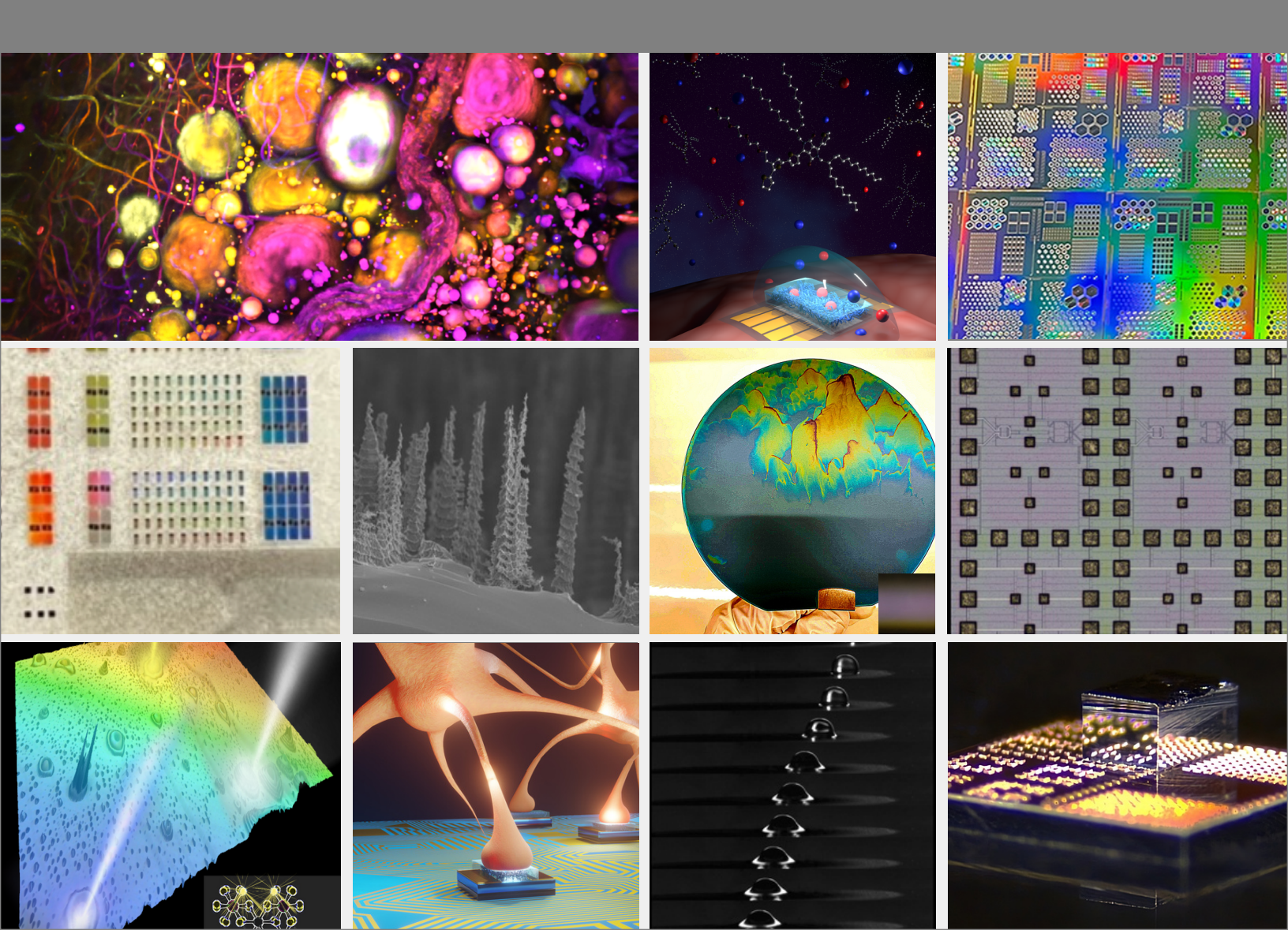


MIT.nano

RESEARCH REPORT 2025



| 1 | | 2 | 3 |
|---|---|----|----|
| 4 | 5 | 6 | 7 |
| 8 | 9 | 10 | 11 |

Front Cover Credits

- 1. "3D imaging of bacteria invading skin microenvironment in Lyme disease" submitted by Kunzan Liu.
- 2. "A Rocket Organic Electrochemical Transistor (OECT) lands on the 'planet Brain,' where the channel material, made of semiconducting polymer stars, begins communicating with the brain." submitted by Camille Cunin.
- 3. "GaN Power Transistors on 8" Si Wafers" submitted by Josh Perozek.
- 5. "Cross section of black silicon formed during DRIE, the "trees" are 5-15 microns tall" submitted by Gillian Micale.
- 6. "Mountains of silane on the backside of a wafer. Captured in MIT.nano (L6)" submitted by Camille Cunin.
- 7. "Intel 16 Si CMOS BEOL Chip for World's First GaN/Si CMOS 3D-mmWIC" submitted by Pradyot Yadav.
- 8. "PhD student Abhishek Mukherjee from Multifunctional Metamaterials research lab demonstrates how one can harness a combination of chemical and structural material defects to tune and enhance photoluminescence from AgScP2S6 a new layered semiconductor material recently synthesized in the Air Force Research Lab" submitted by Syetlana Boriskina.
- 9. "Listening to Synaptic Potentials: Organic Electrochemical Transistors at the Brain-Machine Interface" submitted by Camille Cunin.
- 10. "Capillary Catapults: A high-speed timelapse capturing the inertio-capillary propulsion of a water drop on a nanograss surface. The imbibition front of silicone oil, hemi-wicking through the (nano)structures, contacts the "foot" of the drop sitting atop the superhydrophobic surface. This triggers an immediate dynamic reconfiguration of the drop from a sphere to a hemisphere in milliseconds, as the oil cloaks the drop with a Van der Waals film (first four frames). The sudden change in surface energy induces strong lateral propulsion, with inertio-capillary speeds reaching up to 10 cm/s. This seemingly simple phenomenon arises from a complex interplay of capillarity, geometry, and inertia, forming the foundation for novel droplet transport (and removal) devices currently under development in our lab, in collaboration with Tal Joseph. The video was shot at 50,000 frames per second" submitted by Saurabh Nath.
- 11. "GaN" hattan submitted by Pradyot Yadav.

Microsystems Annual Research Report 2025

Director & Editor-in-Chief Managing Editors & Project Managers Editor Technical Editor Tomás Palacios, Vladimir Bulović Meghan Melvin, Jami L. Mitchell Elizabeth M. Fox Annie Wang

CONTENTS

| Foreword | i |
|--|-----|
| Acknowledgments | ii |
| RESEARCH ABSTRACTS: VOLUME I | |
| 3DHI & Additive Manufacturing | 1 |
| Circuits and Systems | 10 |
| Electronic, Magnetic & Spintronic Devices | 26 |
| Life Science & Semiconductors, Medical Devices & Biotechnology | 45 |
| MEMS, Field-Emitter, Thermal, Fluidic Devices & Robotics | 57 |
| Nanoscience & Nanotechnology | 68 |
| Neuromorphic Devices & Al Hardware Accelerators | 89 |
| Photonics and Optoelectronics | 118 |
| Power Devices and Circuits | 141 |
| Quantum Science and Engineering | 150 |
| RESEARCH ABSTRACTS: VOLUME II | |
| Materials Synthesis and Characterization | 164 |
| In-situ Microscopy / Dynamic Processes | 187 |
| Immersive simulation, design, and visualization | 192 |
| Research Centers | 194 |
| Faculty Profiles | 201 |
| Theses Awards | 241 |
| Startups Affiliated with MTL and MIT.nano Faculty | 243 |
| Glossary | 245 |
| Principal Investigator Index | 248 |

Foreword

We are pleased to announce the publication of the 2025 Microsystems Annual Research Report, a collaborative effort between the Microsystems Technology Laboratories (MTL) and MIT.nano, covering the academic year from July 1, 2024 to June 30, 2025. This report showcases the remarkable accomplishments of the MIT microsystems and nano communities over the past year.

A key highlight was a major milestone for MTL: on November 20, 2024, we commemorated 40 years of pioneering research, cross-disciplinary collaboration, and transformative impact in microelectronics, nanotechnology, and microsystems at the MTL40 Symposium and Gala. The celebration reflected not only MTL's history but also its continued leadership in advancing semiconductor research, fostering strong industry partnerships, and supporting the innovation ecosystem at MIT. Over the past year, MTL welcomed new member companies into the Microsystems Industrial Group (MIG), expanded collaborative research opportunities, and advanced key initiatives such as patent curation and faculty–industry engagement. These efforts continue to strengthen MTL's role as a bridge between fundamental discovery and technological application.

MIT.nano likewise marked FY25 with signature achievements that further demonstrated its role as MIT's hub for nanoscience and nanotechnology. The second annual Nano Summit convened more than 400 researchers, industry leaders, and entrepreneurs to share advances in sustainable materials, nanomedicine, next-generation computing, and artificial intelligence, and to highlight the entrepreneurial ecosystem through a dynamic startup showcase. MIT.nano also hosted the 2025 NNCI Etch Symposium, bringing together national experts to discuss emerging challenges and opportunities in advanced fabrication processes. Together, these events underscored MIT.nano's impact as a catalyst for interdisciplinary collaboration and innovation.

As we mark these important milestones, we take pride in showcasing the various ways we continue to drive innovation and advance research in semiconductor materials, technologies, devices, circuits, and systems, as well as exploring new frontiers in nanoscience and nanoengineering. We find ourselves at a pivotal moment in the field of microelectronics, where we are all called upon to push the boundaries of what is possible. MTL, in close partnership with MIT.nano and its state-of-the-art fabrication and characterization facilities, is well-prepared to meet these challenges.

This year's report provides a comprehensive overview of over 200 research projects across diverse areas of microand nanotechnology. These projects range from advancements in semiconductor materials, the development of new devices, and integrated photonics and circuits, to innovations in insect-scale microrobotics, biomedical systems, and AI hardware accelerators, among many others.

On behalf of MTL and MIT.nano, we extend our deepest gratitude to every contributor to this year's Microsystems Annual Research Report and to the dedicated staff of both organizations, whose tireless efforts have brought this dynamic snapshot of our research to life.

Tomás Palacios Director, Microsystems Technology Laboratories

Vladimir Bulović Director, MIT.nano

Acknowledgments

MICROSYSTEMS INDUSTRIAL GROUP

Analog Devices, Inc.
Applied Materials
Draper
Edwards
Ericsson
GlobalFoundries
Hitachi High-Tech Corporation
IBM Research
Lam Research Corporation
Lockheed Martin Corporation
muRata
NEC
Soitec
TSMC

MTL LEADERSHIP TEAM

Texas Instruments

Tomás Palacios, Director Ruonan Han, Associate Director Charles H. Hsu, Consortium Manager Bilge Yildiz, Associate Director

MTL TECHNICAL STAFF

Michael J. Hobbs, Systems Administrator Thomas J. Lohman, Project Leader, Computation William T. Maloney, Systems Manager Michael McIlrath. Research Scientist

MTL ADMINISTRATIVE STAFF

Ava Bowen, Administrative Assistant
Elizabeth Green, Senior Administrative Assistant
Preetha Kingsview, Project Coordinator
Elizabeth Kubicki, Administrative Assistant
Maria Markulis, Administrative Assistant
Meghan Melvin, Communications Administrator
Jami L. Mitchell, Project Coordinator
Katey Provost, Program Coordinator

MTL SEMINAR SERIES COMMITTEE

Luis F. Velásquez-García, Chair Jeffrey H. Lang Jami L. Mitchell Vivienne Sze

ii

MARC2025 CONFERENCE ORGANIZERS

STEERING COMMITTEE

Mingran Jia, Conference Co-Chair Emma Wawrzynek, Conference Co-Chair Tomás Palacios, MTL Director Vladimir Bulović, MIT.nano Director Kelly Gavin, MIT.nano Meghan Melvin, MTL Jami L. Mitchell, MTL Amanda Stoll DiCristofaro, MIT.nano

CORE COMMITTEE

Emma Batson, Publicity and Web Chair
Adina Bechhofer, Social Chair
Patrick Darmawi-Iskander, Graphics Chair
Julia Estrin, MIG/MAP Coordinator Co-Chair
Amanda Jackson, Registration & Conference Package Chair
Tamar Kadosh Zhitomirsky, Winter Activities & Transportation Chair
Stella Lessler, MIG/MAP Coordinator Co-Chair
Jinchen Wang, Technical Program Chair

SESSION CHAIRS

Zoey Bigelow, 3DHI & Additive Manufacturing
Sabrina Corsetti, Optoelectronics & Integrated Photonics
Julia Estrin, Energy, Power, and Sustainability
Ayush Gupta, Electronic Devices
Patricia Jastrzebska-Perfect, Medical Devices & Biotechnology
Shivam Kajale, Nanotechnology & Nanomaterials
Chao Li, Quantum Technologies
Shi-Yuan Ma, Neuromorphic Devices & AI Hardware Accelerators
Saransh Sharma, Integrated Circuits & Systems
Abigail Wang, Materials & Manufacturing
Hao-Tung Yang, MEMS, Field-Emitter, Thermal, Fluidic Devices & Robotics

MIT.NANO CONSORTIUM

Analog Devices, Inc.
Applied Materials, Inc.
Edwards Vacuum, LLC
Fujikura, Ltd.
IBM
Lam Research
Lockheed Martin Corporation
NC
NEC Corporation
Shell Global Solutions (US) Inc.
SLB
UpNano, Inc.
VIAVI Solutions

MIT.NANO LEADERSHIP TEAM

Vladimir Bulović, Faculty Director, MIT.nano
Brian Anthony, Associate Director
Kathleen Boisvert, Director,
Administration and Finance
Tom Gearty, Communications and Initiatives Director
Nicholas Menounos, Associate
Director of Infrastructure
Anna Osherov, Associate Director,
Characterization.nano
Kristofor Payer, Assistant Director of Operations
Jorg Scholvin, Associate Director, Fab.nano

MIT.NANO STAFF

Daniel A. Adams, Research Specialist Shereece Beckford, Events and Projects Coordinator Robert J. Bicchieri, Research Specialist Kurt A. Broderick. Research Associate Cody Corey, Research Specialist Jordan Cox, Research Specialist Dane Craighead, Research Specialist James Daley, Research Specialist David Dunham, EHS DLC Officer Samantha Farrell. Senior Administrative Assistant Juan Ferrera, Research Scientist Kelly Gavin, Program and Events Manager Shayne Harrel, Research Specialist Justin Hill, Chemical Safety Engineer Donal Jamieson, Research Specialist Ludmila Leoparde-Adams, Financial Officer Hanqing Li, Research Scientist Eric Lim, Research Engineer Lars Llorente, EHS Coordinator John McGlashing, Technician C - Electro - Mechanical Mark K. Mondol, Domain Expert Connor Moorman, Research Specialist Benjamin Newcomb, Operations Engineer Maansi Patel, Research Specialist

Justin Pellegrine, Technician B Electro-Mechanical

Aubrey Penn, Research Specialist Scott J. Poesse, Research Specialist Talis Reks, AR/VR/Gaming/Big Data IT Technologist Gary Riggott, Research Associate Alan Schwartzman, Research Scientist Charlie Settens, Research Specialist Libby Shaw, Research Specialist Elijah Shirman, Program Scientist Amanda Stoll DiCristofaro, Communications and Marketing Manager David M. Terry, Sponsored Research Technical Staff Timothy K. Turner, Project Technician Electro - Mechanical Annie I. Wang, Research Scientist Dennis J. Ward, Research Specialist Joyce Wu, START.nano Program Manager Yong Zhang, Research Specialist Zhenyuan Zhang, Research Specialist Anderson Zu, Administrative Assistant Victoria Zurman, Financial and

AFFILIATED MIT.NANO STAFF

Contract Administrator

Anuradha Murthy Agarwal, Principal Research Scientist. MRL Elham Rafie Borujeny, Postdoctoral Associate, RLE Rami Dana, Research Scientist, DMSE Thomas Lohman, Senior Software Developer/Systems Manager Bill Maloney, Systems Manager Joe Masello, Area Manager, Dept. of Facilities Praneeth Namburi, Research Scientist, Institute for Medical Engineering and Science Jennifer Podgorski, Research Scientist, Biology Haden Quinlan, Senior Program Manager, Mechanical Engineering Mark Rapoza, Area Manager, Dept. of Facilities Ardalan SadeghiKivi, STUDIO.nano liaison, CMS/Writing Sarah Sterling, Cryo-EM Facility Director, Biology Katie Torrence, Senior Administrative Assistant, VPR Luis Velasquez-Garcia, Principal Research Scientist, MTL Travis Wanat, Project Manager, Dept. of Facilities Wade Warman, Technical Instructor, Mechanical Engineering James Weaver, Visiting Scientist Samantha Young, Administrative, Assistant II/ Mechanical Engineering

MIT.NANO LEADERSHIP COUNCIL

Brian Anthony, MIT.nano Robert Atkins, Lincoln Laboratory Kathy Boisvert, MIT.nano

MIT.NANO LEADERSHIP COUNCIL CONTINUED

Vladimir Bulović, MIT.nano
Pablo Jarillo-Herrero, Physics
James LeBeau, DMSE
Farnaz Niroui, EECS
Will Oliver, RLE, Physics
Tomás Palacios, EECS
Carlos Portela, MechE
Katharina Ribbeck, Biological Engineering
Frances Ross, DMSE
Thomas Schwartz, Biology
Carl Thompson, MRL, DMSE
Kripa Varanasi, MechE

MIT.NANO FACULTY ADVOCATES WORKING GROUP - CHARACTERIZATION.NANO

Jim LeBeau, Faculty Lead, DMSE
Anna Osherov, Technical Lead, MIT.nano
Karl Berggren, NSL, EECS
A. John Hart, MechE
Long Ju, Physics
Benedetto Marelli, CEE
Farnaz Niroui, EECS
Yogesh Surendranath, Chemistry

MIT.NANO FACULTY ADVOCATES WORKING GROUP - FAB.NANO

Tomás Palacios – Faculty Lead, EECS Jorg Scholvin – Technical Lead, MIT.nano Tayo Akinwande, EECS Karl Berggren, EECS Jesus del Alamo, EECS Dirk Englund, EECS Juejun Hu, MechE Pablo Jarillo-Herrero, Physics Jeehwan Kim, MechE/DMSE Jing Kong, EECS Paulo Lozano, AeroAstro Farnaz Niroui, EECS Will Oliver, EECS Deblina Sarkar, MAS Caroline Ross. DMSE Bilge Yildiz, NSE & DMSE

RESEARCH ABSTRACTS: VOLUME I

3DHI & Additive Manufacturing

| In-situ Magnetization of Additively Manufactured, Permanent Magnets | 2 |
|--|---|
| Fully 3D-printed, Soft Magnetic Cores Via Material Extrusion | 3 |
| Semiconductor-Free, Fully 3D-printed Logic Gates | 4 |
| Miniaturized, 3D-printed Retarding Potential Analyzer | 5 |
| 3D-printed Triaxial Electrospray Devices | 6 |
| Unsupervised Anomaly Detection on Irregular Time Series Data | 7 |
| Additive Manufacturing of Hybrid Electrospray Emitter Geometries via Two-Photon Polymerization | 8 |
| 3D-Printed Hard Magnets | 9 |

In-situ Magnetization of Additively Manufactured, Permanent Magnets

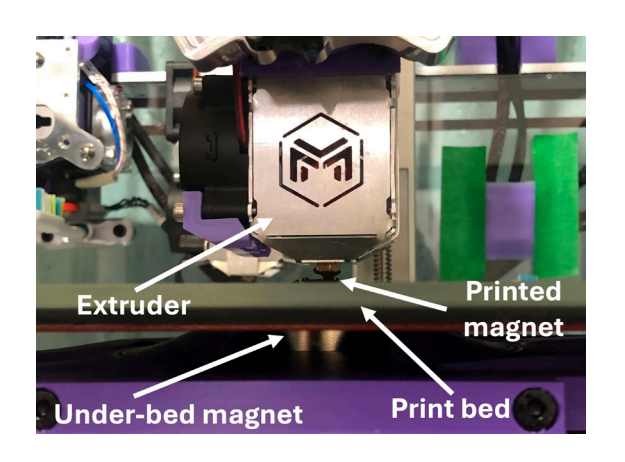
Z. Bigelow, L. F. Velásquez-García Sponsorship: Empiriko Corporation

Hard ferrite magnets are widely used due to their low cost, chemical stability, and resistance to demagnetization, making them attractive for applications in motors, sensors, and consumer electronics. However, traditional fabrication methods are limited to predefined shapes and rely on post-processing magnetization steps, restricting design freedom and integration into complex devices.

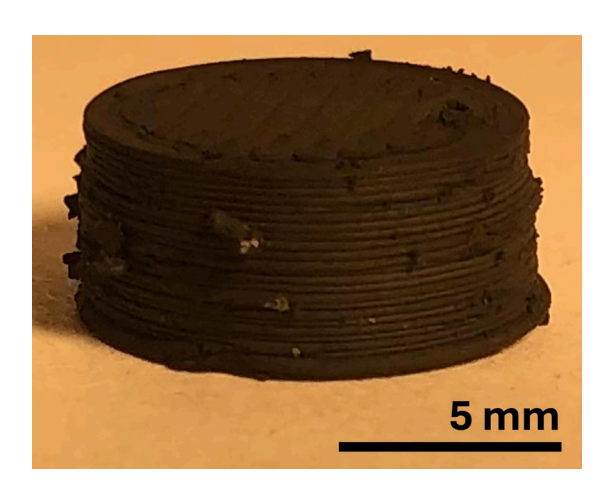
In this project, we explore the in-situ magnetization of ferrite-based composites during the printing process itself—a feat not previously demonstrated, to our knowledge. Our work represents a departure from conventional post-print magnetization techniques and

opens the door to freeform fabrication of functional, magnetic architectures, particularly in applications where shape complexity and miniaturization are critical.

By placing a high-strength, permanent magnet beneath the printer bed (Figure 1), we successfully magnetized ferrite-doped, Nylon 12 feedstock as it was extruded and cooled (Figure 2). This process resulted in a net surface magnetic field on the printed part—a significant step toward additive manufacturing of magnetized components. Current research efforts focus on feedstock optimization, magnetization direction control, and magnetic strength optimization.



▲ Figure 1: Side view of magnet secured beneath printer bed.



▲ Figure 2: 3D-printed, hard ferrite magnet.

- A. P. Taylor, J. Izquierdo-Reyes, and L. F. Velásquez-García, "Compact, Magnetically Actuated, Additively Manufactured Pumps for Liquids and Gases," J. of Physics D – Applied Physics, vol. 53, no. 35, 355002, Aug. 2020. DOI: 10.1088/1361-6463/ab8de8
- A. P. Taylor, C. Vélez Cuervo, D. Arnold, and L. F. Velásquez-García, "Fully 3D-Printed, Monolithic, Mini Magnetic Actuators for Low-Cost, Compact Systems," J. of Microelectromechanical Systems, vol. 28, no. 3, pp. 481-493, Jun. 2019. DOI: 10.1109/JMEMS.2019.2910215
- J. Cañada, H. Kim, and L. F. Velásquez-García, "Three-dimensional, Soft Magnetic-cored Solenoids via Monolithic, Multi-Material Extrusion,"
 Virtual and Physical Prototyping, vol. 19. no. 1, e2310046, Feb. 2024. DOI: 10.1080/17452759.2024.2310046

Fully 3D-printed, Soft Magnetic Cores Via Material Extrusion

J. Cañada, L. F. Velásquez-García Sponsorship: Empiriko Corporation, "la Caixa" Foundation

Electrical machines are the key elements in the generation, distribution, and utilization of electrical energy. Recently reported works demonstrate that additive manufacturing (AM) technologies can produce all the parts involved in the fabrication of electrical machines including magnetic cores, conductive coils, permanent magnets, and mechanical couplings. By harnessing the virtues of AM (e.g., multi-material fabrication, waste reduction, feasibility to create freeform, geometrically complex structures), the fabrication of electrical machines can become cheaper and easier, and their performance can be improved.

The performance of electrical machines is closely tied to that of their magnetic cores, which are made of soft magnetic materials. Multiple studies have reported on the development of AM-compatible, soft magnetic feedstock. However, the performance of most of the proposed materials is poor, exhibiting relative magnetic permeabilities of 2-3. Processes that yield parts with higher magnetic permeabilities (up to ~600) have been reported, but they rely on heat post-processing at temperatures close to 1000 °C, which is incompatible with thermoplastics-based, multi-

material three-dimensional (3D) printing and often introduces geometrical distortions on the fabricated components.

This work reports the single-step 3D printing of soft magnetic cores that attain relative magnetic permeabilities above 30, while not requiring heat post-processing (Figure 1). The 3D-printed cores exhibit a narrow hysteresis loop and negligible electrical conductivity—qualities desirable for the fabrication of soft magnetic cores for electrical machines. Furthermore, the magnetic permeability of the cores can be modulated by tuning specific 3D printing parameters (Figure 2), enabling the monolithic fabrication of multi-permeability cores.

The cores are fabricated from pellets of FeSiAl-doped nylon using a multi-material extrusion 3D printer capable of handling other functional materials (e.g., electrically conductive, elastic). This feat entails significant progress towards the monolithic AM of electrical machines and has immediate relevance for the on-site fabrication of electromechanical devices in remote areas.



 \blacktriangle Figure 1: 3D-printed toroidal cores of different sizes made in FeSiAl-doped nylon next to a US quarter.

▲ Figure 2: Real component of the relative magnetic permeability of 3D-printed cores at 1 MHz versus the "extrusion multiplier" 3D printing parameter.

- J. Cañada, S. F. Nagle, N. Vidal, J. M. López-Villegas, and L. F. Velásquez-García, "3D-Printed Soft Magnetic Cores for Compact Electromechanical Devices Via Material Extrusion," 2024 IEEE 23rd International Conference on Micro and Miniature Power Systems, Self-Powered Sensors and Energy Autonomous Devices (PowerMEMS), Tonsberg, Norway, 2024, pp. 255-258. DOI: 10.1109/ PowerMEMS63147.2024.10814238
- J. Cañada, H. Kim, and L. F. Velásquez-García, "Three-dimensional, Soft Magnetic-cored Solenoids via Multi-material Extrusion," Virtual and Physical Prototyping, vol. 19, no. 1, 2024. DOI: 10.1080/17452759.2024.2310046
- A. P. Taylor, J. Izquierdo-Reyes, and L. F. Velásquez-García, "Compact, Magnetically Actuated, Additively Manufactured Pumps for Liquids and Gases," J. of Physics D – Applied Physics, vol. 53, no. 35, p. 355002 August 2020. DOI: 10.1088/1361-6463/ab8de8

Semiconductor-Free, Fully 3D-printed Logic Gates

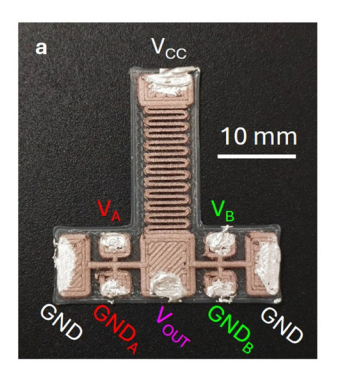
J. Cañada, L. F. Velásquez-García Sponsorship: Empiriko Corporation, "la Caixa" Foundation

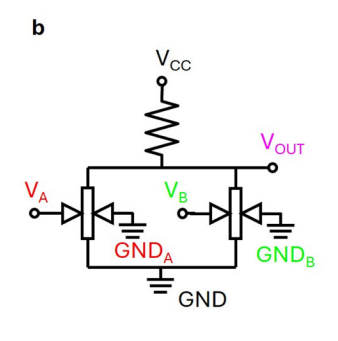
Additive manufacturing (AM) has the potential to enable the inexpensive, single-step fabrication of fully functional electromechanical devices. However, while the three-dimensional (3D) printing of mechanical parts and passive electrical components is well developed, the fabrication of fully 3D-printed active electronics, which are the cornerstone of intelligent devices, remains a challenge. Existing examples of 3D-printed active electronics show potential but lack integrability and accessibility.

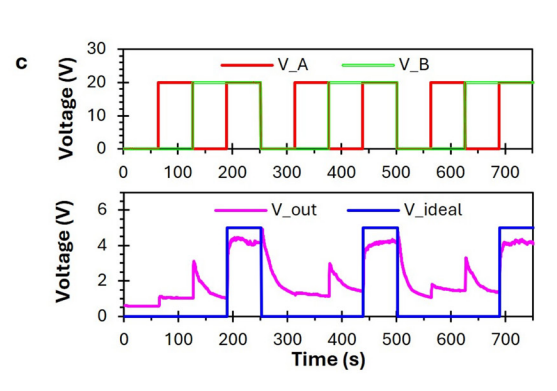
This work reports the first instance of active electronics fully 3D-printed via material extrusion. Material extrusion is one of the most accessible and versatile additive manufacturing technologies, and it is among the few techniques capable of monolithic multi-material fabrication. The proposed devices harness a polymeric positive temperature coefficient phenomenon observed in thin 3D-printed traces of copper-reinforced polylactic acid. This phenomenon, which entails a temperature-driven, reversible, and repeatable spike in resistivity, can be leveraged for

the implementation of 3D-printed electrical switches. The proposed switches behave as normally closed switches, and their combination with other 3D-printed components (e.g., resistors) enables the fabrication of fully 3D-printed integrated circuits. This capability is demonstrated through the implementation of the first fully 3D-printed, semiconductor-free, solid-state logic gates (Figure 1). The devices are fabricated in a single operation using commercially available hardware and materials.

Although the reported switches and logic gates do not perform competitively against semiconductor-enabled integrated circuits, the customizability and accessibility intrinsic to material extrusion make this technology promisingly disruptive. Furthermore, the combination of the proposed control devices with the ability of material extrusion to fabricate electromagnetic devices and mechanically functional components can enable the single-step fabrication of complex hardware, such as functionalized prostheses and robots.







▲ Figure 1: Fully 3D-printed AND gate: picture of fabricated device (a), schematic (b), and input-output characteristics with Vcc set to 5 V (c)

- J. Cañada and L. F. Velásquez-García, "Semiconductor-free, Monolithically 3D-printed Logic Gates and Resettable Fuses," Virtual and Physical Prototyping, vol. 19, no. 1, 2024. DOI: 10.1080/17452759.2024.2404157
- J. Cañada, H. Kim, and L. F. Velásquez-García, "Three-dimensional, Soft Magnetic-cored Solenoids via Multi-material Extrusion," Virtual and Physical Prototyping, vol. 19, no. 1, 2024. DOI: 10.1080/17452759.2024.2310046
- A. P. Taylor, J. Izquierdo-Reyes, and L. F. Velásquez-García, "Compact, Magnetically Actuated, Additively Manufactured Pumps for Liquids and Gases," J. of Physics D – Applied Physics, vol. 53, no. 35, p. 355002 Aug. 2020. DOI: 10.1088/1361-6463/ab8de8

Miniaturized, 3D-printed Retarding Potential Analyzer

B. I. Quintanar, Z. Bigelow, L. F. Velásquez-García Sponsorship: Lam Research

Retarding potential analyzers (RPAs) are gridded instruments that estimate the energy distribution of plasma ions; the information is important for optimizing plasma-based processes in fields such as semiconductor manufacturing, materials processing, and fusion energy research. This project aims at conducting a proof-of-concept demonstration of an additively manufactured RPA capable of measuring cold, dense plasmas, which have associated a small Debye length. The fabrication of the RPAs uses a combination of two different

vat-photopolymerization techniques: two-photon polymerization for the grids and digital light projection for the housing, allowing for precise control over the device's geometry and dimensions while minimizing the printing time. Computational fluid dynamics simulations using COMSOL Multiphysics have guided the design of the RPA. Current efforts focus on fabricating the devices and testing them in experimental plasmas of relevance.



▲ Figure 1: Miniaturized RPA, showing the active zone at the top and a PCB for electrical connections at the bottom.

J. Izquierdo-Reyes, Z. Bigelow, N. Lubinsky, and L. F. Velásquez-García, "Compact Retarding Potential Analyzers Enabled by Glass-ceramic vat Polymerization for CubeSat and Laboratory Plasma Diagnostics," Additive Manufacturing, vol. 58, p. 103034, Jul. 2022. DOI: 10.1016/j. addma.2022.103034

E. V. Heubel and L. F. Velásquez-García, "Microfabricated Retarding Potential Analyzers with Enforced Aperture Alignment for Improved Ion Energy Measurements in Plasmas," J. of Microelectromechanical Systems, vol. 24, no. 5, pp. 1355-1369, Oct. 2015. DOI: 10.1109/ JMEMS.2015.2399373

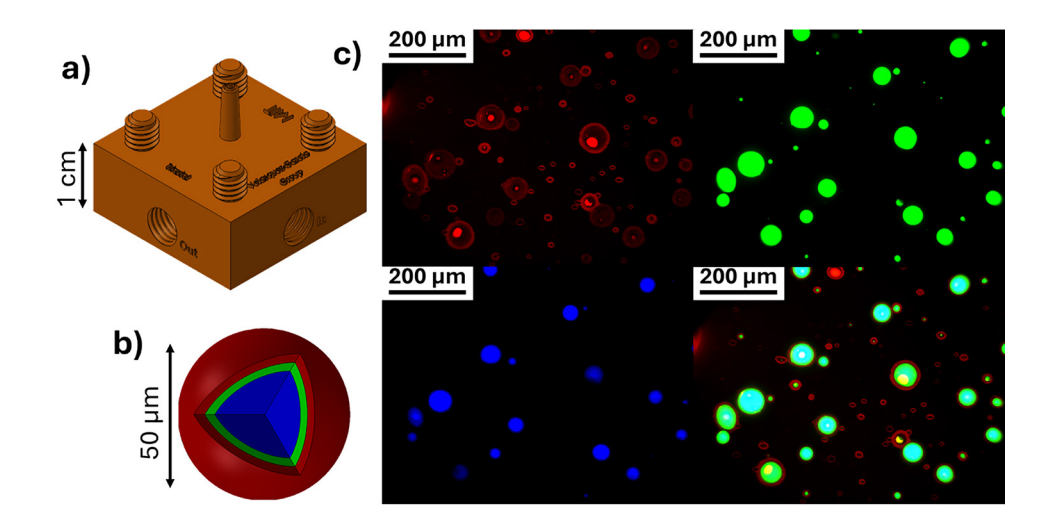
L. F. Velásquez-García, J. Izquierdo-Reyes, and H. Kim, "Review of in-space Plasma Diagnostics for Studying the Earth's Ionosphere," J. of Physics D – Applied Physics, vol. 55, no. 26, pp. 263001-263027, Jun. 2022. DOI: 10.1088/1361-6463/ac520a

3D-printed Triaxial Electrospray Devices

B. I. Quintanar, L. F. Velásquez-García Sponsorship: Monterrey Tec - MIT Nanotechnology Program

Electrospraying is a versatile technique that utilizes electrostatic forces to atomize liquids into fine droplets, enabling the encapsulation of a wide range of materials, including sensitive bioactive agents, drugs, and food ingredients. This project reports the proof-of-concept demonstration of the first three-dimensional (3D)-printed, triaxial electrospray microparticle generators. Made via vat photopolymerization, the devices' spouts have three concentric microchannels that facil-

itate the simultaneous and controlled release of multiple solutions, generating structured, multi-layered (core-shell-shell), compound microparticles (Figure 1). The compound particles have applications in drug delivery, self-healing materials, and micro- and nano-reinforced composites. Current research efforts focus on increasing the throughput of the devices by implementing arrays of emitters that uniformly operate in parallel.



▲ Figure 1: a) CAD of a 3D-printed, triaxial electrospray device; b) Core-shell-shell particle schematic identifying with colors its layers (red − outer shell, green − inner shell, and blue − core), c) Fluorescent microscopy images of compound particles generated by the 3D-printed devices (from left to right and from top to bottom): outer shell, inner shell, core, superposition.

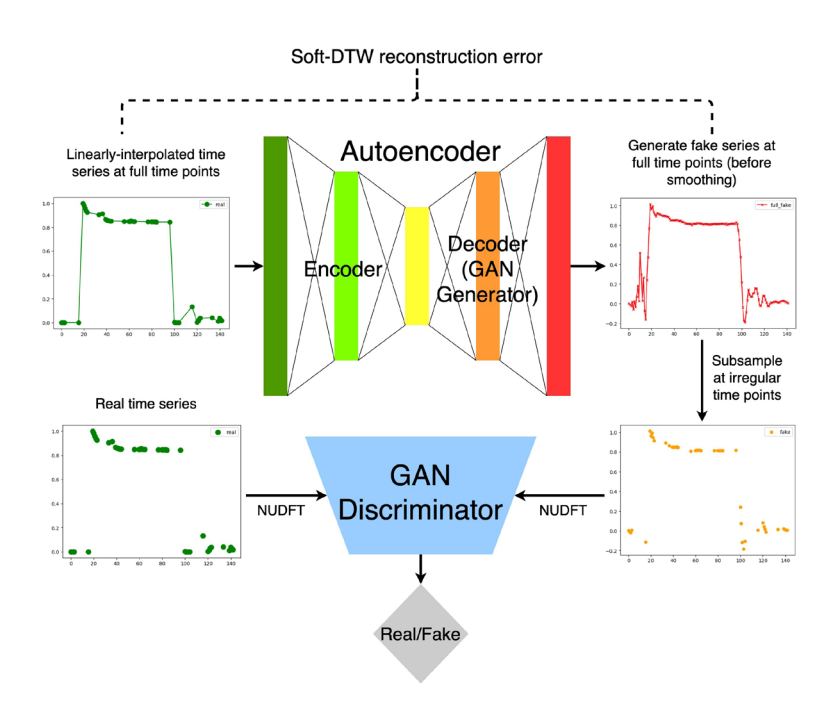
- D. Olvera-Trejo and L. F. Velásquez-García, "Additively Manufactured MEMS Multiplexed Coaxial Electrospray Sources for High-throughput, Uniform Generation of Core-shell Microparticles," Lab on a Chip, vol. 16, no. 21, Jan. 2016. DOI: 10.1039/c6lc00729e
- H. Kim and L. F. Velásquez-García, "High-impulse, Modular, 3D-printed CubeSat Electrospray Thrusters Throttleable via Pressure and Voltage Control," Advanced Science, vol. 12, no. 13, pp. 2413706-2413719 Apr. 2025. DOI: 10.1002/advs.202413706
- B. Garcia-Farrera and L. F. Velásquez-García, "Ultrathin Ceramic Piezoelectric Films via Room-temperature Electrospray Deposition of ZnO Nanoparticles for Printed GHz Devices," ACS Applied Materials & Interfaces, vol. 11, no. 32, pp. 29167-29176, Aug. 2019. DOI: 10.1021/ acsami.9b09563

Unsupervised Anomaly Detection on Irregular Time Series Data

F.-K. Sun, R. K. Owens, D. S. Boning Sponsorship: Analog Devices

Anomaly detection in semiconductor manufacturing is essential for maintaining production quality and efficiency. However, data from semiconductor equipment sensors can form irregular (i.e. unevenly-spaced) time series due to sporadic instabilities, which challenge the regularity assumption in most machine learning algorithms.

Our anomaly detection uses an autoencoder as its backbone. To address time shifts commonly seen in signals, we compute the reconstruction error using Soft-Dynamic Time Warping (Soft-DTW), a technique resilient to temporal misalignments. We also employ the Non-Uniform Discrete Fourier Transform (NUDFT) to convert irregular time series into fixed-size representations in the frequency domain, making the data suitable for processing. To further enhance the ability to reconstruct realistic series, even with irregular timing, we integrate a Generative Adversarial Network. This combined approach enables robust anomaly detection in irregular time series without performance degradation.



▲ Figure 1: Overall model architecture.

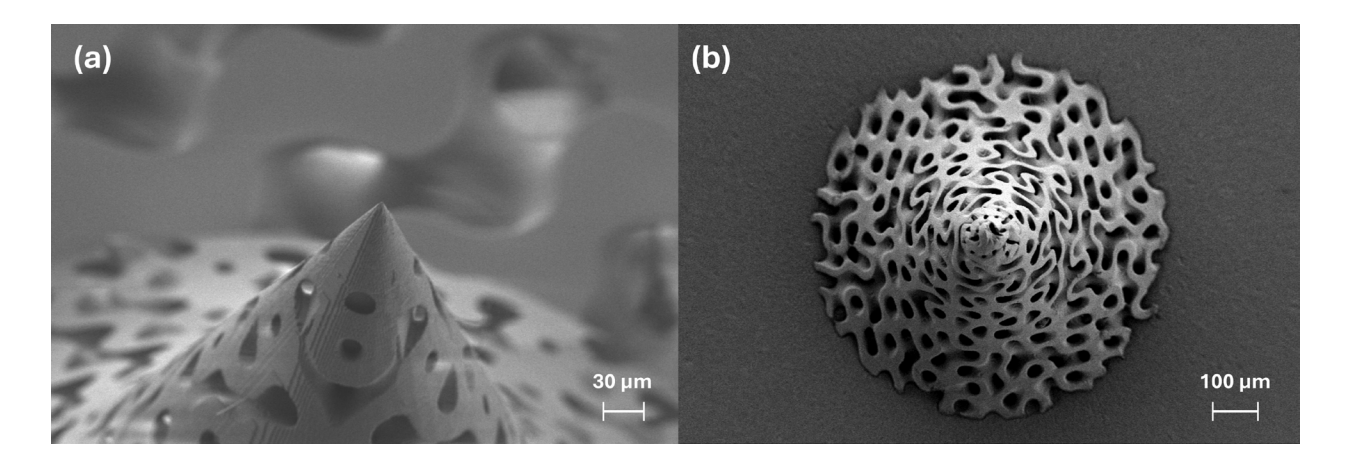
Additive Manufacturing of Hybrid Electrospray Emitter Geometries via Two-Photon Polymerization

R. A. Davis, G. D'Orazio, J. H. Fang, S. Sobhani, E. Petro, B. L. Wardle Sponsorship: NASA Space Technology Graduate Research Opportunities Grant

Electric propulsion provides precise, in-space propulsion with mass savings and high specific impulse. Electrospray propulsion, using microfluidics and electrostatics to accelerate ions and droplets, has low-thrust applications and can scale to larger systems. Key failure modes are dependent on the propellant wetting properties and emitter geometry.

Current manufacturing methods face challenges in creating precise, repeatable emitter geometries, leading to long development times and unstable performance.

This work aims to improve individual emitter accuracy with nanoscale additive manufacturing and tailor wetting properties via dielectric atomic layer deposition. Single emitters are printed including triply periodic minimal surfaces (TPMS) to achieve uniform porosity, followed by alumina coating to adjust wetting. Key electrospray performance parameters are estimated, revealing the potential for convenient, repeatable emitter fabrication and tailored geometries for specific applications.



▲ Figure 1: Scanning electron microscope (SEM) images of additively-manufactured (a) Schwarz diamond TPMS electrospray emitter, (b) and alumina-coated gyroid TPMS electrospray emitter.

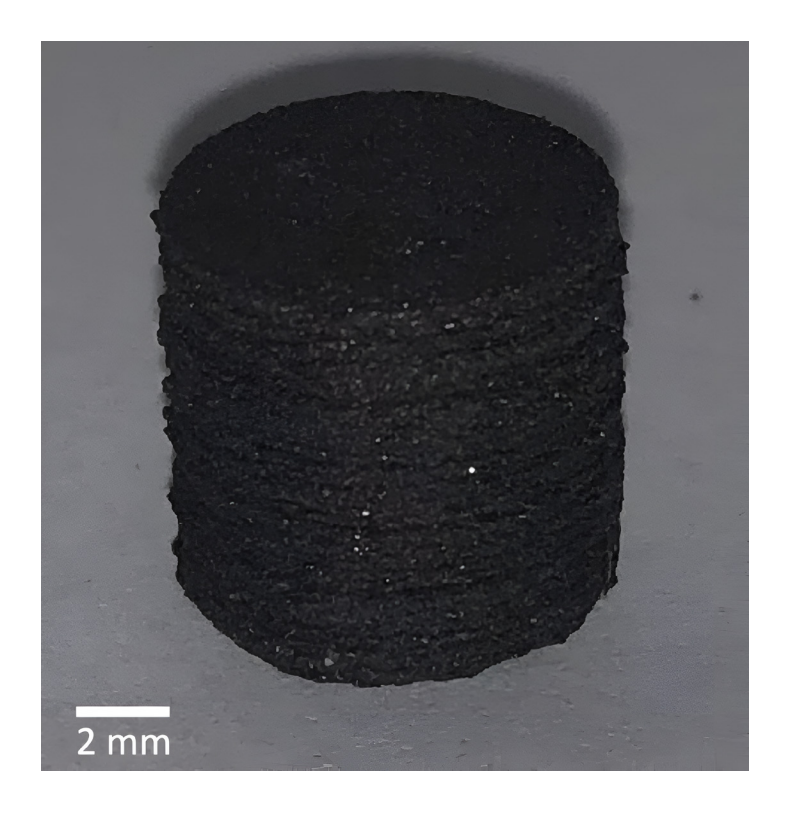
3D-Printed Hard Magnets

Z. Bigelow, L. F. Velásquez-García Sponsorship: Empiriko Corporation

Hard magnets are extensively used across numerous industries, including electronics, automotive, renewable energy, healthcare, and consumer goods. However, conventional methods for producing these magnets are limited to simple shapes and require assembly, leading to increased production costs and constrained geometries and devices.

We present a novel 3D printing process capable of producing hard magnets using micro- and nanoreinforced materials, thereby expanding the scope of their practical applications. Our research is focused on the fabrication of isotropic magnets at a miniature

scale, typically ranging in size from a few millimeters. The material composition utilized in our printing process consists of a blend comprising 75% NdFeB and 25% Nylon 12 by volume. This work demonstrates the feasibility of 3D printing hard magnets and underscores the potential for fine-tuning magnetic properties through additive manufacturing techniques. These advancements offer precise control over magnet geometry and performance, presenting significant opportunities for industries seeking tailored magnetic solutions.



▲ Figure 1: 3D printed 75% NdFeB magnet.

Circuits & Systems

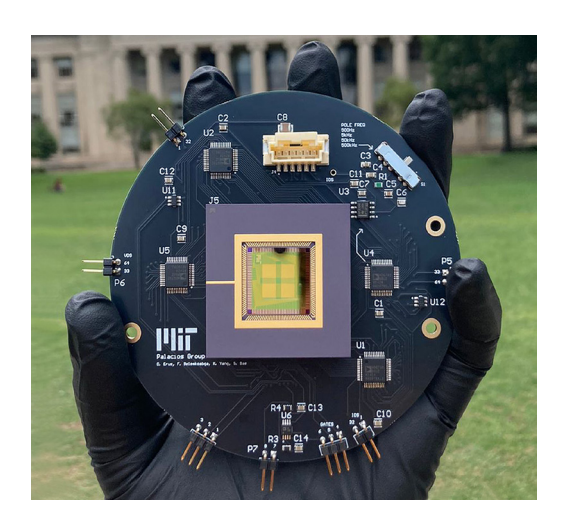
| Integrated System to Control and Measure Graphene Field-effect Transistor Arrays | 11 |
|--|----|
| High-Angular-Resolution Sub-THz Imaging System with Antenna-in-Package (AiP) Technology | 12 |
| SPIPE: Differentiable SPICE-level Co-simulation Program for Integrated Photonics and Electronics | 13 |
| Terahertz Tactile and Non-contact Sensors for Robotic Manipulation and Training | 14 |
| Reinforcement Learning for Verilog Code Generation with Functional Feedback | 15 |
| Highly Selective Harmonic-resilient Sub-6G Front Ends | 16 |
| Defining and Optimizing Write/Clear Margin for a Nanoantenna-Based Petahertz Electronic Memory Cell | 17 |
| Memory-Efficient Gaussian Mapping on Micro-Robots: Algorithm and Chip | 18 |
| Design and Modeling of High Temperature Gallium Nitride RF Amplifiers | 19 |
| Harmonic-Resilient Low-Power Receiver Architecture with Pipeline Mixing for IoT Applications | 20 |
| A 28 GHz Coupled PLL-Based CMOS Quadrature Oscillator | 21 |
| Interface Circuits for Analog In-Memory Computing | 22 |
| An Analog Front End with Sparse-Image Capturing for Energy-Efficient Bladder Ultrasound Imaging | 23 |
| A 232-to-260GHz CMOS Amplifier-Multiplier Chain with a Matching-Sheet-Assisted Radiation Package and 11.1dBm Total Radiated Power | 24 |
| Efficientvit-SAM: Accelerated Segment Anything Model without Performance Loss | 25 |

Integrated System to Control and Measure Graphene Field-effect Transistor Arrays

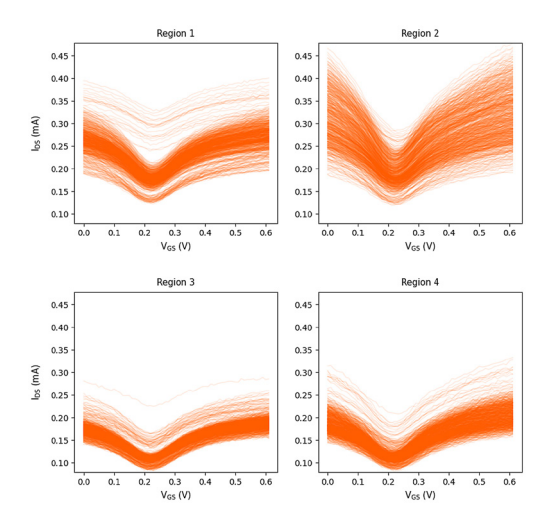
S. Bae, D. Erus, F. Belemkoabga, C. Lopez, C.-H. Liu, T. Palacios Sponsorship: NSF CIQM, NSF Convergence

Two-dimensional materials such as graphene have shown great promise as biochemical sensors. As a zero-bandgap material, graphene field effect transistors (GFETs) exhibit a Dirac point shift when different ions (i.e., dopants) come into contact with the transistor. This shift can be observed from the GFET's I-V characteristics, enabling the detection of changes in chemical environments.

Our group has designed and fabricated a scalable, handheld chemical sensing system with 4096 sensing units, each consisting of a GFET (Figure 1). While previous research has demonstrated the feasibility of ion detection with electrolytegated transistors, we propose an integrated system that controls and measures both liquid-gated and gas-sensing transistors. Specifically, the custom-designed printed circuit board (PCB) enables extraction of the electrical characteristics of 4096 functional GFETs individually by multiplexing a single pair of drain and source connections to the measurement circuitry (Figure 2). This PCB facilitates automated, real-time analysis of data regardless of transistor quality, applied dopant, and sensing medium, advancing its potential for use as a portable biomedical diagnostic device.



▲ Figure 1: Proposed integrated measurement system incorporating a GFET array chip. The platform supports both liquid-gated and gas-sensing modalities, enabling the characterization of 4,096 transistors in under three seconds.



▲ Figure 2: I_{DS}-V_{GS} characteristics of 4096 functionalized GFET units measured in PBST. The system automatically determines the Dirac point—the gate voltage at minimum conductivity—of each unit using fifth-order polynomial fitting.

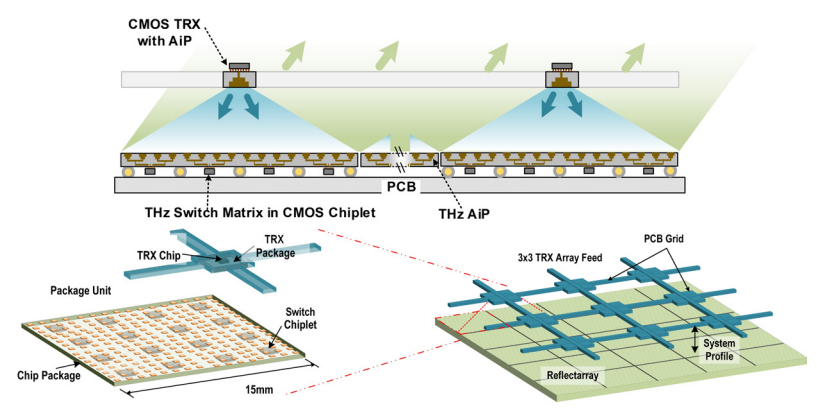
M. Xue, C. Mackin, W.-H. Weng, J. Zhu, Y. Luo, S.-X. L. Luo, A.-Y. Lu, M. Hempel, et al., "Integrated Biosensor Platform Based on Graphene Transistor Arrays for Real-Time High-Accuracy Ion Sensing," Nature Communications, vol. 13, no. 5064, 2022.

[•] Y. Ohono, K. Maehashi, Y. Yamashiro, and K. Matsumoto, "Electrolytegated Graphene Field-effect Transistors for Detecting pH and Protein Adsorption," Nano Letts., vol. 9, pp. 3318–3322, 2009.

High-Angular-Resolution Sub-THz Imaging System with Antenna-in-Package (AiP) Technology

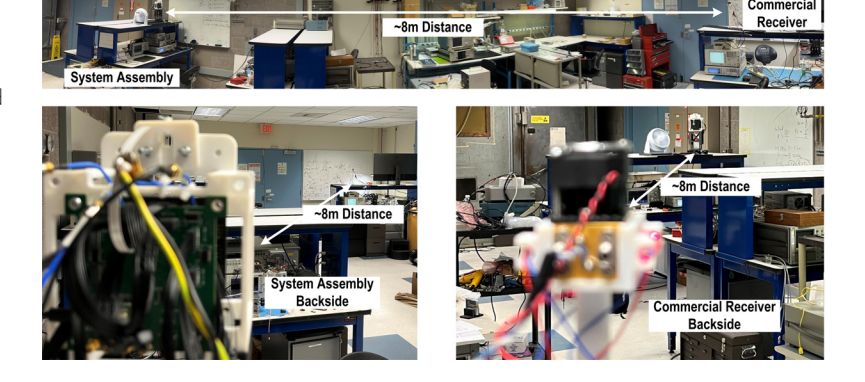
X. Chen, G. C. Dogiamis, R. Han Sponsorship: Intel Corporation

The high-angular-resolution imaging capability of future automotive and security sensing systems is in favor of compact, fully integrated, and reconfigurable antenna arrays. The adoption of sub-terahertz (sub-THz) frequencies in such systems relieves the hardware requirements for the physical size and fractional bandwidth. This project proposes a sub-THz four-dimensional (4D) imaging system that decouples the designs of active circuits (transceivers) and a large passive antenna array (reflectarray), which naturally circumvents those challenges of circuit complexities, electronic density, and computation power in traditional phased/Multiple-Input Multiple-Output arrays. On the transceiver (TRX) side, a 250-GHz TRX system with antenna-in-package (AiP) technology is developed and assembled; it shows a significant radiation efficiency improvement over the on-chip solution. On the reflectarray side, AiP is used for the antenna array. Only digital circuits and memories are integrated on 400 tiny chiplets mounted on 25 package modules, which reduces the total silicon area by more than 10x compared to a full-silicon solution. To further enhance the aperture size and address the small gaps between adjacent package modules in the assembly process, the array is designed in an aperiodic manner, so that the grating lobes can be well suppressed. Combining the two sub-systems (TRX & reflectarray) with a full-duplex technique based on reflectarray-TRX cooperation enables the complete 4D imaging system with a needle-beam. Simulation shows a 0.5° round-trip beamwidth, which leads to a 0.25° angular resolution for radar imaging. Figure 1 shows the system architecture, and Figure 2 shows one typical measurement setup of the assembled system.



◆ Figure 1: Proposed sub-THz system with multi-transceiver feeds and AiP technology.

Figure 2: Die micrograph of the proposed harmonic rejection receiver.



- X. Chen, "A 265-GHz CMOS Reflectarray With 98×98 Elements for 1°-Wide Beam Forming and High-Angular-Resolution Radar Imaging," IEEE
 J. of Solid-State Circuits, vol. 59, no. 11, pp. 3655-3669, Nov. 2024. DOI: 10.1109/JSSC.2024.3393021
- X. Chen, "A 140-GHz FMCW TX/RX-Antenna-Sharing Transceiver With Low-Inherent-Loss Duplexing and Adaptive Self-Interference Cancellation," IEEE J. of Solid-State Circuits, vol. 57, no. 12, pp. 3631-3645. Dec. 2022. DOI: 10.1109/JSSC.2022.3202814

SPIPE: Differentiable SPICE-level Co-simulation Program for Integrated Photonics and Electronics

Z. Gao, D. S. Boning

Heterogeneous photonic-electronic systems, such as co-packaged optics and photonic-electronic artificial intelligence (AI) accelerators, are rapidly gaining traction but also pose significant design challenges due to distinct design methodologies. Digital and analog electronics are typically described using hardware description languages and Software Improvement and Capability Determination (SPICE), respectively, whereas photonic devices and systems are represented using permittivity tensors on the Yee grid and the scattering matrix formulation. This disparity necessitates an end-to-end photonic-electronic co-simulation tool to streamline co-design. Most preliminary co-simulation approaches rely on translating photonic compact models into Verilog-A or SPICE models to simulate everything there, which not only introduces the additional complexity of model conversion but also has potential numerical stability problems. Additionally, another critical functionality missing from the current implementation is enabling gradient calculation in these co-simulators, which will be crucial for end-to-end gradient-based electronic-photonic system optimization.

We propose a differentiable SPICE-level cosimulation program for integrated photonics and electronics (SPIPE). We develop a customized differentiable frequency-domain scattering matrix simulation for the photonic components and, leveraging the time-domain adjoint method,

enable differentiable transient simulation for the electronic components as well. SPIPE accepts a text file using an extended SPICE syntax to describe the photonic-electronic circuit and outputs both the analytical optical signal values (i.e., complex numbers representing the magnitude and phase of the electromagnetic (EM) mode coefficients) and the electrical signal values (i.e., real numbers representing voltage or current). SPIPE is the first co-simulator to overcome model conversion issues (e.g., eliminating the need to convert photonic compact models into Verilog-A or SPICE) and provide differentiability. Numerical experiments on several circuits confirm the accuracy of SPIPE when compared to analytical solutions and real-world experimental data. Further, in cases where existing simulators are applicable, SPIPE achieves a runtime reduction of 2~85x compared to an industry-standard simulator. In summary, SPIPE has two major advantages. First, SPIPE eliminates model conversion issues (i.e., translating photonic models into Verilog-A or SPICE). Instead, it directly utilizes SPICE for electronic simulation and the scattering matrix method for photonic simulation, with a customized interface to facilitate seamless interaction between the two domains. Second. SPIPE is differentiable. enabling the computation of derivatives of an optical signal with respect to voltage or current signals.

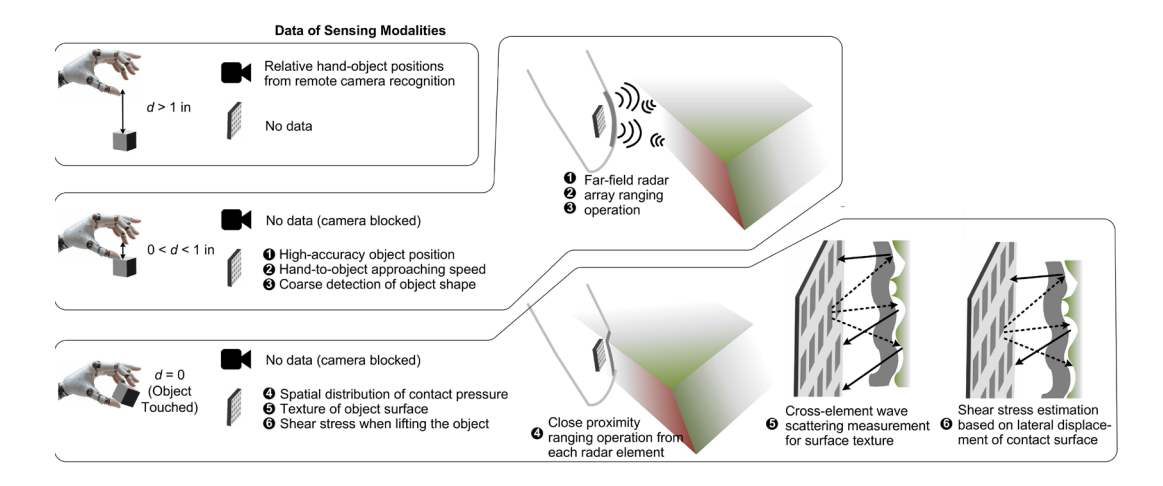
C. S. Agaskar, J. Leu, M. R. Watts, and V. Stojanovic, "Electro-optical Co-simulation for Integrated CMOS Photonic Circuits with VerilogA,"
 Optics Express, pp. 27180-27203, 2015.

Terahertz Tactile and Non-contact Sensors for Robotic Manipulation and Training

K. R. Pochana, R. Han Sponsorship: Analog Devices/MIT Generative AI Impact Consortium

Similar to Large Language Models, Large Behavior Models in robotics have shown promise in learning general capabilities for interacting in dynamic environments, essential for robots that will operate in human environments and alongside humans. Within these efforts, tactile sensors, which provide contact-based shape and force information about objects as they are touched, have become widely regarded as critical to robust performance. However, current mainstream tactile sensors use optical and vision systems, resulting in bulky and rigid-frame packages that limit robot form factors and learning approaches. We aim to develop a thin-package solution for tactile sensing that reduces robot design constraints and lowers the barrier to data collection needed for robotic learning methods. In addition to high-resolution (<0.5 mm) contact pressure spatial mapping, we aim to provide pre-contact position and shape information, a new modality of information for robotic manipulators.

The key enabler of this technology is the use of an on-chip micro-radar array that operates in the subterahertz probing frequency. The corresponding small wavelength (~1 mm) allows for a dense array (0.25 mm element pitch) and sub-mm-level accuracy in distance and shape detection. The proposed system consists of a 5x5 micro-radar array implemented in a custom sensor chip and coupled to in-package antennas to minimize the amount of silicon used for a potentially flexible sensor system. A deposited layer of elastic material on top of these antennas serves as a skin-like interface to contact environmental objects. As the surface deforms, the micro-radar array measures it. Since distance measurements can be taken before an object contacts the sensor, pre-contact shape information can be constructed as well. This modality of information can allow more reliable and precise maneuvers in conditions where vision is occluded and complements vision-based sensing in ideal conditions, ultimately expanding the capabilities of robotic manipulation.



▲ Figure 1: Operation of the proposed sensor. The sensor consists of a 2D-antenna array with bonded chiplets and an elastomer contact surface. In ranges where a camera cannot provide data for behaviors, our sensor provides pre-contact information and high-resolution tactile information, including important components such as shear forces.

- B. Romero, H.-S. Fang, P. Agrawal, and E. Adelson, "EyeSight Hand: Design of a Fully Actuated Dexterous Robot Hand with Integrated Vision-Based Tactile Sensors and Compliant Actuation," IEEE/RSJ International Conference on Intelligent Robots and Systems (IROS), 2024.
- Toyota Robotics Institute, "Large Behavior Models," [Link]

Reinforcement Learning for Verilog Code Generation with Functional Feedback

J. Shi, Z. Gao, D. S. Boning

The increasing complexity of hardware systems has made the automatic generation of register-transfer-level code an important yet challenging problem. While large language models (LLMs) have demonstrated strong capabilities in generating syntactically correct hardware code, ensuring functional correctness and optimizing for design constraints remains a major challenge.

In this work, we propose a reinforcement learning (RL)-based framework for Verilog code generation, where an LLM is fine-tuned with functional feedback. The model takes as input a natural language description of a hardware module's functionality, along with its interface specification, and generates the corresponding Verilog implementation. Our framework employs proximal policy optimization. We leverage simulation tools like Icarus Verilog and functional equivalence checking with Yosis to compute

feedback for each generated candidate. The reward is shaped to encourage both successful compilation and functional equivalence with a reference design, allowing the model to learn effective exploration strategies.

Preliminary results demonstrate that RL training significantly improves functional pass rates compared to baselines. The trained model is capable of generating Verilog programs that not only compile successfully but also satisfy formal equivalence checks with reference designs

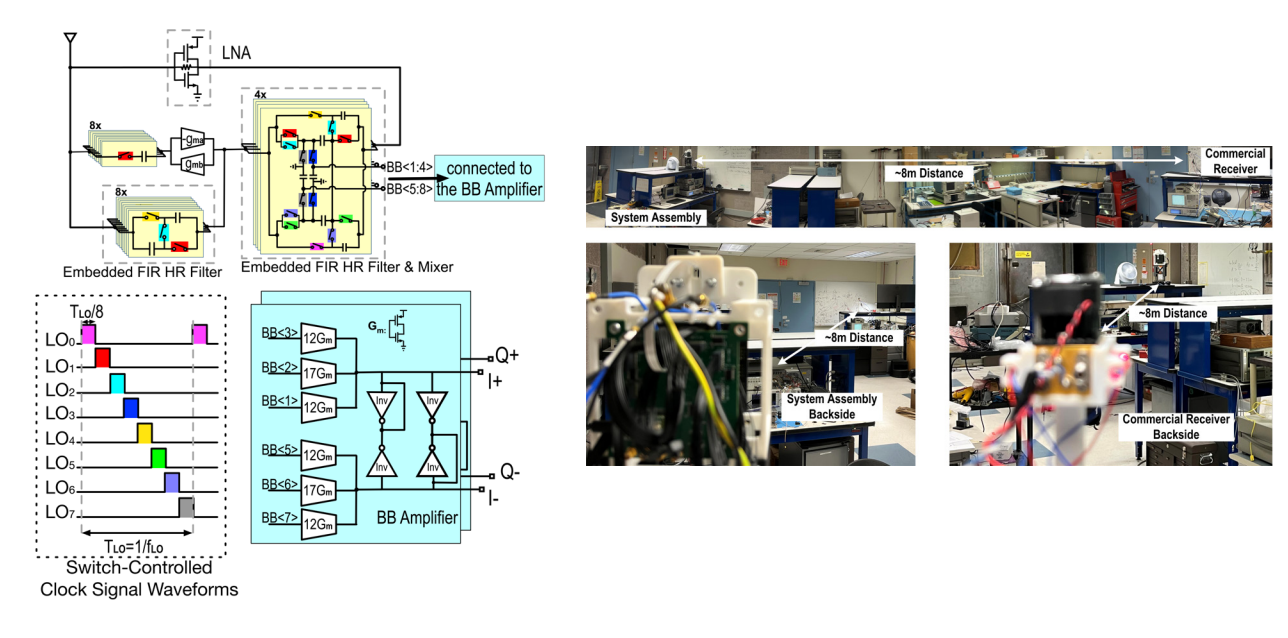
This work contributes to the development of AI-driven electronic design automation (EDA) tools and highlights the role of exploration in program synthesis. Our method offers a scalable and generalizable framework that can be extended to other hardware description language domains or integrated into existing EDA pipelines for agile hardware design.

Highly Selective Harmonic-resilient Sub-6G Front Ends

H. Yang, S. Araei, M. Barzgari, N. Reiskarimian

Widely tunable and reconfigurable front ends are heavily in demand to support multi-band communication, such as the Internet of Everything. Recent developments have shown increased radio selectivity to improve linearity performance with respect to interference in the adjacent channel. One of the crucial features required for a widely tunable receiver is the ability to suppress harmonic blockers efficiently and at the earliest opportunity, because powerful harmonic blockers can saturate the front end early in the chain before being rejected, hindering receiver functionality. We have proposed a highly selective sub-6GHz reconfigurable receiver resilient to both harmonic blockers and close-in blockers, achieving a 40dB/decade filtering along with >10 dB 3rd/5th order harmonic rejection directly at the antenna input, a radio frequency (RF) bandwidth of 100 MHz, a +15dBm out-of-band (OOB)

third-order intercept point (IIP3) at the frequency twice of the RF bandwidth, and a -3dBm OOB blocker 1-dB compression point (B1dB). The proposed receiver includes a single-stage low-noise amplifier (LNA) crossed by a high-order feedback composed of a gyrator, N-path filters, and mixers, followed by samplers to extract the baseband signal and single-stage baseband amplifiers to realize the I/Q recombination. Harmonic-rejecting mixers previously proposed by our group are added across the LNA, as a built-in structure to generate transmission zeros in the high-order feedback and simultaneously achieve harmonic resonance. The proposed design, to be taped out in 65-nm complementary metal-oxide-semiconductor technology, showcases a novel approach that simultaneously rejects closein and harmonic blockers.



▲ Figure 1: Architecture of the Proposed RX.

▲ Figure 2: Conversion Gain.

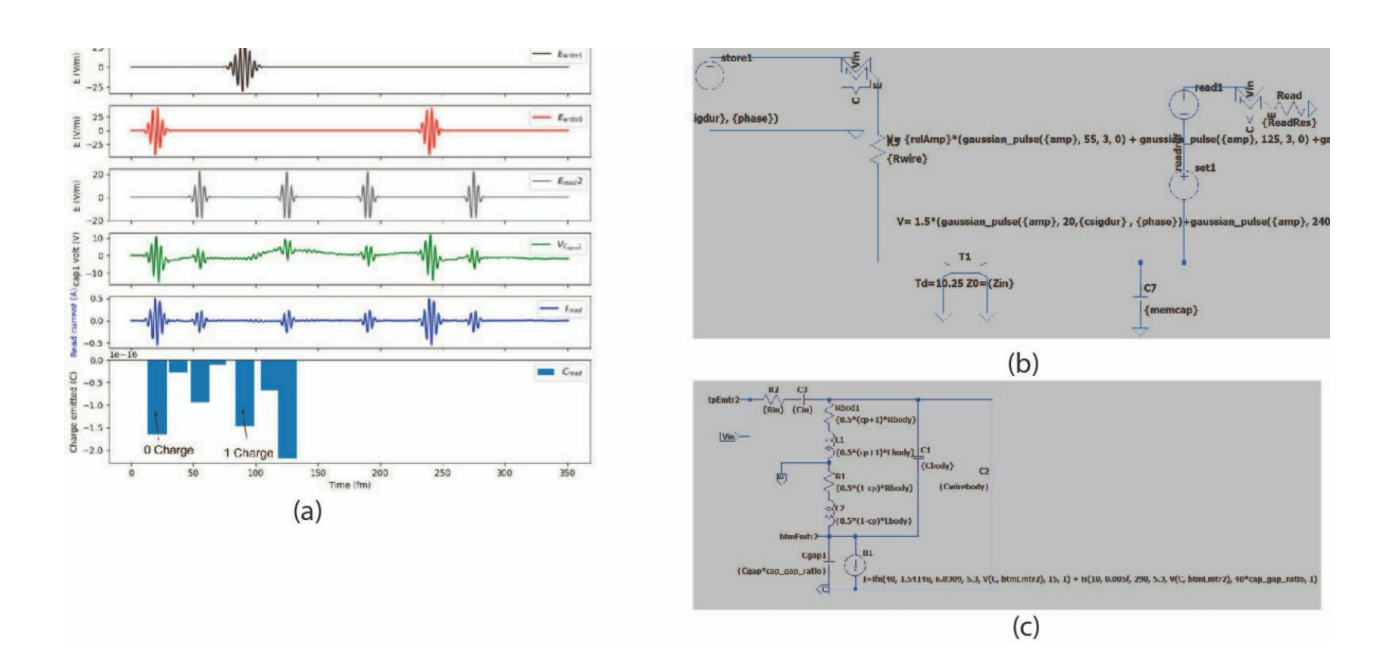
FURTHER READING

• S. Araei, S. Mohin, and N. Reiskarimian, "5.2 0.25-to-4GHz Harmonic-Resilient Receiver with Built-In HR at Antenna and BB Achieving +14/+16.5dBm 3rd/5th IB Harmonic B1dB," 2024 IEEE International Solid-State Circuits Conference (ISSCC).

Defining and Optimizing Write/Clear Margin for a Nanoantenna-Based Petahertz Electronic Memory Cell

A. Chen, A. R. Bechhofer, J. Simonaitis, F. Ritzowsky, K. K. Berggren, P. D. Keathley Sponsorship: MIT UROP, NSF, AFOSR

Nanoantennas leverage the unique properties of metallic nanostructures to enable tunneling of low-voltage currents. The compact and integrable design of the nanoantennas makes them a promising approach for realizing ultrafast electronic components. It is possible to construct complex structures using these nanoantennas. One possible structure is a memory cell. In this study, SPICE circuit models will be employed to explore and optimize various parameters, such as input intensity and input signal frequency, in an operational nanoantenna-based memory cell. Performance metrics will be defined and numerical techniques will be applied to refine these parameters, ensuring a robust and clear distinction between the 'write' and 'clear' states for reliable memory cell performance. Modelling the nanoantenna as a circuit component would take significantly less time than traditional physical simulations.



▲ Figure 1: The current model of the nanoantenna has indistinguishable write 1/0 as can be seen from (a). A simplified model of the nanoantenna component (b) can be used to create memory cells (c).

Memory-Efficient Gaussian Mapping on Micro-Robots: Algorithm and Chip

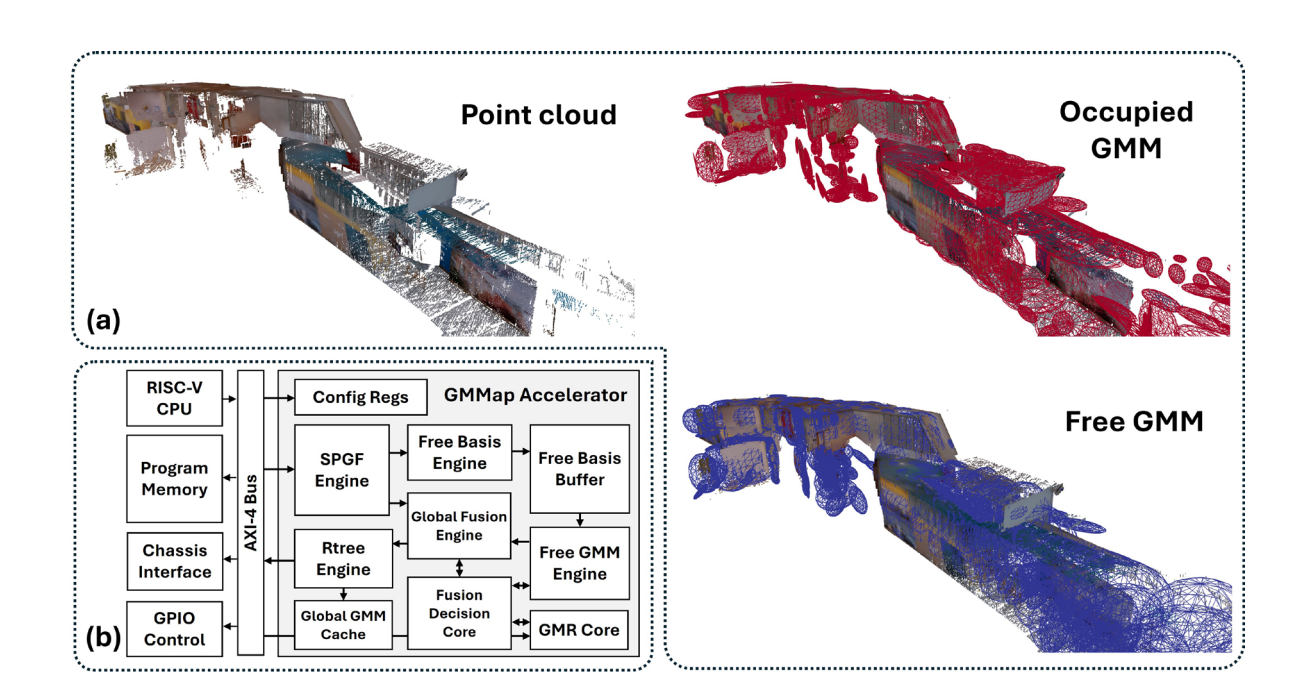
P. Z. X. Li, Z. S. Fu, K. Gupta, S. Karaman, V. Sze Sponsorship: Amazon, MathWorks Fellowship, National Science Foundation CPS

Constructing a compact map of 3D environments in real-time is essential for enabling autonomy on energy-constrained robots. During construction, the memory usage is not limited to map storage, but also includes overheads for storing the sensor measurements and temporary variables. Prior works reduce the map size while incurring a large memory overhead (MBs) which increases energy consumption and limits throughput.

To reduce memory and energy, we present GMMap, a memory-efficient algorithm that compresses each depth image into Gaussians which are directly fused across multiple images to form a compact 3D map. Using a low-power ARM Cortex-A57 CPU, GMMap can

be constructed in real-time with comparable accuracy as prior works while reducing the map size by at least 56%, memory overhead by at least 88%, and energy by at least 69%.

To further reduce energy, we present LEANC, a System-On-Chip with an accelerator for GMMap. On an FPGA, LEANC enables real-time 3D mapping using only milliwatts of power. Thus, LEANC not only enables autonomy on micro-robots but also illustrates the importance of memory-efficient algorithms and specialized hardware design for low-energy applications.



▲ Figure 1: (a) Visualization of the first floor of Stata Center, MIT, and its GMMap representation consisting of Gaussians representing occupied (red) and free (blue) regions. Each Gaussian is visualized as an ellipsoid in 3-D. (b) Hardware architecture of LEANC.

Design and Modeling of High Temperature Gallium Nitride RF Amplifiers

A. Goodnight, J. Niroula, M. Taylor, P. Yadav, T. Palacios Sponsorship: AFOSR (Grant No. FA9550-22-1-0367), NSF Graduate Research Fellowship

High temperature electronics play an important role in many applications such as space exploration, hypersonic flight, geothermal energy, and automotive industry. However, an RF circuit operating at 500°C has never been demonstrated, which, in part, is due to a lack of sufficient high temperature device modeling and process design kits (PDKs). Such frameworks are critical in designing robust circuits with high first pass yield as they enable accurate estimations of circuit performance and allow exploration of design space parameters.

Over the last couple years, our group has been developing and exercising a CAD framework of gallium

nitride technologies [1]. In this work, we expand upon this modeling effort, exploring the design space of high temperature GaN RF HEMTs. We use the MIT Virtual Source GaN FET (MVSG) model to predict the influence of temperatures from a wide temperature range on the electrical and RF device performance. Based on this model, we are developing a PDK for design optimization within industry-standard CAD tools such as Keysight ADS and Cadence. These device characterizations can then be used to investigate different amplifier topologies with a focus on the output power, efficiency, and linearity operating over a wide temperature range from 25°C to 500°C.

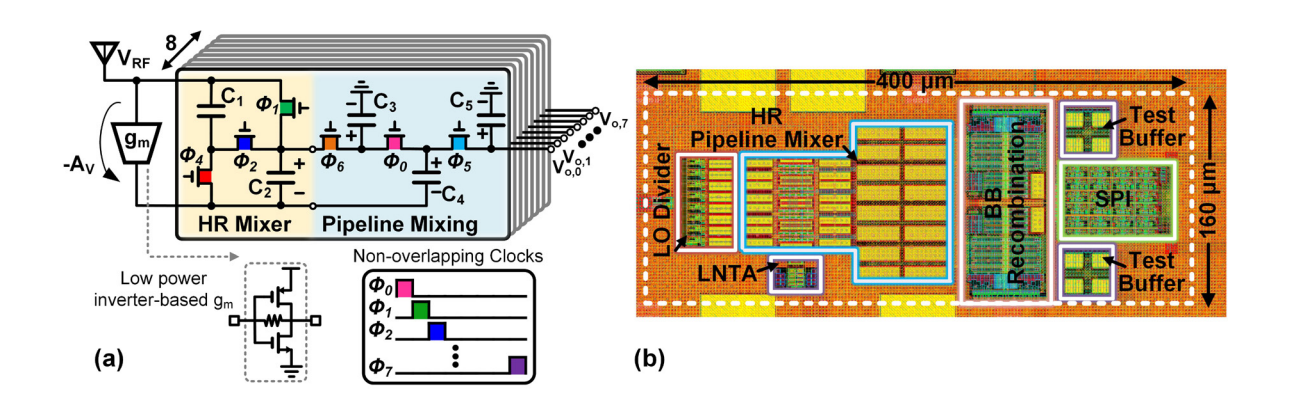
Q. Xie et al., "Towards DTCO in High Temperature GaN-on-Si Technology: Arithmetic Logic Unit at 300°C and CAD Framework up to 500°C,"
 2023 IEEE Symposium on VLSI Technology and Circuits (VLSI Technology and Circuits), Kyoto, Japan, 2023, pp. 1-2.

Harmonic-Resilient Low-Power Receiver Architecture with Pipeline Mixing for IoT Applications

S. Araei, M. Barzgari, N. Reiskarimian

The rapid growth of Internet of Things (IoT) applications in wearable devices, smart homes, and healthcare demands receivers (RXs) that integrate seamlessly into this expanding network. Achieving low power consumption, high linearity, and wide tunability is crucial for efficient operation in the congested sub-7GHz frequency band. In this work, we present an RX topology tailored for IoT needs, featuring a harmonic-resilient N-path filter embedded within negative feedback to provide robust blocker protection for all active cir-

cuits. By leveraging the Miller effect, the proposed RX achieves a reduced capacitor area and minimal dynamic power consumption. Furthermore, the use of pipeline down-mixing eliminates the need for power-hungry baseband amplifiers, enabling passive gain in a low-noise manner. This RX topology consumes sub-mW power, relies solely on switches and capacitors, and is highly scalable, making it an ideal choice for battery-operated IoT devices.



▲ Figure 1: (a) Block diagram of the proposed architecture (b) Chip Layout.

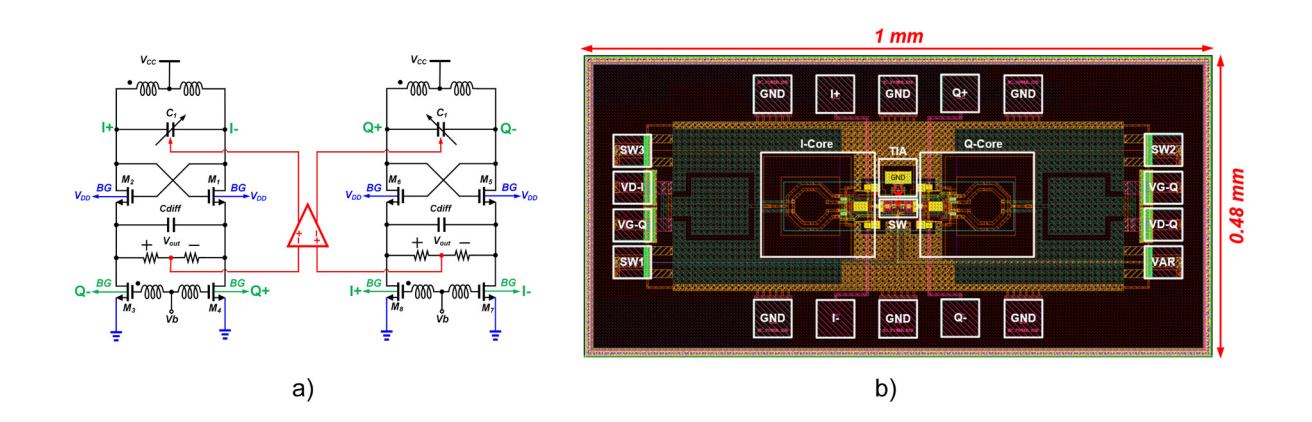
A 28 GHz Coupled PLL-Based CMOS Quadrature Oscillator

M. Barzgari, S. Araei, H. Yang, N. Reiskarimian

One of the most critical challenges in RF and mm-wave transceivers for the further development of wireless communications is generating quadrature signals for receiver down-conversion. Quadrature voltage-controlled oscillators are among the most promising candidates for 5G/6G frequency bands due to their lower power consumption and reduced area. However, achieving a higher Figure-of-Merit (FoM) for the oscillator while maintaining perfect quadrature accuracy remains a significant challenge.

In this work, a coupled PLL-based approach for

generating quadrature signals at the local oscillator (LO) is implemented and fabricated using 22nm fully depleted silicon-on-insulator (FDSOI) CMOS technology. In this approach, each oscillator serves as a reference for the other, and the entire structure functions as a type-II phase-locked loop (PLL). This topology relaxes the trade-off between phase noise and quadrature accuracy while achieving a high FoM. It not only improves the image rejection ratio in mmwave transceivers but also enhances overall system efficiency.



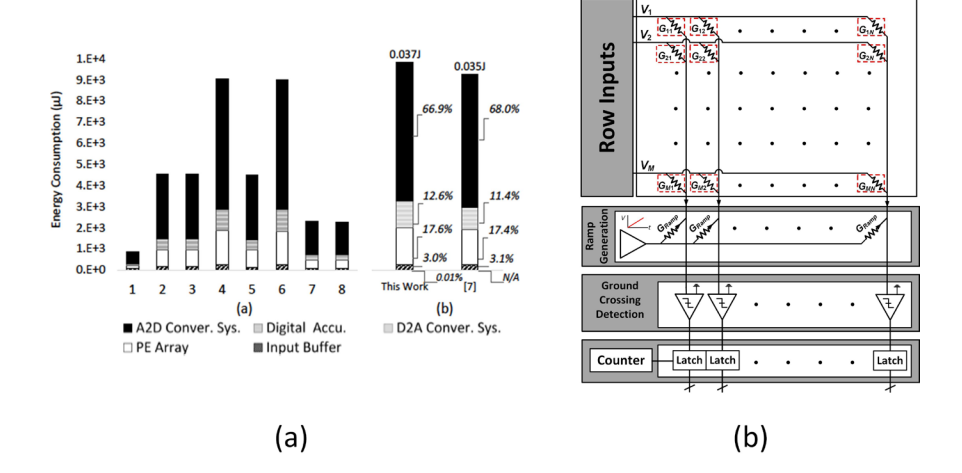
▲ Figure 1: (a) Simplified schematic and (b) Chip Micrograph.

Interface Circuits for Analog In-Memory Computing

M. A. G. Elsheikh, H.-S. Lee Sponsorship: MIT/MTL Samsung Semiconductor Research Fund

The increased adoption of machine learning (ML) in mobile devices demands high performance at low energy consumption. General purpose hardware is limited in speed and efficiency by the data movement between the memory and the processing unit. Alternatively, compute-in-memory (CIM) accelerators perform the required arithmetic by the integration of memory and processing elements to mitigate this problem. Analog CIM accelerators use voltage and current laws for the parallel generation and addition of partial sums, rapid-

ly and efficiently. However, the read-out circuitry poses a substantial overhead in energy consumption. In this work, we propose single-slope an analog-to-digital converter with non-linear characteristics, which maintains the inference accuracy at a reduced number of bits, to leverage the statistical properties of partial sum outputs to optimize performance and efficiency. This will enable more widespread adoption of ML in more energy-constrained applications.



▲ Figure 1: (a) Energy breakdown in analog CIM systems (b) proposed single-slope analog to digital converter readout circuits for analog CIM.

An Analog Front End with Sparse-Image Capturing for Energy-Efficient Bladder Ultrasound Imaging

M. Manohara, S. Schoen, D. U. Yildirim, M. Perrot, P. Garcha, A. Samir, A. Bahai, A. P. Chandrakasan Sponsorship: Texas Instruments

Continuous bladder monitoring is important for patients unable to excrete their urine. One method for bladder volume calculation is capturing ultrasound images and utilizing image segmentation algorithms for bladder volume estimation. These algorithms typically search for the boundary of the bladder and ignore other regions of the image. In this work, we design an analog front end (AFE) utilizing an algorithm called Power Gating for Intra-Image Sparsity (PGIIS). This AFE simultaneously generates beamformed TX pulses

and amplifies the RX signals with good signal-to-noise ratio. For each TX event, the PGIIS algorithm identifies time intervals corresponding to the bladder boundary and power-gates the RX amplifiers outside of these time intervals, generating a sparse image. The AFE was tested on a custom phantom with a bladder proxy. After calibration, the PGIIS algorithm demonstrated 75% power savings in RX amplification, enabling low-power imaging suitable for wearable ultrasound systems.

General Purpose Ultrasound Imaging Continuous Bladder Fetus Ultrasound Image Monitoring Beam Scanned Every feature Capture all image features Constant Power Consumption Low battery life Bladder Application Specific Ultrasound + PGIIS Wearable Bladder Ultrasound Image Ultrasound **VDD** Device Power $t_1 t_2 t_3 t_4$ Gate Beam Scanned · Enables continuous measurement of bladder Border is the most volume for patients important High battery life desired so patients do not need to feature swap the device often Only capture necessary features RX power consumption greatly reduced

▲ Figure 1: Motivation for continuous bladder monitoring and motivation behind Power-Gating for Intra Image Sparsity algorithm

A 232-to-260GHz CMOS Amplifier-Multiplier Chain with a Matching-Sheet-Assisted Radiation Package and 11.1dBm Total Radiated Power

J. Wang, R. Han

Sponsorship: Intel University Shuttle Program, Jet Propulsion Laboratory Strategic University Research Partnerships Program

Terahertz (THz) signal sources and radiators are essential for a variety of future applications, such as high-resolution radar imaging, molecular spectroscopy, and clocks, as well as high-speed or miniature-platform communications. For over a decade, the growing interest in complementary metal-oxide semiconductor (CMOS) compact THz radiation sources has been driven by their small form factor and integration with other analog/digital systems. However, the total radiated power of prior CMOS THz sources was still only several mW, not only due to the limited fmax and breakdown voltages of the CMOS transistors, but also due to the inefficient on-chip radiation approaches. Due to the large dielectric constant contrast between the silicon and air, the radiated waves undergo strong reflection at the sil-

icon-air interface, and with a small outward angle, total internal reflection occurs. To alleviate this problem, cm-sized, high-resistivity silicon lenses affixed to the chip back have been used. However, they dramatically increase the cost and size of the overall assembly. In this work, we introduce a CMOS THz amplifier-multiplier chain array generating radiation between 232 and 260GHz. Instead of using a silicon lens, a patterned dielectric matching sheet is applied onto the flipped-chip back, which enhances the wave coupling from silicon to air and enables low-cost and planar packages. That, in conjunction with broadband gain-peaking power amplifiers built with a high-power radio frequency FinFET transistor technology in the CMOS process, enables a measured peak total radiated power of 11.1dBm.

Efficientvit-SAM: Accelerated Segment Anything Model without Performance Loss

Z. Zhang, H. Cai, S. Han Sponsorship: National Science Foundation, MIT-IBM Watson AI Lab, MIT AI Hardware Program, Amazon, Samsung, Hyundai

Segment Anything Model (SAM) has gained widespread recognition as a milestone in the field of computer vision, showcasing its exceptional performance and generalization in image segmentation. SAM defines image segmentation as a promptable task, that aims to generate a valid segmentation mask given any segmentation prompt. SAM has shown its high versatility in a wide range of downstream applications, including image in-painting, object tracking, and 3D generation. Nevertheless, SAM imposes significant computational costs, leading to high latency that restricts its practicality in time-sensitive scenarios and edge devices. In particular, SAM's main computation bottleneck is its image encoder, which requires 2973 GMACs per image at the inference time. To accelerate SAM, numerous efforts (MobileSAM, EdgeSAM, EfficientSAM) have been made to replace SAM's image encoder with lightweight models. While these methods reduce the computation cost, they all suffer from significant performance drops. We introduce EfficientViT-SAM to address this limitation by leveraging EfficientViT to replace SAM's image encoder. Meanwhile, we retain the lightweight prompt encoder and mask decoder architecture from SAM. Our training process consists of two phases. First, we train the image encoder of EfficientViT-SAM using SAM's image encoder as the teacher. Second, we train EfficientViT-SAM end-to-end on the whole SA-1B dataset. We thoroughly evaluate EfficientViT-SAM on a series of zero-shot benchmarks. EfficientViT-SAM provides a significant performance/efficiency boost over all prior SAM models. In particular, on the COCO dataset, EfficientViT-SAM achieves 48.9× higher throughput on A100 GPU without mAP drop compared with SAM-ViT-H. We believe that EfficientViT-SAM enables the segment anything technique to be widely applied in time-sensitive scenarios, such as autonomous driving and robotic manipulation, while also making it easily deployable on edge devices like mobile phones.

Electronic, Magnetic & Spintronic Devices

| Magnetically Modulated Electrical Switching in an Antiferromagnetic MOSFET | |
|--|----|
| Frequency-dependent Wake-up in Ferroelectric Hf _{0.5} Zr _{0.5} O ₂ Devices | 28 |
| Towards 65-GHz Capacitance-voltage Characterization of Ferroelectric $\mathrm{Hf_{0.5}Zr_{0.5}O_{2}}$ | 29 |
| Direct van der Waals Integration of 2D Materials for High-performance Chemical Sensors | 30 |
| 3D-integrated Circuits in GaN/Si CMOS/Glass for High-frequency, High-data-rate Applications | 31 |
| Dipole-Engineered Contacts to Two-Dimensional Semiconductors | 32 |
| Electrical-controlled Magnetism in Rhombohedral Graphene | 33 |
| Materials Study of Flip-Processed Nitrogen-Polar GaN HEMTs | 34 |
| High Temperature RF GaN Electronics. | 35 |
| Gate Stack Design of p-GaN Gate GaN High Electron Mobility Transistors | 36 |
| Singlet Fission Sensitized Planar Silicon Solar Cells | 37 |
| Photon-Assisted Quantum Tunneling in Two-Dimensional Nil2/hBN Heterostructures | 38 |
| Systematic Study of Dielectric Materials for GaN MISHEMTs | 39 |
| High-performance Multi-channel ${ m MoS}_2$ Transistors for Front-end-of-line Integration Beyond 1 nm Node | 40 |
| AFM-Based Alignment of MATBG with hBN | 41 |
| Non-Toxic Solvent System for Ubiquitous Coatings of Perovskite Solar Cells | 42 |
| Towards a Ferroelectric High Electron Mobility Transistor for Memory Applications | 43 |
| Anomalous Hall Effect and Superconductivity in BN-aligned Magic-angle Twisted Bilayer Graphene | 44 |

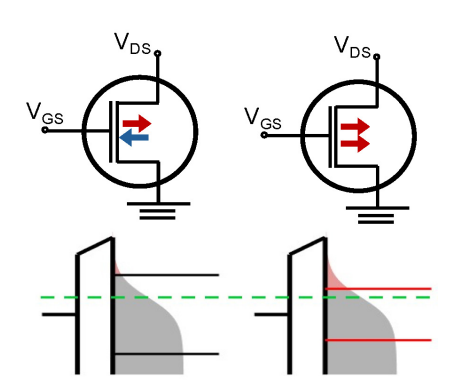
Magnetically Modulated Electrical Switching in an Antiferromagnetic MOSFET

C.-T. Chou, E. Park, J. Ingla-Aynes, J. Klein, K. Mosina, J. S. Moodera, Z. Sofer, F. M. Ross, L. Liu Sponsorship: SRC, Defense Advanced Research Projects Agency, NSF

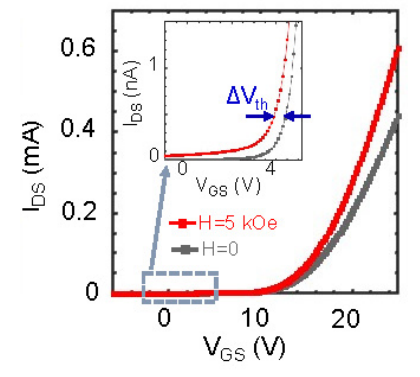
The metal-oxide-semiconductor field-effect transistor (MOSFET) is a foundational component of modern electronics, relying on electric fields to control charge flow in a semiconductor. Spintronic devices, in contrast, leverage the electron's spin to enable new functionalities like non-volatile memory and logic. A long-standing goal in spintronics has been to integrate spin control into transistors, enabling spin-based switching to enhance performance and reduce energy consumption. While concepts like the Datta-Das spin transistor offer promising designs, practical realization has been hindered by challenges in spin injection, detection, and maintaining coherence—making high-performance, locally integrated spin transistors difficult to achieve.

In this work, we study a magnetic MOSFET using CrSBr, a van der Waals (vdW) antiferro-magnetic semiconductor, as the channel material. Many two-dimensional vdW magnetic semiconductors exhibit moderate bandgaps and weak interlayer antiferromagnetic coupling, enabling magnetic

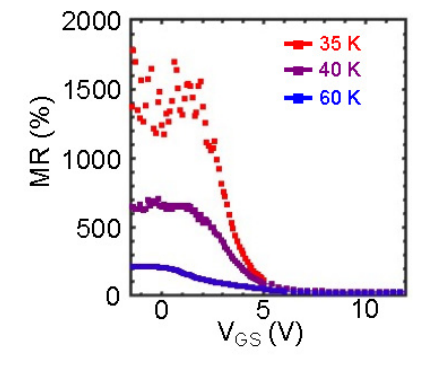
transitions such as spin-flip and spin-flop under external stimuli. These transitions not only alter magnetic states but can also modify the electronic band structure via exchange interactions between local magnetic moments and conduction electrons. As adjacent layers switch from antiparallel to parallel alignment, interlayer spin-dependent hopping becomes allowed, significantly reducing the bandgap and altering carrier concentration. We show that both gate voltage and magnetic transitions modulate the channel current, achieving an ON/OFF ratio over 106 and magnetoresistance (MR) up to ~1500% at 35 K. Modeling reveals that spin-flip transitions drive significant carrier density changes, enabling strong magnetic tunability of channel conductance—beyond conventional MR mechanisms. Furthermore, by analyzing transport signatures alongside magnetic transitions, we demonstrate the potential of this magnetic MOSFET platform to distinguish interfacial magnetic switching from bulk effects.



 \blacktriangle Figure 1: Schematics of magnetic MOSFET in parallel (right) and antiparallel (left) magnetic states. Parallel state results in smaller band gap, thus increasing carrier density.



 \blacktriangle Figure 2: $I_{\rm D}$ vs. $V_{\rm G}$ curves of magnetic MOSFET in antiparallel (gray) and parallel (red) states. Clear shift of subthreshold voltage $\Delta V_{\rm th}$ is observed.



■ Figure 3: MR of magnetic MOSFET vs. gate voltage and temperature. Gate-voltage-dependent MR with large MR plateau in subthreshold regime are consistent with theoretical calculations.

FURTHER READING

• C.-T. Chou, et al., "Magnetically Modulated Electrical Switching in an Antiferromagnetic Transistor," arXiv preprint arXiv: 2505.09019 (2025).

Frequency-dependent Wake-up in Ferroelectric Hf_{0.5}Zr_{0.5}O₂ Devices

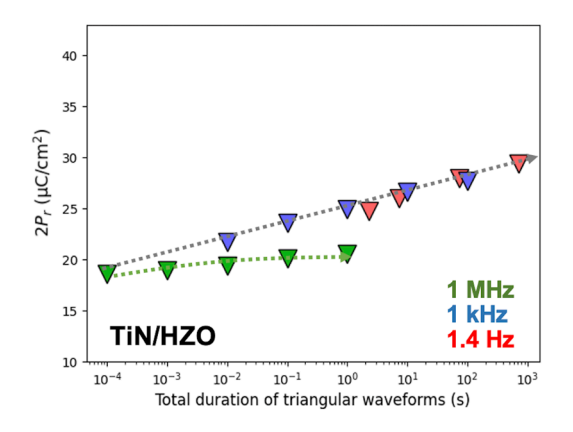
T. E. Espedal, Y. Shao, J. C-C. Huang, E. R. Borujeny, D. A. Antoniadis, J. A. del Alamo Sponsorship: MIT Undergraduate Research Opportunity Program, SRC, MIT AI Hardware Program

Among non-volatile memory technologies, ferroelectric (FE) memory based on com-plementary metal-oxide-semiconductor-compatible $\mathrm{Hf_{0.5}Zr_{0.5}O_2}$ (HZO) has emerged as a promising one due to its potential for low-voltage, fast switching, long data retention, and high memory endurance. A drawback of this technology is the need for device "wake-up." Typically, >10³ voltage cycles are required to sufficient wake-up metal-FE-metal (MFM) capacitors, while FE transistors usually wake up after a single direct current (DC) sweep, typically taking a few seconds. The frequency dependence of wake-up cycling is a poorly understood phenomenon, but it has great relevance for device performance and reliability.

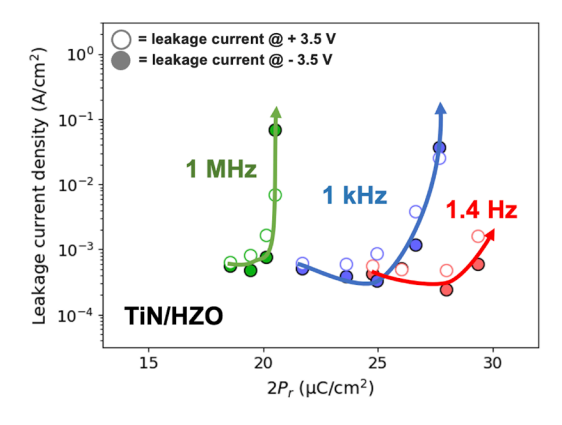
In this work, we study the frequency-dependent wake-up behavior of 30x30µm TiN- and W-based FE-HZO capacitors. We apply repeated triangular voltage cycles at frequencies between 1.4 Hz and

1 MHz, monitoring polarization-voltage (P-V) and quasi-static DC current-voltage characteristics. We find a reproducible frequency depend-ence of P-V characteristics after some N wake-up cycles, a result which has not been reported thus far. We also find that high-frequency cycling leads to ineffective wake-up, likely due to domain pinning through high-voltage-induced defect generation.

Furthermore, we observe leakage current degradation upon repeated cycling that appears to be primarily determined by N rather than the total stress time. This contrasts with the wake-up behavior associated with increasing remanent polarization $(2P_r)$ shown in Figure 1. This result evidences wake-up (increasing $2P_r$ early in device life) and device breakdown (observed in an upturn in leakage current, as shown in Figure 2) as distinct physical phenomena taking place within the HZO thin film.



ightharpoonup Figure 1: Frequency-dependence of $2P_r$ over total duration of applied triangular waveforms, measured in capacitors with TiN elec-trodes.



ightharpoonup Figure 2: Evolution of leakage current density and $2P_r$ with repeated cycling for TiN-electrode capacitors.

Y. Shao, E. R. Borujeny, J. N. Fidalgo, J. C-C. Huang, T. E. Espedal, D. A. Antoniadis, and J. A. del Alamo. "Discrete Ferroelectric Polarization Switching in Nanoscale Oxide-Channel Ferroelectric Field-Effect Transistors," Nano Letts. 2025.

T. E. Espedal, Y. Shao, J. C-C. Huang, E. R. Borujeny, D. A. Antoniadis, J. A. del Ala-mo, "Frequency-Dependent Wake-Up in Ferroelectric Hf_{0.x}Zr_{0.5}O₂ Devices," to be presented at *Devices Research Conference (DRC)*, Durham, NC, Jun. 2025.

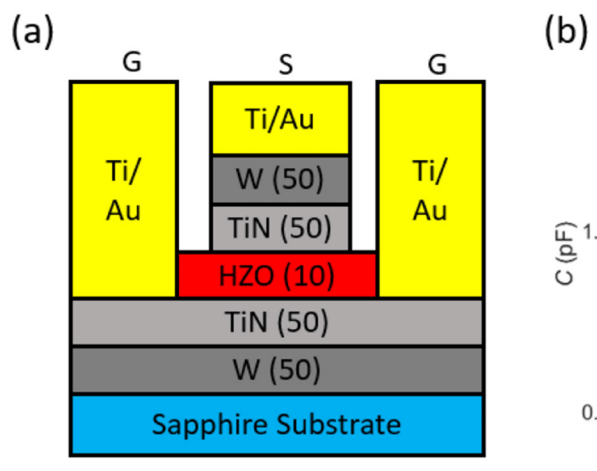
Towards 65-GHz Capacitance-voltage Characterization of Ferroelectric Hf_{0.5}Zr_{0.5}O₂

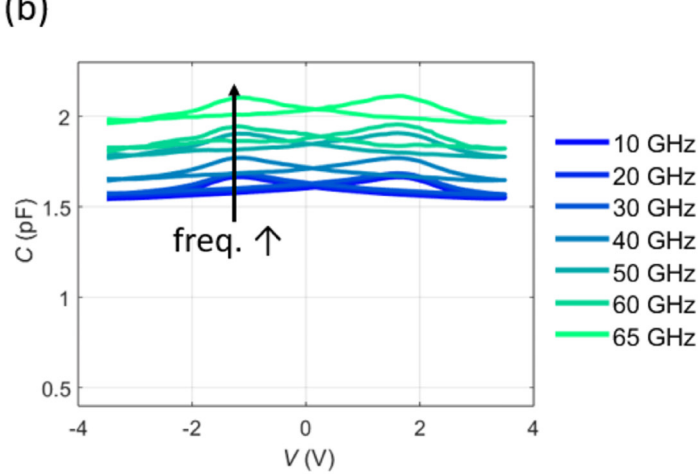
J. C.-C. Huang, Y. Shao, E. Borujeny, T. Espedal, H. Choi, J. Grajal, D. A. Antoniadis, J. A. del Alamo Sponsorship: SRC

Doped hafnia has emerged as a popular family of materials in the field of microelectronics because of its surprising ferroelectric (FE) properties and compatibility with complementary metal-oxide semiconductor fabrication process. Among various hafnia, $\mathrm{Hf_{0.5}Zr_{0.5}O_2}$ (HZO) stands out owing to its large remnant polarization and low coercive field, which is desirable for device applications. In such FE oxides, though the butterfly-like capacitance-voltage (CV) characteristic is a well-known phenomenon, its underlying physics has not been studied comprehensively. Our group has previously conducted CV characterization on HZO-based metal/FE/metal (MFM) capacitors across a broad frequency range up to 10 GHz, providing insights into the impact of defect dynamics in these devices.

In this study, we aim to extend the frequency range of CV characterization up to 65 GHz on HZO-

based MFM structures built on impedance-matched coplanar waveguide structures. Our results highlight the significant influence of the intrinsic inductance of the coplanar waveguide on accurate capacitance extraction. Through the application of several de-embedding approaches, we demonstrate that the CV characteristics exhibit minimal frequency dependence across the GHz range, remaining stable up to approximately 40 GHz. More importantly, the butterfly-like feature of the CV curve persists even at 65 GHz. These findings shed light on the defect dynamics and FE switching behavior in HZO-based devices and promise to advance the understanding of undesired phenomena such as wake-up and fatigue, underscoring their potential relevance in high-speed memory and radio-frequency circuit applications.





▲ Figure 1: Schematic diagram of a W/TiN/HZO/TiN/W coplanar waveguide device.

 \blacktriangle Figure 2: CV curves of W/TiN/HZO/TiN/W measured from 10 GHz to 65 GHz.

Y. Guo, Y. Lin, K. Xie, B. Yuan, J. Zhu, P.-C. Shen, A.-Y. Lu, C. Su, et al., "Designing Artificial Two-dimensional Landscapes Via Atomic-layer Substitution," Proc. National Academy of Sciences, vol. 118, p. 32, 2021.

[•] J. Zhu, J.-H. Park, S. A. Vitale, W. Ge, G. S. Jung, J. Wang, M. Mohamed, T. Zhang, et al., "Low-thermal-budget Synthesis of Monolayer Molybdenum Disulfide for Silicon Back-end-of-line Integration on a 200 mm Platform," *Nature Nanotechnology*, vol. 18, pp. 456-463, 2023.

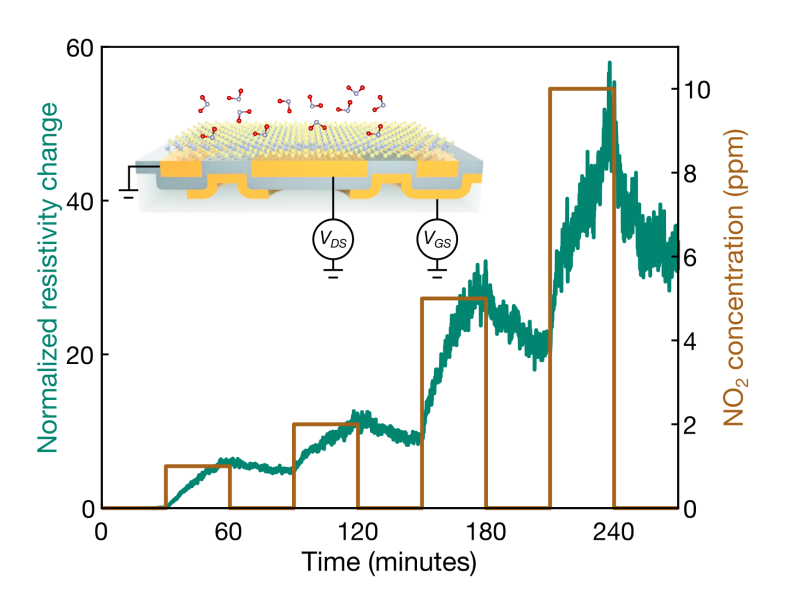
Direct van der Waals Integration of 2D Materials for High-performance Chemical Sensors

P. F. Satterthwaite, S. O. Spector, J. Song, F. Niroui Sponsorship: MathWorks, NSF Division of Civil, Mechanical and Manufacturing Innovation, 2135846

Two-dimensional (2D) materials have the potential to serve as a platform for the fabrication of high-performance chemical sensors. Their atomically thin nature results in high surface area-to-volume ratios, allowing for high-sensitivity, low-power devices. Furthermore, the existing library of 2D materials includes diverse chemical and electronic properties, providing opportunities for selective sensing of different analytes. However, performance of current devices can often be limited by fabrication and design artifacts. Thus, platforms that overcome these limitations are desired.

Van der Waals (vdW) integration, where layers are physically contacted and held together by vdW forces, presents an alternative approach that enables the realization of diverse heterostructures

with clean interfaces. Despite the clean interfaces, current vdW integration strategies typically result in encapsulated 2D materials where the top surface is not exposed for sensing applications. Using our newly developed adhesive matrix transfer platform, we have demonstrated direct integration of 2D materials into functional sensors. This allows for scalable, facile fabrication of 2D sensors with clean interfaces, in a design where the surface is fully exposed to maximize interaction with the analyte. The unique combination of these features enables high-performance chemical sensors, which we highlight by demonstrating a 50-fold enhancement in sensitivity of molybdenum disulfide-based sensors to nitrogen dioxide, a benchmark gas.



▲ Figure 1: Clean vdW integration for high-performance chemical sensors. Normalized change in resistance of an example device exposed to increasing concentrations of nitrogen dioxide. Inset shows schematic of fabricated device.

[•] P. F. Satterthwaite, W. Zhu, P. Jastrezebska-Perfect, M. Tang, S. O. Spector, H. Gao, H. Kitadai, A.-Y. Lu, et al., "Van der Waals Device Integration Beyond the Limits of van der Waals Forces using Adhesive Matrix Transfer," *Nature Electronics*, vol. 7, p. 17, 2024.

3D-integrated Circuits in GaN/Si CMOS/Glass for High-frequency, High-data-rate Applications

P. Yadav, J. Wang, D. Baig, X. Li, J. Pastrana, J. Niroula, M. Bakir, M. Swaminathan, R. Han, T. Palacios Sponsorship: SRC Joint University Microelectronics Program 2.0 and National Defense and Science Graduate Fellowship

Gallium nitride (GaN) transistors are enabling the next generation of high-efficiency, high-power, and high-frequency integrated circuits. Furthermore, demonstrations of low-voltage GaN radio frequency (RF) switches for front-end modules (FEM) and low-noise figures in GaN low-noise amplifiers (LNAs), are broadening the applications of GaN into the mobile, artificial intelligence (AI), and quantum sectors. But this excellent performance comes with a high cost, due to limited wafer sizes and back-end-of-line (BEOL) metallization options. On the other hand, a Si complementary metal-oxide-semiconductor (CMOS) allows access to state-of-the-art 300-mm BEOL and digital circuit design.

Revolutionizing GaN chip design requires a holistic approach through integration with Si CMOS. This work, through these two approaches, makes three-dimensional (3D) GaN chips design more cost-effective while providing orders of magnitude improvement

over convention 2D-circuits in Si or GaN-only frontend-of-line (FEOL). With the combination of Si CMOS digital, bias, and matching chips, high-frequency GaN dielets are integrated in a highly scaled manner through using direct Cu-Cu bonding for several 3D-amplifier first demonstrations. Such integration offers low RF losses as well as near-seamless-bonding interfaces. Similarly, glass offers a low-cost packaging option for multi-chiplet systems. Large substrate sizes and panel thickness down to 30 µm enable the next generation of packaging for nano-systems at scale, while also allowing for novel thermal cooling solutions such as microfluidic, two-phase vapor, etc. With the lamination of low-loss dielectric Ajinomoto build-up film (ABF) layers in glass, a highly capable package for 3D-RF stacking can be created. This work integrates GaN dielets directly in this glass package for the first time; it also studies and quantifies their properties.

Dipole-Engineered Contacts to Two-Dimensional Semiconductors

A. S. Gupta, J. Zhu, Y.-R. Peng, J. Kong, T. Palacios Sponsorship: Army Research Office

Power transistors for fast-switching, high-voltage applications require wide bandgaps to enable large breakdown fields. Emerging ultrawide-bandgap (UWBG) two-dimensional (2D) semiconductors such as hexagonal boron nitride (hBN) and 2D gallium nitride (GaN) have bandgaps above 5 eV and are expected to provide better performance than current WBG semiconductors thanks to their higher critical fields and atomic thinness. However, forming low-resistance contacts to UWBG 2D materials is challenging due to their extreme energy band misalignment with conventional metal contacts and the Fermi level pinning effect, which both contribute to large Schottky barrier heights (SBHs).

Here, we propose using dipoles to reduce the SBH. Inserting a material with an appropriate builtin electric field at the contact interface will enhance carrier injection from the metal to the 2D channel. In this work, we study contacts to ${\rm MoS}_2$ with ${\rm MoSSe}$, a so-called "Janus" 2D material, which has vertical asymmetry and therefore an inherent dipole. We demonstrate higher current density in Janus 2D material contacts than in conventional ${\rm MoS}_2$ contacts to bilayer ${\rm MoS}_2$ transistors, confirming the positive impact of dipole-tuned contacts. Future work will focus on contact materials with stronger dipoles, as well as wider bandgap channel materials such as hBN and 2D GaN. Overall, this work is a step towards forming ohmic contacts with WBG and UWBG 2D materials, thus enabling the next generation of power electronic devices with higher operation voltage as well as future integrated circuits with increased functionalities.

Electrical-Controlled Magnetism in Rhombohedral Graphene

E. Aitken, T. Han, Z. Lu, J. Yang, J. Seo, S. Ye, Z. Wu, M. Zhou, L. Ju

Magnetism typically arises from the alignment of electron spin, which can only be indirectly influenced by an electric field. In contrast, orbital magnetism can be directly controlled by an electric field, enabling faster and more energy-efficient operation. Rhombohedral-stacked multilayer graphene, with its flat electronic bands and concentrated Berry curvature, facilitates the spontaneous ordering of electron orbital motion, resulting in a pure carbon-based orbital magnet. In this study, we investigate orbital magnetism in rhombohedral graphene by measuring the anomalous Hall effect, a Hall effect observed in the absence of an external magnetic field. By applying an out-of-plane magnetic field,

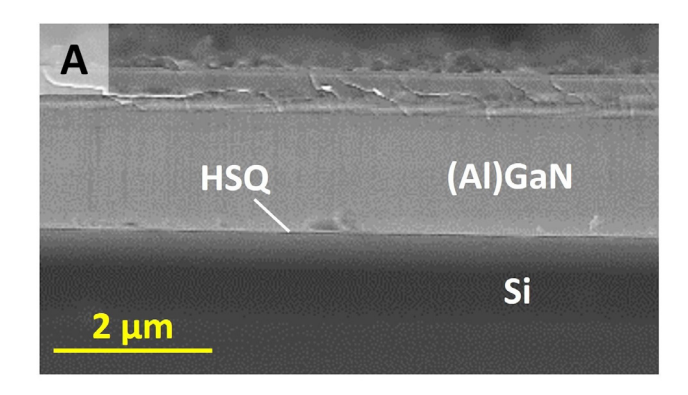
we observe a hysteretic Hall resistance loop, providing clear evidence of magnetic ordering. Given graphene's negligible spin-orbit coupling, this anomalous Hall effect must arise from the ordering of electron orbital motion. Remarkably, an out-of-plane electric field can effectively modulate the magnitude of the anomalous Hall effect and magnetic hysteresis loop, demonstrating the electric-field control of magnetism. This control arises from the coupling of the electric field to the electron wave function, underscoring the potential for fast, low-energy magnetic memory and computation applications.

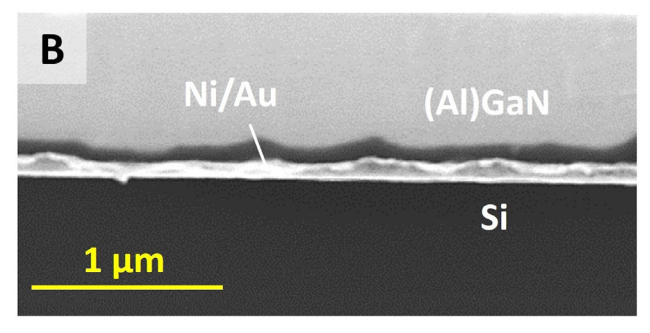
Materials Study of Flip-Processed Nitrogen-Polar GaN HEMTs

G. K. Micale, J. Niroula, P. Yadav, J. Hsia, H. Pal, Q. Xie, T. Palacios Sponsorship: SRC Jump 2.0 SUPREME

GaN high electron mobility transistors (HEMTs) are the leading technology for high-power and high-frequency applications thanks to the high breakdown voltages and high electron saturation velocity of GaN. Utilizing wafer bonding, flip processing, and Si substrate removal, we demonstrate a technology for making N-polar devices from Ga-polar GaN-on-Si heteroepitaxy, which provides the flexibility to create innovative gate designs for greater electrostatic control. Here we present an in-depth study of this technology and the resulting

N-polar AlGaN/GaN structure. Specifically, we investigate the adhesion between GaN and Si bonded with a hydrogen silsesquioxane (HSQ) interlayer and included back gate metal, looking at thermal compressive bonding variables and particle inclusions in the HSQ layer. Applying this technology for the fabrication of multichannel devices offers a path towards high current densities with superior gate control compared to previously demonstrated architectures.





▲ Figure 1: SEM cross-sections of (A) the bonding interface between the Ga-face GaN and the Si mechanical wafer, and (B) the bonding interface with the included Ni-Au gate metal.

High Temperature RF GaN Electronics

J. Niroula, M. Oh, M. Taylor, P. Yadav, Q. Xie, T. Palacios Sponsorship: AFOSR (Grant No. FA9550-22-1-0367)

High temperature electronics has received much interest recently due to emerging applications in geothermal well exploration, hypersonic flight electronics, and space exploration. GaN based devices are an exciting contender for extremely high temperature environments due to their high mobility, high saturation velocity, especially beyond 250°C, which is the limit of traditional silicon-based devices. In this project we aim to develop a high performing GaN based RF devices that operates at both room temperature as well as 500°C, by developing highly scaled, high temperature refractory tungsten T-gates with AlN gate dielectric that has record current density at 500°C. Such high temperature ready devices will allow high performing RF communication systems operating in the extreme conditions needed to enable the aforementioned applications.

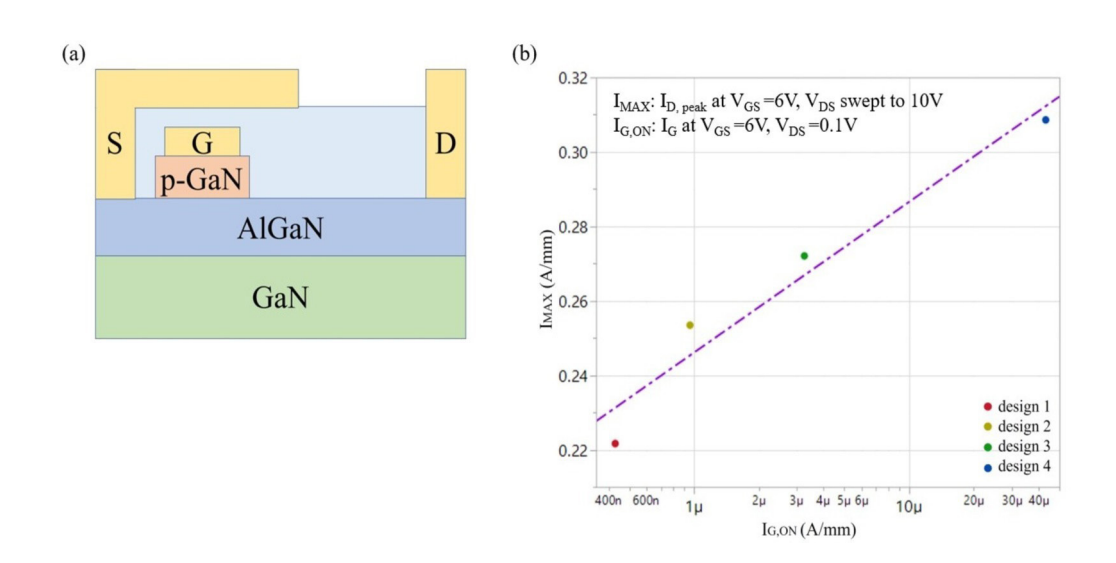
Gate Stack Design of p-GaN Gate GaN High Electron Mobility Transistors

Y. Yu, J. A. del Alamo Sponsorship: Texas Instruments

Gallium nitride (GaN) high electron mobility transistors (HEMTs) represent a breakthrough in semiconductor technology, offering superior high-frequency and high-power performance. However, reliability issues, particularly related to p-GaN gate designs, remain a challenge. This study investigates the impact of this design and fabrication on transistor performance, focusing on the trade-off between peak saturation drain current (I_{MAX}) and ON-state current ($I_{G,ON}$). Modest structural design and fabrication process changes have shown significant variations in I_{MAX} and $I_{G,ON}$, high-

lighting the need for strict process control.

In our work, we are carrying out extensive electrical characterization of prototype industrial transistors. In addition, we are performing Sentaurus TCAD simulations built to model such GaN HEMTs. By comparing experimental and simulated data, we aim to understand the dominant underlying physical mechanisms and refine predictive models for future GaN HEMT designs, ultimately improving device performance and reliability.



▲ Figure 1: (a) Cross-sectional view of p-GaN gate GaN HEMT (S is source, G is gate, D is drain), and (b) trade-off between I_{MAX} and $I_{G,ON}$ of prototype transistors from four differently-designed wafers.

Singlet Fission Sensitized Planar Silicon Solar Cells

J. Z. Wang, A. Li, K. Lee, N. Nagaya, M. A. Baldo Sponsorship: DOE Materials Chemistry Program (DE-FG02-377 07ER46454), NSF Graduate Research Fellowship (112237)

Integrating singlet fission materials with silicon solar cells presents a pathway to surpassing the Shockley-Quiesser power conversion efficiency limit for single-junction solar cells. Singlet fission is a spin-allowed process in which one high energy singlet exciton is converted into two lower energy triplet excitons. These triplet excitons can transfer to silicon in a solar cell, enabling external quantum efficiencies over 100% and increasing the photocurrent output for the same incident light. Previous work in our group demonstrated enhanced external quantum efficiency in devices employing tetracene as the singlet fission material and zinc phthalocyanine as a charge transfer layer on silicon microwire cells, a geometry optimized to reduce re-

flection losses. In this work, we focus on a planar silicon system to further study and optimize the interface between singlet fission materials and silicon for efficient triplet exciton transfer. We examine new singlet fission materials such as rubrene, which introduces an uphill triplet exciton transfer to silicon, as well as more stable tetracene derivatives. Another key consideration is silicon surface passivation: the oxide layer must be thick enough to reduce surface recombination losses but also thin enough to allow efficient triplet transfer from the singlet fission material. This study contributes insights into the interface engineering required to leverage singlet fission in planar silicon solar cells towards the development of high-efficiency photovoltaic devices.

Photon-Assisted Quantum Tunneling in Two-Dimensional Nil2/hBN Heterostructures

J. Li, R. Comin Sponsorship: NSF under Grant No. DMR-2405560

Quantum tunneling plays a fundamental role in modern physics and technology. Understanding the intricate relationships between quantum tunneling, light, and magnetic ordering expands the frontiers of quantum physics. Here, we demonstrate photon-assisted quantum tunneling in NiI2/hBN heterostructures in the two-dimensional material NiI2. Our measurements reveal a remarkable ten-fold enhancement in tunneling current through the junction at specific photon energies during the multiferroic phase (low-T) compared to the non-multiferroic phase (high-T).

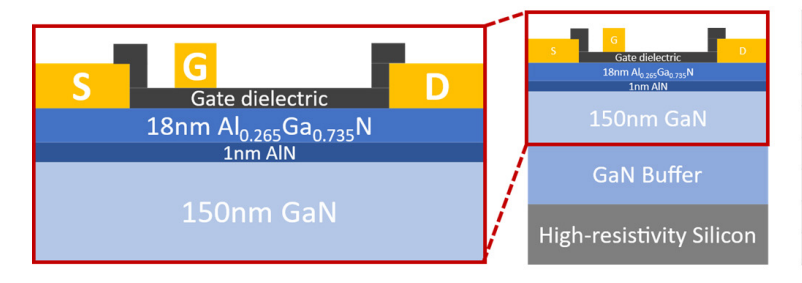
This phenomenon suggests a complex interplay between photonic excitation, multiferroic ordering, and electron tunneling dynamics. Our findings open new possibilities for controlling quantum tunneling through light-matter interactions in multiferroic systems, and paving the way for integration of photonic, spintronic, and electronic quantum devices.

Systematic Study of Dielectric Materials for GaN MISHEMTs

K. Limanta, T. Palacios Sponsorship: U. S. Army Research Office (ARO), AFOSR

Gallium nitride (GaN) heterojunction high-electron-mobility-transistors (HEMTs) are promising candidates for next-generation high-frequency and power electronics due to their superior performance characteristics. While Schottky-gate HEMTs are the current standard for lateral GaN transistors, metal-insulator-semiconductor HEMTs (MISHEMTs) are attractive due to their high on/off ratio and low gate leakage current. A comprehensive review of different insulators is necessary

to identify the optimal gate dielectric material for GaN MISHEMTs. In this study, we cover a wide range of insulators, including conventional oxides (SiO2, Al2O3), high-k dielectrics (HfO2, ZrO2), and nitrides (SiNx, AlN), comparing their impact on device characteristics such as gate leakage, threshold voltage shift, and interface quality. By fabricating and measuring hundreds of MISHEMTs, we can systematically evaluate the feasibility of these dielectrics for GaN MISHEMTs.



| Dielectric | Deposition technique | t _{ox} (nm) |
|--------------------------------|----------------------|----------------------|
| AIN | PEALD | 18 |
| SiN _x | PECVD | 18 |
| Al ₂ O ₃ | Thermal ALD | 15 |
| Al ₂ O ₃ | PEALD | 18 |
| SiO ₂ | PECVD | 18 |
| HfO ₂ | PEALD | 18 |
| ZrO ₂ | PEALD | 15 |

▲ Figure 1: Device diagram (enlarged on the left). Source and drain are alloyed metal contacts. Table: Deposition technique and thicknesses of gate dielectrics. PEALD – Plasma Enhanced Atomic Layer Deposition. PECVD – Plasma Enhanced Chemical Vapor Deposition.

High-performance Multi-channel MoS₂ Transistors for Front-end-of-line Integration Beyond 1 nm Node

A. Yao, J. Zhu, Y. Jiao, A. S. Gupta, J. Kong, T. Palacios Sponsorship: SRC Jump 2.0 SUPREME Center

Front-end-of-line (FEOL) integration of transistors based on two-dimensional (2D) materials, e.g., molybdenum disulfide (MoS₂), provide exciting opportunities for device scaling by leveraging the unique material properties of 2D materials, e.g., atomic channel thickness, large band gap, to ensure excellent gate modulation and minimum leakage. The advancements of two-dimensional (2D) materials-based microelectronics have sparked notable efforts for both industry and academic research of novel 2D front-end-of-line (FEOL) device structures such as Gate-All-Around (GAA), stacked nanosheets, multi-channel transistors (MCT), and multi-fin transistors. However, functional multi-channel transistors (2 or more channels) have not been demonstrated, and sacrificial layers (SALs) or suspended structures are also required in previous fabrication flows, which could lead to potential damage and contaminations and more complexity in the fabrication.

Here, we demonstrated double-gate, single-channel ${\rm MoS}_2$ transistors based on a novel reduced lithography step, low-temperature, high-quality ${\rm MoS}_2$ synthesis. These devices demonstrate a high on-current (${\rm I}_{\rm ON}$) of 386 ${\rm \mu A}/{\rm \mu m}$ at ${\rm V}_{\rm DS}$ =1 V, a subthreshold swing (SS) of 85 mV/dec and low drain-induced-barrier-lowering (DIBL) of 28 mV/V, showcasing record performance among 2D GAA transistors and MCTs. Additionally, we presented the first high-performance, functional 2-channel ${\rm MoS}_2$ transistor, which achieves 673 ${\rm \mu A}/{\rm \mu m}$ ${\rm I}_{\rm ON}$ and 88 mV/dec SS at a channel length (${\rm L}_{\rm ch}$) of 400 nm. Further with design-technology co-optimization (DTCO) analysis, our studies enable projections of 2D MCT scaling, addressing power and performance demands for the "1 nm" technology node and beyond.

AFM-Based Alignment of MATBG with hBN

D. Kumawat, S. Rao, T. Iwasaki, A. L. Sharpe, K. Watanabe, T. Taniguchi, P. Jarillo-Hererro Sponsorship: Department of Defense

In van der Waals heterostructures, two adjacent layers with similar lattice constants and a small angle alignment create a large length-scale moire pattern, changing periodically as the atoms modulate in and out of registry. When two moire patterns are overlaid, a larger supermoire can emerge. This supermoire pattern may be relevant in magic-angle twisted bilayer graphene (MATBG) aligned with hexagonal boron nitride (hBN), where it is possible to observe a quantum anomalous hall effect (QAHE) instead of the canonical superconducting phase [1, 2]. Recent theory papers suggest that quantization relies on the percolation of a well-defined non-zero Chern number throughout the sample, arising precisely when the two moire patterns are commensurate [3, 4]. However, crystal alignment between MATBG

and hBN layers at precise angles close to zero degrees is challenging, requiring the identification of crystallographic edges as armchair- or zigzag-type cleavages. We use lateral force microscopy (LFM) techniques to determine the crystal orientation with high precision. We then use torsional force microscopy (TFM) to analyze the supermoire formed by the moire patterns. By constructing devices with well-characterized stacks, we aim to connect the supermoire length scale back to stable Chern insulators in MATBG. Partially filled Chern insulator bands in such moire systems have been suggested to host fractional quasiparticles, which are candidate platforms for topological quantum computation.

41

Non-Toxic Solvent System for Ubiquitous Coatings of Perovskite Solar Cells

K. Yang, T. Kadosh, R. Swartwout, J. Mwaura, S. Lessler, R. Zhang, V. Bulović Sponsorship: Department of Energy Grant – ADDEPT Center

Perovskite Solar Cells (PSCs) have the potential to greatly disrupt the solar landscape due to their lightweight form factors as well as their simple manufacturing process. Bottom-up analysis performed on flexible PSC photovoltaics using Monte-Carlo simulation methods shows that, at scale, flexible perovskite modules cost \$0.19/W, compared to \$0.30/W/module for crystalline silicon. This reduction in cost also requires the lifetime of these modules to only be around 13 years to reach similar LCOE levels, which is in direct contrast with the 25 years required for silicon. From an industrial scalability perspective, the additional air handling costs required to keep toxic solvents under the governmental guidelines for permissible exposure levels increase exponentially with factory capacity. A recent internal study shows that the air handling costs for a DMF-based system, a commonly used solvent in perovskite manufacturing, would account for up to 12.3% of the overall module cost, whereas a less toxic alternative, THF, would only account for about 0.6% of the module cost. However, because the perovskite community has not settled on one particular architecture or deposition technique, it is advantageous to develop a perovskite ink which can be used ubiquitously across device designs. Therefore, in this project we developed a non-toxic solvent system for perovskite manufacturing which can be applied to both PIN and NIP architectures and two different thin film deposition techniques for the SnO₂ ETL in NIP. Thus far we have been able to demonstrate up to 15% power conversion efficiency (PCE) for the archetypical fully slot-die coated NIP stack and greater than 10% PCE for the slot-die coated PIN architecture and chemical bath deposited (CBD) SnO₂. These results demonstrate the first non-toxic ink able to be ubiquitously applied to three different solar cell stacks, and the first scalable demonstration of coating perovskite on an underlying layer grown by CBD.

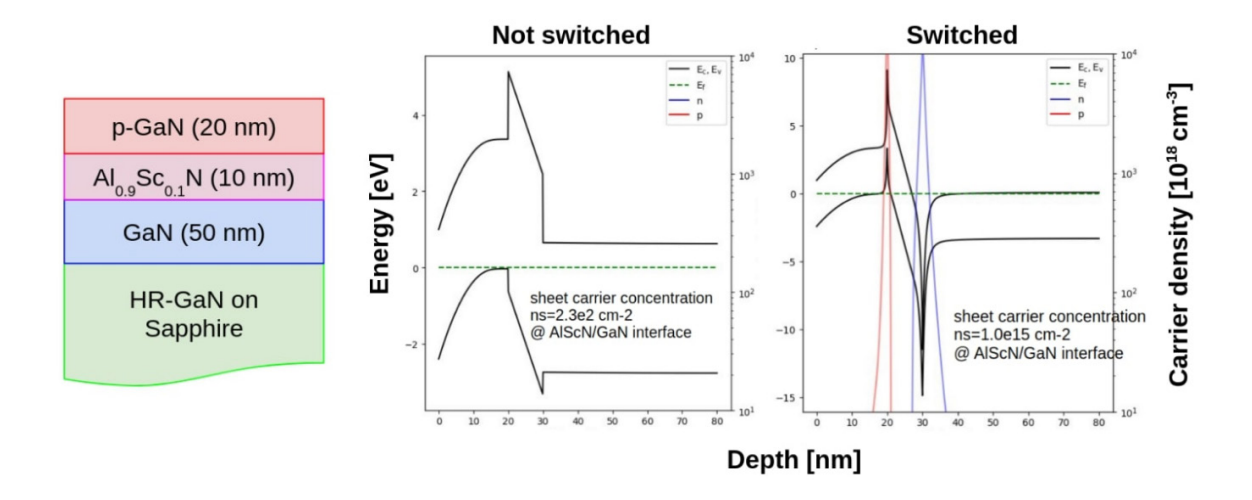
Towards a Ferroelectric High Electron Mobility Transistor for Memory Applications

L. Talli, D. Kang, J. Casamento

The development of ferroelectric high electron mobility transistors (FeHEMTs) presents a compelling pathway for memory applications. However, current demonstrated devices exhibit limited polarization switching capabilities, a critical feature for memory functionality. This challenge underscores the necessity for further advancements in FeHEMT design.

In this work, I used 1D Poisson simulation software to explore gate stack configurations suitable for a p-type FeHEMT (pFeHEMT) that depletes the

two-dimensional electron gas (2DEG) at zero bias. This design strategy aims to achieve an enhancement-mode (E-mode) FeHEMT device controllable by polarization switching, supporting memory-like operation. Following simulation, I attempted device fabrication, but encountered significant challenges with achieving robust ohmic contacts to the 2DEG and demonstrating reliable polarization switching. These issues highlight critical areas for future research.



▲ Figure 1: (a) Gate stack design. (b) 1D Poisson band structure simulation showing E-mode behavior and switching capability.

Anomalous Hall Effect and Superconductivity in BN-aligned Magic-angle Twisted Bilayer Graphene

S. V. Rao, A. L. Sharpe, T. Iwasaki, D. Kumawat, L. A. Benitez, K. Watanabe, T. Taniguchi, P. Jarillo-Herrero Sponsorship: Department of Defense

Magic-angle twisted bilayer graphene (MATBG) hosts many exotic electronic states due to its combination of strong electron-electron correlations and band topology. Results published in 2019 reveal that MATBG, when tuned to a charge carrier density of 3 electrons per moiré cell (v=+3), exhibits a quantum anomalous Hall effect, but not the canonical superconducting state typically observed near v=+2]. These results are likely explained by the added moiré potential of an aligned BN which breaks inversion symmetry, gapping the otherwise protected Dirac cones of MATBG.

Using atomic force microscopy-based techniques, we verify BN alignment in a MATBG heterostructure prior to device fabrication. Subsequent transport mea-

surements of a fabricated device reveal an anomalous Hall effect when filling 1 electron or hole per moiré cell ($v=\pm 1$). The anomalous Hall signal is comparable in both fillings, in contrast to earlier studies showing a strong particle-hole asymmetry. Additionally, we find hints of superconductivity near v=2 despite the BN-induced inversion symmetry breaking, suggesting superconductivity and the quantum anomalous Hall effect might coexist in the same device. These findings contribute to a deeper understanding of stabilizing Chern bands in mesoscopic moiré systems, a critical step toward realizing novel fractional Chern insulator states that can serve as platforms for topological quantum computing.

Life Science & Semiconductors, Medical Devices & Biotechnology

| Capturing Methanogenic Carbon Monoxide Dehydrogenase/Acetyl-CoA Synthase Complexes via Cryogenic-Electron Microscopy | 46 |
|--|----|
| Ultrasound-based System for Emboli Detection and Sizing | |
| Towards Scalable Screening for the Early Detection of Parkinson's Disease: Validation of an iPad-based Eye Movement Assessment System Against a Clinical-grade Eye Tracker | |
| Miniaturized Ingestible Temperature Sensing System with Enhanced Safety and Versatility for Continuous Internal Monitoring | 49 |
| Structural Mechanisms of Catalysis in Ribonucleotide Reductase by Cryogenic-Electron Microscopy | 50 |
| Ingestible Gastric Electrical Stimulation System Using Bioresorbable Electromechanical Systems | 51 |
| Highly Integrated Graphene-based Chemical Sensing Platform for Structural Monitoring Applications | 52 |
| Deep and Dynamic Metabolic and Structural Imaging in Living Tissues | 53 |
| New NMR Probe Configurations for Spectroscopy and Relaxometry of Moving Fluids | 54 |
| Surface Patch Coils and Pulse Sequences for Noninvasive Blood Tests Using Magnetic Resonance | 55 |
| System Prototype for Electromagnetic Breast Cancer Detection | 56 |

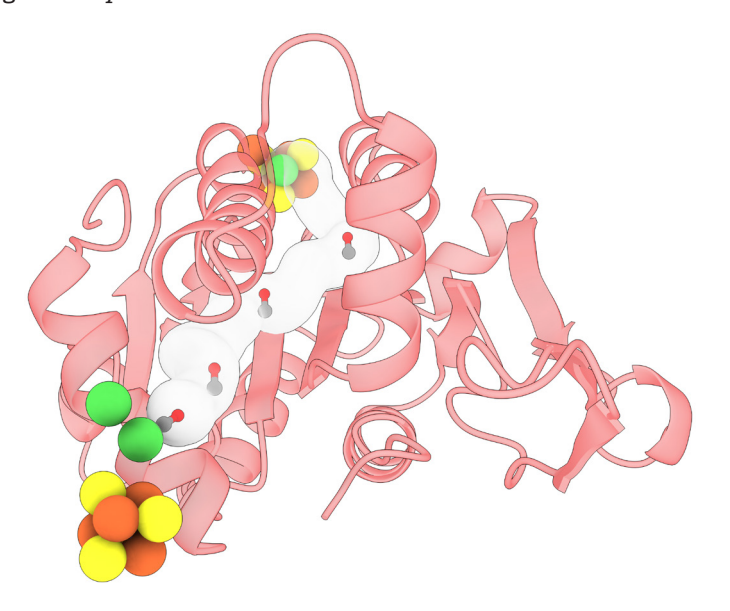
Capturing Methanogenic Carbon Monoxide Dehydrogenase/Acetyl-CoA Synthase Complexes via Cryogenic-Electron Microscopy

A. Biester, C. L. Drennan Sponsorship: Howard Hughes Medical Institute, National Institutes of Health

Carbon monoxide dehydrogenases (CODHs) and acetyl-CoA synthases (ACSs) are major players in the global carbon cycle. Approximately two-thirds of the estimated one-billion metric tons of methane produced annually by methanogens on Earth is derived from the ACS-catalyzed cleavage of acetate. A nickel-iron-sulfur (Ni-Fe-S)-containing ACS cleaves acetyl-CoA into a methyl group, carbon monoxide (CO), and coenzyme-A (CoA). The methyl group goes on to form the greenhouse gas methane, and the CO is oxidized to form the greenhouse gas CO2. The latter reaction is catalyzed by a Ni-Fe-S-containing CODH. The reactions of CODH and ACS are reversible; acetogenic bacteria, like Moorella thermoacetica and Clostridium autoethanogenum, employ CODH/ACSs to synthesize acetyl-CoA from one-carbon units derived from CO₂.

Although our lab determined the first structure of an acetogenic CODH/ACS over twenty years ago, the structure of the methanogenic enzyme has been elusive.

Methanogenic CODHs cannot be recombinantly expressed, and the protein as isolated from native methanogens exists as a massive 2.2 MDa acetyl-CoA decarbonylase/synthase (ACDS) complex—a size that has precluded crystallography. Due to the cryogenic electron microscopy (cryo-EM) "resolution revolution" and the amazing cryo-EM facility run by Sarah Sterling in MIT.nano, it is now possible to obtain structures at atomic resolution of methanogenic CODH/ACS enzyme complexes. We visualize the Ni-Fe-S metal cluster that is responsible for the first step in the biological production of methane from acetate. This research is timely, as metabolic engineering efforts are underway to employ acetogens and methanogens and their CODH/ACS enzymes in producing biofuels from greenhouse gases. Clostridium autoethanogenum is already being used by LanzaTech in the conversion of CO₂ to ethanol.



▲ Figure 1: Cryo-EM has allowed us to visualize a methanogenic CODH/ACS complex that contains an internal gas channel. This channel provides a route for CO to travel between a Ni-Fe-S cluster (green, orange, and yellow spheres) that produces CO from acetate and one that converts the CO to CO₂.

FURTHER READING

 A. Biester, D. A. Grahame, C. L. Drennan, "Capturing a Methanogenic Carbon Monoxide Dehydrogenase/Acetyl-CoA Synthase Complex via Cryogenic Electron Microscopy," Proc. Natl. Acad. Sci., vol. 121, no. 41, p. e2410995121, 2024. DOI.org/10.1073/pnas.2410995121 PMCID: PMC11474084. PMID: 39361653

Ultrasound-based System for Emboli Detection and Sizing

I. Romero Estevez, S. M. Imaduddin, T. Heldt, L. Bourouiba Sponsorship: Boston Children's Hospital Anaesthesia Foundation

Extracorporeal membrane oxygenation (ECMO) is a life-support mechanism designed to aid individuals whose lungs and/or hearts are failing. It continuously pumps blood through an external system that adds oxygen and removes carbon dioxide. However, ECMO carries risks, including the potential formation of emboli–either solid, such as blood clots, or gaseous, such as air bubbles. In a study involving 1,095 ECMO-patients, 53% developed deep vein thrombosis. Emboli in the micrometer range, when entering the body, can cause tissue damage through ischemia and may lead to stroke or pulmonary obstruction. Detecting, counting, and differentiating (solid vs. gaseous) such emboli remain major technological challenges.

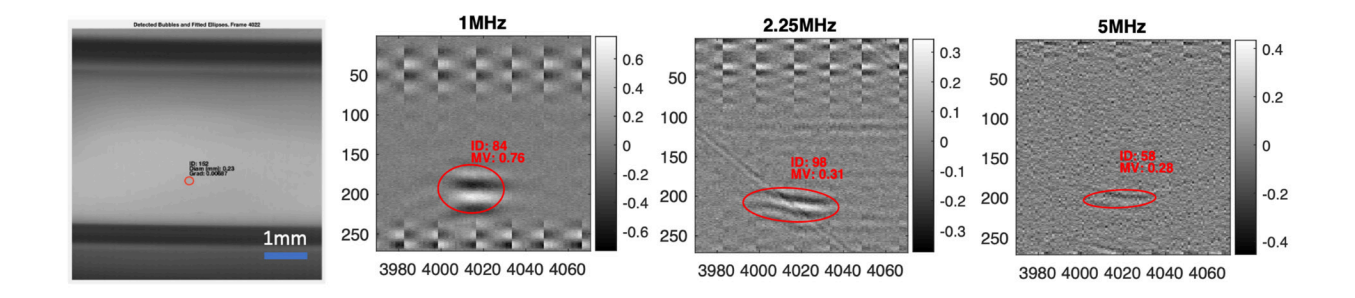
Ultrasound-based methods seem ideally suited to fill this technological gap, but current research methods face limitations. These include the need for a reliable base-line power measurement to accurately detect emboli, the lack of ground truth data, and reliance on small datasets of embolic signals.

In ultrasound signals, emboli appear as high intensity transient signals, and there is a relationship

between air bubble size, for example, and the received backscatter intensity. The proposed solution is an ultrasound system—in collaboration with colleagues from Boston Children's Hospital—for the detection, differentiation, counting, and sizing of emboli in ECMO.

Some of our key achievements include 1) the development of a lab-based flow phantom system; 2) acquisition of ground truth data using a high-speed camera; 3) controlled experiments varying parameters such as bubble size and flow rate; 4) implementation of a tracking algorithm for video analysis and a detection algorithm for ultrasound signals; and 5) establishment of an initial relationship between the ultrasound signal and the bubble size.

Future work will extend to solid emboli and physiological fluid mimicking blood's acoustic properties. Expanding this technology to other extracorporeal support systems will be a priority, broadening its impact across different critical care domains.



▲ Figure 1: A 150-micrometer bubble detected in high-speed camera videos. Corresponding M-mode ultrasound signals from the same bubble are shown at 1, 2.25, and 5 MHz, with object detection and maximum voltage extraction highlighted.

B. D. Kussman, S. M. Imaduddin, M. H. Gharedaghi, T. Heldt, and K. L. La-Rovere, "Cerebral Emboli Monitoring Using Transcranial Doppler Ultrasonography in Adults and Children: A Review of the Current Technology and Clinical Applications in the Perioperative and Intensive Care Setting," International Anesthesia Research Society, vol. 133, no. 2, Aug. 2021.

[•] S. M. Imaduddin, K. L. LaRovere, B. D. Kussman, and T. Heldt, "A Time-Frequency Approach for Cerebral Embolic Load Monitoring," *IEEE Transactions on Biomedical Engineering*, vol. 67, no. 4, Jul. 2019.

Towards Scalable Screening for the Early Detection of Parkinson's Disease: Validation of an iPad-based Eye Movement Assessment System Against a Clinical-grade Eye Tracker

J. Koerner, E. Zou, J. A. Karl, C. Poon, L. Verhagen-Metman, C. G. Sodini, V. Sze, F. J. David, T. Heldt Sponsorship: Analog Devices, Inc., MIT Aging Brain Initiative, the Northwestern University Department of Physical Therapy and Human Movement Sciences, the Northwestern Medicine Enterprise Data Warehouse

Early detection and monitoring of Parkinson's disease (PD) remain challenging, underscoring the need for accessible and cost-effective methods. Abnormalities in saccadic eye movements have emerged as promising noninvasive biomarkers for early PD detection and disease progression tracking. Although clinical-grade eye tracking devices provide high accuracy and precision, their clinical adoption is constrained by cost and complexity. Here, we introduce and validate a cost-effective and accessible iPad-based system for assessing saccadic eye movements, benchmarking it directly against the clinical-grade EyeLink 1000 Plus eye tracker. Our approach utilizes the iPad's front-facing camera combined with a deep learning algorithm for gaze estimation. Validation involved 25 participants (10 with PD, 15 healthy controls) performing standardized pro-saccade (PS), anti-saccade (AS), memory-guided-saccade (MGS), and self-generated saccade (SGS) tasks. The iPad system demonstrated subject-level error magnitudes aver-

aging 2 ms (SD = 2 ms) for latency and 0.7° (SD = 0.6°) for amplitude in the PS, AS, and MGS tasks and 0.003 s-1 (SD = $0.004 \, \text{s}^{-1}$) for instantaneous primary saccade rate and 1.6° (SD = 1.5°) for amplitude in the SGS task. To contextualize our findings, we reviewed studies reporting saccadic impairments in PD relative to healthy individuals. By compiling data from studies that included PD participants at varying stages of disease severity, we established benchmarks for clinically meaningful changes in saccade metrics. Our results indicate that the iPad system achieves accuracy and precision—particularly in temporal measurements—that meet or exceed these benchmarks, supporting its potential use in clinical screening and longitudinal monitoring of PD. Our findings underscore the iPad-based system's potential as an accessible, cost-effective, and scalable solution for routine clinical screening and longitudinal monitoring of PD.

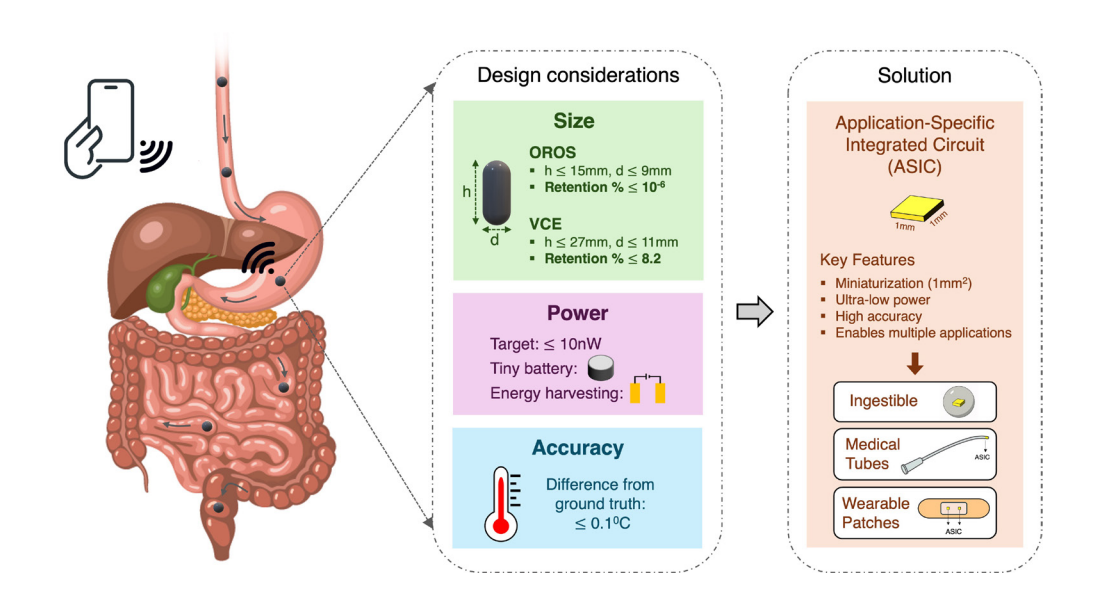
Miniaturized Ingestible Temperature Sensing System with Enhanced Safety and Versatility for Continuous Internal Monitoring

S. Sharma, Y. Cai, I. Moon, M. Yang, P. Chai, N. Fabian, K. Schmidt, A. Hayward, A. Pettinari, M. Platero, B. Laidlaw, A. Guevara, J.-G. Rosenboom, A. Chandrakasan, G. Traverso

Sponsorship: Defense Advanced Research Project Agency, Advanced Research Projects Agency for Health

Ingestible electronic systems provide a minimally invasive approach for continuous monitoring of core body temperature, offering critical insights into gastrointestinal (GI) physiology and pathophysiological conditions. Despite significant progress, existing ingestible temperature sensors typically exceed dimensions that restrict universal applicability, particularly in pediatric populations. Here, we introduce the Miniaturized Ingestible Temperature Sensing (MITS) system, a compact temperature monitoring device comprising a highly miniaturized (1 mm x 1 mm) and ultra-low power (10 nW) integrated circuit chip, coupled with a custom-designed and miniaturized antenna (5 mm x 5 mm) for wireless communication through backscattering, and a tiny coin-cell battery for power (Figure 1).

The completely assembled system with encapsulation measures 6 mm in diameter and 4 mm in height, which aligns with the established safety dimensions validated by clinically successful OROS® systems and presents minimal risk for GI retention as indicated by clinical experiences with video capsule endoscopy. Preclinical evaluation in swine across diverse physiological conditions—including induced inflammation, variable GI transit times, alterations in circulation, and multi-day monitoring—demonstrate the system's broad potential applicability. These findings underscore how significant size reduction of ingestible devices enhances safety, facilitates pediatric use, and expands monitoring applications across various clinical scenarios.



▲ Figure 1: Overview: The MITS device is designed for continuous, real-time, and wireless monitoring of core body temperature. MITS can be orally ingested and can measure the temperature inside the GI tract, serving as an important tool both inside and outside the clinic.

- C. M. Blatteis, Physiology and Pathophysiology of Temperature Regulation. New Jersey: World Scientific, 1998.
- S. R. Madhvapathy, M. I. Bury, L. W. Wang, J. L. Ciatti, R. Avila, Y. Huang, A. K. Sharma, and J. A. Rogers, "Miniaturized Implantable Temperature Sensors for the Long-term Monitoring of Chronic Intestinal Inflammation," *Nature Biomedical Engineering*, vol. 8, pp. 1040–52, 2024.
- S. Sharma, K. B. Ramadi, N. Poole, S. S. Srinivasan, K. Ishida, J. Kuosmanen, J. Jenkins, F. Aghlmand, M. B. Swift, M. G. Shapiro, G. Traverso, and A. Emami, "Location-aware Smart-pills for Wireless Monitoring of Gastrointestinal Dynamics," *Nature Electronics*, vol. 6, pp 242-256, 2023.

Structural Mechanisms of Catalysis in Ribonucleotide Reductase by Cryogenic-Electron Microscopy

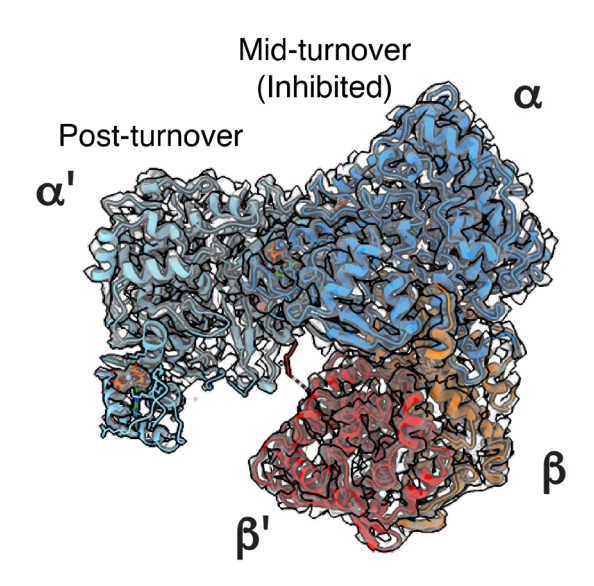
D. E. Westmoreland, C. L. Drennan Sponsorship: Howard Hughes Medical Institute, National Institutes of Health

Antibiotic resistance is anticipated to be a major challenge of the 21st century. To address this concern, we are studying class Ia ribonucleotide reductases (RNRs), which are present in a number of pathogenic organisms and are responsible for catalyzing the only known de novo biosynthetic route to deoxyribonucleotides from the corresponding RNs. As such, class Ia RNRs represent a promising target for novel antibacterial drugs. The active state of this enzyme—a heterodimer of two homodimeric subunits, $\alpha 2$ and $\beta 2$ —however, is transiently associated and has only been observed using cryogenic electron microscopy (cryo-EM) and either mutations or substrate analogs as inhibitors (Figure 1).

Our work focuses, therefore, on the use of cryo-EM to understand how the class Ia RNR from *Escherichia coli* structurally regulates its catalysis in an effort to design antibiotics that inhibit the active state of RNR. In particular, the C-terminal tails of both the

 $\alpha 2$ and $\beta 2$ subunits are known to play critical roles in the catalytic mechanism of RNR, but the tail regions of these subunits are conformationally dynamic and have not yet been resolved by any structural method, including cryo-EM.

Here, we use high-resolution cryo-EM data sets in combination with machine learning-based data processing techniques (cryoDRGN, developed by the Davis Lab in the Department of Biology) to curate particle stacks of tens of thousands of particles with increased resolution for both the $\alpha 2$ and $\beta 2$ tail regions. This work helps explain how the conformational dynamics of these tail regions function within the larger catalytic mechanism of RNR. Further work in this area will compare the human RNR, also a class Ia RNR, with the E. coli RNR to design novel antibiotics with reduced cytotoxicity in humans.



 \blacktriangle Figure 1: Active state structure of E. coli class la RNR in which one side of the enzyme has already undergone catalysis (post-turnover) and one side has not yet completed catalysis (mid-turnover). The $\alpha 2$ subunit is shown in light and dark blue; the $\beta 2$ subunit is shown in red and orange).

D. E. Westmoreland, P. R. Feliciano, G. Kang, C. Cui, A. Kim, J. Stubbe, D. G. Nocera, and C. L. Drennan, "2.6-Å Resolution Cryo-EM Structure of a Class Ia Ribonucleotide Reductase Trapped with Mechanism-based Inhibitor N₃CDP," Proc. Natl. Acad. Sci., vol. 121, no. 45, p. 32417157121, Oct. 2024.

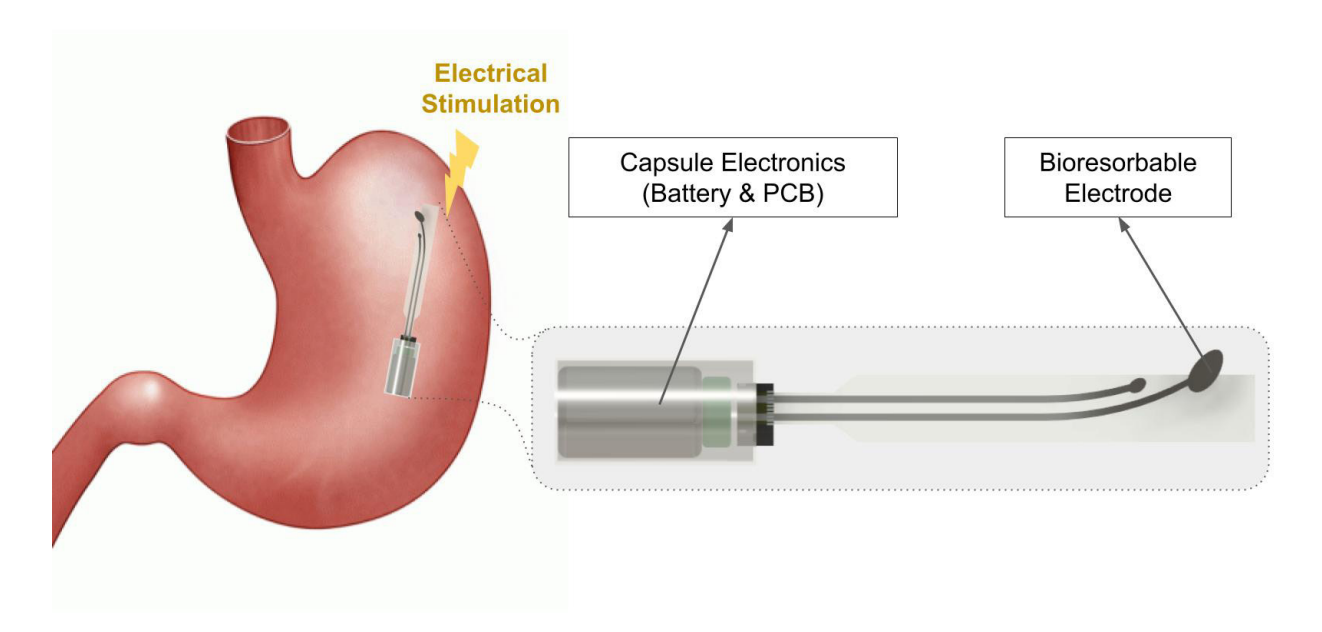
[•] B. L. Greene, G. Kang, C. Cui, M. Bennati, D. G. Nocera, C. L. Drennan, and J. Stubbe, "Ribonucleotide Reductases: Structure, Chemistry, and Metabolism Suggest New Therapeutic Targets," Ann. Rev. Biochem., vol. 89, pp. 45–75, Jun. 2020.

Ingestible Gastric Electrical Stimulation System Using Bioresorbable Electromechanical Systems

A. O. Erus, M. G. Say, I. Moon, G. Traverso Sponsorship: ARPA-H

The gut-brain axis, a bidirectional communication network between the gastrointestinal (GI) tract and the central nervous system, regulates various physiological functions via neurohormonal signaling. Electrical stimulation of the GI tract can modulate hormone release, offering therapeutic potential. However, current gastric electrical stimulation (GES) systems require invasive surgery for implantation and removal. To address this limitation, we developed an ingestible GES system composed of a bioresorbable electrode array in-

tegrated with capsule-based electronics. The bioresorbable substrate and thin film metal are chosen for their low dissolution rate and high mechanical strength. The electrodes are fabricated using laser systems, offering a faster, cost-effective alternative to traditional photolithography. In vitro testing, including dissolution, stress-strain, and impedance assessments, demonstrates the system's viability, supporting its potential for non-invasive GES.



▲ Figure 1: Simplified schematic of gastric electrical stimulation system (not to scale) in the stomach.

Highly Integrated Graphene-based Chemical Sensing Platform for Structural Monitoring Applications

C. Lopez Angeles, T. Palacios Sponsorship: Ferrovial

Two-dimensional materials, such as graphene, hold promise for sensing applications. Graphene's remarkable surface-to-volume ratio, when employed as a transducer, enables the sensor channel to be readily modulated in response to chemical changes in proximity to its surface, effectively converting chemical signals into the electrical domain. However, their utilization has been constrained due to variations in device-to-device performance arising from synthesis and fabrication processes.

To address this challenge, we employ Graphene Field Effect Transistors (GFETs) in developing a robust and multiplexed chemical sensing array comprising tens of sensing units. This array is coupled with custom-designed high-speed readout electronics for structural monitoring applications.

For example, in harsh environmental conditions,

structures constructed from reinforced concrete may experience degradation due to corrosion, a chemical process initiated by carbonation and significant fluctuations in temperature and humidity. Under normal conditions, concrete maintains a pH level within the alkaline range of 13 to 14. However, when subjected to carbonation, its pH decreases to values between 8 and 9.

Our platform excels in real-time pH monitoring. By conducting I-V sweep measurements in the sensor channel, we have established a correlation between [H+] concentration and the gate-source voltage (Vgs) at graphene's Dirac point with an accuracy of roughly 98%. This system and correlation allows for the prompt detection of any deviations induced by corrosion within a concrete environment.

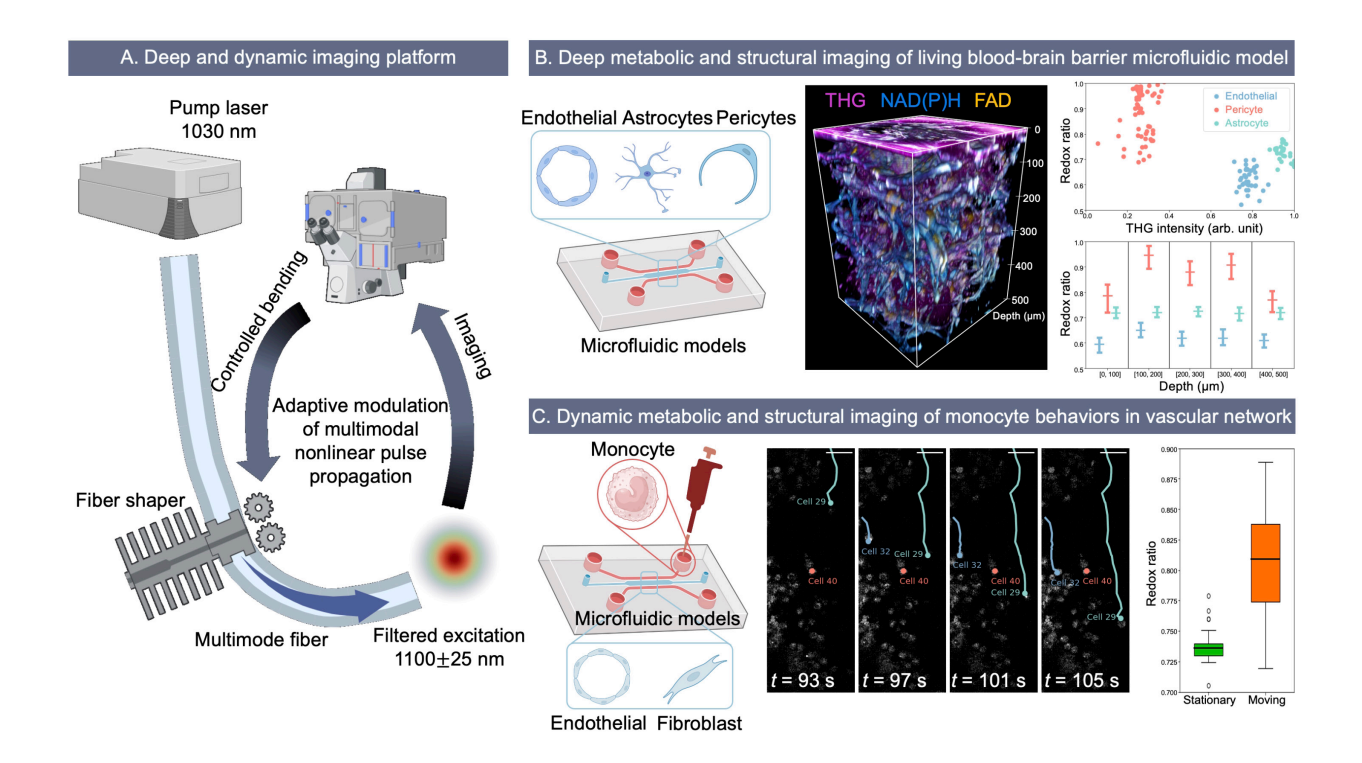
52

Deep and Dynamic Metabolic and Structural Imaging in Living Tissues

K. Liu, H. Cao, R. Kamm, L. Griffith, F. Wang, T. Qiu, S. You Sponsorship: Mathworks Fellowship

Label-free imaging through two-photon autofluorescence (2PAF) of NAD(P)H allows for non-destructive and high-resolution visualization of cellular activities in living systems. However, its application to thick tissues and organoids has been restricted by its limited penetration depth, largely due to tissue scattering at the typical excitation wavelength required for NAD(P) H. Here, we demonstrate that the imaging depth for NAD(P)H can be extended to over 700 μ m in living engineered human multicellular microtissues by adopting multimode fiber (MMF)-based low-repetition-rate high peak-power three-photon (3P) excitation of NAD(P)H at

1100 nm. This is achieved by having over 0.5 MW peak power at the band of 1100±25 nm through adaptively modulating multimodal nonlinear pulse propagation with a compact fiber shaper. Moreover, the 8-fold increase in pulse energy enables faster imaging of monocyte behaviors in the living multicellular models. These results represent an advance for deep and dynamic imaging of intact living biosystems. The modular design is anticipated to allow wide adoption for demanding in vivo and in vitro imaging applications, including cancer research, autoimmune diseases, and tissue engineering.



▲ Figure 1: (a) Deep and dynamic imaging platform. (b) Deep imaging over the entire depth of 500 µm in the living human blood-brain barrier microfluidic model. (c) Dynamic imaging of monocyte trafficking in vascular network.

New NMR Probe Configurations for Spectroscopy and Relaxometry of Moving Fluids

H. Gaensbauer, A. Bevacqua, D. H. Park, J. Han Sponsorship: Singapore MIT Alliance for Research and Technology, CAMP IRG

Nuclear Magnetic Resonance (NMR) spectroscopy and relaxometry are widely used and well-established techniques that can detect and identify chemical compounds in samples with significant background. Because NMR measurements are nondestructive, they have many applications in industrial process control, where they can be used to track reaction progress, detect contaminants, and provide insight into the quality of the product being produced. However, movement of the sample through the NMR system during the experiment reduces the resolution of NMR spectroscopy and confounds NMR relaxometry measurements. This makes it difficult or impossible to use NMR to continuously monitor flowing fluids in industrial settings, es-

pecially when the flow rate is variable or unknown. In this work, we present an RF coil geometry that produces NMR measurements that are completely insensitive to the flow behavior of the sample. We show that these coils can be designed for different ranges of flow rates and demonstrate in-line monitoring of a commercial dairy sample over a period of several hours. These coils enable in-line high resolution spectroscopy and relaxometry for process monitoring applications without needing to control or even know the flow rate, making it possible to retrofit state-of-the-art NMR systems for continuous quality control on a wide range of biomanufacturing and industrial processes that would traditionally require regular invasive sampling.

Surface Patch Coils and Pulse Sequences for Noninvasive Blood Tests Using Magnetic Resonance

A. Huang, H. Gaensbauer, J. Han Sponsorship: MIT Research and Innovation Scholars Program, MIT Lincoln Labs

Traditional blood tests for diseases such as malaria and diabetes require drawing blood, which is painful and time-consuming. Our lab has shown that magnetic resonance (MR) relaxometry can be used to perform these blood tests electromagnetically, opening the door to contact-free, noninvasive diagnostic blood tests. While our low-cost, gradient-free MR systems have been demonstrated in vitro, they have not yet been demonstrated in vivo, due to the movement of blood in the body and the chaotic tissue signal background. In this work, we demonstrate the use of custom surface coils designed for blood signal detection with standard time-of-flight MR pulse sequences to isolate signals from blood and compensate for the blood flow velocity. We go on to perform relaxometry measurements in a model of a human arm. This brings us one step closer to noninvasive blood monitoring with low-cost equipment.

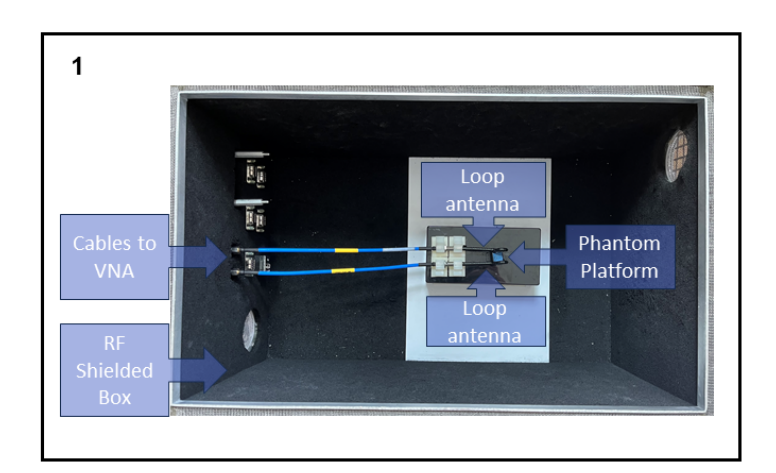
System Prototype for Electromagnetic Breast Cancer Detection

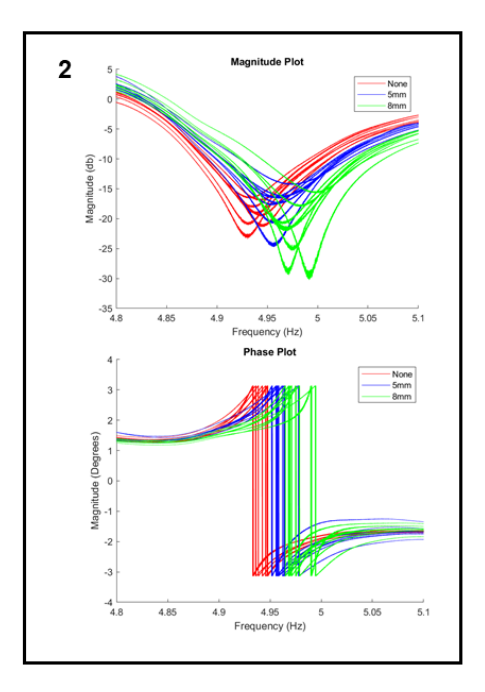
M. St. Cyr, S. Sabouri

Breast cancer detection is ideally quick, accurate, and comfortable. An emerging technology to fill the gaps in current diagnostic methods is microwave imaging, which sends and receives microwave signals through the breast in order to detect tumors of various sizes. This method has potential for a more comfortable patient experience at a lower cost than the current standards in breast cancer imaging [1].

In this work, a prototype system is developed for

determining tumor size in breast tissue by utilizing microwave imaging techniques. The system consists of RF shielding components, custom loop antennas, and a vector network analyzer for signal generation and data collection. Additionally, post processing is completed by a ML algorithm to classify tumor sizes. By sending and receiving signals in the GHz range, this system can detect and distinguish between tumors of varying sizes on the millimeter scale within breast phantoms.





▲ Figure 1: (1) System overview (2) Transmission coefficient of various tumor sizes.

FURTHER READING

• N. Nikolova, "Microwave Imaging for Breast Cancer," IEEE Microwave, vol. 12, no. 7, pp. 78–94, Dec. 2011, doi: 10.1109/MMM.2011.942702.

MEMS, Field-Emitter, Thermal, Fluidic Devices, and Robotics

| Modular, 3D-printed Electrospray Thrusters for High-impulse Maneuvers in CubeSats | 58 |
|---|----|
| Advanced Cooling of Electronics via Additive Manufacturing and Al | 59 |
| 2-photon Photolithography Fabrication of "Pixel" Electrospray Thrusters | 60 |
| Tailored Ultrasound Propagation in Microscale Metamaterials via Inertia Design | 61 |
| 3D-integrated Circuits in GaN/Si CMOS/Glass for High-frequency, High-data-rate Applications | 62 |
| GEVO: Memory-Efficient Monocular Visual Odometry Using Gaussians | 63 |
| Ultra-thin Ruthenium Electrochemical Actuators | 64 |
| DecTrain: Deciding When to Train a Monocular Depth DNN Online | 65 |
| Flexible Acoustically Active Surfaces Based on Piezoelectric Microstructures | 66 |
| Anode Engineering to Reduce On-Resistance of Field Emitter Arrays | 67 |

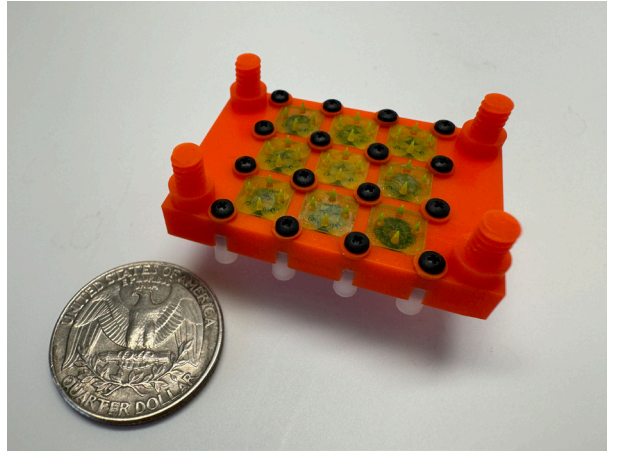
Modular, 3D-printed Electrospray Thrusters for High-impulse Maneuvers in **CubeSats**

H. Kim. L. F. Velásquez-García Sponsorship: MathWorks Fellowship, the MIT Portugal Program

Electrospray thrusters are a type of electric propulsion system that offers high specific impulse, making them ideal for maneuvering small satellites. Traditionally, the fabrication of electrospray thrusters has been conducted in semiconductor cleanrooms to achieve precise micro-scaled features. However, this process is expensive, time-consuming, and incompatible with in-space manufacturing. This study presents a proof-of-concept demonstration of a novel, droplet-emitting electrospray thruster array design for CubeSats that is fully additively manufactured.

study integrates two vat photopolymerization three-

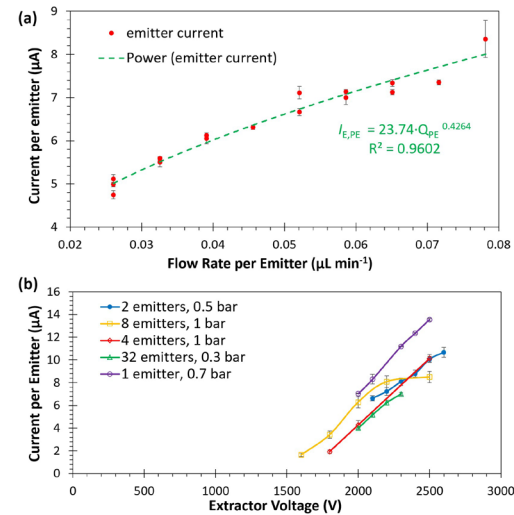
The electrospray thruster design developed in this dimensional (3D) printing technologies, i.e., digital light processing (DLP) for the meso-scaled features, and two-photo polymerization (2PP) for the micro-scaled features. Each 2PP-printed module contains 4 emitters with optimized, 50-µm-diameter microfluidic channels to ensure uniform operation across the emitter arrays. propulsion. (a)



▲ Figure 1: Optical image of a device with 9 modules, without the extractor electrode, next to a US quarter. From first Reading.

These modules are connected in parallel using a DLPprinted manifold block to increase the thruster's throughput (Figure 1).

Testing of devices with up to 8 modules (32 emitters in total) in vacuum demonstrated stable and uniform operation for the first time as a 3D-printed, droplet-emitting electrospray emitter array with near 100% beam transmission (Figure 2). Both pressure and voltage were evaluated as ways to control the emitted current and thrust, with voltage control proving to be a more effective and simpler approach, despite being less explored in the literature for electrospray in the droplet emission regime. The estimated thrust and specific impulse are comparable to, or better than, those reported for other droplet-emitting electrospray thrusters. These results suggest that the proposed manufacturing approach is a promising method for developing efficient electrospray thrusters for space



▲ Figure 2: (a) Per-emitter current versus flow rate for a device biased at 2000 V, and (b) per-emitter current versus extractor voltage for a device tested with different pressures. Emitter electrode was grounded; error bars represent one standard deviation.

- H. Kim and L. F. Velásquez-García, "High-impulse, Modular, 3D-printed CubeSat Electrospray Thrusters Throttleable via Pressure and Voltage Control," Advanced Science, p. 2413706, 2025. DOI: 10.1002/advs.202413706
- A. A. Fomani, A. I. Akinwande, and L. F. Velásquez-García, "Resilient, Nanostructured, High-current, and Low-voltage Neutralizers for Electric Propulsion of Small Spacecraft in Low Earth Orbit," IOP J. of Physics: Conference Series, vol. 476, p. 012014, 2013. DOI: 10.1088/1742-6596/476/1/012014
- D. Melo Máximo and L. F. Velásquez-García, "Additively Manufactured Electrohydrodynamic Ionic Liquid Pure-ion Sources for Nanosatellite Propulsion," Additive Manufacturing, vol. 36, p. 101719, Dec. 2020. DOI: 10.1016/j.addma.2020.101719

Advanced Cooling of Electronics via Additive Manufacturing and Al

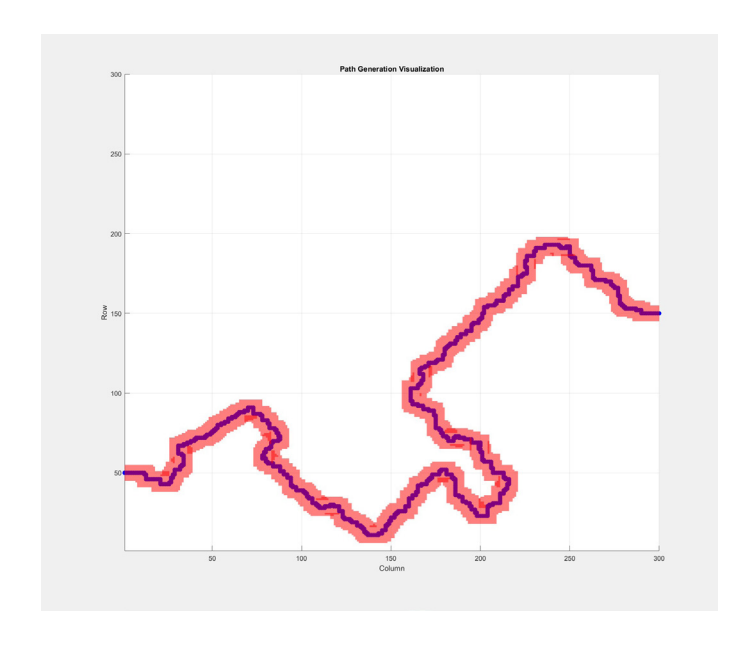
H. Kim, L. F. Velásquez-García Sponsorship: MathWorks Fellowship

The increasing demand for compact and efficient power electronics highlights the need for advanced thermal management solutions. Traditional liquid-cooled heat sinks, typically fabricated via subtractive or formative manufacturing, are limited in their ability to address nonuni-form heat loads due to their simple geometries. This research aims to develop a low-cost, high-performance, liquid-cooled heat sink for electronics by integrating generative artificial in-telligence (AI)-driven design with three-dimensional (3D) printing using highly thermally conductive composite resins. Leveraging additive manufacturing can realize complex, freeform internal cavities tailored to specific thermal profiles to significantly enhance heat dissipation. The devices will be made via vat photopolymerization using ceramic-loaded polymer resin as feedstock. The ceramic filler increases the thermal conductivity of the composite.

Current work focuses on developing a genetic algorithm to generate printable, 2D liquid channel designs that maximize heat transfer performance. The

algorithm includes initialization, evaluation, mutation, and crossover stages, iteratively refining designs based on simulated temperature distributions. To address manufacturability constraints inherent to the chosen 3D printing method, the initialization phase generates non-intersecting centerline paths on a discretized grid, ensuring that resulting channel geometries are printable (Figure 1). The evaluation phase, which integrates automated 3D model generation and thermal simulation, assesses the effectiveness of each design. The algorithm then iteratively seeks the best-performing designs by mutating and merging features from the previous iterations.

Future research will explore transitioning from genetic algorithms to other generative AI techniques and extend the design framework to full 3D heat exchanger architectures. This integrated approach aims to unlock the full potential of additive manufacturing for custom, high-performance thermal management solutions.



◄ Figure 1: A random, constant-width path generated between designated start and end points for the initialization phase of the genetic algorithm, with printability constraints taken into account.

[•] T. Wu, B. Ozpineci, and C. Ayers, "Genetic Algorithm Design of a 3D Printed Heat Sink," 2016 IEEE Applied Power electronics Conference and Exposition (APEC), pp. 3529-3536, 2016. DOI: 10.1109/APEC.2016.7468376

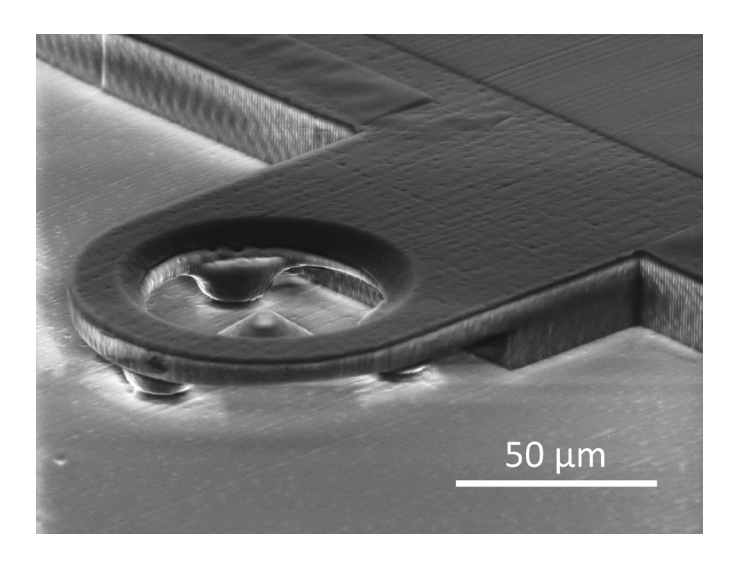
[•] Y. Manaserh, A. R. Gharaibeh, M, I. Tradat, S. Rangarajan, B. G. Sammakia, and H. A. Alis-sa, "Multi-objective Optimization of 3D Printed Liquid Cooled Heat Sink with Guide Vanes for Targeting Hotspots in High Heat Flux Electronics," *International J. of Heat and Mass Transfer*, 184, p. 122287, 2022. DOI: 10.1016/j.ijheatmasstransfer.2021.122287

H. Kim and L. F. Velásquez-García, "High-impulse, Modular, 3D-printed CubeSat Electrospray Thrusters Throttleable via Pressure and Voltage Control," Advanced Science, p. 2413706, 2025. DOI: 10.1002/advs.202413706

2-photon Photolithography Fabrication of "Pixel" Electrospray Thrusters

C. J. Nachtigal, S. Dhulipala, C. M. Portela, P. C. Lozano Sponsorship: NASA Space Technology Graduate Research Office Grant (80NSSC23K1174), U.S. Air Force Office of Scientific Research (FA9550-19-1-0104)

Electrospray thrusters (ESTs) are a promising form of electric propulsion in small satellite and deep space applications due to their high specific impulse and low thrust. ESTs consist of an array of micro emission sites where propellant is fed to and propelled from via a voltage application to the emitter with respect to a downstream grounded extractor electrode. ESTs lack in the length of their lifetime, due to electrical shortages at a single emission site causing premature full array shortage. They also lack efficiency, due to improper extractor alignment and poor emitter manufacturing precision affecting emission site stability and purely ionic regime emission. To remedy this, we propose an EST design consisting of precise capillary emitters with an integrated extractor array consisting of single extractors connected via fuses to prevent shortage propagation and ensure extractor alignment. To realize this design, this work uses 2-photon photolithography to build the emitter capillaries and integrated extractor base and liftoff of sputter-coated nichrome to pattern the extractors and fuses. We examine the fabrication feasibility on porous glass substrates and on 50-100- μ m-diameter etched through-holes in silicon wafers to allow for passive propellant uptake. We determined the contact angle and dielectric breakdown of the structure and designed a prototype to be compatible with voltages over 1200 V, which is well within the necessary firing voltage range that is simulated. Further, the design allows for an emitter pitch of less than 80 μ m, which can be reduced further in future iterations, greatly densifying arrays and increasing the potential thrust per area of ESTs.



▲ Figure 1: Scanning electron microscope image of single 3-µm-diameter "pixel" emitter capillary fabricated in UpBrix with connected extractor contact pad and patterned Ag and Ti on Si over 100-µm-diameter propellant-feeding through hole.

C. J. Nachtigal and P. Lozano, ""Pixels" in Electrospray Thrusters for Ultra-Reliable Flat-Panel Electric Propulsion," AIAA 2024-1345. AIAA SCITECH 2024 Forum, Jan. 2024.

C. Nachtigal and P. Lozano, "Flat-panel Pixel Electrospray Thrusters for Increased Reliability and Efficiency: Preliminary Design and Testing," 08 Jan.2025, PREPRINT (Version 1) available at Research Square [Link]

Tailored Ultrasound Propagation in Microscale Metamaterials via Inertia Design

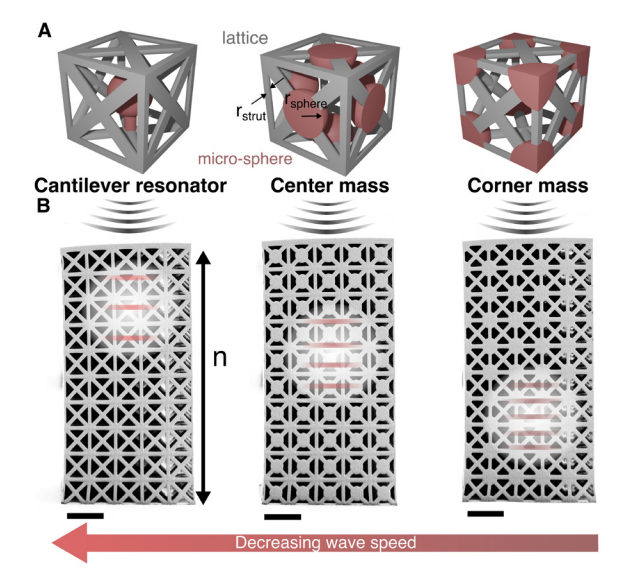
R. Sun, J. Lem, Y. Kai, W. DeLima, C. M. Portela Sponsorship: Kansas City National Security Campus, MIT Institute for Soldier Nanotechnolgies, MIT Mechanical Engineering MathWorks Seed Fund, NSF Graduate Research Fellowship Program

The quasi-static properties of micro-architected (meta) materials have been extensively studied, but their dynamic responses, especially in acoustic metamaterials with engineered wave propagation behavior, represent a new frontier. However, challenges in miniaturizing and characterizing acoustic metamaterials in high-frequency (megahertz, MHz) regimes have hindered progress toward experimentally implementing ultrasonic-wave control.

We present and validate a micro-inertia design framework for programming quasi-static and dynamic (MHz range) responses of three-dimensional micro-architected materials. Using a simple braced-cubic unit cell design, we present two micro-inertia placement strategies and explain how each tunes quasistatic stiffness and dynamic longitudinal-wave velocities differently in these metamaterials. We fabricate all designs in a single-step, single-material two-photon lithography process, which enables their microscale implementation. Through quasi-static nanomechanical compression experiments and finite-element analysis, we demonstrate that micro-inertia location changes

stress distribution within the materials and lowers the effective stiffness increase per added unit of mass. This presents a deviation from the classical stiffness scaling laws for architected materials, which we describe as partially "decoupling" mass and stiffness properties. Using the laser-induced resonant spectroscopy method, we experimentally demonstrate that decoupling mass and stiffness enables tunable elastic-wave velocities in the MHz regime. Our framework provides a vast design library of elasto-dynamic properties via simple geometric changes, which we use to spatially and temporally program ultrasonic wave propagation in microscale materials and an acoustic demultiplexer.

Altogether, the capabilities of this micro-inertia design framework expand the achievable property space by partially decoupling mass and stiffness. This parametric design framework establishes independently tunable quasi-static and elastodynamic properties without requiring complex design algorithms, enabling straightforward design and fabrication of microscale acoustic metamaterials and devices.



▲ Figure 1: (A) Three braced-cubic sample designs increase relative density by increas-ing strut radius and nodal mass radii. (B) Various mass-addition schemes provide a route to achieve both tunable quasi-static stiffness and longitudinal wave velocities. Scale bars 20µm.

FURTHER READING

 Y. Kai, S. Dhulipala, R. Sun, J. Lem, W. DeLima, T. Pezeril, and C. M. Portela, "Dynamic Diagnosis of Metamaterials through Laser-induced Vibrational Signatures," Nature, vol. 623, no. 7987, p. 514-521, 2023.

3D-integrated Circuits in GaN/Si CMOS/Glass for High-frequency, High-data-rate Applications

P. Yadav, J. Wang, D. Baig, X. Li, J. Pastrana, J. Niroula, M. Bakir, M. Swaminathan, R. Han, T. Palacios Sponsorship: SRC Joint University Microelectronics Program 2.0 (Grant no. 2023-JU-3136), National Defense and Science Graduate Fellowship

Gallium nitride (GaN) transistors are enabling the next generation of high-efficiency, high-power, and high-frequency integrated circuits. Furthermore, demonstrations of low-voltage GaN radio frequency (RF) switches for front-end modules (FEM) and low-noise figures in GaN low-noise amplifiers (LNAs), are broadening the applications of GaN into the mobile, artificial intelligence (AI), and quantum sectors. But this excellent performance comes with a high cost, due to limited wafer sizes and back-end-of-line (BEOL) metallization options. On the other hand, a Si complementary metal-oxide-semiconductor (CMOS) allows access to state-of-the-art 300-mm BEOL and digital circuit design.

Revolutionizing GaN chip design requires a holistic approach through integration with Si CMOS. This work, through these two approaches, makes three-dimensional (3D) GaN chips design more cost-effective while providing orders of magnitude improvement

over convention 2D-circuits in Si or GaN-only frontend-of-line (FEOL). With the combination of Si CMOS digital, bias, and matching chips, high-frequency GaN dielets are integrated in a highly scaled manner through using direct Cu-Cu bonding for several 3D-amplifier first demonstrations. Such integration offers low RF losses as well as near-seamless-bonding interfaces. Similarly, glass offers a low-cost packaging option for multi-chiplet systems. Large substrate sizes and panel thickness down to 30 µm enable the next generation of packaging for nano-systems at scale, while also allowing for novel thermal cooling solutions such as microfluidic, two-phase vapor, etc. With the lamination of low-loss dielectric Ajinomoto build-up film (ABF) layers in glass, a highly capable package for 3D-RF stacking can be created. This work integrates GaN dielets directly in this glass package for the first time; it also studies and quantifies their properties.

GEVO: Memory-Efficient Monocular Visual Odometry Using Gaussians

D. Gao, P. Z. X. Li, V. Sze, S. Karaman Sponsorship: Amazon, MathWorks Fellowship, NSF CPS

High-fidelity 3D scene reconstruction with a monocular camera supports applications on mobile devices like micro-robots and AR/VR headsets, where access to the off-chip memory dominates the compute energy. While Gaussian Splatting (GS) enables detailed reconstruction, existing GS-based SLAM systems are memory-inefficient because they store numerous past images to retrain Gaussians to prevent catastrophic forgetting, leading to excessive memory usage.

Thus, we present GEVO, a GS-based SLAM

framework that achieves comparable fidelity as prior works by rendering (instead of storing) them from the existing map. Novel Gaussian initialization and optimization methods are proposed to delay the degradation of the rendered images over time. In various environments, GEVO achieves comparable map fidelity with up to 94x lower memory overhead than prior works. Ultimately, GEVO facilitates the design of ASIC accelerators for real-time, high-fidelity, and low-energy reconstruction on mobile devices.



(a) Reconstruction before catastrophic forgetting



(b) MonoGS no past images 8 images stored (7 MB)



(c) GEVO (This work) 8 images stored (7 MB)



(d) MonoGS 114 images stored (100 MB)

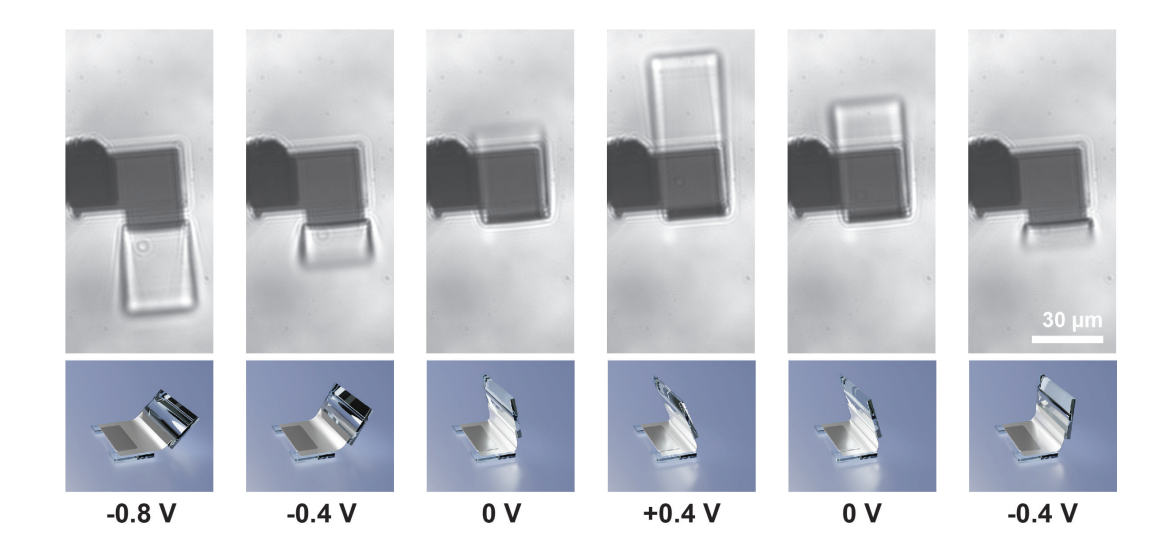
▲ Figure 1: The region (a) catastrophically forgets (b) when no past images are used to retrain. GEVO (d) maintains high fidelity with significantly lower memory overhead for storing images compared with prior work (c).

Ultra-thin Ruthenium Electrochemical Actuators

Z. Zheng, M. F. Reynolds, J. Clark, S. Norris, Q. Liu, N. L. Abbott, I. Cohen, P. L. McEuen Sponsorship: Cornell Center for Materials Research (DMR-1719875)

Electrochemical micro-actuators are essential components in micro-robotics, micro-fluidics, and biomedical devices. The surface electrochemical actuator (SEA) platform was developed by our group with atomic layer deposited (ALD) platinum and shown to provide locomotion in CMOS integrated micro-scale robots. Prior to the SEAs, there had been a lack of micron-scale actuator systems that can be processed with the standard semiconductor technology and well-integrated with on-board CMOS for control. Besides platinum, materials with similar properties have the potential to accomplish comparable functions and may possess advantageous properties like higher force output or

better durability. In this work, we investigate such actuators of nano-scale thickness fabricated with ALD ruthenium. Similar to the platinum version, these actuators operate at low-voltages, low-power, with high durability, and ample force output, while being entirely compatible with industrial standard microelectronics processing. Distinguishingly, though, these actuators show atomic layer etching (ALE) when driven at certain higher voltages, which allows us to have special control over the precise thickness and thereby motions of these actuators. Thus, we show ruthenium as a viable option for electrochemical micro-actuators with unique additional features.



 \triangle Figure 1: A sequence of optical images and schematics showing an actuator's motion in a 1 Hz sweep cycle between +0.4 and -0.8 V.

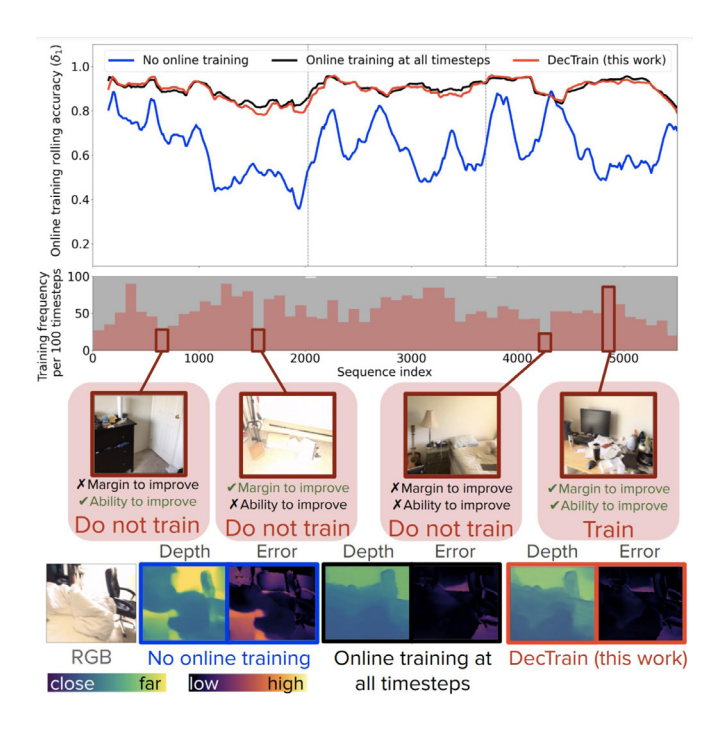
64

DecTrain: Deciding When to Train a Monocular Depth DNN Online

Z.-S. Fu, S. Sudhakar, S. Karaman, V. Sze Sponsorship: NSF, Real-Time Machine Learning Program Grant no. 1937501, MIT-Accenture Fellowship, Huang Phillips Fellowship, Gift from Intel

Monocular depth deep neural network (DNN) is useful for 3D reconstruction by predicting per-pixel depth of an RGB image. While using a monocular depth DNN can be more energy efficient and has a smaller form factor than traditional bulky and high-power physical depth sensors, it can deteriorate in accuracy when deployment data differs from training data. While performing online training at all timesteps can improve accuracy, it is computationally expensive. We propose DecTrain, a new algorithm that decides when to train a monocular depth DNN with self-supervision by comparing the cost of training with the predicted ac-

curacy gain. DecTrain maintains accuracy compared to online training at all timesteps on out-of-distribution data, while training only 44% of the time on average. We also compare the recovery of a low inference cost DNN using DecTrain and a more generalizable high inference cost DNN, and find DecTrain recovers the majority (97%) of the accuracy gain of online training at all timesteps while reducing computation compared to the high inference cost DNN which recovers only 66%. DecTrain enables low-cost online training for a smaller DNN to have competitive accuracy with a larger DNN at a lower overall computational cost.



▲ Figure 1: Compared to the baseline of online training at all timesteps (black) or no timesteps (blue), DecTrain (red) maintains the accuracy improvement of adaptation while training on only a subset of the timesteps.

Flexible Acoustically Active Surfaces Based on Piezoelectric Microstructures

T. Dang, J. Han, Z. Zheng, J. H. Lang, V. Bulović

Flexible acoustic transducers have gained significant attention due to their diverse applications in modern technologies, including active noise control, human-machine interfaces, ultrasonic imaging, and tactile sensing. Flexible speakers typically utilize electrostatic or piezoelectric effects to generate sound, with piezoelectric loudspeakers standing out for their ease of fabrication and low power consumption. Despite their advantages, most demonstrated flexible speakers show limited performance or require high operating voltages, restricting their practical use in applications involving potential human contact.

In this project, we develop a flexible thin-film acoustic transducer based on an ensemble of free-standing microstructures using a piezoelectric polyvinylidene fluoride (PVDF) sheet, targeting

potential wearable applications. The microstructure arrays are encapsulated between two layers of flexible substrates that not only protect the piezoelectric microstructures but also define their shapes while allowing free vibration. The performance evaluation of these speakers demonstrates excellent sound generation, achieving 60 dB at 1 kHz under 20V excitation. The speakers display broad bandwidths reaching up to 100 kHz, thanks to the high resonant frequencies of the fabricated microstructures. Additionally, the device consumes power at the milliwatt level, offering a substantial efficiency advantage over dynamic and thermoacoustic loudspeakers. Therefore, this lightweight, flexible and low-cost speaker could perform as an innovative interface for acoustic applications.

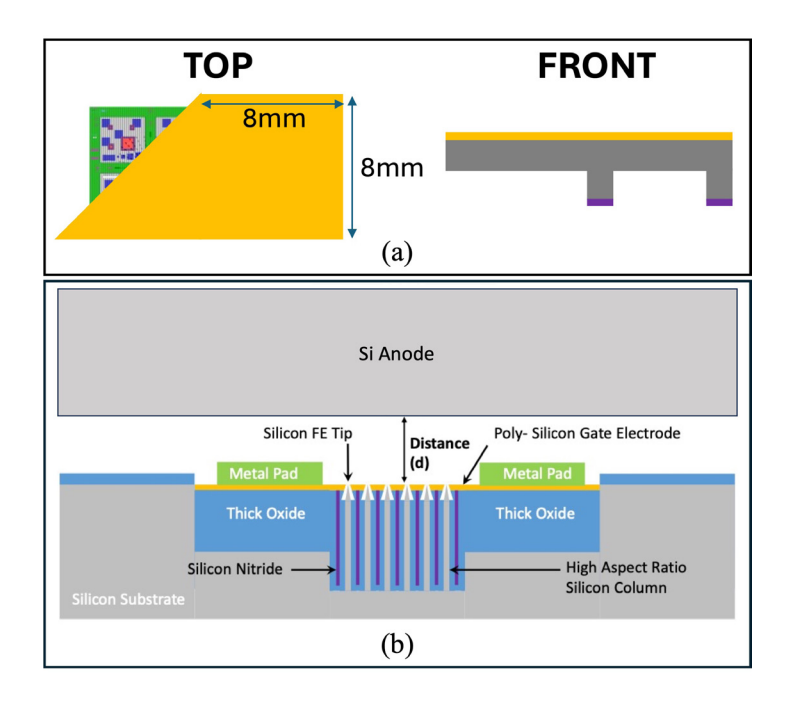
66

Anode Engineering to Reduce On-Resistance of Field Emitter Arrays

Y. Shin, W. Chern, N. Karaulac, A. I. Akinwande Sponsorship: AFOSR

Field emitter arrays (FEAs) are promising electron sources for high-power and high-frequency devices such as power switches and electric jet propulsion. The property of ballistic transport and high breakdown field make FEAs capable of low switching losses and on-resistance. However, prior optimization methods fail to account for changes in electrostatics along the vacuum channel due to the anode geometry and position, causing unfavorable phenomena in device characteristics.

In this work, we attempt to engineer the anode of FEAs, specifically for anodes configured with anode-to-emitter distances of 100m, using a MEMS fabricated silicon anode for on-chip integration. We find that the geometry and position of the anode improves the space charge limited (triode) regime of the FEA output characteristics, achieving lower on-resistance. These results pave a way to integrate FEAs into compact high-power switches for megawatt operation with comparable on-resistances with GaN and SiC.



▲ Figure 1: (a) Anode design of three layers consisting of silicon oxide (purple), silicon (gray), and TiAu (gold). The relative size of the flat anode is compared to a sample device chip. (b) Schematic of the experimental setup relative to the device.

Nanoscience & Nanotechnology

| Directly Grown Graphene Buffer Layers on Silicon Carbide Enable Remote Epitaxy of Gallium Nitride | 69 |
|--|----|
| Scalable Device Integration via III-V Epitaxy on Patterned 2D Materials | 70 |
| Revealing Metal Redox Pathways up to Ambient Pressure via in-situ Transmission Electron Microscopy | 71 |
| Atomic Lift-off of Epitaxial Membranes for Cooling-free Infrared Detection | 72 |
| Cross-correlated AFM and TERS Imaging of Janus Transition Metal Dichalcogenide Monolayers | 73 |
| Scalable, Defect-tolerant Spinodal Metamaterials with Tunable Mechanical Properties | 74 |
| Dynamic Mechanical Responses of Shell-based Spinodal Metamaterials | 75 |
| Atomic Layer Etching of Overlying Epitaxial Graphene on Graphene Buffer Layer for a Scalable Remote Epitaxy Template | 76 |
| Fluctuations in Superconducting Nanowires | 77 |
| Laser-induced Graphene Supercapacitors | 78 |
| Hydrogen Gas Detection with MoS2-based Chemical Sensing Platform | 79 |
| Signatures of Chiral Superconductivity in Rhombohedral Graphene | 80 |
| Domain-controlled Growth of Two-dimensional Tin Selenide | 81 |
| Molecular Probe Adsorption as a Technique to Elucidate Corona Phase Molecular Recognition (CoPhMoRe) through Structure Property Relationships | 82 |
| Optimizing Contact Resistance of GaN p-FET Devices for CMOS Applications | 83 |
| Optical Detection of Proximity Effect Between WSe2 and Multiferroic Helimagnet Nil2 | |
| On-site Growth of Perovskite Nanocrystal Arrays for Integrated Nanodevices | 85 |
| Probing Operational Degradation Mechanism on Cd-free Red and Blue QD-quantum dot LEDs | |
| Solid State Solar Energy Storage from Persistently Luminescent Solar Concentrators | 87 |
| Electrical Double Layer Force Enabled Wafer-scale Transfer of van der Waals Materials | 88 |

Directly Grown Graphene Buffer Layers on Silicon Carbide Enable Remote Epitaxy of Gallium Nitride

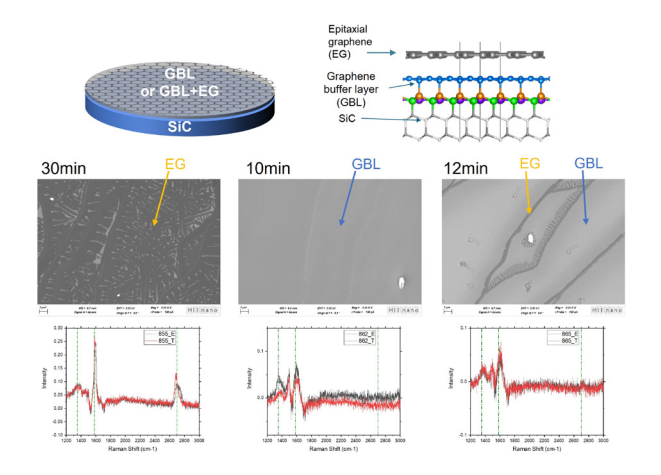
J. Kim, S. Lee, H. Kim, J. Kim, J. Lee, J. Feng, J. Kim Sponsorship: Samsung Display, Softepi

In the emerging technique of remote epitaxy, epitaxial films are grown on single-crystalline sub-strates coated with two-dimensional (2D) materials. Among these, graphene has been widely studied as a buffer layer and is typically transferred onto substrates via nickel-assisted delamination. However, this transfer process can damage the graphene, compromising the quality of the subsequent epitaxial film. To make matters worse, conventional epitaxial methods such as metal-organic chemical vapor deposition (MOCVD) present challenges, as reactive gases like H2 and NH3 can degrade graphene during high-temperature growth. To address this, we employ graphene buffer layers (GBLs) directly grown on silicon carbide (SiC), leveraging covalent bonding at the GBL-SiC interface while maintaining a van der Waals gap between GBL and the epitaxial films. This configuration enhances the stability of graphene under harsh growth conditions.

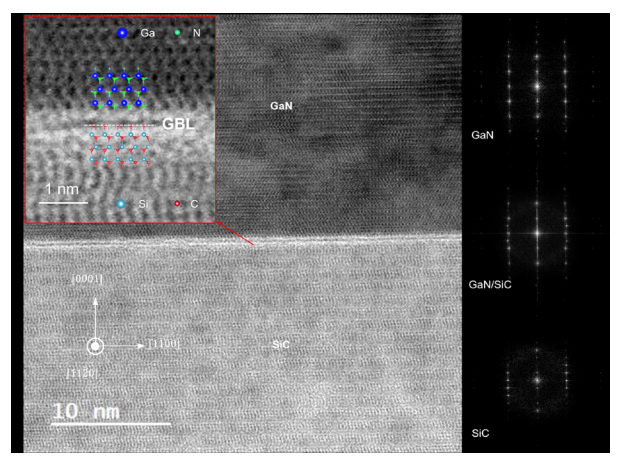
As Figure 1 shows, epitaxial graphene (EG) initially nucleates at step edges and subsequently extends

across terraces. Raman spectra, after subtraction of pristine SiC signals, exhibit the characteristic D (~1350 cm⁻¹), G (~1580 cm⁻¹), and 2D (~2700 cm⁻¹) peaks of graphene. The enhanced D peak and suppressed 2D peak confirm GBL formation. Based on these measurements, we identify the optimized growth conditions that suppress EG formation at step edges while enabling GBL growth on the substrate.

Subsequently, gallium nitride (GaN) is grown on GBL-coated SiC via MOCVD, as shown in Figure 2. Scanning transmission electron microscopy (STEM) confirms the preservation of the GBL after GaN growth, indicating its resilience under harsh MOCVD growth conditions. Corresponding fast Fourier transform (FFT) patterns indicate that GaN maintains a heteroepitaxial relationship with the SiC substrate, despite the presence of the GBL. These findings validate remote epitaxy, where the substrate's lattice information is transmitted through the graphene layer, enabling single-crystal GaN growth.



▲ Figure 1: Schematics of GBL and EG and their characterization by SEM and Raman. Fully covered EG shows strong 2D peaks; GBL-dominant regions exhibit stronger D peaks due to increased sp³ bonding.



▲ Figure 2: STEM cross section of GaN on SiC and corresponding FFT of GaN, GaN/SiC, and SiC. GBL remains after growth, confirming its stability. Diffraction confirms single-crystal GaN via remote epitaxy.

FURTHER READING

- S. Lee, J. Kim, B.-I. Park, H. Ik Kim, C. Lim, E. Lee, J. Y. Yang, J. Choi, et al. "GaN Remote Epitaxy on a Pristine Graphene Buffer Layer via Controlled Graphitization of SiC", Applied Physics Letts., vol. 125, p. 25, 2024.
- K. Qiao, Y. Liu, C. Kim, R. J. Molnar, T. Osadchy, W. Li, X. Sun, H. Li, et al. "Graphene Buffer Layer on SiC as a Release Layer for High-quality Free-standing Semiconductor Membranes," *Nano Letts.*, vol. 21, no. 9, pp. 4013-4020, 2021.
- Y. Kim, S. S. Cruz, K. Lee, B. O. Alawode, C. Choi, Y. Song, J. M. Johnson, C. Heidelberger, et al. "Remote Epitaxy Through Graphene Enables Two-dimensional Material-based Layer Transfer," *Nature*, vol. 544, no. 7650, pp. 340-343, 2017.

Scalable Device Integration via III-V Epitaxy on Patterned 2D Materials

N. M. Han, K. Lu, D. Kwon, C. Chang, J. Kim Sponsorship: Defense Advanced Research Projects Agency

The integration of high-mobility III-V semiconductors on scalable platforms is a critical step toward advancing future generations of high-performance electronic and optoelectronic devices. However, conventional III-V/Si heteroepitaxy faces severe challenges due to lattice and polarity mismatch, leading to high densities of threading dislocations and antiphase boundaries that degrade device performance. Existing approaches such as graded buffer layers and aspect ratio trapping have achieved partial success but still suffer from thick buffers, residual defects, and limited scalability.

Our research explores a novel integration strategy based on selective-area epitaxy of III-V materials on patterned two-dimensional (2D) materials. 2D materials like graphene serve as atomically thin, flexible buffer layers that mediate the lattice mismatch and allow lateral strain relaxation without generating dislocations. By engineering nanometer-scale openings (nanoholes) in the 2D layer, we localize III-V nucleation on the underlying substrate while suppressing unwanted nucleation elsewhere, enabling selective and defect-minimized epitaxy.

As a first step, we have demonstrated successful deoxidation of silicon substrates beneath nanoholes, enabling the nucleation of relaxed and dislocation-free GaAs crystals directly on silicon, as verified by high-resolution transmission electron microscopy. Furthermore, we have achieved a lateral-to-vertical growth rate ratio of approximately 20×, allowing efficient lateral overgrowth without significantly

increasing the vertical thickness. This high lateral growth rate is critical for eventual coalescence of adjacent III-V nuclei without the need for thick layers, offering a pathway toward ultrathin device channels.

Looking ahead, our next milestones include achieving full merging of III-V nuclei, characterizing the presence and nature of any defects at the coalescence boundaries, and fabricating and testing devices to benchmark electrical performance. While ${\rm SiO}_2$ trench confinement has been proposed to further control nucleation density and merging, it has not yet been implemented in the current stage of the work.

Ultimately, our approach aims to enable monolithic, transfer-free integration of III-V materials onto complementary metal-oxide-semiconductor-compatible platforms with minimal defects and atomically sharp heterojunctions. By circumventing the limitations of traditional heteroepitaxy, this technique could significantly advance the development of high-mobility transistors, such as III-V multiquantum well metal-oxide semiconductor field-effect transistors and gate-all-around structures, as well as low-defect optoelectronic devices.

Our preliminary success in demonstrating dislocation-free nucleation and efficient lateral overgrowth represents a major step toward scalable heterogeneous integration using 2D material-assisted epi-taxy. This platform holds promise for revolutionizing device scaling strategies and extending Moore's Law into new frontiers.

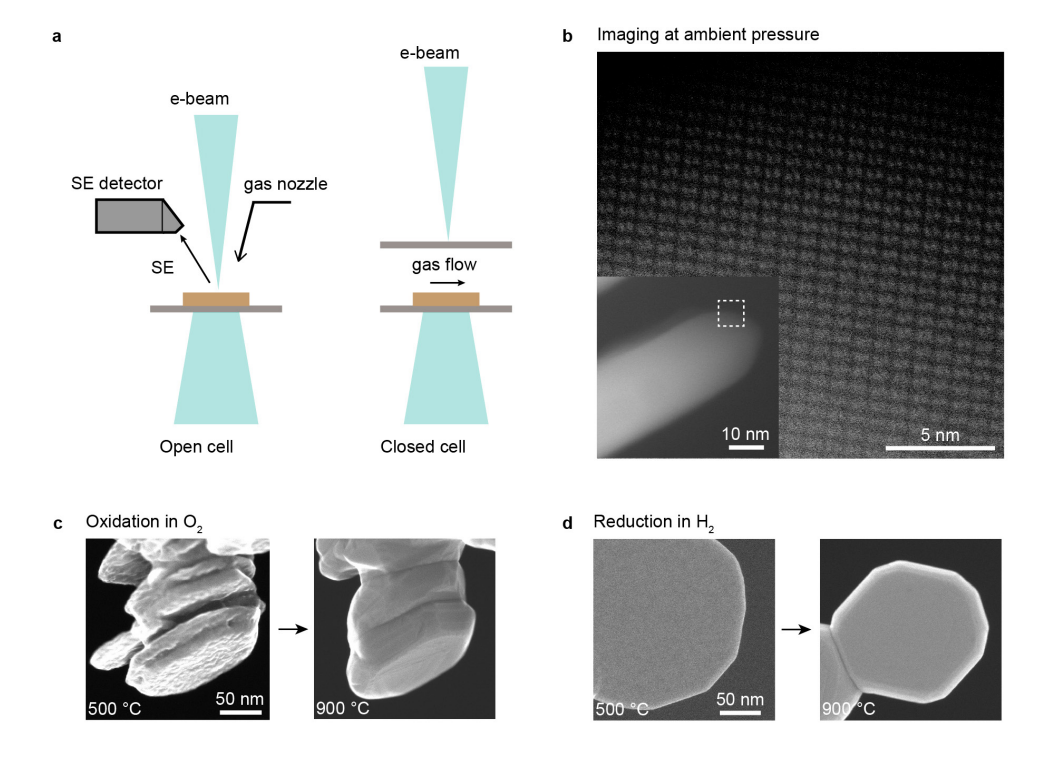
Revealing Metal Redox Pathways up to Ambient Pressure via in-situ Transmission Electron Microscopy

H. Wu, F. M. Ross

Sponsorship: Center for Electrification and Decarbonization of Industry, Seagate

Metal redox reactions are ubiquitous in nature (e.g., geological processes) and industrial applications. Understanding how materials evolve in morphology and structure at the nanoscale during such reactions in gaseous environments is critical for advancing catalysis, energy storage, and semiconductor technologies. Advances in transmission electron microscopy (TEM), microfabrication, and microelectromechanical systems have enabled the direct exposure of samples to a controlled gas environment at elevated temperatures within the microscope column. Gas can be introduced at low pressures (up to tens of millibars) using differential pumping or confined between two thin silicon nitride membranes in a closed-cell specimen holder (up to ambient pressure). Both approaches have proven effective in revealing atomistic mechanisms governing metal redox reactions. However, the effects of gas pressure on kinetic phase transformation pathways, particularly on transient surface morphological evolution during redox reactions, remain poorly understood.

In this project, we investigate metal redox reactions in various gaseous environments across different pressures using Characterization.nano's Hitachi HF5000-IS environmental TEM (ETEM) with a secondary electron (SE) detector (Figure 1). We visualize redox reactions occurring in a range of metal and alloys (Fe-, Zn-, and Ni-based alloys) under gases, including H2, O2, methanol, and water vapor, up to ambient pressure. These experiments demonstrate that atomic resolution can be obtained under ambient pressure conditions and enable us to identify several transient phase transformation pathways during the early stages of oxidation and reduction of metals. The simultaneous SE imaging enabled us to understand the surface morphological changes taking place during these reactions, including the removal of surface ligand layers and the development of surface faceting. We anticipate these advances will broaden the application of in-situ gas phase TEM for studying dynamic material processes.



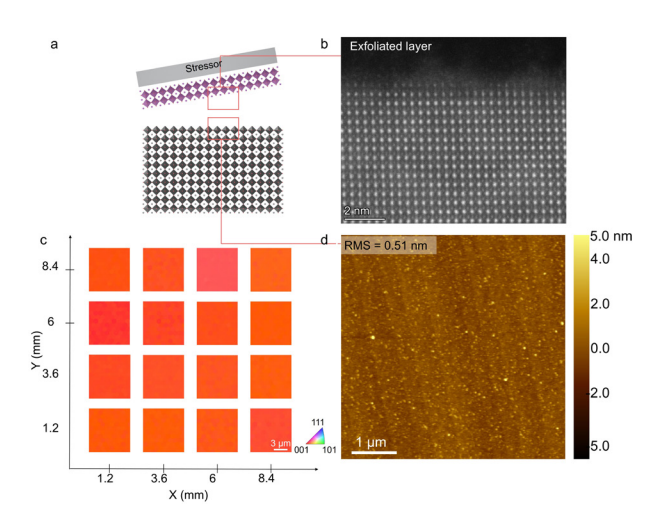
 \triangle Figure 1: (a) Schematics of setups for gas-phase TEM imaging. (b) Atomic-resolution image of magnetite in O_2 at am-bient pressure. (c-d) Secondary electron images showing the morphological evolution of magnetite oxidation in O_2 (c) and hematite reduction in H_2 (d).

Atomic Lift-off of Epitaxial Membranes for Cooling-free Infrared Detection

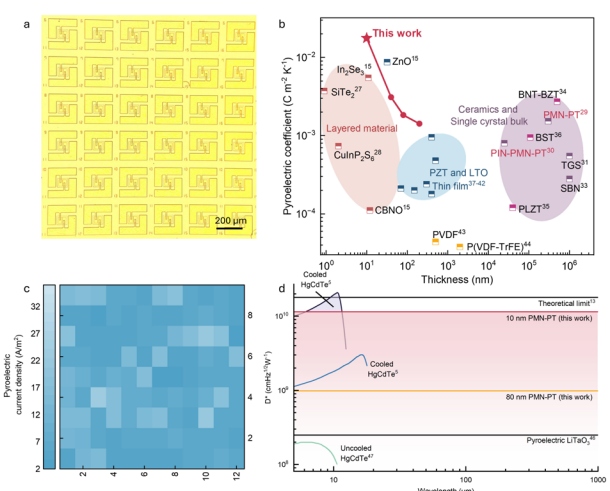
X. Zhang, O. Ericksen, S. Lee, M. Akl, M-K. Song, H. Lan, P. Pal, J. M. Suh, S. Lindemann, J-E. Ryu, Y. Shao, X. Zheng, N. M. Han, B. Bhatia, H. Kim, H. S. Kum, C. S. Chang, Y. Shi, C.-B. Eom, J. Kim Sponsorship: Air Force Office of the Scientific Research

Recent breakthroughs in ultrathin, single-crystalline, freestanding complex oxide systems have sparked industry interest in their potential for next-generation commercial devices. However, the mass production of these ultrathin complex oxide membranes has been hindered by the challenging requirement of inserting an artificial release layer between the epilayers and substrates. Here we introduce a technique that achieves atomic precision lift-off of ultrathin membranes without artificial release layers to facilitate the high-throughput production of scalable, ultrathin, freestanding perovskite systems (Figure 1). Leveraging both theoretical insights and empirical evidence, we

have identified the pivotal role of lead in weakening the interface. This insight has led to the creation of a universal exfoliation strategy that enables the production of diverse ultrathin perovskite membranes less than 10 nm thick. Our pyroelectric membranes demonstrate a record-high pyroelectric coefficient of 1.76×10^{-2} C m⁻² K⁻¹, attributed to their exceptionally low thickness and freestanding nature (Figure 2). Moreover, this method offers an approach to manufacturing cooling-free detectors that can cover the full far-infrared (FIR) spectrum, marking a notable advancement in detector technology.



▲ Figure 1: Atomic lift-off (ALO) of epitaxial ultrathin membranes at a large scale. (a) Schematic of ALO process. (b) Cross-section transmission electron microscopy image of exfoliated membrane. (c) Electron backscatter diffraction maps over the entire membrane. (d) Atomic-force microscopy image of substrate after exfoliation.



▲ Figure 2: Potential application towards cooling-free FIR imaging. (a) Optical image of pyroelectric device array fabricated on $Pb(Mg_{1/3}Nb_{2/3})O_3$ - $PbTiO_3$ membrane. (b) Benchmark plot showing pyroelectric coefficients. (c) Mapping of the performance of device array. (d) Specific detectivity evaluations as a function of wavelength for our detector vs. commercial ones.

FURTHER READING

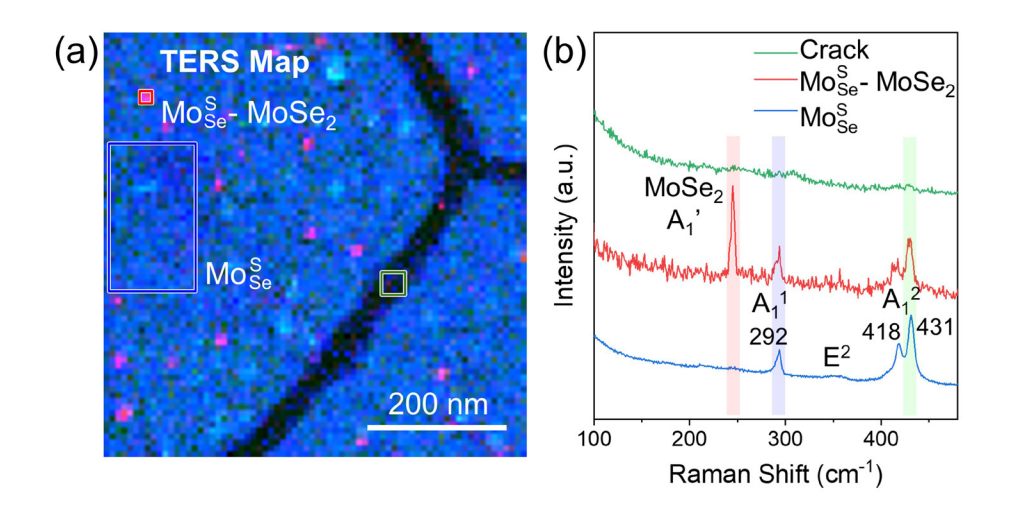
 X. Zhang, O. Ericksen, S. Lee, M. Akl, and J. Kim, "Atomic Lift-Off of Epitaxial Membranes for Cooling-Free Infrared Detection," Nature, vol. 641, pp. 98-105, May 2025.

Cross-correlated AFM and TERS Imaging of Janus Transition Metal Dichalcogenide Monolayers

T. Zhang, A. Krayev, T. H. Yang, N. Mao, L. Hoang, Z. Wang, H. Liu, Y. R. Peng, A. Mannix, J. Kong Sponsorship: U.S. Department of Energy, Office of Science, Basic Energy Sciences under Award DE-SC0020042.

Two-dimensional (2D) Janus transition metal dichalcogenides (TMDs) are intriguing material candidates for various applications such as non-linear optics, energy harvesting, and catalysis. These materials are usually synthesized via chemical conversion of pristine TMDs, and reliable and high-resolution characterization of the obtained Janus materials' morphology and composition is highly desired for both the synthesis optimization and device applications. In this work, we present a cross-correlated atomic force microscopy (AFM) and tip-enhanced Raman spectroscopy (TERS) study of Janus and Janus monolayers synthesized by the hydrogen plasma-assisted chemical conversion of MoSe₂ and MoS₂, respectively. Effects of strain and substrates

during the Janus conversion process on the morphology of resulting Janus TMD materials are revealed. Moreover, the TERS characterization shows nanoscale MoSe₂-Janus vertical heterostructures (~20-nm sizes) that become hidden under conventional far-field optical characterization, suggesting the power of using near-field approaches to avoid misconceptions in the composition of Janus TMDs. Our work indicates that cross-correlated AFM and TERS have great capability for studying nanoscale composition and defects in Janus TMD monolayers. The obtained insights into morphology and composition should be useful for further optimizing the Janus conversion approach towards uniform and wrinkle-/crack-free Janus materials.



▲ Figure 1: (a) TERS map showing intensity distribution of correspondingly highlighted Raman modes in panel (b): $MoSe_2A_1$ ' (red), A_1 ' (green), and $A1^1$ (blue). Map clearly identifies Janus monolayer (blue rectangle), nanoscale $MoSe_2$ -Janus vertical heterostructures (red square), and crack (green square) regions. (b) TERS spectra averaged over Janus monolayer , nanoscale $MoSe_2$ -Janus vertical heterostructures, and crack regions marked in (a).

FURTHER READING

[•] T. Zhang, A. Krayev, T. H. Yang, N. Mao, L. Hoang, Z. Wang, H. Liu, Y. R. Peng, et al., "Synthesis-related Nanoscale Defects in Mo-based Janus Monolayers Revealed by Cross-correlated AFM and TERS Imaging," arXiv:2503.22861 [cond-mat.mtrl-sci].

Scalable, Defect-tolerant Spinodal Metamaterials with Tunable Mechanical Properties

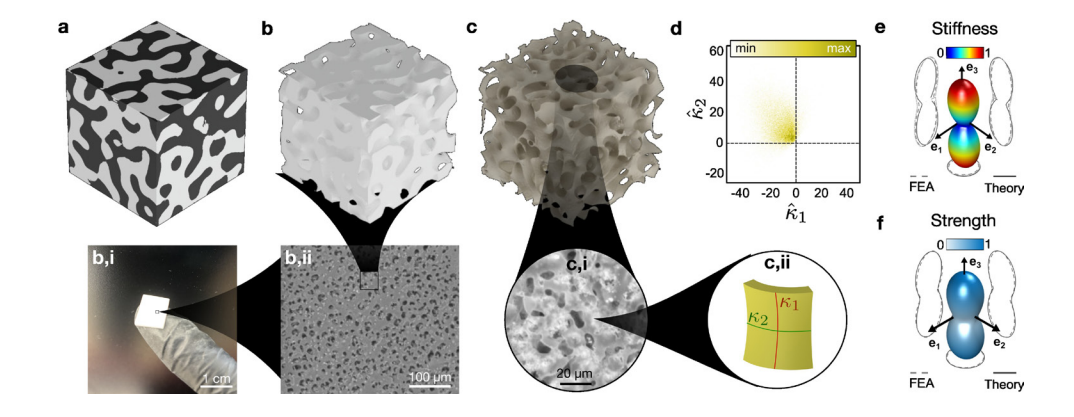
S. Dhulipala, M. A. Espinal, C. M. Portela Sponsorship: NSF CAREER

Spinodal metamaterials, non-periodic, bicontinuous structures inspired by nature, offer a scalable pathway to fabricating lightweight, high-performance materials with exceptional mechanical properties. Unlike truss-based lattices, which concentrate stress and rely on geometric periodicity, spinodal architectures eliminate sharp junctions and distribute stress smoothly through doubly curved shells. These features, combined with their compatibility with self-assembly and coating-based synthesis, open avenues for scale-bridging fabrication.

This work presents scalable strategies for generating spinodal geometries. We induce spinodal decomposition in epoxy-based polymer systems to produce large-scale templates with smooth, interconnected channels. Conformal nanocoating of these templates using ceramic thin films such as alumina followed by removal of the polymer template produces hollow, shell-based spinodal metamaterials with controlled wall thickness and curvature. Additionally, these templates are digitally

reconstructed using micro-scale X-ray computed tomography (XCT), enabling both structural characterization and theoretical modeling. To quantify how geometry affects performance, we introduce new curvature-based metrics for predicting anisotropic stiffness and strength. Local curvature distributions, derived from principal curvature maps, strongly correlate with measured and simulated mechanical response. These predictions are validated through two-photon lithography prototypes tested under in-situ nanomechanical compression, as well as finite element simulations. Our approach enables rational design and optimization of spinodal structures by controlling curvature anisotropy to tune mechanical properties.

With this scalable fabrication platform and new geometric framework, spinodal meta-materials emerge as a versatile solution for next-generation lightweight structures, overcoming the limitations of periodic lattices in defect tolerance, scalability, and mechanical tunability.



▲ Figure 1: Overview of scalable spinodal metamaterials. (a) Three-dimensional (3D) rendering of the spinodal decomposition process. (b) Epoxy template derived from spinodal decomposition, including (b,i) a large-scale fabricated template and (b,ii) scanning electron microscopy (SEM) image showing its bicontinuous morphology. (c) 3D rendering of a shell-based spinodal metamaterial, with (c,i) SEM image of an alumina spinodal shell structure and (c,ii) schematic illustrating the principal curvature directions on a representative shell element. (d) Distribution of principal curvature in the shell-based spinodal geometry. Theoretically predicted anisotropic (e) stiffness and (f) strength, derived from curvature-based geometric metrics.

FURTHER READING

C. M. Portela, A. Vidyasagar, S. Krödel, T. Weissenbach, D. W. Yee, J. R. Greer, and D. M. Kochmann, "Extreme Mechanical Resilience of Self-assembled Nanolabyrinthine Materials," Proc. Natl. Acad. Sci. U.S.A., vol. 117, no. 11, pp. 5686-5693, 2020. DOI.org/10.1073/pnas.1916817117

[•] S. Dhulipala, and C. M. Portela, "Curvature-Guided Mechanics and Design of Spinodal and Shell-Based Architected Materials," arXiv preprint arXiv:2505.21509, 2025. [Link]

Dynamic Mechanical Responses of Shell-based Spinodal Metamaterials

R. T. Kommalapati, C. M. Portela

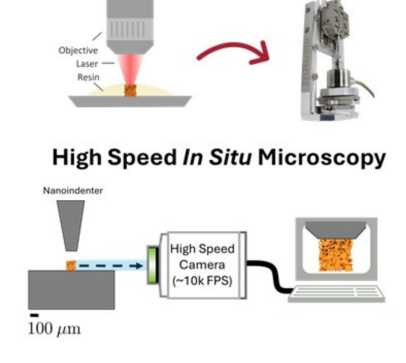
Architected materials are engineered materials that realize unique properties like near-optimal stiffness, strength, and energy absorption, mitigating vibrations or even focusing and guiding waves. There is high demand for lightweight materials with high energy absorption in many applications such as energy-absorbing bumpers, lightweight protective cladding, or shock-resistant medical impacts. Traditionally, architected materials have required high-resolution additive manufacturing to construct their carefully designed microstructure, a time- and cost-intensive process that can introduce significant performance-degrading defects. One area of recent interest has been spinodal metamaterials, which are the result of a natural phase separation process, granting a potential path to defect-free, inexpensive, and scalable fabrication. The resulting structures are aperiodic and asymmetric, consisting of smoothly connected shells with double curvature, analogous to an eggshell. Existing work has demonstrated that these spinodal metamaterials exhibit near-optimal stiffness-to-density, have highly customizable directional properties (anisotropy), and high recoverability. However, their performance under dynamic loading—pertinent to their potential application to engineering problems—remains unexplored.

this work, we computationally and experimentally demonstrate how curvature in shellbased spinodal metamaterials determines their ratedependent mechanical responses. To do this, we model the phase separation process and fabricate spinodal structures using two-photon lithography—a highresolution, three-dimensional printing process—and then perform nanomechanical dynamic experiments with high speed in situ microscopy to observe deformation modes and behavior. We demonstrate ratestiffening in spinodal metamaterials that surpasses (by ~50%) the expected rate-stiffening of the constituent material. Through computational studies of both spinodal and reference periodic architectures, we reveal that shell-based spinodal metamaterials exhibit a wide range of localization responses due to their double curvature and aperiodicity relative to periodic architectures. These findings offer a pathway for the design of energy-absorbing metamaterials with enhanced and programmable rate sensitivity and suggest spinodal architectures as a promising route toward scalable, application-ready dynamic materials.

Dynamic Behavior of Architected Materials

Shell-Based Architectures Periodic Beam-Based Architectures

Dynamic Nanomechanical Experiments Fabrication Experiment



▲ Figure 1: Dynamic behavior of Shell-based architected materials.

Atomic Layer Etching of Overlying Epitaxial Graphene on Graphene Buffer Layer for a Scalable Remote Epitaxy Template

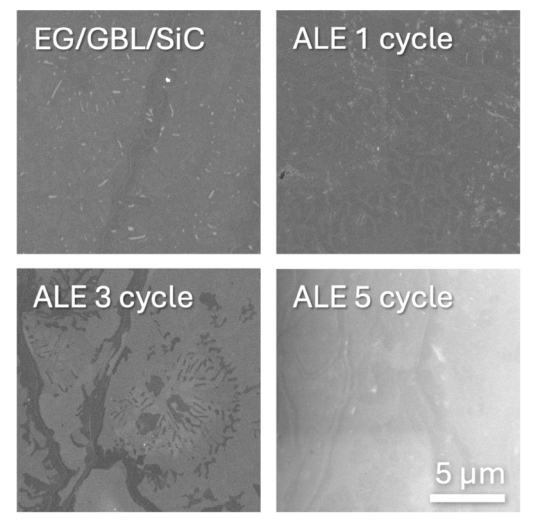
J. Lee, J. Feng, J. Kim, S. H. Cho, S. Lee, J. Kim, J. Kim

Freestanding single-crystal membranes hold transformative potential for next-generation electronic and optoelectronic devices due to their ultrathin form factor, flexibility, and integra-tion versatility. Among fabrication techniques, remote epitaxy has emerged as a powerful route to produce transferable single-crystal membranes by leveraging long-range electrostatic interactions through atomically thin two-dimensional (2D) interlayers. Graphene buffer layers (GBLs) formed on silicon carbide (SiC) substrates via high-temperature graphitization have gained attention as ideal 2D templates. However, conventional graphitization unavoidably gen-erates overlying epitaxial graphene (EG) layers on top of the GBL, which must be selectively removed to maximize remote interaction and substrate pattern transfer. Previous EG removal methods—such as mechanical exfoliation or chemical etching-often degrade the underlying GBL, hindering remote epitaxy performance.

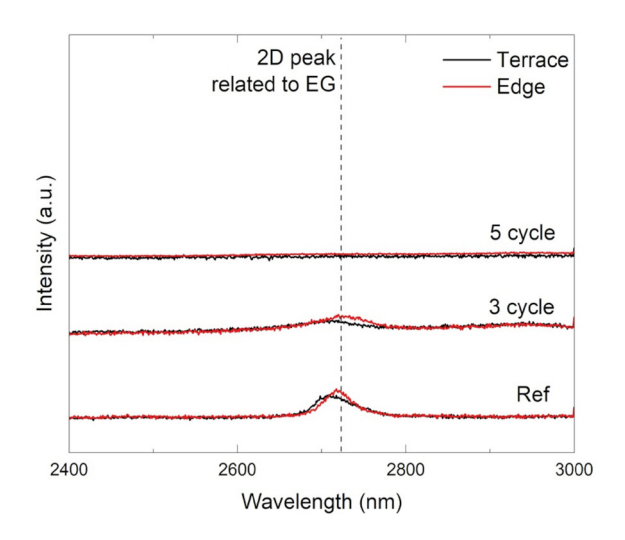
In this work, we introduce a selective atomic layer etching (ALE) technique to remove EG while

preserving the integrity of the underlying GBL. Our approach exploits the differential bonding strengths: EG is weakly bound to the sp²-hybridized GBL, whereas the GBL is partially covalently bonded to the SiC substrate. By tailoring etching conditions to this interfacial energy contrast, we achieve layer-by-layer removal of EG without damaging the GBL. Surface and structural analyses confirm the preservation of a pristine, atomically flat GBL surface—essential for enhancing remote substrate interaction and enabling high-quality remote epitaxi-al growth.

This ALE-based approach provides a scalable route to prepare high-quality GBL templates for remote epitaxy. Building on this foundation, we aim to demonstrate the growth and exfoli-ation of freestanding GaN membranes via remote epitaxy in future work. Our results lay the groundwork for defect-free GBL engineering and highlight a critical step toward realizing wafer-scale manufacturing of freestanding semiconductor membranes.



▲ Figure 1: Scanning electron microscopy (SEM) top-view for before/after of atomic layer etching of EG on GBL/SiC substrate – EG removal in SEM with ALE 5 cycle.



▲ Figure 2: Raman analysis for ALE of EG on GBL/SiC substrate – 2D peak disappearance in Raman with ALE 5 cycle.

FURTHER READING

S. Lee, J. Kim, B.-I. Park, H. I. Kim, C. Lim, E. Lee, J. Y. Yang, J. Choi, Y. J. Hong, C. S. Chang, H. S. Kum, J. Kim, K. Lee, H. Kim, and G.-C. Yi, "GaN Remote Epitaxy on a Pristine Graphene Buffer Layer via Controlled Graphitization of SiC," Appl. Phys. Letts. DOI: 10.1063/5.0235653

Fluctuations in Superconducting Nanowires

E. Batson, A. Jacquillat, A. Simon, F. Incalza, R. Foster, K. K. Berggren Sponsorship: NSF GRFP Grant No. 2141064, NSF CQN Grant No. EEC1941583

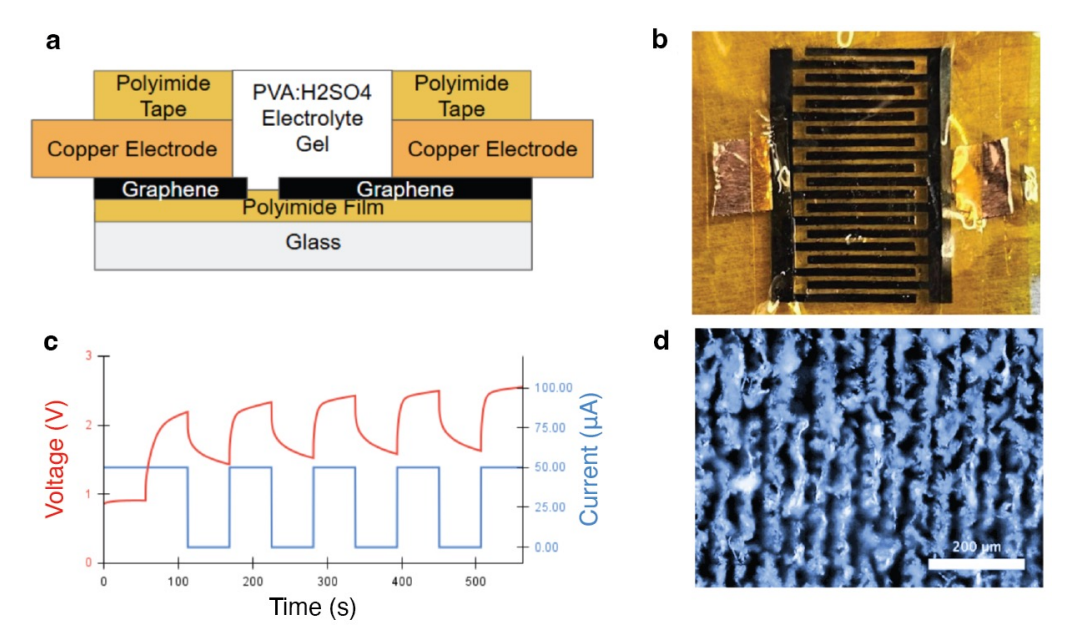
Superconducting nanowire single photon detectors (SNSPDs) provide sensitive, highly efficient detection out into the mid-infrared, suitable for low-signal applications like exoplanet search, quantum networking, and biomedical imaging. However, the physics of these devices is complex, and the detection mechanism is not well understood, which makes it difficult to predict the success of new material platforms or develop designs that decrease dark counts while preserving high detection efficiency. In this work, we study dark fluctuations in niobium nitride nanowires of various lengths and widths and compare the fluctuation rates to various models of the underlying mechanism. We evaluate whether it is more appropriate to attribute these fluctuations to one-dimensional phase slips or two-dimensional vortices activated by either flux entry or a topological phase transition. We also consider the role of external noise sources such as blackbody radiation or current source noise.

Laser-induced Graphene Supercapacitors

A. Arroyo, C. Lowe, F. Kelley, E. Szczepaniak, K. Muhammad, P. Jastrzebska-Perfect Sponsorship: MIT EECS, 6.2540 class

Supercapacitors, which demonstrate power densities comparable to those of batteries while providing fast charging and discharging capabilities, have gained favor in energy storage applications requiring fast power transfer, like electric vehicles or power grids. To achieve high capacitances, porous electrodes, which maximize electrolyte-electrode interaction, are utilized. For supercapacitors to be generally applied, scalable, repeatable, and cost-effective methods for fabricating such electrodes are required. Here, we demonstrate a meth-

od for manufacturing supercapacitors based on high surface area laser-induced graphene electrodes. We use a laser-based fabrication process that enables tuning of the electrode conductivity through empirically-determined power-conductivity relationships. Through optimization of laser power level, substrate choice, and details of the optical setup, we achieve devices with a specific capacitance of 0.7 mF/cm². This approach provides an accessible and scalable method for manufacturing graphene supercapacitors.



▲ Figure 1: a) Illustration of the designed supercapacitor's cross section. b) Image of a working supercapacitor. c) Charge and discharge curves of a working capacitor when applying pulses of current. d) Microscope image of laser-induced graphene surface.

Hydrogen Gas Detection with MoS₂-based Chemical Sensing Platform

C.-H. Liu, J. Zhu, C. Lopez Angeles, H. Feng, T. Swagger, J. Kong, T. Palacios Sponsorship: Palacios Lab

Hydrogen is a promising candidate as a clean energy carrier for its high energy density, clean combustion byproduct, and versatile end use. However, its explosive nature calls for the need for rapid and accurate detection. Two dimensional (2D) materials are ideal candidates for such application thanks to their naturally surface-sensitive properties and large surface-to-volume ratio, providing high sensitivity towards the target gas.

In this work, we developed a field effect transistor-based sensor that employs functionalized molybdenum disulfide (MoS₂) as the channel material.

Threshold voltage shift under hydrogen and surface functionalization of the ${\rm MoS}_2$ to further enhance sensitivity are demonstrated. Thanks to the 8" low-temperature (< 400 °C) synthesis of high-quality ${\rm MoS}_2$, the ${\rm MoS}_2$ sensors can be further integrated into a robust sensing array in which each device can be functionalized with different sensing materials and combinations. Future work involves the development of a high-speed readout electronic circuit with a total processing speed below 1 second, establishing an integrated system that can perform rapid measurement, analysis, and real-time chemical recognition.

FURTHER READING

[•] J. Zhu, J. Park, S. A. Vitale, et al., "Low Thermal Budget Synthesis of Monolayer Molybdenum Disulfide for Silicon Back-end-of-line Integration on 200 mm Platform," Nat. Nanotechnol. 18, 456-463 (2023).

Signatures of Chiral Superconductivity in Rhombohedral Graphene

T. Han, Z. Lu, Y. Yao, L. Shi, J. Yang, J. Seo, S. Ye, Z Wu, M Zhou, H. Liu, G. Shi, Z. Hua, K. Watanabe, T. Taniguchi, P. Xiong, L. Fu, L. Ju

Sponsorship: DOE (DE-SC0025325), NSF (DMR-2225925), NSF (DMR-1231319)

Chiral superconductors are unconventional superconducting states that break time reversal symmetry spontaneously and typically feature Cooper pairing at non-zero angular momentum. Such states may host Majorana fermions and provide an important platform for topological physics research and faulttolerant quantum computing. Despite intensive search and prolonged studies of several candidate systems, chiral superconductivity has remained elusive so far. Here we report the discovery of robust unconventional superconductivity in rhombohedral tetra-layer graphene. We observed two superconducting states in the gate-induced flat conduction bands with Tc up to 300 mK and charge density no as low as 2.4 x 10^{11} cm^{-2} in three different devices, where electrons reside close to a proximate WSe, layer, far away from WSe, and in the absence of WSe, respectively. Spontaneous time-reversal-symmetry-breaking (TRSB) due to electron's orbital motion is found,

and several observations indicate the chiral nature of these superconducting states, including: 1. In the superconducting state, R_{xx} shows fluctuations at zero magnetic field and magnetic hysteresis in varying outof-plane magnetic field B_⊥, which are absent from all other superconductors; 2. one superconducting state develops within a spin- and valley-polarized quartermetal phase, and is robust against the neighboring spin-valley-polarized quarter-metal state under B1; 3. the normal states show anomalous Hall signals at zero magnetic field and magnetic hysteresis. We also observed a critical B₊> 0.9 T, higher than any graphene superconductivity reported so far and indicates a strong-coupling superconductivity close to the BCS-BEC (Bardeen-Cooper-Schrieffer - Bose-Einstein condensate) crossover. Our observations establish a pure carbon material for the study of topological superconductivity, and pave the way to explore Majorana modes and topological quantum computing.

Domain-controlled Growth of Two-dimensional Tin Selenide

Y. Zhu, T. Zhang, N. Mao, J. Wang, J. Kong Sponsorship: DOE Basic Energy Sciences under Award DE-SC0020042

Two-dimensional (2D) van der Waals (vdW) layered materials have become a hot research topic in the fields of condensed matter physics and materials science due to their unique low-dimensional crystal structures and physical properties. 2D tin selenide (SnSe) is a vdW layered material with a strong spontaneous ferroelectric polarization and second-order nonlinear optical response, whose ferroelectric properties and second-order nonlinear optical characteristics are enhanced in its ferroelectric-stacking (FE-stacking) phase, a metastable phase at room temperature. Large-sized ultrathin 2D SnSe crystals have been synthesized via a physical vapor deposition (PVD) approach, but the control of FE-stacking and domain distribution remains a challenge.

In this work, the domain control of 2D SnSe

is preliminarily achieved by growth condition modulation and substrate engineering. A PVD growth recipe for 2D SnSe is optimized, that yields the most FE-stacking phase crystals, and a dependence of domain distribution density on substrate condition is identified. A pre-annealing treatment of the mica substrate in air not only improves the 2D SnSe samples' size and distribution on substrate, but also promotes the synthesis of samples with dense FE-stacking domains. The next step is to apply an electric field to the 2D SnSe material during PVD growth, which modulates the energy of the FE-stacking metastable phase compared to the stable phase, providing a possible pathway to achieve the controlled growth of FE-stacking 2D SnSe.

Molecular Probe Adsorption as a Technique to Elucidate Corona Phase Molecular Recognition (CoPhMoRe) through Structure Property Relationships

G. Sánchez-Velázquez, D. T. Khong, M. Park, X. Jin, X. Gong, Z. Yuan, M. C.-Y. Ang, M. S. Strano Sponsorships: NSF Graduate Research Fellowship Program, Singapore-MIT Alliance for Research & Technology (SMART)

The nanoparticle corona—a molecular layer adsorbed on nanoparticle surfaces—is critical in controlling molecular interactions for applications in catalysis, separations, and sensing technologies like Corona Phase Molecular Recognition (CoPhMoRe). While tailoring the corona has enabled detection of diverse analytes, quantitatively characterizing it remains challenging. Here, we advance Molecular Probe Adsorption (MPA) to address this issue. MPA employs a fluorescent probe quenched upon adsorption to quantify the solvent-exposed surface area via adsorption isotherms. We use MPA to elucidate recognition mechanisms in various corona phases and expand the library by characterizing new CoPhMoRe constructs, enabling comprehensive comparative analyses. We further develop structureproperty relationships linking MPA area to adsorption parameters. Additionally, we investigate how polymer

stiffness, characterized by persistence length, influences corona formation on single-walled carbon nanotubes (SWCNTs). Contrary to the assumption that stiffer polymers enhance adsorption efficiency, our results indicate that more flexible polymers achieve greater surface coverage, offering new insights for optimizing polymer-based corona phases. We also tackle the inverse problem of predicting analyte binding affinities by integrating MPA with molecular dynamics simulations and thermodynamic modeling, demonstrating that computational CoPhMoRe screening is feasible. This integration paves the way for rational sensor design without extensive experimental screening. Our findings highlight MPA's utility in advancing nanomaterial-based sensing technologies through quantitative corona characterization and provide a framework for the rational design of selective nanosensors.

Optimizing Contact Resistance of GaN p-FET Devices for CMOS Applications

J. Park, J. Niroula, J. Hsia, T. Palacios Sponsorship: Lincoln Laboratory

Gallium nitride (GaN) transistors have a much higher break-down voltage, switching frequency, and maximum operating temperature than their silicon (Si) counterparts. However, because GaN transistors are largely limited in performance by the Si gate driver and other ancillary chips, GaN transistors need to be integrated with GaN driver chips to fully realize their energy efficiency in power electronics applications and high-temperature environments. The most energy-efficient architecture for integrated circuits and drivers is complementary metal oxide semiconductor (CMOS) circuitry, which requires n-type field effect transistors (n-FETs) and p-type field effect transistors (p-FETs). While GaN n-FETs have been widely demonstrated,

GaN p-FETs are traditionally difficult to fabricate with good performance and integrate into CMOS circuits.

A primary source behind the current density limitations of a GaN p-FET device is the high contact resistance. Prior work in the Palacios group at the Massachusetts Institute of Technology (MIT) has shown record GaN p-FET performance; however, these devices are still largely limited by the contacts. In this project, we will explore different deposition methods and metals for achieving low contact resistance on GaN p-FETs. Ultimately, this work on improving contact resistance of GaN p-FETs will enable a fully integrated GaN-based CMOS platform.

Optical Detection of Proximity Effect Between WSe_2 and Multiferroic Helimagnet Nil_2

M. Shankar, Q. Song, R. Comin Sponsorship: National Science Foundation (DMR-2405560), Peskoff Physics Fellowship

Magnetic proximity effects have been widely investigated in layered heterostructures to imprint the properties of one material to be detected on the other. In many cases, studying the proximity effect of a magnetic material on another material can reveal properties about the former that are not otherwise straightforward to detect. NiI, is a type-II multiferroic that exhibits a simultaneous ferroelectric and non-collinear helimagnetic transition at T_N = 59.5 K, where the spin helix has propagation vector q = (0.138, 0, 1.457) RLU. It exhibits strong optical linear dichroism related to the ferroelectric transition, but direct optical detection methods of the chirality of the spin helix, which is coupled to the direction of the ferroelectric polarization, have remained elusive. Monolayer WSe, is effective for studying a variety of optical phenomena due to its direct bandgap and spin-valley locking, namely exhibiting very strong photoluminescence; thus, putting it in

proximity to NiI, enables additional optical techniques to interpret properties of the latter. In this study, we report circular dichroism in the photoluminescence of a monolayer WSe, and NiI, heterostructure that switches sign upon reversing the electric polarization of the NiI₂. We attribute the dichroism to the type-II band alignment of the semiconductor-insulator interface and the spin-polarized momentum splitting of the Nil, bands along the direction of the spin helix. In addition, we compare the reflective circular dichroism of the heterostructure to the reflective magnetic circular dichroism (RMCD) of the isolated WSe, monolayer to estimate the magnitude of the magnetic proximity effect. These results demonstrate a novel optical detection method of magnetic chirality switching in an odd-parity multiferroic, expanding the methods to distinguish symmetry breaking phenomena in unconventional magnetic systems.

On-site Growth of Perovskite Nanocrystal Arrays for Integrated Nanodevices

P. Jastrzebska-Perfect, W. Zhu, M. Saravanapavanantham, Z. Li, S. O. Spector, R. Brenes, P. F. Satterthwaite, R. Ram, F. Niroui Sponsorship: NSF

Known for their superior optoelectronic properties, halide perovskites have been utilized to realize applications such as solar cells, light-emitting diodes, memristors, and single photon-sources. However, integrating halide perovskites in nanoscale devices has remained challenging, given the chemical incompatibilities of these materials with conventional lithographic processing techniques. Here, we introduce a bottom-up approach for precise and scalable formation of perovskite nanocrystals and their integration into functional nanodevices. Our approach uses topographical templates with asymmetric surface wettability to guide the site-selective growth of the perovskite nanocrystals. With this platform, we demonstrate arrays of CsPbBr₂ nanocrystals with tunable dimensions down to < 50 nm and placement accuracy < 50 nm. We further apply our approach to develop nanoscale light-emitting diodes (nanoLEDs), highlighting the potential this platform offers for enabling on-chip perovskite nanodevices.

Probing Operational Degradation Mechanism on Cd-free Red and Blue QD-quantum dot LEDs

R. Zhang, V. Bulović Sponsorship: Samsung Electronics, MIT 2024 Mathworks Fellowship

With a variety of emerging display products like AR/VR, smart watch, etc., high quality display materials are required. Cadmium-free colloidal quantum dots have been reported as promising candidates in quantum dot light-emitting diodes (QD-LEDs) due to their tunable optical properties, quantum confinement effects and scale-up capability. However, comparing to the high operational lifetime of red and green QD-LEDs counterparts, the blue QD-LEDs offer a much lower operation lifetime. In this work, we probe the operation degradation mechanisms on both InP/ZnSe/ZnS (red) and ZnSe(Te)/ZnSe/ZnS (blue) QD-LEDs from a perspective of nanoscale device morphology and interlayer elemental tracing. A coarsening and thinning phenomenon is observed in both quantum dots and Mg-doped

zinc oxide nanoparticles (ZnMgO NPs) layers after red QD-LED LT-50 aging and blue QD-LED LT-70 aging. An extra oxygen peak shows up in the InP/ZnSe QD layer after biasing the device, where the compositional oxygen level enhances at the Al electrode / ZnMgO NPs junction. Additionally, our findings indicate that long-time high-dose electron beam irradiation contributes to the coarsening of the ZnMgO NP layer, and the presence of hydrogen significantly accelerates the coarsening process under electron beam exposure. This study reveals the morphological thinning and particle coarsening in the electron transporting layer (ETL) and active layer after diode aging, establishing a framework for understanding QD-LED degradation mechanisms during operation.

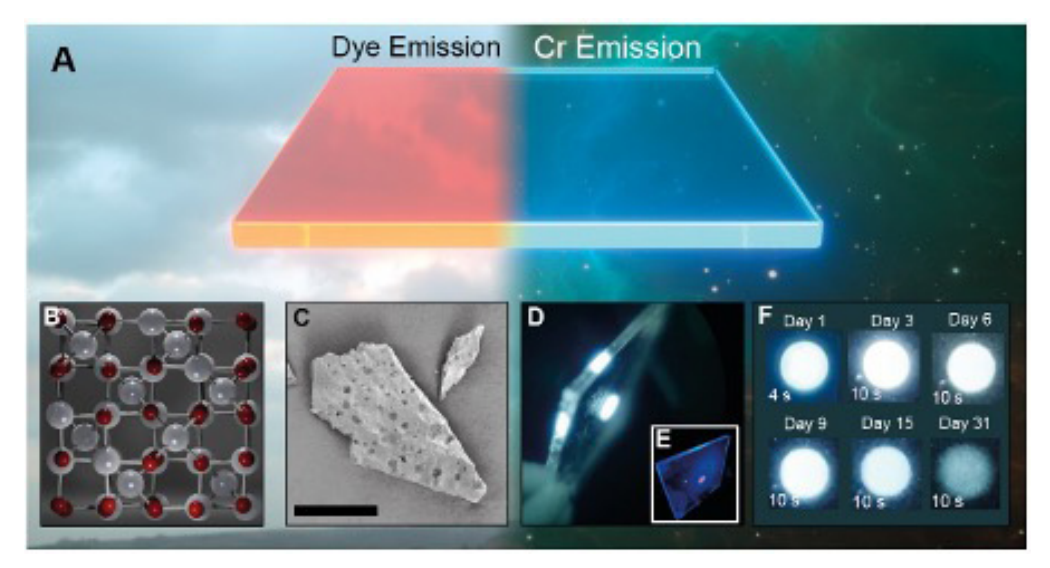
Solid State Solar Energy Storage from Persistently Luminescent Solar Concentrators

T. K. Baikie

Sponsorship: Schmidt Science Fellowship, Lindemann Trust Fellowship

The remarkable reduction in the levelized cost of energy (LCOE) for solar power has meant that photovoltaics have become increasingly competitive with fossil fuels, yet challenges remain in achieving the widespread adoption necessary to meet global climate targets. One of the primary barriers is the inherent variability of photovoltaic (PV) output, driven by short-term fluctuations in environmental conditions, which undermine the output stability and predictability re-

quired in energy markets that rely on spot pricing. We propose an alternative approach to stabilize solar output by artificially delaying the photon flux incident on conventional solar cells using persistently luminescent chromophores within solar concentrator devices. This approach aims to smooth the output power with minimal impact on overall efficiency, providing a pathway to enhance the economic viability and reliability of solar energy in grid-scale applications.



▲ Figure 1: **A** – Cartoon depiction of the two emission modes. Dye emission under bright conditions and long lifetime emission from Cr. **B** – Structure of long-lived emissive crystal determined from XRD. A single unit cell of $Zn_3GaGe_2O_8$, where Zn, Ga and Ga are shown in grey, Ga is shown in red. Thermal parameters were refined by element and are not shown to scale. **C** - Indicative SEM image of particles. Scale bar is X um. **D** – 10 by 10 cm PLSC device photographed 1 hour after illumination in dark conditions in the IR with **E** inset a photo at visible wavelengths under blue illumination. **F** Active area photographed in the IR for a period of a month after illumination with different integration times inset.

Electrical Double Layer Force Enabled Wafer-scale Transfer of van der Waals Materials

X. Zheng, J. Wang, J. Jiang, T. Zhang, J. Zhu, T. Dang, P. Wu, A. Lu, D. Chen, T. H. Yang, X. Zhang, K. Zhang, K. Y. Ma, Z. Wang, Y. Hsieh, V. Bulović, T. Palacios, J. Kong

Sponsorship: US Army Research Office, Air Force Office of Scientific Research (AFOSR) Multi-University Research Initiative

The transfer and integration of van der Waals (vdW) materials to target substrates is critical to their applications in high-end electronics, optics, moiré electronics, etc. The transfer step typically requires the use of either chemical etchants, electrochemical bubbling, or mechanical strain to detach vdW materials from growth substrate. However, these approaches often have issues regarding contamination, degradation of vdW materials or damage of growth substrates (adding significant cost to the manufacturing process, especially for single crystalline substrates). In this work, we present an electrical double layer (EDL) force enabled transfer method that is etching-free, fast, highly reliable and widely applicable to various types of substrates (e.g., oxide, nitride, etc.) and materials (e.g., carbon nanotube, MoS₂, h-BN, etc.). The unique strategy is to leverage the negative zeta potential of both the substrate and the

vdW material in concentrated ammonia solution. With the formation of the EDL, the vdW material is repelled from the substrate by the strong EDL repulsion force. The as-transferred vdW materials show minimized wrinkles, cracks, contaminations, and other transfer-induced defects. The $\rm MoS_2$ field effect transistors fabricated with EDL transfer show 100% yield, near-zero hysteresis (7 mV) and near-ideal subthreshold swing (65.9 mV/dec), evidencing an ultra-clean interface and minimized damage. The combination of EDL transfer and bismuth contact further enables an ultra-high on-current of 1.3 mA/ μ m. This EDL transfer approach offers a facile and manufacturing-viable solution for vdW material integration, which will significantly advance the future development of atomically thin electronics.

88

Neuromorphic Devices & Al Hardware Accelerators

| Electronic-protonic Conduction in Electrochemical RAM | 90 |
|--|-----|
| Impact of Annealing on Ferroelectric Properties of HZO for Non-volatile Memory | 91 |
| Atomistic Simulations on Ion Incorporation in 2D Channel Materials for Fast Conductivity Modulation in Electrochemical Random-access Memory Devices | 92 |
| Accelerated Analog In-memory Computing for Neural Network Training | 93 |
| Predicting Energy Materials Properties with Artificial Intelligence | 94 |
| Oxide Interface Coatings in Proton-based Electrochemical Ionic Synapse Devices | 95 |
| Understanding the Role of Space Charge Resistances in ECRAM | 96 |
| Quantifying and Deconvoluting the Variability in Protonic Electrochemical Random-access Memories | 97 |
| Toward Fast, Nanoscale, and Accurate Fabrication of Diffractive Optical Neural Networks | |
| Discrete Domain Switching in Scaled Amorphous Metal-oxide Channel Ferroelectric FETs | 99 |
| Electrochemical Random-access Memory with Monolayer MoS ₂ Channels for Fast Conductivity | |
| Modulation and Dynamically Tunable Transistors | 100 |
| Dynamic Modeling of WO ₃ -PSG Protonic Devices for Analog Computing | 101 |
| RDIT: Residual-based Diffusion Implicit Models for Probabilistic Time Series Forecasting | 102 |
| Design Considerations of Analog Accelerators for Machine Learning Applications | 103 |
| Development of a Neuromorphic Network using BioSFQ Circuits | 10∠ |
| CiMLoop: A Flexible, Accurate, and Fast Compute-In-Memory Modeling Tool | 105 |
| Ultra-low Power Superconducting Electronics for Deep Learning Accelerator Architectures: Evaluating Energy Efficiency and Scalability | 106 |
| Single-Shot Matrix-Matrix Multiplication Optical Processor for Deep Learning | 107 |
| 200 mm Wafer Diameter Process of Pd/PSG/WO3 Protonic Synapses for Analog Deep Learning | 108 |
| Tailor Swiftiles: Accelerating Sparse Tensor Algebra by Overbooking Buffer Capacity | 109 |
| Stable and Accurate Nano-Resistor for Reliable Fixed AI Inference Tasks | 110 |
| DuoAttention: Efficient Long-Context LLM Inference with Retrieval and Streaming Heads | 111 |
| Quest: Query-Aware Sparsity for Efficient Long-Context LLM Inference | 112 |
| SORBET: Secure Off-chip Memory Interface for Deep Neural Network Accelerators | 113 |
| LoopTree: Exploring the Fused-layer Dataflow Accelerator Design Space | 114 |
| SVDQuant: Absorbing Outliers by Low-Rank Components for 4-Bit Diffusion Models | 115 |
| LongVILA: Scaling Long-Context Visual Language Models for Long Videos | 116 |
| QServe: W4A8KV4 Quantization and System Co-design for Efficient LLM Serving | 117 |

Electronic-protonic Conduction in Electrochemical RAM

S. Bitton, J. A. del Alamo

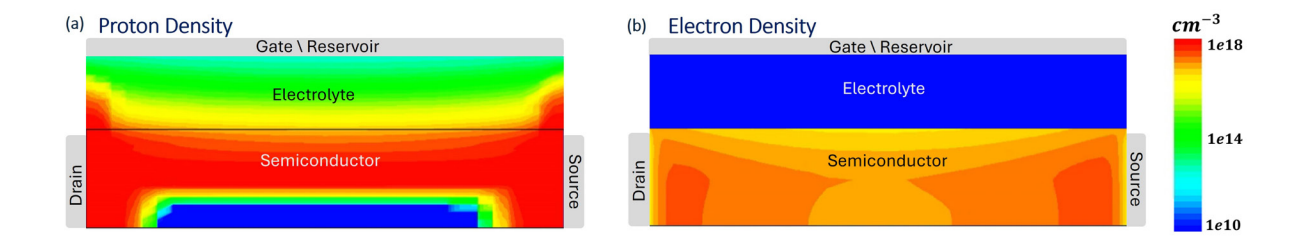
Sponsorship: MIT-IBM Watson AI Lab, Fulbright Fellowship, Intel International Science and Engineering Fair Fellowship, Zuckerman STEM Leadership Program, Schmidt Israeli Women's Postdoctoral Fellowship

Electrochemical random-access memory (ECRAM) is a promising candidate for analog in-memory neural network accelerators. Unlike traditional digital memory, which stores binary states (0 or 1), ECRAM can store a continuous range of values by modulating the conductivity of a semiconductor channel. This enables efficient analog computation directly within memory, reducing data movement between memory and processor, lowering energy consumption, and enhancing performance for artificial intelligence workloads.

The non-volatile analog states in ECRAM are achieved through proton (i.e., hydrogen cations) intercalation from a hydrogen reservoir, through an electrolyte, into a semiconductor channel. As protons accumulate in the semiconductor channel, they attract electrons, which increases the channel's conductivity.

While this basic mechanism is known, the underlying electronic–protonic interactions that govern device behavior are not yet fully understood. These interactions are key to unlocking the full potential of ECRAM for neuromorphic computing.

In this work, we investigate these mechanisms using a combination of advanced two-dimensional (2D) device simulations and targeted experiments. Our simulation framework provides a theoretical foundation that complements the experimental results, offering insights into proton dynamics and their effect on conductivity. This integrated approach helps identify the key factors that influence device performance and guides strategies for further optimization.



 \blacktriangle Figure 1: Simulated 2D ECRAM structure based on a WO₃ channel showing the spatial distribution of (a) proton density and (b) electron density after 50 potentiation pulses.

FURTHER READING:

M. Onen, N. Emond, B. Wang, D. Zhang, F. M. Ross, J. Li, B. Yildiz, and J. A. del Alamo, "Nanosecond Protonic Programmable Resistors For Analog Deep Learning," Science, vol. 377, pp. 539-43, 2022.

M. Onen, J. Li, B. Yildiz, and J. A. Del Alamo, "Dynamics of PSG-Based Nanosecond Protonic Programmable Resistors for Analog Deep Learning," 2022 International Electron Devices Meeting (IEDM), vol. 2, no. 6, pp. 1-4, 2022.

Impact of Annealing on Ferroelectric Properties of HZO for Non-volatile Memory

H. Choi, J. C.-C. Huang, Y. Shao, T. E. Espedal, D. A. Antoniadis, J. A. del Alamo Sponsorship: SRC

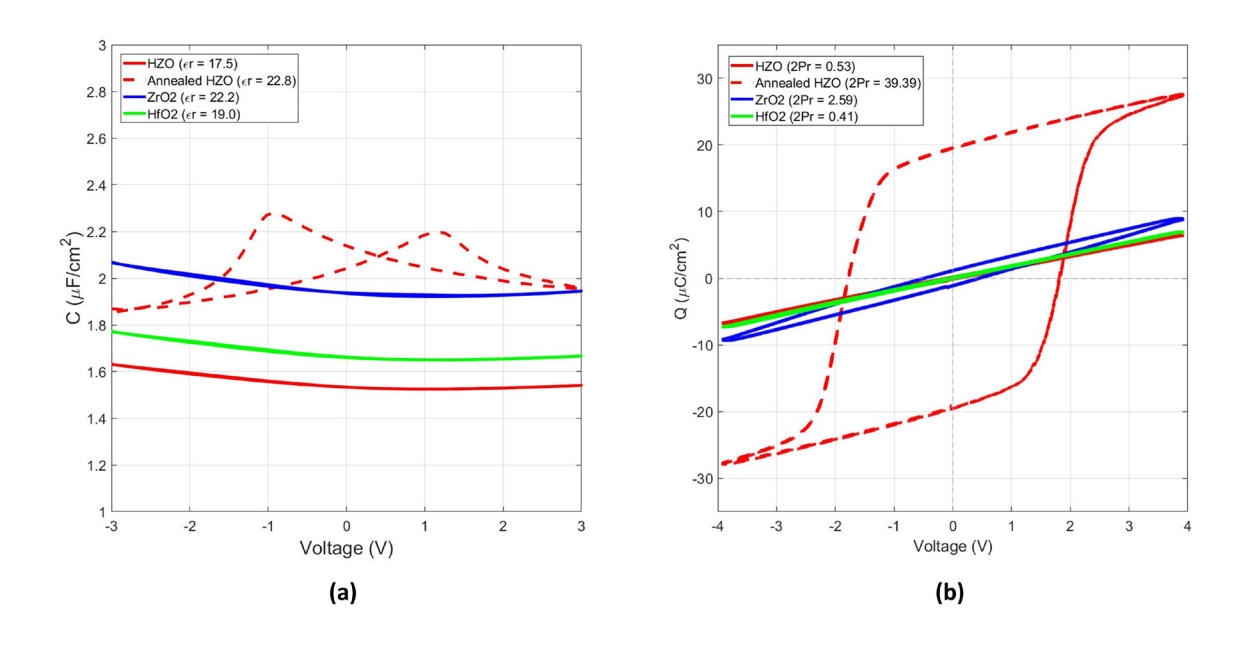
Ferroelectric (FE) materials, particularly hafnium oxide (HfO₂)-based thin films, have attracted significant interest for complementary metal-oxide-semiconductor-compatible non-volatile memory technologies. In this study, we examine how thermal annealing affects the FE properties of HZO thin films compared to unannealed films (HZO, pure HfO₂, and ZrO₂). We fabricated metal-insulator-metal structures using plasma-enhanced atomic layer deposition for the insulator and sputtering for the tungsten electrodes.

Capacitance-voltage (C-V) and charge-voltage (Q-V) measurements at 100 kHz reveal clear differences between annealed and unannealed films. Annealed HZO samples show distinct butterfly-shaped C-V loops (Figure 1a), indicating robust FE behavior. The strong hysteresis in the Q-V characteristics (Figure 1b) demonstrates a remnant polarization (2Pr) of approximately 39.4 μ C/cm², where each polarization state

represents a distinct memory state suitable for non-volatile memory.

Unannealed HZO, HfO₂, and ZrO₂ films exhibit relatively featureless C-V characteristics but subtle yet measurable hysteresis in their Q-V characteristics, suggesting previously over-looked polarization. Although significantly smaller than annealed HZO, the observed remnant polarization (below 3 μ C/cm²) challenges the assumption that these materials lack ferroelectricity without annealing.

These findings highlight that annealing greatly enhances polarization stability and ferroelectricity in HZO thin films, guiding the development of efficient, high-performance FE memory devices. Additionally, unannealed HfO₂ and ZrO₂ films may also be useful for applications requiring minor polarization effects. Future research should explore other activation methods to optimize FE polarization properties.



▲ Figure 1: (a) C-V loops and (b) Q-V loops of metal/ferro/metal with different FE materials.

FURTHER READING:

[•] T. Kim, J. A. del Alamo, and D. A. Antoniadis, "Switching Dynamics in Metal–Ferroelectric HfZrO2–Metal Structures," *IEEE Transactions on Electron Devices*, vol. 69, no. 7, pp. 4016-4021, July 2022. DOI: 10.1109/TED.2022.3175444

T. Kim, J. A. del Alamo, and D. A. Antoniadis, "Dynamics of HfZrO₂ Ferroelectric Structures: Experiments and Models," 2020 IEEE International Electron Devices Meeting (IEDM), vol. 21, no. 4, pp. 1-4, 2020. DOI: 10.1109/IEDM13553.2020.9372013

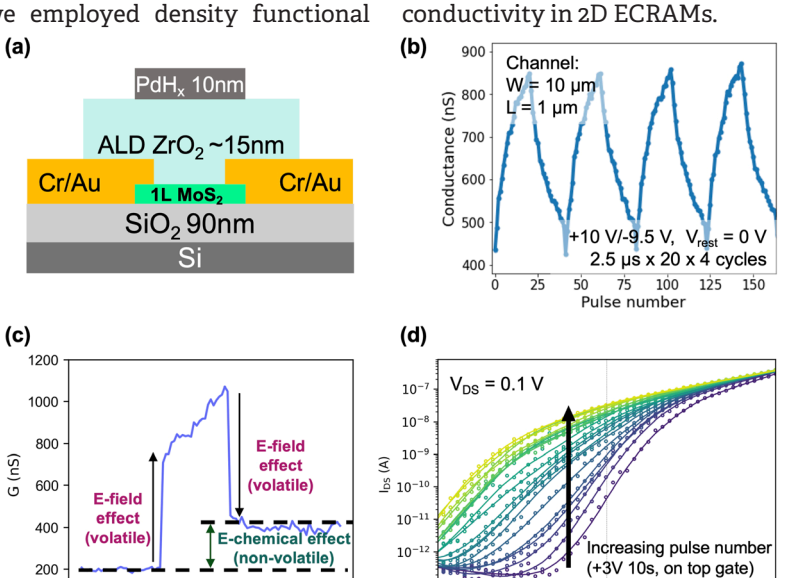
Atomistic Simulations on Ion Incorporation in 2D Channel Materials for Fast Conductivity Modulation in Electrochemical Random-access Memory Devices

V. Fotopoulos, M. Siebenhofer, M. Huang, L. Xu, B. Yildiz Sponsorship: SRC

Electrochemical random-access memory (ECRAM) has emerged as a novel type of pro-grammable resistor for crossbar arrays—a promising architecture for implementing energy-efficient artificial neural networks. ECRAMs consist of three key functional layers: an ion reservoir, a solid electrolyte, and a channel (Figure 1(a)). Through voltage-driven intercalation of mobile ions (e.g., H+), the electronic conductivity of the channel can be finely modulated, enabling precise control over the resistance state of the device. Mixed ionic and electronic conducting oxides, e.g., WO₃, have been investigated as channel materials. However, their bulk nature necessitates three-dimensional ion redistribution, leading to undesirably long conductivity settling times. Two-dimensional (2D) materials, including monolayers of transition metal dichalcogenides (TMDs), such as MoS2, offer a promising alternative, yet the mechanisms of interfacial ion transport and their impact on the conductivity of the channel remain underexplored.

In this work, we employed density functional

-10



 \triangle Figure 1: (a) ECRAM device. (b) MoS₂/SiO₂ interface. (c) (i) At fully saturated interfaces, H is stable on MoS₂. (ii) In interfaces with dangling bonds, H is stable on SiO₂. (d) (i) Density of states (DOS) of MoS₂ in saturated interface. (ii) DOS of MoS₂ in interface with dangling bonds.

-20 -10

10 20

FURTHER READING:

- A. A. Talin, J. Meyer, J. Li, M. Huang, M. Schwacke, H. W. Chung, L. Xu, E. J. Fuller, Y. Li, and B. Yildiz, "Electrochemical Random-Access Memory: Progress, Perspectives, and Opportunities," Chemical Reviews, vol. 125, no. 4, pp. 1962-2008, 2025.
- M. Schwacke, P. Žguns, J. A. del Alamo, J. Li, and B. Yildiz, "Electrochemical Ionic Synapses with Mg2+ as the Working Ion," Advanced Electronic Materials, vol. 10, no. 5, p. 2300577, 2024.
- M. Huang, M. Schwacke, M. Onen, J. A. del Alamo, J. Li, and B. Yildiz, "Electrochemical Ionic Synapses: Progress and Perspectives," Advanced Materials, vol. 35, no. 37, p. 2205169, 2023.

10

Time (s)

theory to investigate hydrogen (H) incorporation at

interfaces between a solid electrolyte (SiO₂) and a

monolayer (MoS2) channel (Figure 1(b)). We explored a

range of SiO, surface chemistries—including surfaces

with unsaturated Si and O dangling bonds and

reconstructed surfaces with fully saturated bonds-

and showed that surface termination determines

the most stable H incorporation sites. For defect-free

MoS₂, H is stable on MoS₂ only when the underlying SiO₂ surface is fully saturated (Figure 1(c)(i)), in-

creasing the channel's conductivity through n-type

doping (Figure 1(d)(i)). In contrast, when unsaturated

O and/or Si dangling bonds are present (Figure 1(c)

(ii)), H preferentially binds to the electrolyte surface,

remaining electronically decoupled from MoS₂ (Figure

1(d)(ii)). Additionally, introducing a sulfur vacancy

(V_s) in MoS₂ alters this behavior: across all surfaces, H

stabilizes inside the vacancy, leading to n-type doping.

These findings highlight how interfacial structure and defect engineering can enhance ionic modulation of

Accelerated Analog In-memory Computing for Neural Network Training

I. J. Gallo, J. A. del Alamo Sponsorship: MIT-IBM Watson AI Lab

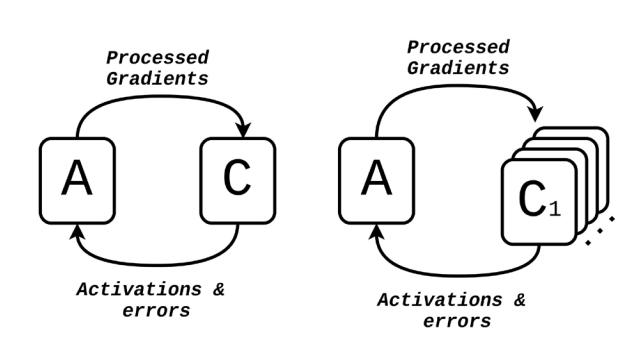
Neural network training demands enormous computational resources, leading to high energy consumption and long processing times. Analog in-memory computing offers a promising solution by performing matrix-vector multiplications directly within memory arrays, leveraging the physical properties of analog devices such as protonic synapses. However, a fundamental limitation of analog crossbar arrays is their inability to process multiple inputs simultaneously.

We propose a multi-tile parallel processing architecture that accelerates existing algorithms such as Tiki-Taka by introducing parallelism at the algorithmic level, as shown in Figure 1. Our approach distributes computation across multiple crossbar arrays, enabling the parallel processing of inputs while

maintaining high accuracy. Using IBM's AIHWKIT simulation frame-work, we demonstrate that this parallel architecture achieves comparable accuracy to conventional sequential implementations while significantly reducing training time.

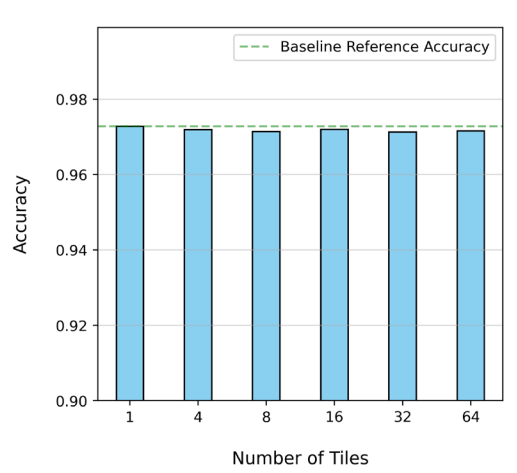
As shown in Figure 2, our parallel implementation maintains over 97% accuracy on the Modified National Institute of Standards and Technology (MNIST) dataset while achieving substantial speedup compared to standard Tiki-Taka implementations. By combining parallelization with analog in-memory computing, our approach delivers both dramatic improvements in energy efficiency over conventional digital methods and significantly accelerated training times.

Tiki-Taka Multi-Tile Tiki-Taka



▲ Figure 1: Architecture diagram of the pro-posed multi-tile parallel processing approach for accelerated Tiki-Taka.

Accuracy Across Tile Configurations - 40 epochs



▲ Figure 2: Comparison of classification accuracy in MNIST between standard and parallel implementations, demonstrating maintained performance despite parallelization.

FURTHER READING:

 M. Onen, T. Gokmen, T. K. Todorov, T. Nowicki, J. A. del Alamo, J. Rozen, W. Haensch, and S. Kim, "Neural Network Training with Asymmetric Crosspoint Elements," Frontiers in Artificial Intelligence, vol. 5, Article 891624, 09 May 2022. DOI: 10.3389/frai.2022.891624

Predicting Energy Materials Properties with Artificial Intelligence

R. Okabe, A. Chotrattanapituk, M. Li Sponsorship: NSF, Department of Energy

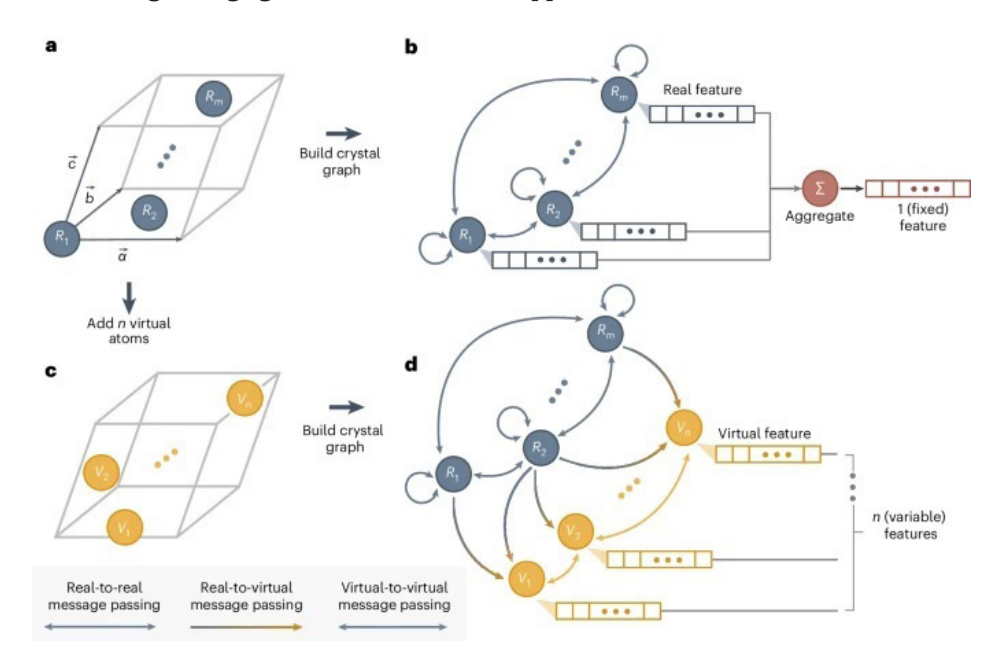
Accurate prediction of materials properties is essential for the discovery and design of next-generation energy materials. While first-principles calculations provide reliable insights, they are often computationally intensive, particularly for complex properties such as optical response and phonon spectra. Recent advances in machine learning offer promising alternatives, but key challenges remain in embedding atomic structures and handling variable-length outputs across materials.

To address these challenges, we introduce two complementary artificial intelligence (AI) frameworks tailored for property prediction: GNNOpt and the virtual node graph neural network (VGNN). GNNOpt is an equivariant graph neural network designed to predict optical properties—including absorption, refractive index, and reflectance—directly from crystal structures. It leverages universal atomic embeddings and the Kramers-Krönig relations to deliver accurate predictions on a dataset of only 944 materials, demonstrating strong agreement with first-

principles calculations. Applications include screening photovoltaic candidates by spectroscopic efficiency and discovering topological quantum materials such as SiOs with high quantum weight.

In parallel, VGNN addresses the challenge of predicting phonon-related properties, which often have materials-dependent dimensionality. By incorporating virtual nodes into the crystal graph, this approach enables efficient and accurate prediction of Γ -point phonon spectra and full phonon dispersion relations. With significantly reduced computational cost and high accuracy, VGNN has generated large-scale databases, including over 146,000 Γ -phonon entries and phonon band structures for zeolites.

Together, these AI models demonstrate how tailored GNNs can achieve scalable, flexible, and high-fidelity prediction of energy-relevant properties, accelerating the discovery and design of functional materials for energy conversion, transport, and storage applications.



▲ Figure 1: A GNN processes a crystalline material with m atoms per unit cell, where each atom is a real node. After message passing, local features are aggregated into a fixed-size output. To enable flexible outputs, n virtual nodes are added to the crystal graph, allowing representations of variable length not limited to real-node aggregation.

FURTHER READING

R. Okabe, A. Chotrattanapituk, A. Boonkird, N. Andrejevic, X. Fu, T. S. Jaakkola, Q. Song, T. Nguyen, N. C. Drucker, S. Mu, B. Liao, Y. Cheng, and M. Li, "Virtual Node Graph Neural Network for Full Phonon Prediction," *Nature Computational Science*, vol. 4, p. 522, 2024.

N. T. Hung, R. Okabe, A. Chotrattanapituk, and M. Li, "Universal Ensemble-Embedding Graph Neural Network for Direct Prediction of Optical Spectra from Crystal Structures," Advanced Materials, vol. 36, p. 2409175, 2024.

Oxide Interface Coatings in Proton-based Electrochemical Ionic Synapse Devices

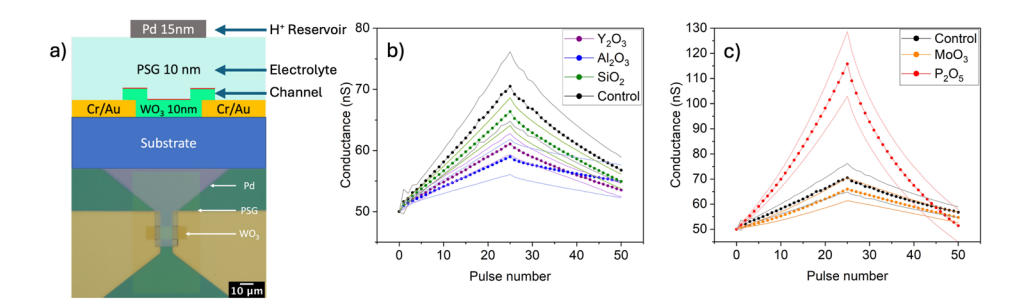
J. Meyer, B. Yildiz

Sponsorship: Department of Defense National Department of Science and Engineer-ing Graduate Fellowship (2022), Department of Energy EFRC Hydrogen in Energy and Information Sciences

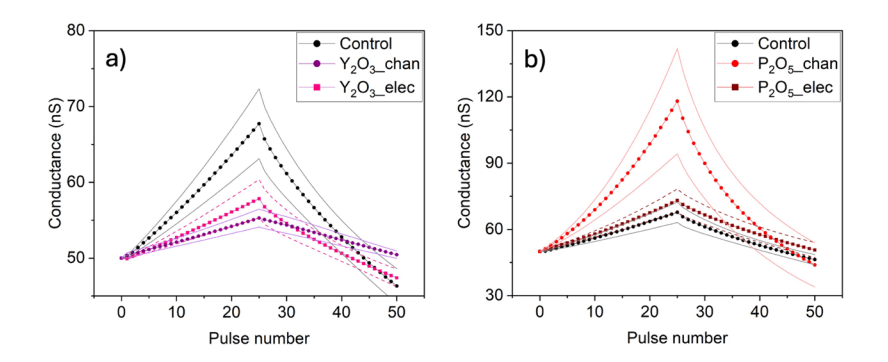
Electrochemical ionic synapses (EIS) that modulate the electronic conductivity of a channel by ion intercalation are promising devices for use in energy-efficient neuromorphic computing hardware. Using protons as the working ions enhances the energy-efficiency and programming speed, but proton transfer through the electrolyte and interfaces of the device faces kinetic limitations. This presents a challenge for achieving nanosecond programming at 1 V or less.

Here, thin binary oxide coatings are deposited at the electrolyte-channel (phosphosilicate glass (PSG)-WO $_3$) interface to modify the interface chemistry and EIS device operation. Figure 1 shows tunable conductance change of the channel in response to voltage gating, depending on the interface oxide. The P_2O_5 interface

coating markedly enhances the conductance change obtained under cycling, relative to both the other oxide-coated and unmodified (control) EIS devices. The position of the oxide coating within the device structure, in the middle of the PSG electrolyte versus at the electrolyte-channel interface, also impacts the magnitude of the effect on conductance change (Figure 2). The P_2O_5 and Y_2O_3 coatings increase and decrease the conductance change, respectively, to a greater degree when deposited at the interface. These results inform interface design for EIS devices with greater conductance change per voltage pulse, which can enable lower voltages as the programming speed increases towards the nanosecond scale.



▲ Figure 1: a) EIS schematic and image. (b-c) Cycling of oxide-coated EIS with 10-nm PSG with ±3 V, 100-ms pulses, 25 positive and 25 negative voltage pulses, showing mean and standard deviation for each device chemistry.



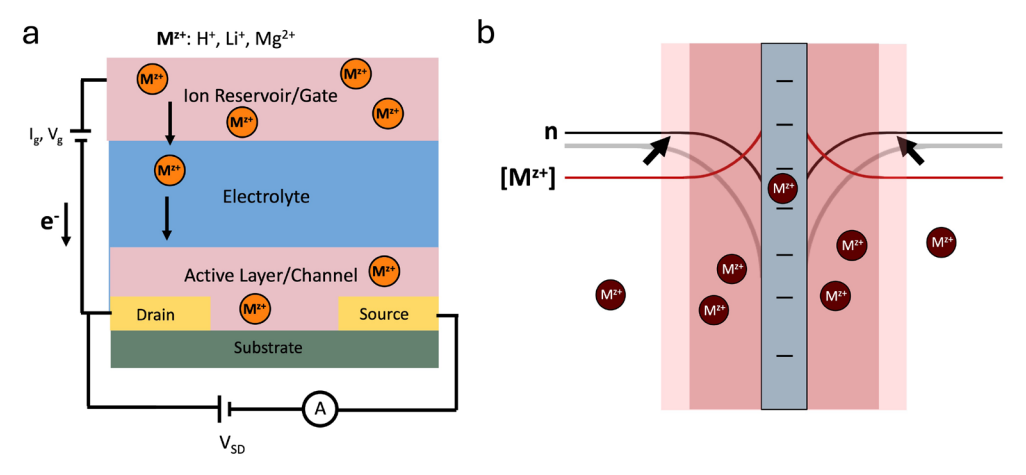
 \blacktriangle Figure 2: Cycling of a) Y₂O₃-coated and b) P₂O₅-coated EIS with 20-nm PSG with ±4 V, 1 s pulses. Position of oxide coating is labeled for deposition in middle of electrolyte (_elec) versus at electrolyte-channel interface (_chan).

Understanding the Role of Space Charge Resistances in ECRAM

M. Schwacke, M. Siebenhofer, T. Defferriere, H. Tuller, B. Yildiz Sponsorship: IBM, MIT School of Engineering Mathworks Fellowship

With the rapid rise in the prevalence of artificial intelligence, the energy consumed by training neural networks is also skyrocketing. Moreover, the energy consumed each year by computing is exponentially increasing and rapidly approaching the world's total energy production, making finding more energy efficient methods of computing imperative. Electrochemical random-access memory (ECRAM) is a promising technology for brain-inspired computing and for energy efficient training of neural networks. ECRAM devices act as programmable resistors, where the resistance of a channel material is programmed by electrochemically controlled intercalation of small cations into or out of the channel. A schematic of an ECRAM device appears in Figure 1a. It is generally thought that resistance modulation occurs due to changes in the bulk carrier concentration of the channel, as electrons must accompany cation intercalation to maintain charge neutrality. However, polycrystalline thin films, which are generally used as ECRAM channels, can have many sources of resistance beyond the bulk, including resistances arising from electron depletion in space charge regions at grain boundaries, contacts, and the electrolyte/channel or channel/substrate interfaces.

We use electrochemical impedance spectroscopy to characterize the contributions of bulk, grain boundary, and contact resistances to the total resistance of sputtered, polycrystalline WO₃ thin films, a common ECRAM channel material, before and after various levels of Mg²⁺ intercalation. We find that space charge resistances actually dominate the total resistance of the films and are also modulated by ion intercalation. To understand the mechanism by which space charge resistances are modulated, we develop an electrostatics model of space charge regions. The modeling results suggest that several mechanisms exist by which small concentrations of mobile cations could dramatically reduce the degree of electron depletion in space charge regions, including by cation accumulation in space charge regions and cation insertion directly into grain boundary or interfacial cores, as Figure 1b shows. This work has important implications for understanding the operating mechanisms of ECRAM. It also opens new avenues for informed device design, including by controlling grain size and interfacial chemistries.



▲ Figure 1: Schematic depictions of (a) an ECRAM device and (b) space charge regions adjacent to grain boundaries.

FURTHER READING

 A. A. Talin, J. Meyer, J. Li, M. Huang, M. Schwacke, H. W. Chung, L. Xu, E. J. Fuller, Y. Li, and B. Yildiz, "Electrochemical Random Access Memory: Progress, Perspectives, and Opportunities," Chemical Reviews, vol. 125, pp. 1962-2008, Feb. 2025.

Quantifying and Deconvoluting the Variability in Protonic Electrochemical Randomaccess Memories

L. Xu, M. Huang, B. Yildiz Sponsorship: SRC

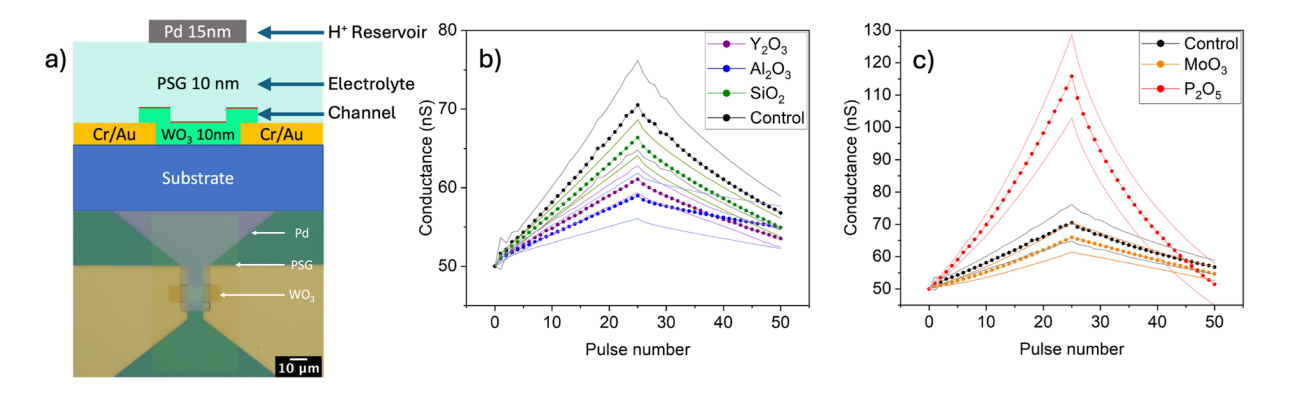
Electrochemical random-access memory (ECRAM) is a novel programmable resistor candidate powering hardware neural networks (HNNs) based on cross-bar arrays, targeting fast and energy-efficient artificial intelligence (AI) training. Low device variability is crucial to high training accuracy in HNNs. ECRAMs are expected to have low variability compared to other candidates such as resistive random-access memory and phase-change memory, enabled by the deterministic dynamic doping of the channel. Some possible sources, such as the material micro-structure and non-ideal fabrication artifacts, can introduce variations in ECRAMs.

This work systematically quantified the variability of complementary metal-oxide-semiconductor-compatible protonic ECRAMs (PdH $_{\rm x}$ /HfO $_{\rm 2}$ or YSZ/WO $_{\rm 3}$ structure, Figure 1). By examining conductance modulation range and symmetry with over 1000 conductance states, we observed low variations in low-conductance regime (Figure 2). Device-to-device

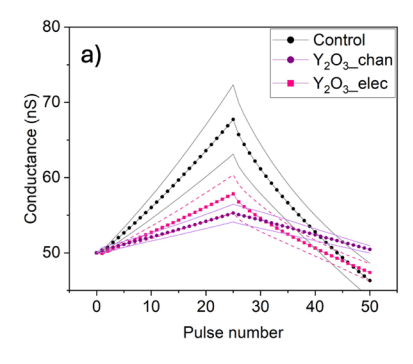
variation showed dependence neither on channel ordering (crystalline/amorphous), nor on channel sizes ranging from 102 μ m² to 1502 nm².

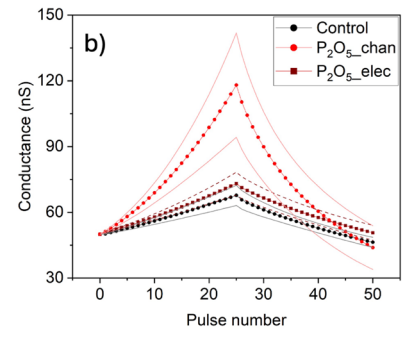
Meanwhile, source/drain contact with the channel was investigated as a possible variation source. Correlation between the contact resistance contribution and device modulation behavior was observed. We explored contact improvement via hydrogen plasma treatment or using Ti transition layer and plan further evaluation to assess its impact on variability.

These findings confirm that ECRAM meets variability targets and demonstrates strong potential for downscaling, indicating it can be a promising candidate for programmable resistors. The results also emphasize the importance of microstructure and contact resistance control for consistent, low-variability operation.



▲ Figure 1: ECRAM device structure. (a) Cross section schematic of device structure. (b) Optical image of a device with 10^2 -µm2 channel size.





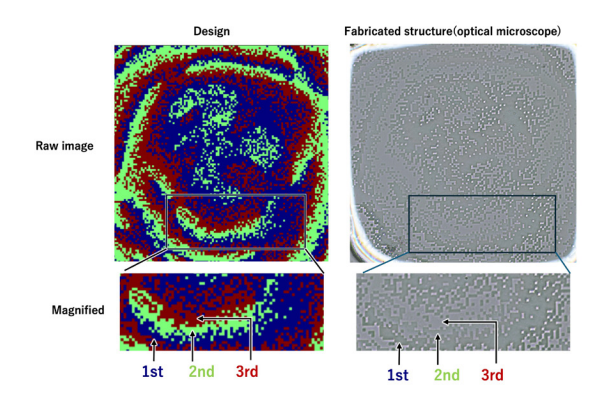
■ Figure 2: Device variability. (a) ECRAM con-ductance modulation with 3V/-3.2V writing voltage. (b) Device-to-device variation of EC-RAM device with amorphous and crystalline channel, showing 15% variation.

Toward Fast, Nanoscale, and Accurate Fabrication of Diffractive Optical Neural Networks

D. Zhang, H. Kusaka, T. Nambara, Y. Kunai, G. Barbastathis Sponsorship: Fujikura Ltd.

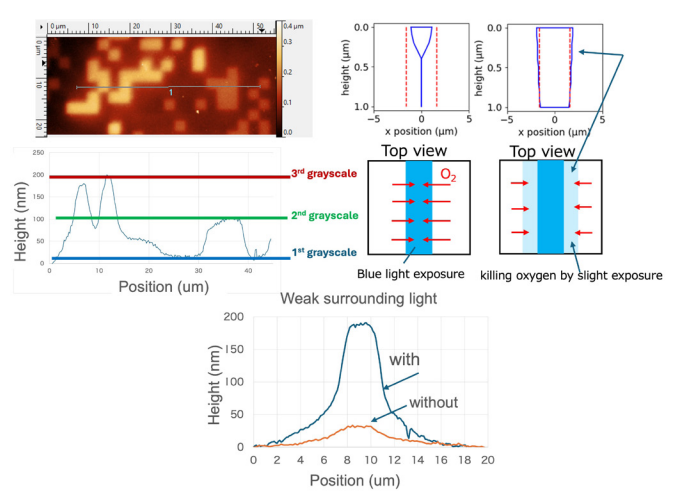
The fusion of machine learning and optics has driven advances in all-optical computing, with diffractive deep neural networks (D2NNs) emerging as a powerful architecture. By using deep learning to design diffractive layers, D2NNs can perform tasks like image classification at the speed of light, offering high parallelism and energy efficiency. However, D2NNs are typically fabricated at the macro scale, which limits their suitability for highly integrated devices. While some have been made at the micron scale using slow, point-bypoint methods, these approaches remain unsuitable for large-scale deployment. Moreover, accurately fabricating these structures at wavelength-level resolution remains a major challenge. Achieving fast, scalable, and precise fabrication is critical for practical implementation.

We systematically address these fabrication challenges. For speed, we used a digital micromirror device as a dynamic mask to fabricate entire layer patterns at once, enabling layer-by-layer lithography rather than traditional point-by-point writing (Figure 1). To achieve the nanoscale, we demonstrated the ability to fabricate 2.5-µm pillar features using blue light only (Figure 2). We will also adopt two-color lithography to exceed the diffraction limit, achieving sub-wavelength ($\lambda/2$) resolution and enabling precise phase control. In terms of accurate fabrication, we discovered that non-local oxygen inhibition coupled with varying light intensity along the vertical axis due to diffraction can significantly degrade the height profiles of printed pillars. This effect results in inconsistent polymerization across depths, resulting in shape distortion and even fabrication failure. To explain this phenomenon, we modeled the underlying photopolymerization dynamics, capturing both chemical reactions and oxygen diffusion. The model successfully describes the observed behavior and provides a predictive framework. Based on this, we proposed an illumination strategy that introduces weak surrounding light to deplete oxygen, improving quality of printed pillars and enabling consistency across printed layers (Figure 2).



◆ Figure 1: Rapidly fabricated 3-layer structures observed under optical microscope.

▼ Figure 2: (Top left) AFM height profiles of 3-layer structures. (Top right) Simulation of coupling between non-local oxygen inhibition and diffracted light intensity profiles. Introducing weak surrounding light to pre-deplete oxygen effectively resolves this issue and enhances fabrication quality. (Bottom) Experimental validation of simulation results.



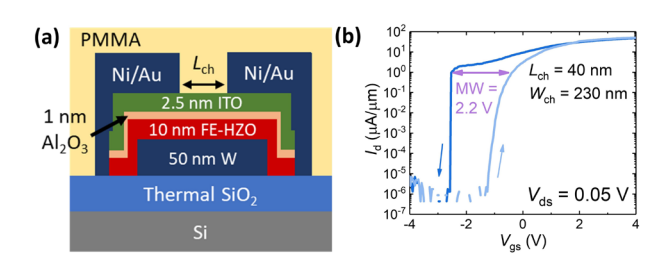
Discrete Domain Switching in Scaled Amorphous Metal-oxide Channel Ferroelectric FETs

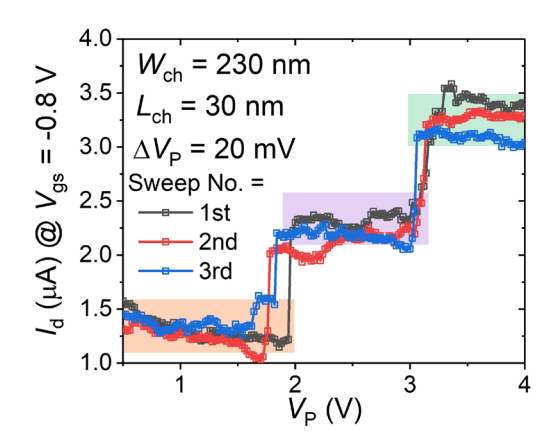
Y. Shao, E. Rafie Borujeny, J. Navarro Fidalgo, J. C.-C. Huang, T. E. Espedal, D. A. Antoniadis, J. A. del Alamo Sponsorship: Intel Corporation, SRC

Understanding domain structures and domain switching mechanisms in ferroelectric (FE) $\mathrm{Hf_{0.5}Zr_{0.5}O_2}$ (HZO) is crucial for its applications in non-volatile memory and analog hardware. Probing the actual size of the FE domains and mapping their individual polarization switching is challenging, but such information is highly valuable for HZO-based FE device design.

In this work, we integrate FE-HZO in complementary metal-oxide-semiconductor (CMOS)-compatible FE-FETs based on an amorphous oxide-semiconductor (AOS) channel (Figure 1a). Extensive electrical characterizations, including large-signal polarization-voltage, small-signal capacitance-voltage, and direct-current current-voltage characteristics, have been carried out on multiple device structures. A large memory window (MW) of 2.2 V @ 1 μ A/ μ m is achieved with a scaled channel length of 30 nm (Figure

1b). Gate voltage pulses with in-creasing amplitudes are applied. After each pulse, channel current is read at a constant gate voltage. Discrete domain switching is observed in narrow devices with reproducible multilevel erasing/programming operations (Figure 2), whereas gradual switching is apparent in wider ones (Figure 2). Moreover, we show that discrete polarization switching acts as a sensitive probe to study intriguing physics in AOS-channel FE-FETs, such as FE fatigue. We observe that FE domain pinning, with domains stuck in the up-polarization state, leads to MW closure and negative threshold voltage shift. Based on a channel length scaling study, we estimate the av-erage FE domain size in our FE-HZO film to be ~40 nm. This work shows the rich physics and countless engineering opportunities in AOS-based FE devices.





▲ Figure 1: (a) Schematic of CMOS-compatible FE-FET. (b) Hysteretic transfer characteristics of a highly scaled FE-FET.

▲ Figure 2: Drain current obtained at a constant gate voltage as a function of applied positive gate pulse amplitude of a narrow device showing three discrete states.

FURTHER READING

[•] Y. Shao, E. Rafie Borujeny, J. Navarro Fidalgo, J. C.-C. Huang, T. E. Espedal, D. A. Antoniadis and J. A. del Alamo, "Discrete Domain Switching in Scaled Oxide-Channel Ferroelectric FETs," presented at 82nd Device Research Conference, 2024.

Y. Shao, E. Rafie Borujeny, J. Navarro Fidalgo, J. C.-C. Huang, T. E. Espedal, D. A. Antoniadis and J. A. del Alamo, "Discrete Ferroelectric Polarization Switching in Nanoscale Oxide-channel Ferroelectric Field-effect Transistors," Nano Letts., vol. 25, no. 8, pp. 3173-3179, Feb. 2025.

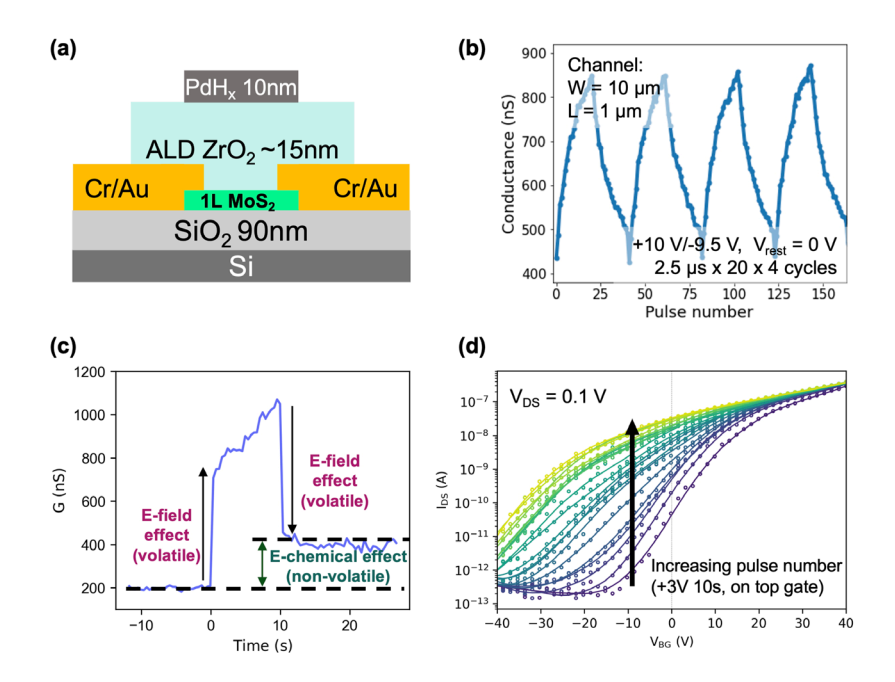
Electrochemical Random-access Memory with Monolayer MoS₂ Channels for Fast Conductivity Modulation and Dynamically Tunable Transistors

M. Huang, L. Xu, X. Zheng, J. Kong, B. Yildiz Sponsorship: SRC

Electrochemical random-access memories (ECRAMs) are promising three-terminal programmable resistors for powering deep neural network hardware accelerators when arranged in crossbar arrays. They are three-terminal devices with an ion reservoir layer, a solid-state electrolyte layer, and a channel layer. The electronic conductivity of the channel can be modulated by electrochemical ion intercalation with good linearity, symmetry, and low variability.

Conventional ECRAMs using bulk channels could suffer from undesirable relaxation transients due to ion diffusion through their finite thickness. In this work, we investigate ECRAMs with a 2H-MoS_2 monolayer as the channel (Figure 1a). Our findings show that the supply of protons to the 2H-MoS_2 channel enables reversible non-volatile conductance modulation with microsecond voltage pulses (Figure

1b). The response of the device to the applied gate voltage exhibits both a non-volatile electrochemical effect and a volatile electric field effect (Figure 1c). When combined with the Si substrate as an electronic back-gate, a transistor structure forms at the back side, where the source-drain current is tunable via the back-gate voltages. Applying top-gate pulses induces a large threshold voltage shift, suggesting that the hydrogen supplied to the MoS, and its surrounding interfaces increases the n-type doping of the channel (Figure 1d) and allows for a large range (105) of nonvolatile conductance modulation at a constant back gate voltage. Our findings offer a pathway to develop high-speed programmable resistors and dynamically tunable transistors with 2D channels for hardware neural networks and other in-memory computation architectures.



▲ Figure 1: (a) Schematic of ECRAM device with monolayer MoS₂ channel. (b) Channel conductance modulation with microsecond voltage pulses. (c) Volatile and non-volatile conductance modulation effect from applied gate voltage. (d) Source-drain current as function of back-gate voltage after increasing number of electrochemical gate voltage pulses applied to top, showing shift of threshold voltage towards lower voltage with hydrogen supplied to channel.

FURTHER READING

 A. A. Talin, J. Meyer, J. Li, M. Huang, M. Schwacke, H. W. Chung, L. Xu, E. J. Fuller, Y. Li, and B. Yildiz, "Electrochemical Random-Access Memory: Progress, Perspectives, and Opportunities," Chemical Reviews, vol. 125, no. 4, pp. 1962-2008, 2025.

Dynamic Modeling of WO₃-PSG Protonic Devices for Analog Computing

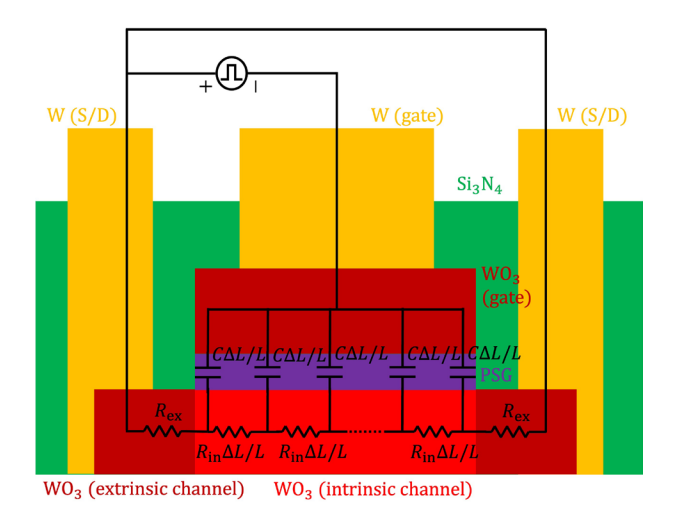
D. Shen, J. A. del Alamo Sponsorship: MIT-IBM Watson AI Lab

By leveraging local information processing through intrinsic physical properties of devices, analog computing presents a promising approach to overcome computational bottlenecks faced by traditional digital deep learning systems. One prominent strategy involves electrochemical ionic interactions in programmable resistors, where device resistance is adjusted by ionic exchange through an electrolyte. Previous research in our group has demonstrated proton-based non-volatile programmable resistors featuring a tungsten oxide (WO₃) channel, phosphorous-doped silicon dioxide (PSG) electrolyte, and palladium (Pd) gate reservoir. However, enhancing performance and making fabrication complementary metal-oxide-semiconductor (CMOS)-compatible remain crucial for application in future accelerators.

In this study, we optimized the device structure into a symmetric WO_3 -PSG- WO_3 stack, making device fabrication fully compatible with standard CMOS fabrication processes. Device programmability is achieved by applying voltage pulses between the gate and source/drain terminals, thereby precisely

controlling channel conductance.

To evaluate programming efficiency, systematically characterized channel conductance responses to various pulse voltages and durations. A distributive resistor-capacitor (RC) model was developed to interpret experimental data and extract critical device parameters by accurately simulating voltage distribution across the electrolyte. This model successfully matched experimental results except under conditions of particularly high voltages or long pulse durations. These discrepancies might highlight the phenomenon of diffusion saturation. When the pulse width is much shorter than the diffusion time of protons inside the WO3, proton flow from the reservoir to the channel will become supply-limited. Diffusion saturation significantly restricts programming speed because conductance changes become proportional to the square root of pulse width. Consequently, improving ion diffusion rates within WO, emerges as a critical factor for further enhancing device performance.



5.2e-02 $R_{\rm ex, sheet} = 1e + 07\Omega$ $\Delta G = kt_{\text{pulse}}^{\beta} \sinh \frac{a_{\text{PSG}}qV_{\text{electrolyte}}}{dt}$ 2.6e-02 $= 5e + 07\Omega$ C = 1.4 pF1.3e-02 k = 4e - 11S6.6e-03 $a_{PSG} = 0.4 \text{Å}$ $\beta = 0.65$ 3.3e-03 1.6e-03 ΔG_{sheet} [S/pulse] 8.2e-04 10⁻⁹ 4.1e-04 2.0e-04 +-1.0e-04 5.1e-05 2.6e-05 1.3e-05 6.4e-06 10⁻¹⁰ 3.2e-06 1.6e-06 V_{pulse} [V]

 \blacktriangle Figure 1: WO₃-PSG-WO₃ protonic device structure and schematic for distributive RC model. We use in-situ protonated WO₃ as both channel and gate reservoir, $\mathrm{Si_3N_4}$ as encapsulation, and W as source/drain/gate contacts. The extrinsic channel is not gated and is heavily doped, while the intrinsic channel is gated and lightly doped.

 \blacktriangle Figure 2: Channel conductance response to different pulse voltages and durations in a 5 µm-by-5 µm device with pulse setup and direction as in Figure 1. Colors indicate pulse durations. Dots show experimental data; lines show simulation results. With the fitting formula on the right, we extract the device parameters on the left.

FURTHER READING

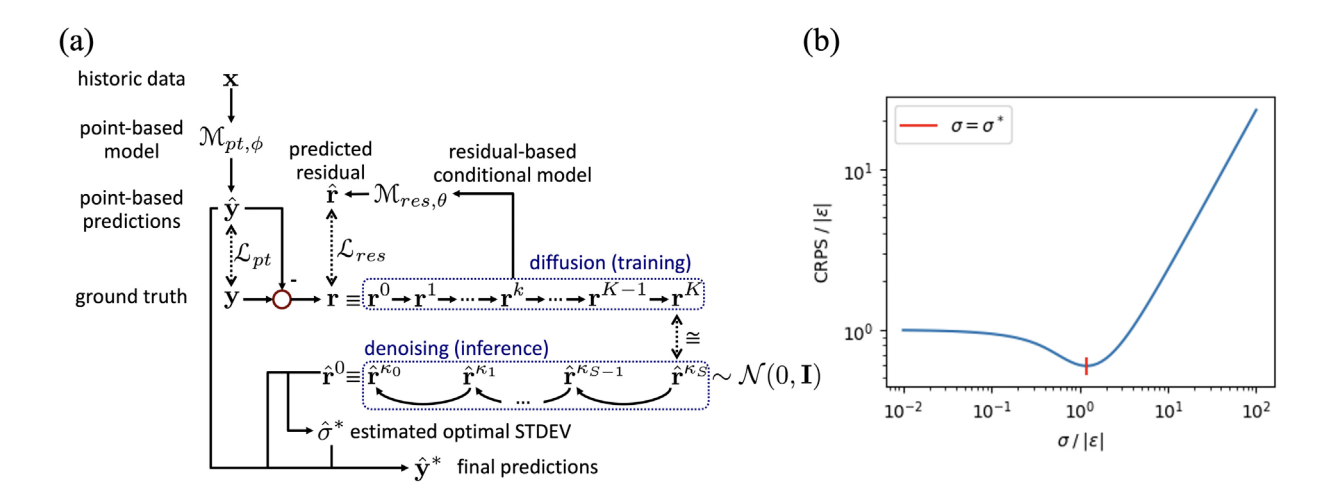
 M. Onen, N. Emond, B. Wang, D. Zhang, F. M. Ross, J. Li, B. Yildiz, and J. A. del Al-amo, "Nanosecond Protonic Programmable Resistors for Analog Deep Learning," Science, vol. 377, no. 6605, pp. 539-543, Jul. 2022.

RDIT: Residual-based Diffusion Implicit Models for Probabilistic Time Series Forecasting

C.-Y. Lai, D. S. Boning

We propose RDIT (Residual-based Diffusion Implicit modeling for probabilistic Time series forecasting), a novel framework designed to address key limitations in recent probabilistic time series forecasting (PTSF) methods. While traditional TSF models have increasingly adopted deep learning architectures, many of these rely on assumptions—such as linear mappings and channel independence—that are ill-suited for accurately modeling uncertainty. Additionally, standard PTSF approaches often conflate point estimation and noise modeling, resulting in reduced flexibility and suboptimal uncertainty quantification. To overcome these issues, RDIT separates the forecasting process into two stages: a plug-and-play model performs point-based prediction (estimating the conditional mean or median), while a conditional diffusion model captures the distribution of the residuals. This modular design not only improves adaptability across different domains but also allows the diffusion model to focus purely on learning noise characteristics. For fast inference, RDIT

employs denoising diffusion implicit models (DDIM), significantly reducing sampling time compared to traditional diffusion models. Furthermore, we derive a theoretical formulation for optimizing the continuous ranked probability score (CRPS), a common metric in probabilistic forecasting, under the assumption of Gaussian-distributed errors. Based on this, we introduce an error-aware expansion mechanism that adjusts the learned distribution to better match the evaluation metric. Experimental results across 8 datasets and 6 forecasting horizons show that RDIT consistently outperforms state-of-the-art TSF and PTSF models in terms of accuracy, uncertainty calibration, and generation speed. Our work provides a practical and theoretically grounded approach to modeling uncertainty in time series forecasting, with potential applications in risk-sensitive domains such as finance, healthcare, environmental monitoring, and industrial process optimization.



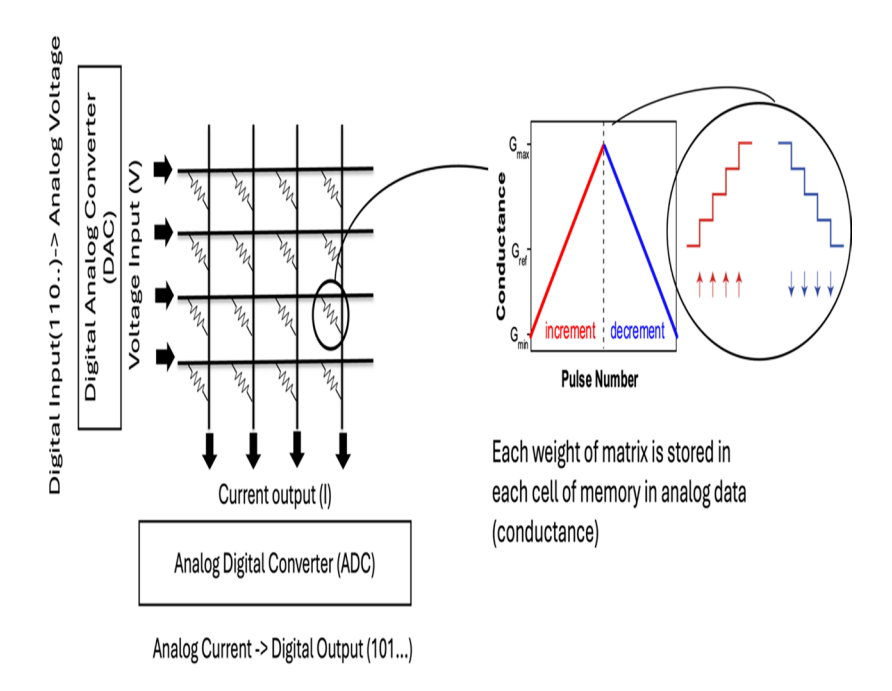
▲ Figure 1: (a) General scheme of this work. The point-based model is used to predict the point-based predictions; the residual-based conditional model is used to predict residuals from the k-th diffusion step residual while conditioning on the input and point-based prediction. (b) Normalized CRPS plotted against normalized standard deviation when the predictions are drawn from a normal distribution with mean and standard deviation, with the ground truth being y.

Design Considerations of Analog Accelerators for Machine Learning Applications

J. Lee, J. A. del Alamo Sponsorship: IBM, Ericsson

Recently, there has been tremendous progress in machine learning, leading to a dramatic increase in its applications, such as image classification and natural language processing. As a result, there has been an explosion in demand for Graphics Processing Units and various accelerators that perform the computation required for machine learning training and inference. The widespread use of currently dominant digital accelerators requires a massive amount of energy, which is becoming a significant global issue. In response, analog computing using devices such as protonic synapses

and ReRAM has been proposed as an alternative that can significantly enhance energy efficiency. Analog devices still face issues such as nonlinearity, asymmetry, and noise. Moreover, their performance heavily depends on components like Analog-to-Digital Converters (ADCs) and Digital-to-Analog Converters (DACs). In this work, we investigate how non-idealities degrade the performance of analog computing. We also evaluate different analog algorithms that mitigate performance degradation in several tasks such as Convolutional and Recursive Neural Networks with IBM AIHWKIT.



▲ Figure 1: Schematics of analog computing with analog crossbar array consisted by non-volatile memory cells.

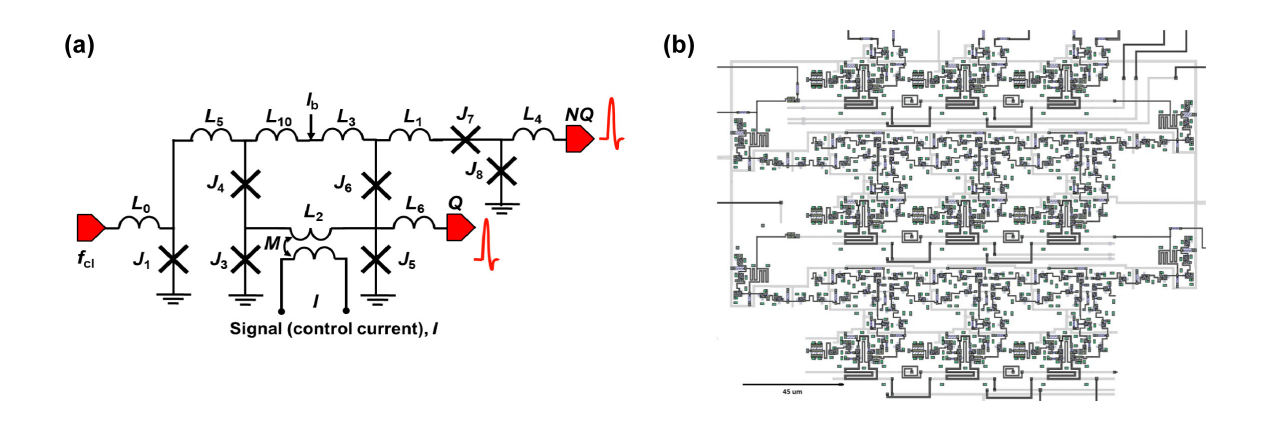
Development of a Neuromorphic Network using BioSFQ Circuits

E. B. Golden, A. Qu, V. K. Semenov, K. K. Berggren, S. K. Tolpygo Sponsorship: Air Force Contract No. FA8702-15-D-0001

Superconducting single-flux quantum (SFQ) circuits are promising candidates for neuromorphic hardware accelerators. They are extraordinarily fast and energy-efficient and use asynchronous pulse-rate data encoding, much like biological neurons. BioSFQ is an SFQ-based family that uses these neuromorphic features of SFQ circuits to process mixed analog/digital logic. BioSFQ circuits are also programmable, enabling

mixed modes of operation and resilience to fabrication variation and flux trapping.

In this work, we design, fabricate, and measure a 3x3 network of bioSFQ comparators, the fundamental building block of bioSFQ circuits. We also demonstrate novel techniques for network calibration, integrating on-chip memory, and image processing using this 3x3 network.



▲ Figure 1: (a) Schematic of a bioSFQ comparator and (b) layout of the 3x3 comparator network.

CiMLoop: A Flexible, Accurate, and Fast Compute-In-Memory Modeling Tool

T. Andrulis, J. S. Emer, V. Sze Sponsorship: Ericsson, TSMC, the MIT AI Hardware Program, MIT Quest, Samsung Semiconductor Fellowship, Siebel Scholars Fellowship

Compute-In-Memory (CiM) is a promising solution to accelerate Deep Neural Networks (DNNs) as it can avoid energy-intensive DNN weight movement and use memory arrays to perform low-energy, high-density computations. These benefits have inspired research across the CiM stack, but CiM research often focuses on only one level of the stack (i.e., devices, circuits, architecture, workload, or mapping) or only one design point (e.g., one fabricated chip). There is a need for a full-stack modeling tool to evaluate design decisions in the context of full systems (e.g., see how a circuit impacts system energy) and to perform rapid early -stage exploration of the CiM co-design space.

To address this need, we propose CiMLoop: an open-

source tool to model diverse CiM systems and explore decisions across the CiM stack. CiMLoop introduces (1) a flexible specification that lets users describe, model, and map workloads to both circuits and architecture, (2) an accurate energy model that captures the interaction between DNN operand values, hardware data representations, and analog/digital values propagated by circuits, and (3) a fast statistical model that can explore the design space orders-of-magnitude more quickly than other high-accuracy models. Using CiMLoop, researchers can evaluate design choices at different levels of the CiM stack, co-design across all levels, fairly compare different implementations, and rapidly explore the design space.

Ultra-low Power Superconducting Electronics for Deep Learning Accelerator Architectures: Evaluating Energy Efficiency and Scalability

L. C. Blackburn, E. Golden, T. Andrulis, V. Sze, J. S. Emer, N. Gershenfeld, K. K. Berggren Sponsorship: MIT Lincoln Laboratory, the MIT AI Hardware Program

Since the invention of the Josephson junction in the 1960s, superconducting electronics have shown promise for high-speed and energy-efficient computing. Since 2013, the Adiabatic Quantum Flux Parametron (AQFP) device has gained popularity for its ultra-low energy dissipation. AQFP inverters dissipate 10-²¹J per switching event, 100 less than other superconductor logic, and 10⁶X less energy than modern-day CMOS transistors or 10³X when including the cryogenic cooling cost. As Moore's law ends and energy efficiency emerges as a limit on today's computing systems, superconducting AQFP logic is a promising technology to address these energy challenges.

Although individual AQFP device performance is impressive, superconducting electronics have failed to replace CMOS systems in the past in part due to the high cost of cryogenic low-noise testing environments and the limitations of superconductor memory scaling.

To realize the promise of superconducting electronics, there is a need to architect full systems that can leverage the benefits of the unique superconductor physics (e.g., low-energy logic, low-energy interconnects on zero-resistance wires) while addressing the challenges (e.g., using low-noise cryogenic environments commoditized by the quantum computing industry, constructing a memory hierarchy that addresses the lack of a scalable, high-density superconducting memory).

In this work, we extend Timeloop/Accelergy accelerator modeling tools to support superconducting accelerators. This framework explores the design space of deep learning accelerator architectures with a toolbox of superconducting circuits from various logic families. We present results demonstrating the tradeoffs between superconductor vs. CMOS accelerators while running a range of deep learning workloads.

Single-Shot Matrix-Matrix Multiplication Optical Processor for Deep Learning

C. Luan, D. Englund, R. Hamerly Sponsorship: NTT Research, TSMC, DARPA NaPSAC

The computational demands of modern AI have sparked interest in optical neural networks (ONNs), which offer the potential benefits of increased capacity and lower power consumption. Notable progress includes the demonstration of optical matrix-vector multiplication (MVM) processors based on cascaded Mach-Zehnder interferometer arrays using coherent light as the data carriers and thermo-optic phase shifters as weighting. Broadcast-and-weight MVM optical processors using different wavelengths as data carriers and tunable add-drop micro-ring resonators as weighting elements have also been demonstrated. Recent advancements in delocalized photonic deep learning also shows the advantages of using optical fan-out and analog time integrator based optical MVM processors on the Internet's edge. So far, limited by the low parallelism, most existing systems operate vector-vector multiplication (VVM) or MVM with O(N) or O(N2) scaling in system throughput. To fully unlock the potential of optical computing, a parallel matrix-matrix multiplication (MMM) processor will allow better throughput and efficiency scaling than ordinary MVMs, but its realization is challenging due to the 3D data structure and high parallelism requirements.

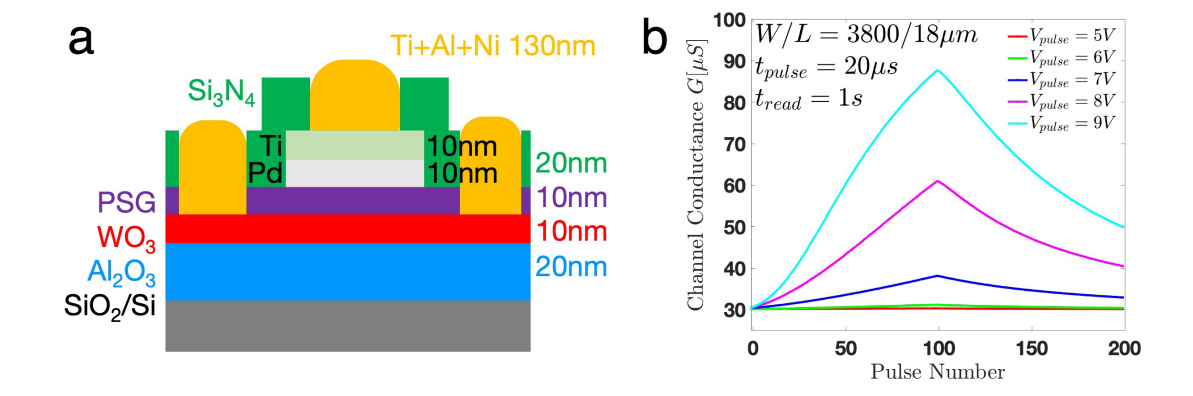
In this work, we propose and experimentally demonstrate a 3D grating-based ONN architecture using time-wavelength-spatial domain data flows with parallel operations in 16 space-degrees of freedom to improve the output capacity and energy efficiency. We experimentally demonstrate a parallel matrix-matrix multiplication processor using 4x4 input and output fiber arrays with 16 channel frequency comb lines of 7 different wavelengths, 32 broadband LiNbO $_3$ intensity modulators for weight matrix and input matrix encoding, a blazed reflective grating for low loss beam routing, and 16 analog time integrators for signal accumulation and network scaling, yielding a total operation-throughput of 64 MACs/shot with a high bit precision of 8-bits.

200 mm Wafer Diameter Process of Pd/PSG/WO3 Protonic Synapses for Analog Deep Learning

D. Shen, J. A. del Alamo Sponsorship: MIT-IBM Watson AI Lab

To solve the overcoming computational bottlenecks for deep learning, analog deep learning accelerators process information locally using special-purpose devices for matrix multiplication calculations and outer product updates. Among them, Electrochemical Random-Access Memories modulate channel resistance by ionic exchange between a semiconductor channel and a gate reservoir via an electrolyte. This design aims to enable neural network training with enhanced energy efficiency, non-volatility, and low latency.

Our research focuses on proton-based ionic synapses featuring in-situ hydrogenated H_xWO_3 (as channel) and PdH_y (as gate reservoir), and phosphosilicate glass (PSG) (as electrolyte). In a close collaboration with IBM Research, we have fabricated devices on a 200-mm wafer from IBM Research using a CMOS back-end-of-line compatible process. We have successfully demonstrated linear and symmetrical channel conductance modulation under different voltage pulses across gate and channel.



 \blacktriangle Figure 1: (a) Schematic of Pd/PSG/WO₃ protonic synapse fabricated in a joint MIT-IBM Research process on 200-mm wafers. (b) Conductance modulation under voltage pulses from 5 V to 9 V with a width of 20 µs that are fired every 1 s.

Tailor Swiftiles: Accelerating Sparse Tensor Algebra by Overbooking Buffer Capacity

Z. Y. Xue, Y. N. Wu, J. S. Emer, V. Sze Sponsorship: MIT AI Hardware Program, Mathworks Fellowship, NSERC PGS-D

Many applications operate on tensor data that has high sparsity (i.e., many zeros) with large variations sparsity between regions of a tensor. Prior sparse tensor algebra accelerators partition the tensor into equal shape tiles that all fit in a buffer, limiting utilization of buffer resources for more sparse tiles. Our key insight is that we can overbook the buffer by allocating tiles that occasionally exceed the capacity of the buffer. We propose to combine a low-overhead data orchestration

mechanism, Tailors, with a statistical tiling approach, Swiftiles, in order to support tiles that overbook the buffer and improve utilization of buffer resources and thus improve on-chip data reuse. Across a suite of 22 sparse tensor algebra workloads, we show that Tailors and Swiftiles introduce an average speedup 2.3x over an existing sparse tensor algebra accelerator with optimized tiling.

Stable and Accurate Nano-Resistor for Reliable Fixed Al Inference Tasks

G. Lee, M. Song, K. Kwon, J. Kim Sponsorship: Samsung Semiconductor Fellowship (3965323)

As artificial intelligence (AI) technology continues to advance in everyday applications, there is a rising demand for seamless, private, and sophisticated AI functionalities. On-device AI solutions, embedded within commercial mobile devices, eliminate the need for external server communication, thereby enhancing response times and data privacy. However, existing on-device AI technologies are limited by substantial power consumption and insufficient computational capacity to support advanced generative AI models. Memristor-based analog AI accelerators have emerged as a potential solution to the von Neumann bottleneck, a major limitation in achieving greater speed and energy efficiency in AI computing. Despite their promise, memristors are hindered by issues with conductance state stability and the complexity of required programming algorithms and circuitry, which constrains

their widespread adoption in industry. In this study, we introduce an ultra-reliable nano-resistor array that enables robust analog AI inference for specific tasks, minimizing the dependence on complex circuitry. Conductance states are fixed and geometrically defined through a single micro-nano patterning process, removing the need for stochastic programming and reducing the complexity of programming circuits typically required in memristor-based accelerators. We achieved 6.8-bit programming accuracy and stable 8-bit conductance levels. Additionally, experimental results from multiply-accumulate (MAC) operations show the feasibility of achieving 8.2-bit accuracy in a passive 28x28 array with simple circuit-level compensation. This nano-resistor array offers a reliable and precise platform for AI computing, tailored for daily AI tasks while reducing peripheral circuitry.

DuoAttention: Efficient Long-Context LLM Inference with Retrieval and Streaming Heads

G. Xiao, J. Tang, J. Zuo, J. Guo, S. Yang, H. Tang, Y. Fu, S. Han Sponsorship: National Science Foundation, MIT-IBM Watson AI Lab, MIT AI Hardware Program, Amazon, Samsung, Hyundai

Deploying long-context large language models (LLMs) is essential but poses significant computational and memory challenges. Caching all Key and Value (KV) states across all attention heads consumes substantial memory. Existing KV cache pruning methods either damage the long-context capabilities of LLMs or offer only limited efficiency improvements. In this paper, we identify that only a fraction of attention heads, a.k.a, Retrieval Heads, are critical for processing long contexts and require full attention across all tokens. In contrast, all other heads, which primarily focus on recent tokens and attention sinks-referred to as Streaming Heads--do not require full attention. Based on this insight, we introduce DuoAttention, a framework that only applies a full KV cache to retriev-

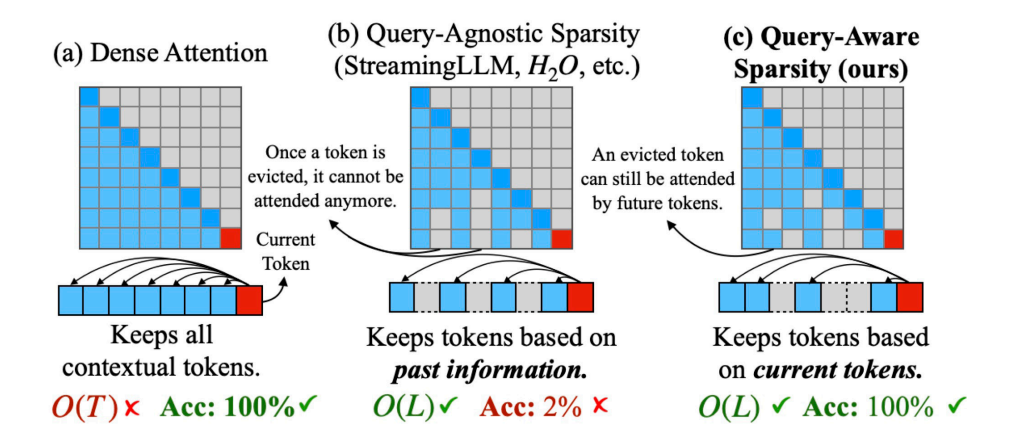
al heads while using a light-weight, constant-length KV cache for streaming heads, which reduces both LLM's decoding and pre-filling memory and latency without compromising its long-context abilities. DuoAttention uses a lightweight, optimization-based algorithm with synthetic data to identify retrieval heads accurately. Our method significantly reduces long-context inference memory by up to 2.55x for MHA and 1.67x for GQA models while speeding up decoding by up to 2.18x and 1.50x and accelerating pre-filling by up to 1.73x and 1.63x for MHA and GQA models, respectively, with minimal accuracy loss compared to full attention. Notably, combined with quantization, DuoAttention enables Llama-3-8B decoding with 3.3 million context length on a single A100 GPU.

Quest: Query-Aware Sparsity for Efficient Long-Context LLM Inference

J. Tang, Y. Zhao, K. Zhu, G. Xiao, B. Kasikci, S. Han Sponsorship: NSF, MIT-IBM Watson AI Lab, MIT AI Hardware Program, Amazon, Samsung, Hyundai

As the demand for long-context large language models (LLMs) increases, models with context windows of up to 1M tokens are becoming prevalent. However, long-context LLM inference is challenging since the inference speed decreases significantly as the sequence length grows. This slowdown is primarily caused by loading a large KV cache during attention. Previous works have shown that a small portion of critical tokens will dominate the attention outcomes. However, we observe the criticality of a token highly depends on

the query. To this end, we propose Quest, a query-aware KV cache selection algorithm. Quest keeps track of the minimal and maximal Key values in KV cache pages and estimates the criticality of a given page using Query. By only loading the Top-K critical KV cache pages, Quest significantly speeds up attention without sacrificing accuracy. We show that Quest can achieve up to 2.23x attention speedup, which reduces inference latency by 7.03x with negligible accuracy loss.



▲ Figure 1: Quest Algorithm Overview.

SORBET: Secure Off-chip Memory Interface for Deep Neural Network Accelerators

K. Lee, G. Das, D. Han, A. P. Chandrakasan Sponsorship: Samsung Electronics

As deep neural networks (DNNs) are deployed in high-stakes applications, ensuring their confidentiality and integrity becomes crucial. Trusted execution environments (TEEs) offer a potential solution by cryptographically encrypting and authenticating all data traffic to and from DNN accelerators without relying on off-chip hardware or system software to provide security. However, hardware memory encryption and authentication for DNN accelerators is challenging due to the large memory footprints of DNNs and the impact of cryptographic operations on the data access pattern of the accelerators. To address these challenges, we present SORBET, a secure off-chip memory interface for DNN accelerators. SORBET efficiently manages the altered

data access patterns resulting from cryptographic authentication and leverages lightweight cryptography to minimize overhead. Also, we designed our DNN accelerator to support fused-layer processing, a technique that reduces the overall off-chip data traffic, to alleviate pressure on the cryptographic engine. Our implementation of a secure DNN accelerator equipped with SORBET supports memory encryption and authentication with only 1-22% performance overhead, 5.6-7.9% of the chip area, and 18.4% energy overhead. These results are verified with an ASIC implementation using TSMC 28nm technology. Overall, we show that memory security of TEEs can be practically achieved for resource-constrained DNN accelerators.

LoopTree: Exploring the Fused-layer Dataflow Accelerator Design Space

M. Gilbert, Y. N. Wu, V. Sze, J. S. Emer Sponsorship: MIT AI Hardware Program

Deep neural network (DNN) accelerators often process DNNs one layer at a time, keeping intermediate data in off-chip DRAM. However, DRAM data transfers consume more energy than on-chip transfers and may increase latency due to limited DRAM bandwidth. Recent work has proposed fused-layer accelerators, which do not transfer intermediate data to/from DRAM but must recompute or retain data on-chip. This retention-recomputation trade-off results from the order of operations (dataflow) and the data tiles retained

on-chip (partitioning). However, prior work has only explored a subset of this design space. We propose (1) an expanded design space, and (2) a model, LoopTree, to evaluate the latency and energy consumption of accelerators in this design space. We validate LoopTree against prior architectures (worst-case 4% error). Finally, we show how exploring this larger space results in more efficient designs (e.g., up to 10× buffer capacity reduction to achieve the same off-chip transfers).

SVDQuant: Absorbing Outliers by Low-Rank Components for 4-Bit Diffusion Models

M. Li, Y. Lin, Z. Zhang, T. Cai, X. Li, J. Guo, E. Xie, C. Meng, J.-Y. Zhu, S. Han Sponsorship: NSF, MIT-IBM Watson AI Lab, MIT AI Hardware Program, Amazon, Samsung, Hyundai

Diffusion models have been proven highly effective at generating high-quality images. However, as these models grow larger, they require significantly more memory and suffer from higher latency, posing substantial challenges for deployment. In this work, we aim to accelerate diffusion models by quantizing their weights and activations to 4 bits. At such an aggressive level, both weights and activations are highly sensitive, where conventional post-training quantization methods for large language models like smoothing become insufficient. To overcome this limitation, we propose SVDQuant, a new 4-bit quantization paradigm. Different from smoothing which redistributes outliers between weights and activations, our approach absorbs these outliers using a low-rank branch. We first consolidate the outliers by shifting them from activations to weights, then employ a high-precision low-rank branch to take in the weight outliers with Singular Value De-

composition (SVD). This process eases the quantization on both sides. However, naïvely running the low-rank branch independently incurs significant overhead due to extra data movement of activations, negating the quantization speedup. To address this, we co-design an inference engine Nunchaku that fuses the kernels of the low-rank branch into those of the low-bit branch to cut off redundant memory access. It can also seamlessly support off-the-shelf low-rank adapters (LoRAs) without the need for re-quantization. Extensive experiments on SDXL, PixArt-∑, and FLUX.1 validate the effectiveness of SVDQuant in preserving image quality. We reduce the memory usage for the 12B FLUX.1 models by 3.5×, achieving 3.0× speedup over the 4-bit weight-only quantized baseline on the 16GB laptop 4090 GPU, paving the way for more interactive applications on PCs. Our quantization library and inference engine are open-sourced.



A Figure 1: SVDQuant is a post-training quantization technique for 4-bit weights and activations that well maintains visual fidelity. On 12B FLUX.1-dev, it achieves 3.6× memory reduction compared to the BF16 model. By eliminating CPU offloading, it offers 8.7× speedup over the 16-bit model when on a 16GB laptop 4090 GPU, 3× faster than the NF4 W4A16 baseline. On PixArt-Σ, it demonstrates significantly superior visual quality over other W4A4 or even W4A8 baselines. "E2E" means the end-to-end latency including the text encoder and VAE decoder.

LongVILA: Scaling Long-Context Visual Language Models for Long Videos

Q. Hu, H. Tang, S. Yang, S. Han

Long-context capability is critical for multi-modal foundation models, especially for long video understanding. We introduce LongVILA, a full-stack solution for long-context visual-language models by co-designing the algorithm and system. For model training, we upgrade existing VLMs to support long video understanding by incorporating two additional stages, i.e., long context extension and long video supervised fine-tuning. However, training on long video is computationally and memory intensive. We introduce the long-context Multi-Modal Sequence Parallelism (MM-SP) system that efficiently parallelizes long video training and inference, enabling 2M context length training on 256 GPUs without any gradient checkpointing. LongVILA efficiently extends the number of video frames of VILA from 8 to 2048, MM-SP is 2.1x - 5.7x faster than ring style sequence parallelism and 1.1x - 1.4x faster than Megatron with a hybrid context and tensor parallelism.

QServe: W4A8KV4 Quantization and System Co-design for Efficient LLM Serving

Y. Lin, H. Tang, S. Yang, Z. Zhang, G. Xiao, C. Gan, S. Han Sponsorship: NSF, MIT-IBM Watson AI Lab, MIT AI Hardware Program, Amazon, Samsung, Hyundai

Quantization can accelerate large language model (LLM) inference. Going beyond INT8 quantization, the research community is actively exploring even lower precision, such as INT4. Nonetheless, state-of-the-art INT4 quantization techniques only accelerate lowbatch, edge LLM inference, failing to deliver performance gains in large-batch, cloud-based LLM serving. We uncover a critical issue: existing INT4 quantization methods suffer from significant runtime overhead (20-90%) when dequantizing either weights or partial sums on GPUs. To address this challenge, we introduce QoQ, a W4A8KV4 quantization algorithm with 4-bit weight, 8-bit activation, and 4-bit KV cache. QoQ stands for quattuor-octo-quattuor, which represents 4-8-4 in Latin. QoQ is implemented by the QServe inference library that achieves measured speedup. The key insight driving QServe is that the efficiency of LLM serving on GPUs is critically influenced by oper-

ations on low-throughput CUDA cores. Building upon this insight, in QoQ algorithm, we introduce progressive quantization that can allow low dequantization overhead in W4A8 GEMM. Additionally, we develop SmoothAttention to effectively mitigate the accuracy degradation incurred by 4-bit KV quantization. In the QServe system, we perform compute-aware weight reordering and take advantage of register-level parallelism to reduce dequantization latency. We also make fused attention memory-bound, harnessing the performance gain brought by KV4 quantization. As a result, QServe improves the maximum achievable serving throughput of Llama-3-8B by 1.2x on A100, 1.4x on L40S; and Owen1.5-72B by 2.4x on A100, 3.5x on L40S, compared to TensorRT-LLM. Remarkably, QServe on L40S GPU can achieve even higher throughput than Tensor-RT-LLM on A100. Thus, QServe effectively reduces the dollar cost of LLM serving by 3x.

Photonics & Optoelectronics

| Integrated Visible-Light Grating-Based Antennas for Augmented-Reality Displays | 119 |
|---|-----|
| Integrated Photonics for Polarization-Gradient Cooling of Trapped Ions | 120 |
| Tunable Nanophotonic Devices and Cavities based on a Two-dimensional Magnet | 121 |
| Spatially-Adaptive Multi-Beam Optical-Phased-Array-Based Solid-State LiDAR Sensors | 122 |
| Optimized 2D Template for Remote Epitaxy of Efficient Red InGaN | 123 |
| High-resolution, Broadband Integrated Photonic Fourier-transform Spectrometer | 124 |
| Nonreciprocal Reflection of Mid-infrared Light at Low External Magnetic Fields or by Leveraging Internal Pseudo-magnetic Fields in Topological Weyl Semimetals | 125 |
| Low-thermal-budget Monolithic Integration of Magneto-optical Garnet for Silicon Photonic Optical Isolators | 126 |
| Understanding the Relationship Between Environmental Fabrication Conditions and Perovskite Formation, Performance, and Stability | 127 |
| Atomistic Simulations on Ion Incorporation in 2D Channel Materials for Fast Conductivity Modulation in Electrochemical Random-access Memory Devices | 128 |
| Heterogeneous Integration of Remote Epitaxial InP Coupons for Advanced Photonic Integrated Circuits | 129 |
| Modeling Coupling between Optically Driven Nanoantennas and Wires in Petahertz Electronic Circuits | 130 |
| Fully Integrated, Silicon Monolithic Refractive Index Sensor in CMOS for Hydrogen Sensing | 131 |
| Photoinduced Surface Passivation for Singlet Fission-Enhanced Silicon Photovoltaics | 132 |
| Electro-optic Control of AIN Photo-Switch with Sub-bandgap Illumination and Enhanced Switching Speed | 133 |
| Adaptive Nonlinear Pulse Engineering in Optical Multimode Fiber with Wavefront Shaping and Mechanical Perturbation | 134 |
| Superconducting Feedforward Electronics for Photon-Number Discrimination in Quantum Photonic Platforms | 135 |
| Gold Nanostructures for Mid and Long-Wave Infrared Detection | 136 |
| Dark Exciton Signatures in Blue OLEDs Probed by Strong Magnetic Fields in situ | 137 |
| Collaborative Robotics for Free-Space Optics | 138 |
| A Novel SERS-Based Strategy for Rapid and Sensitive Detection of NRR Products Using Janus WSSe/WS2 Heterostructures | 139 |
| Spatially and Spectrally Resolved Electric Field Inhomogeneity in Colloidal Cd-Free QD-LEDs | 140 |

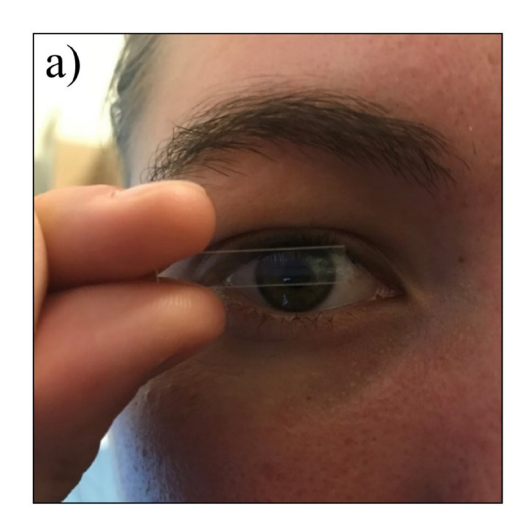
Integrated Visible-Light Grating-Based Antennas for Augmented-Reality Displays

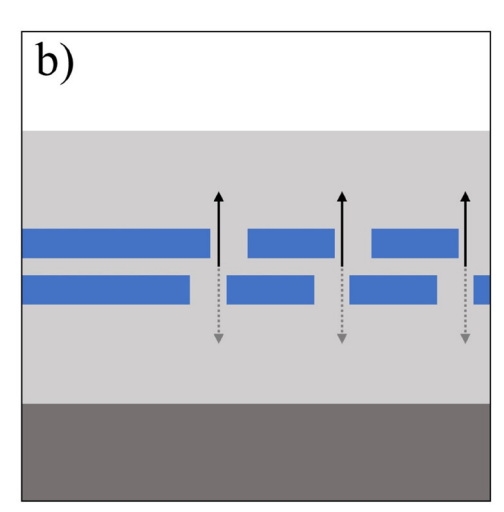
A. Garcia Coleto, M. Notaros, J. Notaros

Sponsorship: NSF CAREER Program, Defense Advanced Research Project Agency Visible Integrated Photonics Enhanced Reality Program, MIT School of Engineering Mathworks Fellowship, NSF Graduate Research Fellowship

Augmented-reality (AR) displays that display information in the user's field of view have many wide-reaching applications in defense, medicine, gaming, etc. However, current commercial AR displays are bulky, heavy, and indiscreet. Moreover, current AR displays are incapable of producing holographic images with full depth cues; this lack of depth information results in eyestrain and headaches that limit long-term and wide-spread use of these displays.

To address these limitations, we are developing an integrated-photonics-based display that consists of a single transparent chip that sits directly in front of the user's eye and projects holograms that only the user can see. Specifically, in this work, we develop and demonstrate uniformly- and unidirectionally-emitting grating-based antennas that enable this integrated-photonics-based display architecture. This work paves the way towards a highly discreet and fully holographic solution for the next generation of AR displays.





▲ Figure 1: (a) Photograph of a transparent integrated-photonics-based holographic display. (b) Simplified cross-sectional conceptual diagram of a partial section of a dual-layer antenna showing unidirectional emission in the upward direction.

FURTHER READING:

A. Garcia Coleto, M. Notaros, and J. Notaros, "Visible-Light Uniform and Unidirectional Grating-Based Antennas for Integrated Optical Phased Arrays," Optics Express, vol. 32, no. 26, pp. 46447-46466, 2024.

A. Garcia Coleto, M. Notaros, and J. Notaros, "Design and Demonstration of Grating-Based Antennas for Visible-Light Integrated Optical Phased Arrays," Proc. Conference on Lasers and Electro-Optics (CLEO) OSA, 2025.

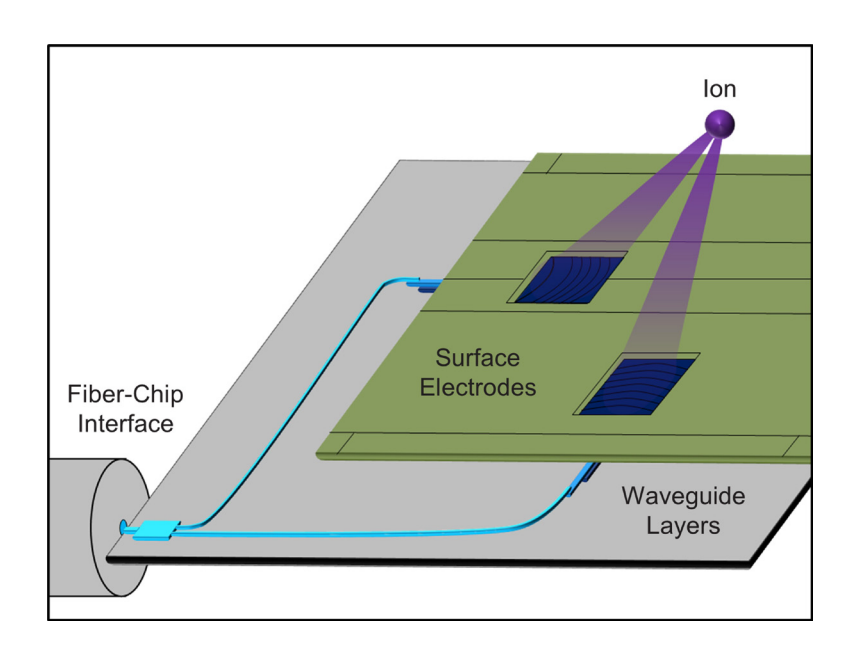
[•] M. Notaros, D. DeSantis, M. Raval, and J. Notaros, "Liquid-Crystal-Based Visible-Light Integrated Optical Phased Arrays and Application to Underwater Communications," Optics Letts., vol. 48, no. 20, pp. 5269-5272, 2023.

Integrated Photonics for Polarization-Gradient Cooling of Trapped Ions

S. M. Corsetti, A. Hattori, E. R. Clements, F. W. Knollmann, M. Notaros, R. Swint, T. Sneh, P. T. Callahan, G. N. West, D. Kharas, T. Mahony, C. D. Bruzewicz, C. Sorace-Agaskar, R. McConnell, I. L. Chuang, J. Chiaverini, J. Notaros Sponsorship: NSF Quantum Leap Challenges Institute (QLCI) Hybrid Quantum Architectures and Networks, NSF QLCI Quantum Systems through Entangled Science and Engineering, MIT Center for Quantum Engineering, NSF Graduate Research Fellowship Program, Department of Defense National Defense Science and Engineering Graduate Fellowship, MIT Cronin Fellowship, MIT Locher Fellowship

Trapped ions are a promising modality for quantum systems, with demonstrated utility as the basis for quantum processors and optical clocks. However, most trapped-ion systems are implemented using free-space optics, whose large size and susceptibility to vibrations and drift inhibit scaling. Integrated photonics offers a potential avenue to address these challenges.

Motional state cooling is a key optical function in trapped-ion systems. However, to date, integratedphotonics-based demonstrations have been limited to Doppler and resolved-sideband cooling. In this work, we develop and demonstrate a variety of integrated-photonics-based systems for polarization-gradient cooling (PGC), resulting in the first experimental demonstration of trapped-ion PGC by an integrated-photonics-based system. By enabling faster and more power-efficient cooling, this work has the potential to improve computational efficiencies for integrated-photonics-based trapped-ion platforms.



▲ Figure 1: Conceptual diagram of an integrated-photonics-based polarization-gradient-cooling experiment, demonstrating the emission of multiple beams from an ion-trap chip designed to intersect and form a polarization gradient at a target ion location.

FURTHER READING:

[•] S. Corsetti, A. Hattori, E. R. Clements, F. W. Knollmann, M. Notaros, R. Swint, T. Sneh, P. T. Callahan, et al., "Integrated-Photonics-Based Systems for Polarization-Gradient Cooling of Trapped Ions," under review. (*Preprint on arXiv: https://arxiv.org/abs/2411.06025*)

[•] E. Clements, F. W. Knollmann, S. Corsetti, Z. Li, A. Hattori, M. Notaros, R. Swint, T. Sneh, et al., "Sub-Doppler Cooling of a Trapped Ion in a Phase-Stable Polarization Gradient," under review. (*Preprint on arXiv: https://arxiv.org/abs/2411.06026*)

A. Hattori*, S. Corsetti*, T. Sneh, M. Notaros, R. Swint, P. T. Callahan, C. D. Bruzewicz, F. Knollmann, et al., "Integrated-Photonics-Based Architectures for Polarization-Gradient and EIT Cooling of Trapped Ions," Proc. Frontiers in Optics (FiO) (Optica), paper FM4B.3, 2022. (*Equal Contributors)

Tunable Nanophotonic Devices and Cavities based on a Two-dimensional Magnet

A. K. Demir, L. Nessi, S. Vaidya, C. A. Occhialini, M. Soljačić, R. Comin

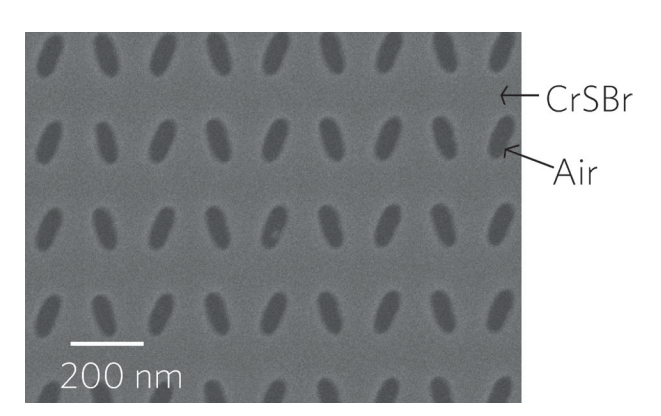
Nanophotonics, the study and manipulation of light at the nanoscale, has experienced rapid growth through the integration of emerging quantum materi-als. These materials offer unique optical properties, particularly when light strongly couples with matter to form hybrid modes known as polaritons. A cen-tral challenge in this field is achieving dynamic control over photonic devices post-fabrication, which is often limited by fixed geometries and weak light-matter interactions. Quantum materials with field-tunable properties might offer a promising path forward, especially when integrated into monolithic photonic de-vices where light is fully confined within the active medium.

We demonstrated a new class of active nanophotonic devices using the low-dimensional magnetic quantum material CrSBr. Through a tailored fabrication process, we nanopattern CrSBr flakes into photonic crystal slabs that support high-Q guided mode resonances and epsilon-below-zero modes within extremely small volumes. Remarkably, by applying external magnetic fields, we achieve a re-versible switch of the mode of the operation of the photonic

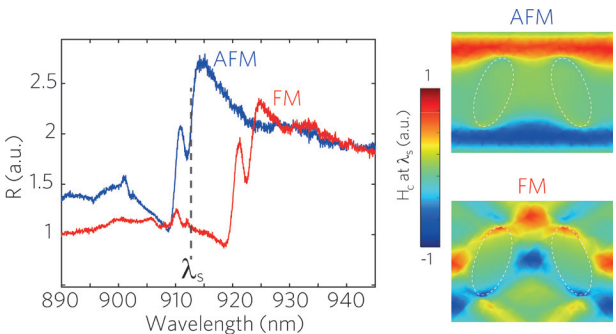
crystal, from elliptic to hyperbolic, without modifying the geometry. This is driven by a giant tunabil-ity in the real permittivity ($\Delta \varepsilon_1 \sim 800$) near CrSBr's excitonic resonance.

Our results highlight two major contributions. First, we show CrSBr-based nanophotonic structures offer intrinsic, in-situ tunability and miniaturization in a monolithic platform. Second, we observe self-hybridized strong light-matter coupling, yielding polariton modes tunable via magnetic fields. With refractive index changes far exceeding those in traditional van der Waals materials, and ob-served Q-factors exceeding 1200, CrSBr emerges as a highly versatile platform. Its tunability spans multiple external stimuli (strain, pressure, ultrafast pulses, and AC/DC magnetic fields) enabling switching speeds up to 30 GHz.

Our findings establish CrSBr as a frontier material for tunable nanophoton-ics and polaritonic devices, combining ultrafast reconfigurability, miniaturization, and strong coupling in a single, compact platform.



▲ Figure 1: Example photonic crystal slab made of 20-nm-thick CrSBr flake.



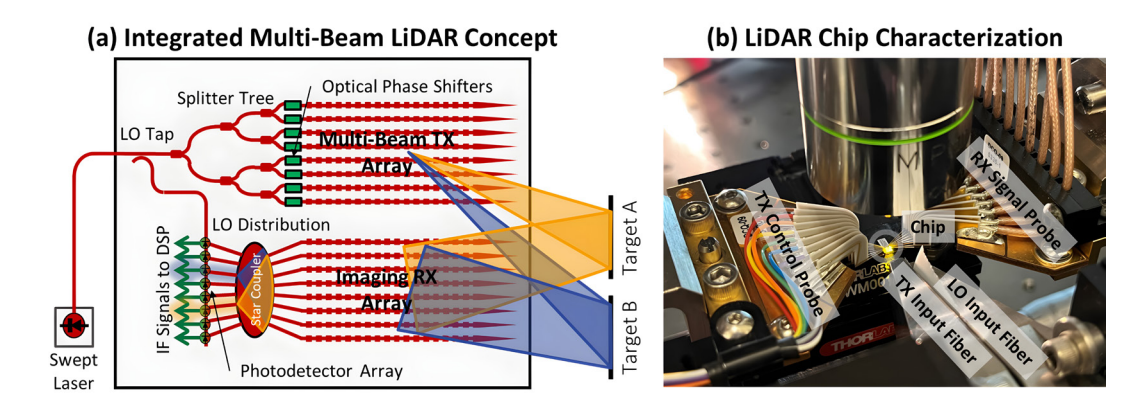
▲ Figure 2: Reflectivity shows that high-Q resonance rigidly redshifts when magnetic ground state goes from antiferromagnetic (AFM) to FM with B-field. Elliptic photonic mode in AFM phase turns into hyperbolic mode in FM.

Spatially-Adaptive Multi-Beam Optical-Phased-Array-Based Solid-State LiDAR Sensors

D. M. DeSantis, B. M. Mazur, M. Notaros, J. Notaros Sponsorship: Semiconductor Research Corporation (SRC) Joint University Microelectronics Program (JUMP) 2.0 CogniSense, MIT Rolf G. Locher Endowed Fellowship, NSF Graduate Research Fellowship

Light detection and ranging (LiDAR) has emerged as a vital and widely-used sensing technology for autonomous systems, such as autonomous vehicles, since it enables three-dimensional mapping with higher resolution than traditional RADAR. However, current commercial LiDAR systems utilize mechanical beam-steering mechanisms that decrease reliability, increase production cost, and limit detection range. To address these limitations, solid-state optical-phased-array-based (OPA-based) LiDAR, which enables low-cost, high-speed, and compact non-mechanical beam steering, has emerged as a promising solution for next-generation Li-DAR sensors.

In this work, we propose, develop, and experimentally demonstrate a novel spatially-adaptive solid-state LiDAR system enabled by multiple-beam OPA subsystems and integrated optical-processing devices. This multi-beam adaptability enhances spatial awareness and reduces the back-end data processing traditionally associated with beam-rastering LiDAR.



▲ Figure 1: (a) Conceptual diagram of our solid-state multi-beam LiDAR system illuminating and ranging two targets simultaneously. (b) Photograph of our fabricated solid-state multi-beam LiDAR system chip under test with light coupled in through optical fibers (bottom) and electrical probes landed (left and right).

FURTHER READING

D. M. DeSantis, B. M. Mazur, M. Notaros, and J. Notaros, "Multi-beam solid-state LiDAR Using Star-coupler-based Optical Phased Arrays,"
 Optics Express, vol. 32, no. 21, pp. 36656-36673, 2024.

[•] Y. Liu, C. Zhang, D. M. DeSantis, D. Hu, T. Meissner, J. Notaros, and J. Klamkin, "High-Resolution Arrayed Waveguide Grating-Assisted Passive Optical Phased Array for 2D Beam Steering," Optics Express, vol. 33, no. 4, pp. 7714-7722, 2025.

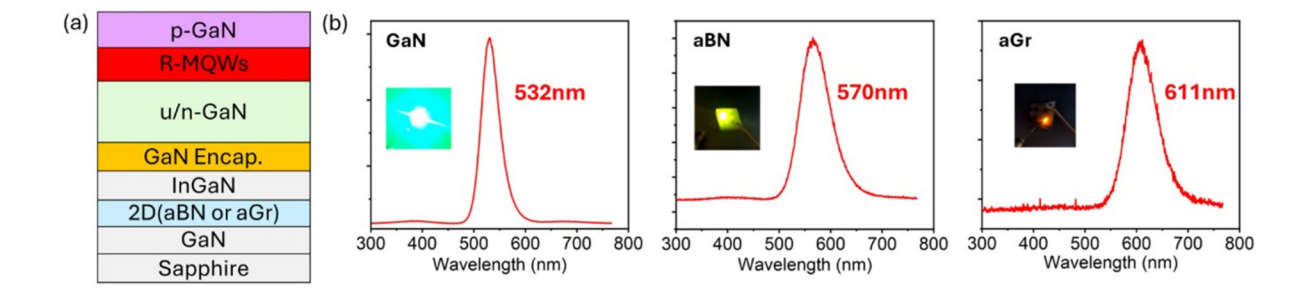
D. M. DeSantis, M. R. Torres, A. Garcia Coleto, B. M. Mazur, S. Corsetti, M. Notaros, and J. Notaros, "Spiral Integrated Optical Phased Arrays for Tunable Near-Field-Focusing Emission," Optics Express, vol. 32, no. 25, pp. 44567-44580, 2024.

Optimized 2D Template for Remote Epitaxy of Efficient Red InGaN

J. Feng, J. Kim, Y. Liu, J. Kim Sponsorship: Samsung Electronics

InGaN-based micro-light-emitting diodes (LEDs) have garnered significant attention for their potential to emit light across the entire visible spectrum. While high external quantum efficiency blue and green InGaN emitters have been achieved, progress in developing high-efficiency red InGaN LEDs remains constrained by the lattice mismatch between III-nitride materials and conventional substrates. This work presents a novel approach using remote epitaxy on two-dimensional (2D) materials, such as amorphous graphene (aGr) and amorphous boron nitride (aBN), to overcome these challenges by strain relaxation. By directly growing

wafer-scale 2D layers on GaN substrates, we enabled relaxed InGaN (up to 100%) with a low dislocation density of 4.4×10⁻⁸ cm⁻². Optimized growth conditions via molecular beam epitaxy (MBE) at 550–600°C facilitated the redshift of luminescence to 611 nm (red light) for InGaN grown on aGr/GaN, a notable improvement com-pared to that grown directly on a GaN template that exhibited 532-nm (green light). These results demon-strate a promising pathway to develop highly efficient InGaN red LEDs for ultra-high-pixel-density micro-LED displays in AR/VR applications, offering a potential alternative to III-As/P-based LEDs.



▲ Figure 1: (a) InGaN red LED quantum well structure and (b) Electroluminescence spectra of InGaN LED on bare GaN, aBN/GaN, and aGr/GaN substrate.

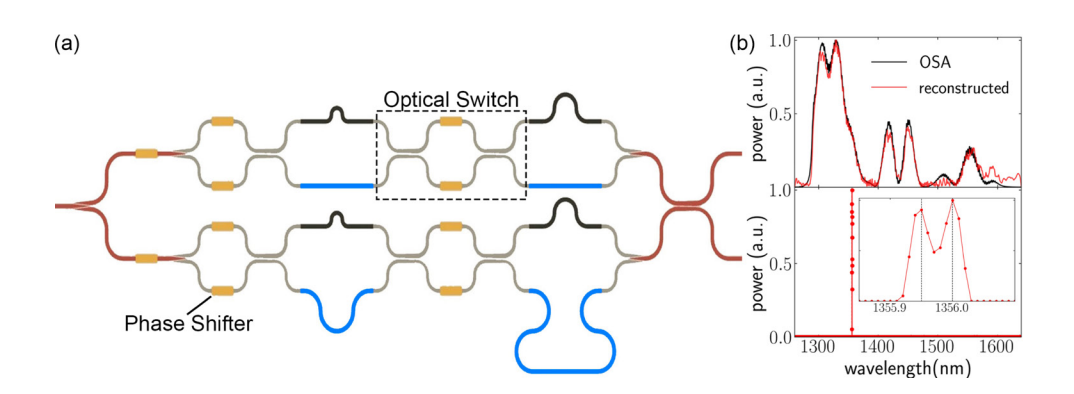
High-resolution, Broadband Integrated Photonic Fourier-transform Spectrometer

M. R. A. Peters, D. Mojahed, B. Neltner, J. Hu Sponsorship: NSF (Grant No. 2122581), LyteChip Inc., Equinor ASA

Spectrometers are powerful and widely used tools for chemical and biological analysis. Low- cost, miniaturized spectrometers enable a wide range of in-the-field, hand-held, or point-of-care spectrometer applications. Integrated photonics provides a unique opportunity for small footprint, on-chip spectrometer devices. In recent years, a variety of integrated spectrometer designs have been proposed; however, most are limited in either bandwidth or resolution.

In this work, we present a digital Fourier-transform spectrometer that overcomes the bandwidth-resolution trade-off faced by other integrated devices. The design employs broad-band 2x2 optical switches to route light through unique optical paths on the silicon-on-insulator chip (Figure 1a), allowing for large optical path length differences and thus high resolution over a broad bandwidth in the near-infrared.

We fabricate and package a digital Fouriertransform spectrometer with 10 optical switches, i.e., 210 = 1024 unique optical path length differences. The full optical package consists of the spectrometer chip, temperature control, and electrical connections to read-out the on-chip photodetector as well as power the thermo-optic phase shifters. We calibrate the device with tunable laser over a 380-nm bandwidth (1260 nm-1640 nm) in steps of 0.01 nm and demonstrate accurate reconstruction of a broadband spectrum (Figure 1b-Top). By measuring the closest spacing between two laser lines that can be accurately resolved, we find a high resolu-tion of 0.05 nm (Figure 1b-Bottom). Our work shows the potential of the digital Fourier-transform spectrometer as a broadly applicable miniaturized spectrometer.



▲ Figure 1: (a) Schematic representation of digital Fourier-transform spectrometer. Thermo-optic phase shifters (yellow) in broadband 2x2 optical switches (grey) allow light to be switched between different waveguides (black and blue, respectively). Each combination of optical switch states results in a unique optical path length difference between the two arms. (b) Top: Reconstructed broadband spectrum (red) and input spectrum as measured with optical spectrum analyzer (black). Bottom: Reconstruction of input spectrum consisting of two laser lines at 1355.95 and 1356.00 nm, respectively.

Nonreciprocal Reflection of Mid-infrared Light at Low External Magnetic Fields or by Leveraging Internal Pseudo-magnetic Fields in Topological Weyl Semimetals

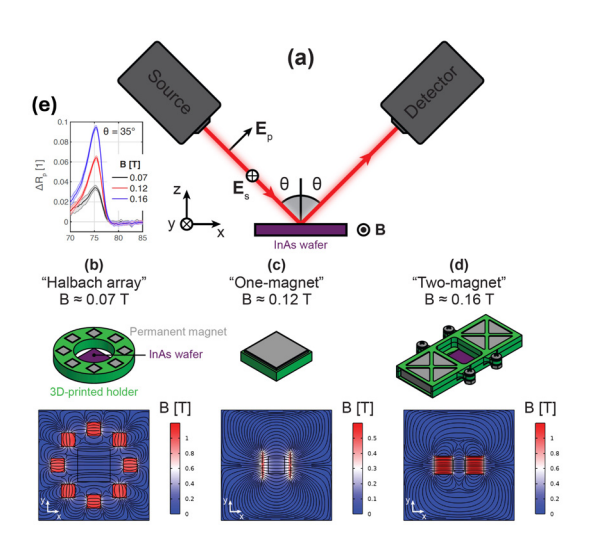
S. Pajovic, H. Gold, Y. Tsurimaki, A. Mukherjee, X. Qian, G. Chen, S. V. Boriskina Sponsorship: ARO-Multidisciplinary University Research Initiatives program

In conventional optical materials, light-matter interactions are reciprocal. This means that a light wave returns to its original state if it travels backwards through the medium following the same trajectory. However, reciprocity of light and energy transport is not a fundamental law. It can be broken by material losses, nonlinearity, or magnetic fields, enabling the "one-way" flow of optical energy and unlocking applications in energy harvesting, signal processing, and thermal emission control.

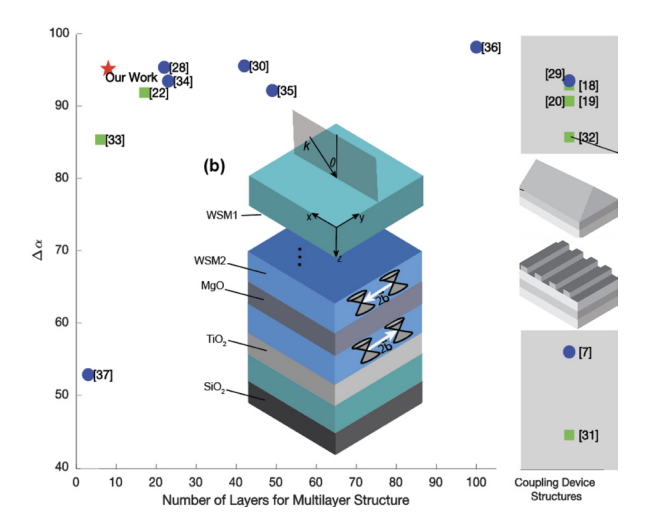
Nonreciprocal surfaces do not obey Kirchhoff's law of thermal radiation, which postulates the equality of spectral directional emissivity and absorptivity. This has implications for the energy efficiency of devices that emit and absorb thermal radiation, such as solar thermal collectors and thermophotovoltaic cells, since they no longer must emit as much energy as they absorb through any given spectral directional channel.

We experimentally observed room-temperature nonreciprocal reflection of mid-infrared light from planar highly doped InAs surfaces at low magnetic fields ranging from 0.07 T to 0.16 T. Prior experiments used larger magnetic fields ranging from 0.5 T to 1.5 T, which limited practical applications of this effect (Figure 1).

Taking a step further, we theoretically predict strong nonreciprocity and violation of Kirchhoff's law in a planar sub-wavelength-thin magnetophotonic crystal composed of dielectric and magnetic Weyl semimetal thin films. The optimized design eliminates the need for an external magnetic field and achieves a large nonreciprocal absorptivity contrast of 0.953. Our work is a step toward the practical implementation of nonreciprocal thermal emitters and absorbers and applications such as remote magnetic field sensing (Figure 2).



▲ Figure 1: (a) Light is incident on InAs wa-fer at polar angle of incidence θ and can be s- or p-polarized. InAs wafer is magnet-ized normal to plane of incidence. Three magnetization schemes provide different magnetic field magnitudes B: (b) Halbach array, $B \approx 0.07$ T. (c) One-magnet, $B \approx 0.12$ T. (d) Two-magnet, $B \approx 0.16$ T. (e) Meas-ured nonreciprocal reflectance contrast of p-polarized light, $\Delta Rp \equiv Rp(\omega, \theta, +B) - Rp(\omega, \theta, -B)$.



▲ Figure 2:1D photonic crystal composed of Weyl semimetal and dielectric layers was optimized to maximize nonreci-procity of infrared radiation absorptance in planar and ultra-compact design, which surpasses other proposed de-signs in performance.

FURTHER READING

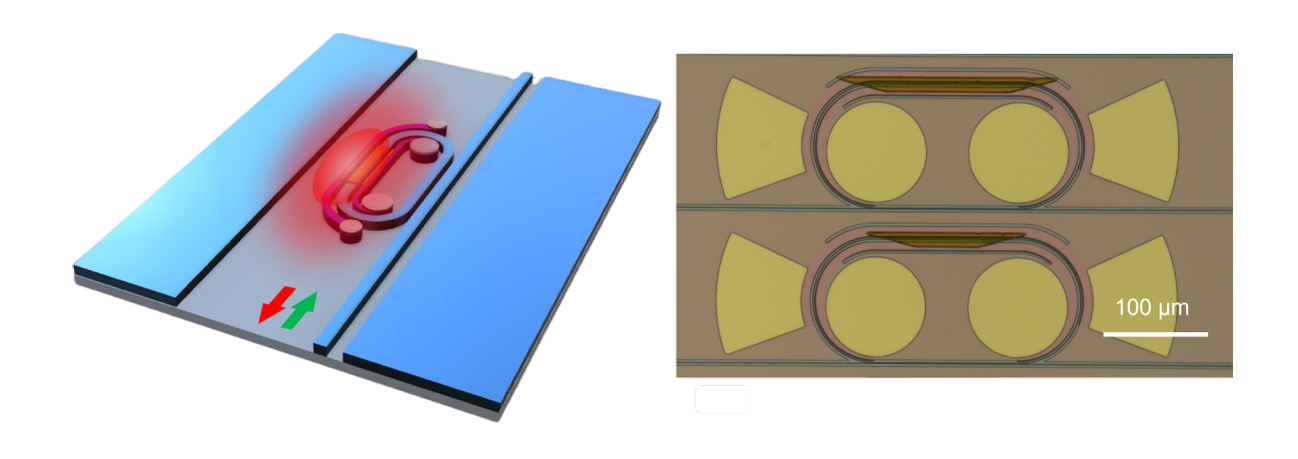
- S. V. Boriskina, M. Blevins, and S. Pajovic, "The Nonreciprocal Adventures of Light," Optics and Photonics News, vol. 33, no. 9, pp. 46-53, 2022.
 DOI.org/10.1364/OPN.33.9.000046
- S. Pajovic, Y. Tsurimaki, X. Qian, G. Chen, and S.V. Boriskina, "Nonreciprocal Reflection of Mid-infrared Light by Highly Doped InAs at Low Magnetic Fields," Opt. Express, vol. 33, pp. 8661-8674, 2025. DOI.org/10.1364/OE.544496
- H. Gold, S. Pajovic, A. Mukherjee, and S.V. Boriskina, "GAGA for Nonreciprocal Emitters: Genetic Algorithm Gradient Ascent Optimization of Compact Magnetopho-tonic Crystals," Nanophotonics, vol. 3, no. 5, pp. 773-792, 2024. DOI.org/10.1515/nanoph-2023-0598

Low-thermal-budget Monolithic Integration of Magneto-optical Garnet for Silicon Photonic Optical Isolators

K. P. Dao, J. M. Chavez, K. Hayashi, Q. Du, C. A. Ross, J. Hu

Integrated optical isolators are crucial components of photonic integrated circuits (PICs) and have garnered significant attention. The two common integration schemes for optical isolators are heterogeneous integration and monolithic integration. Monolithic integration using magneto-optical materials is ideal for optical isolator fabrication due to its compact footprint, broadband, polarization-diverse operation, compatibility with various types of devices, and industrial scalability. However, current monolithic optical isolators face a major challenge: a high thermal budget required for the deposition and crystallization of magneto-optical materials, hindering their integration into foundry-processed PICs. This study introduces a novel approach for monolithic integration

of on-chip optical isolators with a low thermal budget, compatible with standard complementary metal-oxide-semiconductor (CMOS) back-end-of-line processes. The proposed optical isolators employ bismuth-substituted yttrium/terbium iron garnet and integrated micro-doped silicon heaters. By engineering the bismuth concentration within the garnet, we showcase the feasibility to deposit the magneto-optical garnet on silicon substrates at room temperature and crystallize it by post-deposition annealing at a lower temperature window. The integrated micro-doped silicon heaters are utilized to crystallize the garnet locally on-chip while protecting other devices. The study presents a new method for incorporating non-reciprocity into various integrated photonic devices.



▲ Figure 1: Schematic and microscopic images of low-thermal-budget monolithic integration for resonator-based optical isolators.

FURTHER READING

K. Hayashi, K. P. Dao, et al. "Magneto-Optical Bi-Substituted Yttrium and Terbium Iron Garnets for On-Chip Crystallization via Microheaters," Adv. Optical Mater, vol. 12, p. 2400708, 2024.

[•] K. P. Dao, et al. "Low-thermal-budget Monolithic Integration of Optical Isolators for Silicon Photonics," Proc. SPIE 13369, Integrated Optics: Devices, Materials, and Technologies XXIX, 133690G, 2025.

K. P. Dao, J. Hu et al. "Thermal Inverse Design for Resistive Micro-heaters," J. Appl. Phys., vol 136, p. 225101, 2024.

Understanding the Relationship Between Environmental Fabrication Conditions and Perovskite Formation, Performance, and Stability

N. Evans, R. Lee, T. Liu, T. Buonassisi

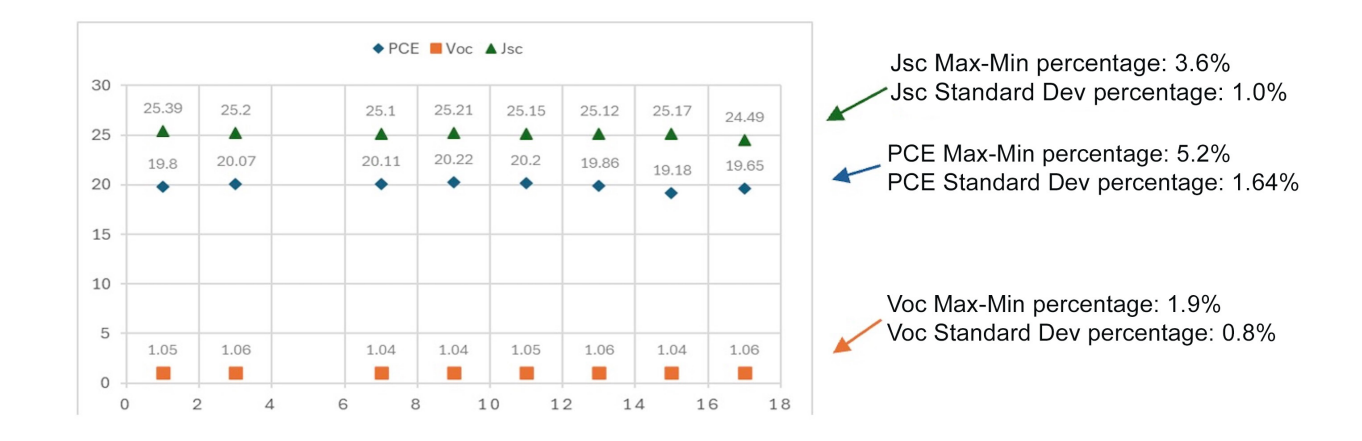
Sponsorships: Centre for Accelerated Co-Design of Durable, Reproducible, and Efficient Perovskite-Silicon Tandems, U.S. Department of Energy Office of Energy Efficiency and Renewable Energy Solar Energy Technologies Office

To achieve perovskite solar cells with recipes that can transfer from lab-to-fab reproducibly and scale from spin-coating to meniscus-coating methods, understanding the impact of environmental variables during the perovskite deposition and drying processes is imperative. These variables, namely the ambient temperature, humidity, and solvent partial pressures, ultimately all affect the growth and formation of the perovskite.

As part of the Centre for Accelerated Co-Design of Durable, Reproducible, and Efficient Perovskite-Silicon Tandems, our team at MIT has designed a setup in which we can control the temperature (T), solvent partial pressure (SPP), and absolute humidity (AH%) during the deposition and annealing steps of perovskite fabrication. In this work, we have explored the effects of these parameters on the device performance of FAPbI $_3$ perovskite devices.

Bayesian optimization was employed with the help of Atinary Self-Driving Labs software to map the relationships between these environmental parameters and the power conversion efficiencies (PCE) of the perovskite solar cell devices. Our findings reveal that the cross-variable relationships between these variables are non-linear and complex, which we show through a tree-diagram analysis, along with supporting GIWAXS data to show the complexity of combined effects on phase-formation during spin coating.

Finally, it was confirmed that with a controlled environment, the repeatability of these devices markedly improved, with tight variance in open circuit voltage, short circuit current, and PCE. By optimizing these parameters for manual spin-coating of stable and efficient small-area perovskite devices, we hope to set a foundation for transitioning to higher throughput printing of both stable and efficient perovskite solar cells.



▲ Figure 1: PCE, Voc, and Jsc of 8 samples fabricated under controlled environmental conditions, resulting in tight variance across the characteristics and exemplifying the positive effect of controlled environment on reproducibility.

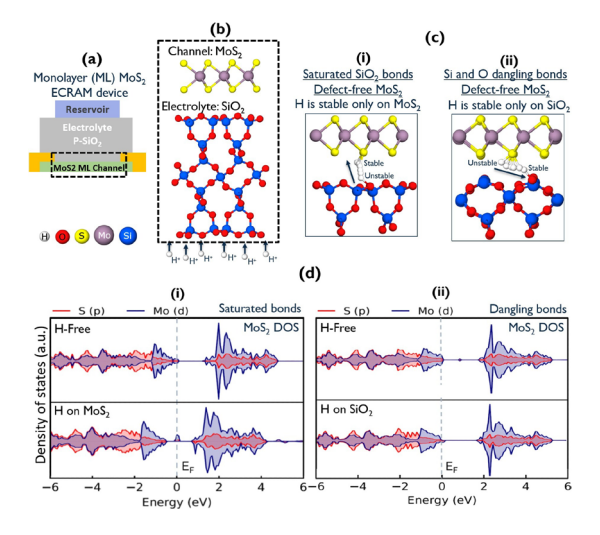
Atomistic Simulations on Ion Incorporation in 2D Channel Materials for Fast Conductivity Modulation in Electrochemical Random-access Memory Devices

V. Fotopoulos, M. Siebenhofer, M. Huang, L. Xu, B. Yildiz Sponsorship: SRC

Electrochemical random-access memory (ECRAM) has emerged as a novel type of programmable resistor for crossbar arrays—a promising architecture for implementing energy-efficient artificial neural networks. ECRAMs consist of three key functional layers: an ion reservoir, a solid electrolyte, and a channel (Figure 1(a)). Through voltage-driven intercalation of mobile ions (e.g., H⁺), the electronic conductivity of the channel can be finely modulated, enabling precise control over the resistance state of the device. Mixed ionic and electronic conducting oxides, e.g., WO₃, have been investigated as channel materials. However, their bulk nature necessitates three-dimensional ion redistribution, leading to undesirably long conductivity settling times. Two-dimensional (2D) materials, including monolayers of transition metal dichalcogenides (TMDs), such as MoS₂, offer a promising alternative, yet the mechanisms of interfacial ion transport and their impact on the conductivity of the channel remain underexplored.

In this work, we employed density functional theory to investigate hydrogen (H) incorporation at

interfaces between a solid electrolyte (SiO2) and a monolayer (MoS₂) channel (Figure 1(b)). We explored a range of SiO₂ surface chemistries—including surfaces with unsaturated Si and O dangling bonds and reconstructed surfaces with fully saturated bonds and showed that surface termination determines the most stable H incorporation sites. For defect-free MoS₂, H is stable on MoS² only when the underlying SiO₂ surface is fully saturated (Figure 1(c)(i)), increasing the channel's conductivity through n-type doping (Figure 1(d)(i)). In contrast, when unsaturated O and/or Si dangling bonds are present (Figure 1(c) (ii)), H preferentially binds to the electrolyte surface, remaining electronically decoupled from MoS₂ (Figure 1(d)(ii)). Additionally, introducing a sulfur vacancy (V_s) in MoS₂ alters this behavior: across all surfaces, H stabilizes inside the vacancy, leading to n-type doping. These findings highlight how interfacial structure and defect engineering can enhance ionic modulation of conductivity in 2D ECRAMs.



▲ Figure 1: (a) ECRAM device. (b) MoS_2/SiO_2 interface. (c) (i) At fully saturated interfaces, H is stable on MoS_2 . (ii) In interfaces with dangling bonds, H is stable on SiO_2 . (d) (i) Density of states (DOS) of MoS_2 in saturated interface. (ii) DOS of MoS_2 in interface with dangling bonds.

FURTHER READING

- A. A. Talin, J. Meyer, J. Li, M. Huang, M. Schwacke, H. W. Chung, L. Xu, E. J. Fuller, Y. Li, and B. Yildiz, "Electrochemical Random-Access Memory: Progress, Perspectives, and Opportunities," Chemical Reviews, vol. 125, no. 4, pp. 1962-2008, 2025.
- M. Schwacke, P. Žguns, J. A. del Alamo, J. Li, and B. Yildiz, "Electrochemical Ionic Synapses with Mg2+ as the Working Ion," Advanced Electronic Materials, vol. 10, no. 5, p. 2300577, 2024.
- M. Huang, M. Schwacke, M. Onen, J. A. del Alamo, J. Li, and B. Yildiz, "Electrochemical Ionic Synapses: Progress and Perspectives," Advanced Materials, vol. 35, no. 37, p. 2205169, 2023.

Heterogeneous Integration of Remote Epitaxial InP Coupons for Advanced Photonic Integrated Circuits

Y. J. Yoo, J. H. Ko, A. Buzzi, K. Lu, L. Follet, K. Alqubaisi, D. R. Englund, J. Kim

Photonic integrated circuits (PICs) are transforming industries by consolidating multiple optoelectronic functions onto a single chip, improving efficiency, and reducing costs across applications such as data centers, autonomous vehicles, and atmospheric sensing. While leveraging silicon (Si) fabrication technologies has significantly enhanced scalability and affordability, integrating efficient light sources remains a major challenge because Si is intrinsically inefficient at light emission.

To address this, III–V semiconductor materials such as indium phosphide (InP) are utilized to generate light although they are often packaged separately, increasing complexity and cost. Recent efforts have focused on integrating III–V lasers directly onto Si photonics platforms, aiming to minimize space constraints, lower system costs, and enhance reliability in laser-dense applications.

Traditional methods of heterogeneous integration typically involve bonding III–V materials onto Si substrates using adhesives or direct bonding techniques, which can introduce thermal and mechanical reliability concerns. To overcome these

challenges, we are developing an adhesive-free remote epitaxial transfer process to integrate thin-film InPbased coupons directly onto Si photonic circuits.

Our approach leverages remote epitaxy to grow single-crystalline III–V layers on two-dimensional (2D) material-coated reusable substrates. These epitaxial layers can be exfoliated cleanly and transferred to Si photonics wafers without the need for adhesives. This method offers several advantages: (1) the reusable growth substrate significantly reduces the overall cost of III–V wafer fabrication, (2) the absence of adhesive layers improves thermal management and mechanical integrity, and (3) the process is compatible with wafer-scale integration techniques, making it scalable for commercial photonic systems.

Furthermore, our method allows precise couponscale transfer, enabling selective placement of III–V emitters where needed without affecting the underlying PIC structures. This adhesive-free, remote epitaxy-enabled integration strategy holds promise for advancing high-density, cost-effective photonic systems by embedding efficient light sources directly into existing Si photonics infrastructures.

FURTHER READING

Y. Kim, et al., "Remote Epitaxy Through Graphene Enables Two-dimensional Material-based Layer Transfer," Nature, vol. 544, pp. 340–343, 2017.

H. Kim, et al., "Graphene Nanopattern as a Universal Epitaxy Platform for Single-Crystal Membrane Production and Defect Reduction," Nature Nanotechnology, vol. 17, no. 10, pp. 1054–1059, 2022.

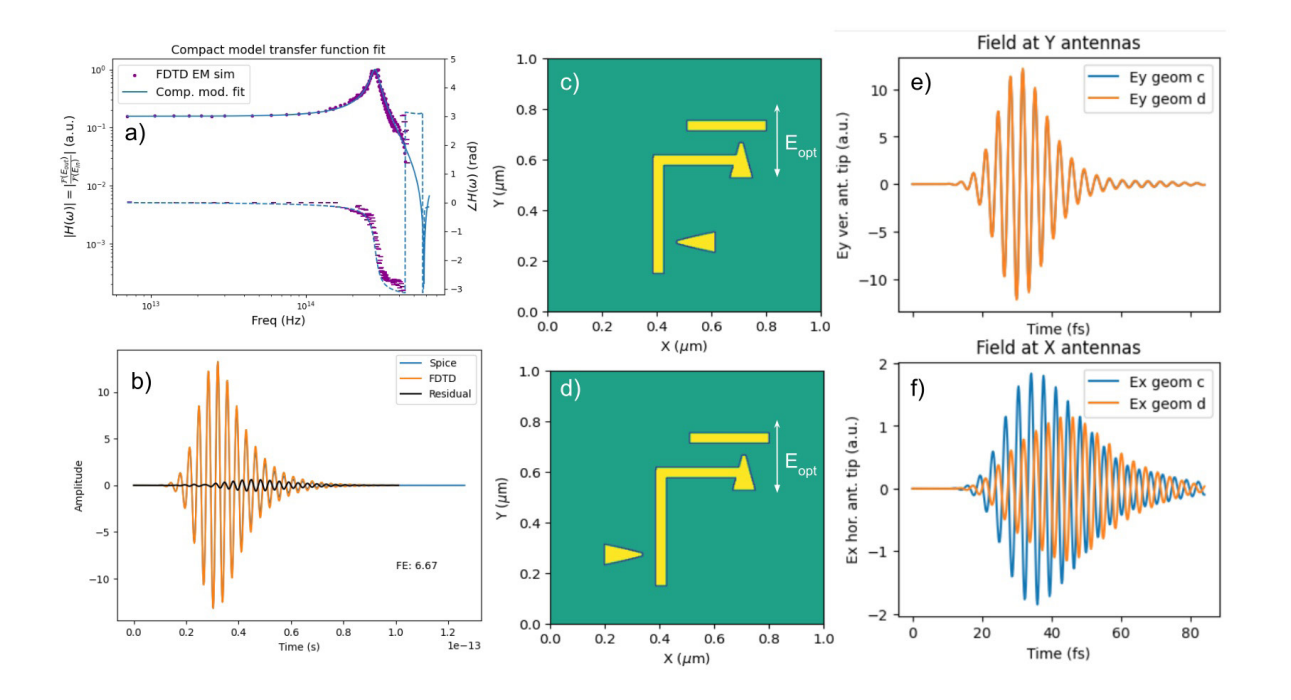
Modeling Coupling between Optically Driven Nanoantennas and Wires in Petahertz Electronic Circuits

A. Bechhofer, J. Simonaitis, F. Ritzkowsky, K. K. Berggren, P. D. Keathley Sponsorship: NSF Career Waveguide Integrated PHz Electronics

Optically driven nanoantennas leverage geometrical field enhancement, plasmonic resonance, and polarization selection of metallic nanostructures. Their subcycle tunneling current responses to optical inputs make them promising candidate components in petahertz electronic circuits, such as memory cells or logic gates. The computational cost of full electromagnetic and particle tracking simulations makes them an infeasible option for design of nanoantenna circuitry. As an alternative, we developed a compact circuit model

describing a nanoantenna which can be simulated efficiently in LTspice, with interconnecting wires modeled as transmission lines.

In this work, we study the coupling between gold triangular nanoantennas and interconnecting wires as well as the free space coupling between neighboring nanoantennas. Describing the wire-mode coupling and distinguishing it from parasitic near-field coupling through free space is essential for reliably simulating nanoantenna circuits in LTspice.



▲ Figure 1: a) Fit of circuit model transfer function to FDTD data. b) Time domain LTspice and FDTD simulation outputs. d-e) Layout of charge coupled devices under Y polarized pulses. e) FDTD simulation of Ey field at vertical antennas. f) FDTD simulation of Ex fields at horizontal antennas.

Fully Integrated, Silicon Monolithic Refractive Index Sensor in CMOS for Hydrogen Sensing

L. S. Hudson, M. de Cea, R. J. Ram Sponsorship: MITei ExxonMobil

Fossil fuels produce high carbon emissions; they can be replaced with cleaner energy sources. Energy storage in the form of chemical bonds is considered an optimal scheme. Hydrogen is a low cost, low emission energy carrier; however, it is difficult to contain, highly flammable, odorless, and a short-lived climate forcer. We need an efficient, scalable, and cost-effective mechanism for in-field hydrogen monitoring.

We introduce a fully integrated silicon monolithic refractive index sensor in CMOS for hydrogen sensing. The system consists of a CMOS LED waveguide, a functionalized sensor in the form of a microring resonator, and a CMOS photodetector. The LED waveguide on-chip light source significantly reduces the cost of the device as opposed to an off-chip light source. The waveguide ring is coated with an active material to adsorb and diffuse hydrogen molecules. The ring is exposed to hydrogen molecules and the

change in refractive index is extracted. We build a testing setup, evaluate, and characterize discrete components of the system. Then, we characterize the full system and establish the sensitivity of the device. This is done through grating coupling into the device and measuring the relationship between the change in refractive index and the change in detected current. Variations of Palladium and Tungsten Trioxide are examined to determine which chemicals are best suited as an active material for the functionalized sensor through optimizing the ratio of the change in refractive index to the change in concentration of hydrogen.

This system represents the first fully integrated refractive index sensor for hydrogen sensing and paves the way for on-site, affordable, and effective gas sensing in the industry.

Photoinduced Surface Passivation for Singlet Fission-Enhanced Silicon Photovoltaics

A. Li, N. Nagaya, C. F. Perkinson, T. Baikie, W. P. A. Verheijen, J. Song, O. M. Nix, Y. Lee, K. Seo, M. G. Bawendi, W. A. Tisdale, M. A. Baldo

Sponsorship: U.S. Department of Energy, Office of Basic Energy Sciences (DE-FG02-377 07ER46454)

Crystalline silicon (c-Si) photovoltaics (PVs) dominate the global production of renewable energy. Capitalizing on the mature industry by sensitizing single junction c-Si PVs with the exciton multiplication process singlet fission (SF) enables generation of two electron-hole pairs per photon and efficiencies that can surpass the single junction limit. SF-enhanced c-Si PV efficiencies are limited by the interfacial transfer of charge carriers from a SF chromophore coupled to the surface of c-Si due to surface recombination and trap loss pathways. Effective surface passivation is essential for achieving high efficiency c-Si PVs and to maximize the contribution of exciton multiplication. Tunnel-oxide layers based on high-k dielectrics have attracted interest in PV architectures to provide chemical passivation of surface defects and electric field-effect passivation, while maintaining favorable charge tunneling characteristics. This passivation layer must be sufficiently

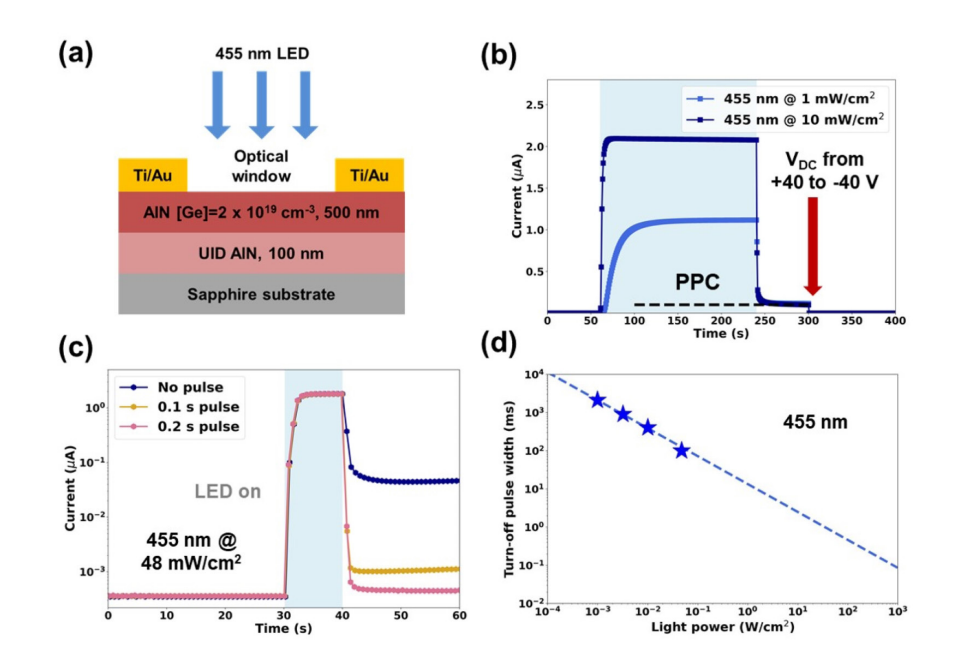
thin for tunneling of electrons and holes from the SF chromophore and sufficiently thick to reduce interfacial recombination loss pathways to successfully enhance the performance of a c-Si PV when coupled to a SF chromophore. In this work we employ a dual-interlayer architecture with an electron donor and a high-k dielectric that enhances the ultra-thin tunnel oxide passivation with a photoinduced charge separation, field-effect passivation contribution while maintaining effective tunneling for charge extraction between the SF chromophore and c-Si surface. Minority carrier lifetime and photoluminescence measurements suggest a reduction in charge recombination loss pathways. Understanding the interplay of charge at the interfaces of SF and c-Si PVs provides a strategic path for employing exciton multiplication in existing PV technology to enhance collection of usable energy from the sun.

Electro-optic Control of AIN Photo-Switch with Sub-bandgap Illumination and Enhanced Switching Speed

J. Dong, R. Jaramillo Sponsorship: Advanced Concepts Committee of MIT Lincoln Laboratory

AlGaN photoconductive switches may be useful for optical control of power electronics. However, switching the intrinsic photoconductivity of high-Al content AlGaN requires deep ultraviolet (UV) illumination, which compromises system cost and reliability. In this work, we study the extrinsic photoconductivity in Gedoped AlN with sub-bandgap visible light. Under blue LED with 455 nm center wavelength and irradiance as low as 1 mW/cm², the AlN photo-switch achieves 1.1 µA photocurrent, 4 orders of magnitude on/off current ratio and 2.8 A/W optical responsivity. However, turn-

off is much slower than turn-on because of persistent photoconductivity (PPC). We show that, in a metal-AlN Schottky junction device, the turn-off speed is limited by charge traps in the space charge region. We demonstrate that electrical bias can annihilate trapped charge on timescales orders-of-magnitude faster than PPC decay. In this way, we remove the limitations of PPC and dramatically improve device response time. The results presented here pave the way for fast switching and high optical gain in high-Al content AlGaN power devices triggered with visible illumination.



▲ Figure 1: (a) Schematic cross-section of sub-bandgap triggered AIN lateral photo-switch. (b) Transient photo response at V_{DC} =40 V. (c) Transient photo response after bias pulse is applied. (d) Width of turn-off bias pulse as function of the light power density.

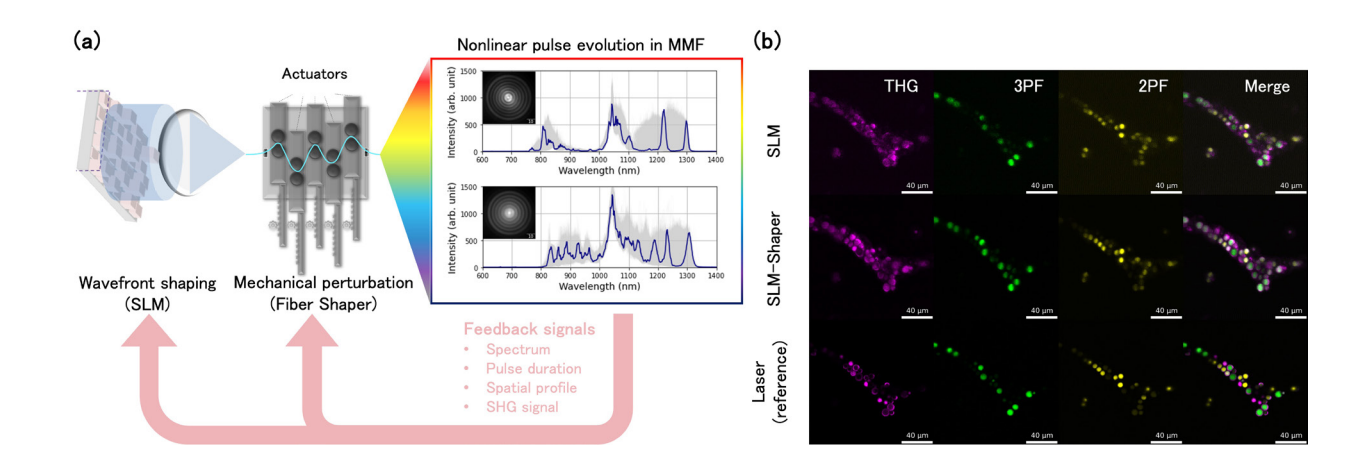
Adaptive Nonlinear Pulse Engineering in Optical Multimode Fiber with Wavefront Shaping and Mechanical Perturbation

L.-Y. Yu, H. Cao, K. Liu, T. Qiu, S. You

Sponsorship: MIT EECS and RLE startup funds, Jameel Clinic, Chan Zuckerberg Initiative, Radon Institute, Koch Institute, Research Corporation for Science Advancement, Mathwork Fellowship, Claude E. Shannon Fellowship

Multimode fibers offer a platform to accommodate intricate light-matter interactions with emerging applications in telecommunications, imaging, and sensing. Controlling light with extended frequency ranges and spatiotemporal characteristics usually requires high-performance photonic devices with considerable degrees of freedom, such as spatial light modulators. However, a more efficient control strategy is demanded to exploit the high dimensionality of nonlinear pulses in a multimode fiber. Here, we demonstrate adaptive

nonlinear pulse engineering from 650 to 1350 nm by leveraging wavefront shaping and mechanical perturbation. We show two control mechanisms have complementary effects on supercontinuum generation in the spectral, temporal, and spatial domains. We leverage the physics priors to establish an efficient adaptive pulse optimization framework, demonstrating the superior capability of femtosecond pulse tailoring and enhanced signal-to-noise ratio in multiphoton microscopy.



▲ Figure 1: (a) Schematic of adaptive nonlinear pulse optimization in a multimode fiber. (b) Multiplexed multiphoton images of fluorescent beads with an excitation at 1300 nm.

Superconducting Feedforward Electronics for Photon-Number Discrimination in Quantum Photonic Platforms

M. Castellani, O. Medeiros, R.A. Foster, E. Batson, F. Incalza, M. Colangelo, N. Sinclair, K. K. Berggren Sponsorship: NSF

Integrating superconducting nanowire single-photon detectors (SNSPDs) on thin-film lithium niobate (TFLN) circuits is a promising step for miniaturizing and advancing quantum photonic platforms. Recent progress has shown SNSPD fabrication on TFLN waveguides, paving the way for system-level applications. Many quantum photonics protocols require feedforward control, where optical operations depend on prior photon measurement outcomes. Therefore, integrating feedforward electronics with SNSPDs-on-TFLN, to support dynamic detector readout and electro-optics control, is an exciting advancement. This approach could enable optical operations based on the observed photon-number state, by using the photon-number resolution (PNR) of SNSPDs. In SNSPDs, PNR is usually achieved by distinguishing output waveform features (e.g., amplitude) with room-temperature electronics. A practical on-chip approach is using nanocryotron (nTron) electronics, an integrated nanowire-based technology that can reach the half-wave-voltage of TFLN optical modulators.

We propose a nanowire-based system that discriminates photon-number detection events. This system includes an SNSPD with PNR coupled to an nTron current-level discriminator. Higher photon numbers produce larger detector output currents, and the discriminator circuit generates an output pulse only if such currents fall within a specific range (set by two tunable thresholds), thus selectively detecting a target photon-number state while ignoring others. This output pulse can drive electro-optic switches to enable feedforward control.

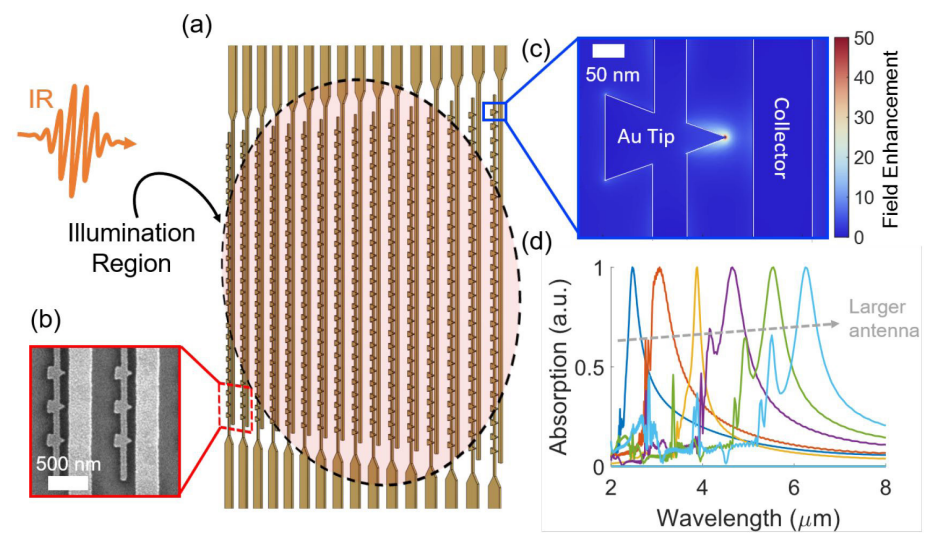
We fabricated the discriminator on a niobium nitride thin film via electron beam lithography, achieving current thresholds compatible with typical SNSPD output levels, and demonstrated successful current discrimination at 4.2 K with a 1-MHz input square wave. Additionally, we simulated the detector-circuit system in SPICE, showing photon-number recognition at 10 MHz. We aim to fabricate and test this system.

Gold Nanostructures for Mid and Long-Wave Infrared Detection

M. A. Sere, M. D. Yeung, K. K. Ryu, I. Prigozhin, K. K. Berggren, P. D. Keathley Sponsorship: Office of Naval Research (Noo0142412350), Lincoln Laboratory ACC (Longwave Infrared-Enhanced Electron Emission from Nanoantennas (L-IREEN)), MIT Presidential Fellowship

Mid-wave infrared (MWIR) and long-wave infrared (LWIR) imaging carries numerous applications such as night vision and security, environmental, and industrial monitoring. However, traditional detectors at these wavelengths have a steep tradeoff between Size, Weight, and Power (SWaP) considerations due to cryogenic cooling requirements and performance metrics in speed and sensitivity.

This work investigates the use of Infrared Enhanced Electron Emission from Nanoantennas (IREEN) for MWIR and LWIR detection at room temperature. Gold antennas of varying geometries are deposited onto silicon and silicon oxide substrates to qualify the effect of geometry on the prominence of field-driven vs Schottky-driven electron emission, providing insights on how to design high-performance, low cost MWIR and LWIR detectors.



▲ Figure 1: (a) Nanoantenna array. (b) SEM of nanoantenna. (c) Field-enhancement simulation of nanoantenna design. (d) Simulation showing spectral tuning of nanoantennas.

Dark Exciton Signatures in Blue OLEDs Probed by Strong Magnetic Fields in situ

O. Nix, J. Tiepelt, J. Song, J. W. Park, M. A. Baldo

Understanding the degradation mechanisms of blue organic light emitting diodes (OLEDs) is key to developing the next generation of bright and stable blue OLEDs for applications in phones, TVs and solid-state lighting. Annihilation processes involving dark excitons are thought to be the primary cause of degradation in blue OLEDs, as they form 6 eV states which break carbon-carbon bonds in the host, emitter, and transport layers, creating defect sites which quench the electroluminescence of the device. While these annihilation processes are thought to be ubiquitous, observing them directly has proven difficult through optical means due to their dark nature, and their connection to device degradation has yet to be fully understood.

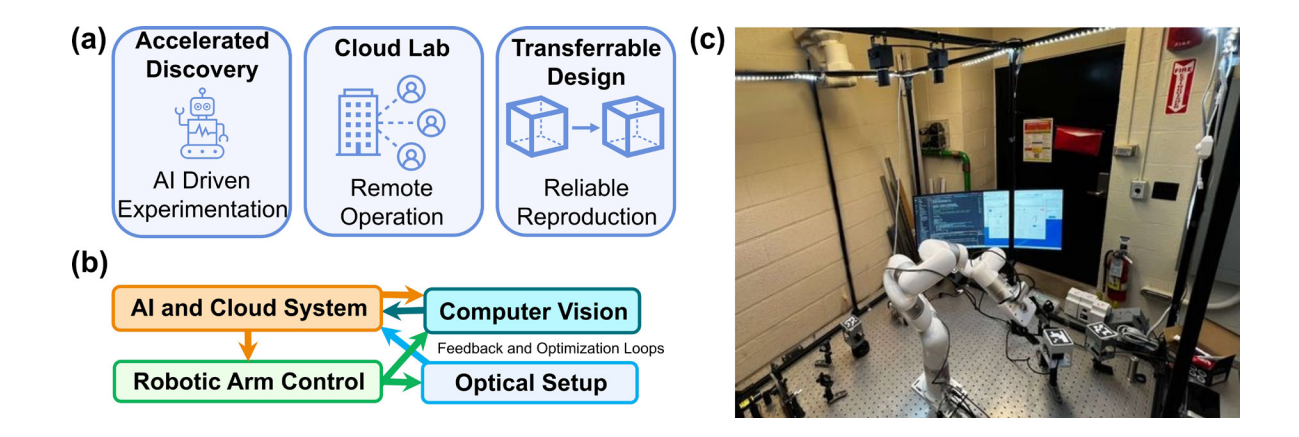
In this work, the annihilation rates of dark excitons are modulated in blue OLEDs in situ through the application of strong DC magnetic fields. By monitoring the response of the electroluminescence efficiency and stability of blue OLEDs to the applied field, unique signatures of these annihilation events are identified and associated with specific nanoscale processes in the device during normal operation. By measuring device degradation under the magnetic fields associated with each annihilation process, a direct link is established between the annihilation of dark excitons and their impacts on blue OLED performance.

Collaborative Robotics for Free-Space Optics

S. Z. Uddin, S. Vaidya, S. Choudhary, R. Salib, L. Huang, M. Soljačić Sponsorship: U. S. Army Research Office through the Institute for Soldier Nanotechnologies at MIT, under Collaborative Agreement Number W911NF-23-2-0121.

Optical beam characterization is essential across multiple fields, from laser development to free-space communication. While traditional manual methods require precise alignment and are prone to human error, collaborative robots integrated with artificial intelligence offer an automated solution for laboratory environments. We present an automation pipeline that combines a robotic arm with AI-driven computer vision and image processing for optical beam characterization. As AI advances, such intelligent systems become

crucial for accelerating experimental science through automated decision-making. Our system autonomously handles precision tasks like camera positioning and lens placement, enabling automated collection of 4×4 beam matrix measurements. Through practical implementation, we show how integrating AI, robotics, and computer vision can streamline complex optical measurements, advancing the field toward more efficient and reliable characterization methods.



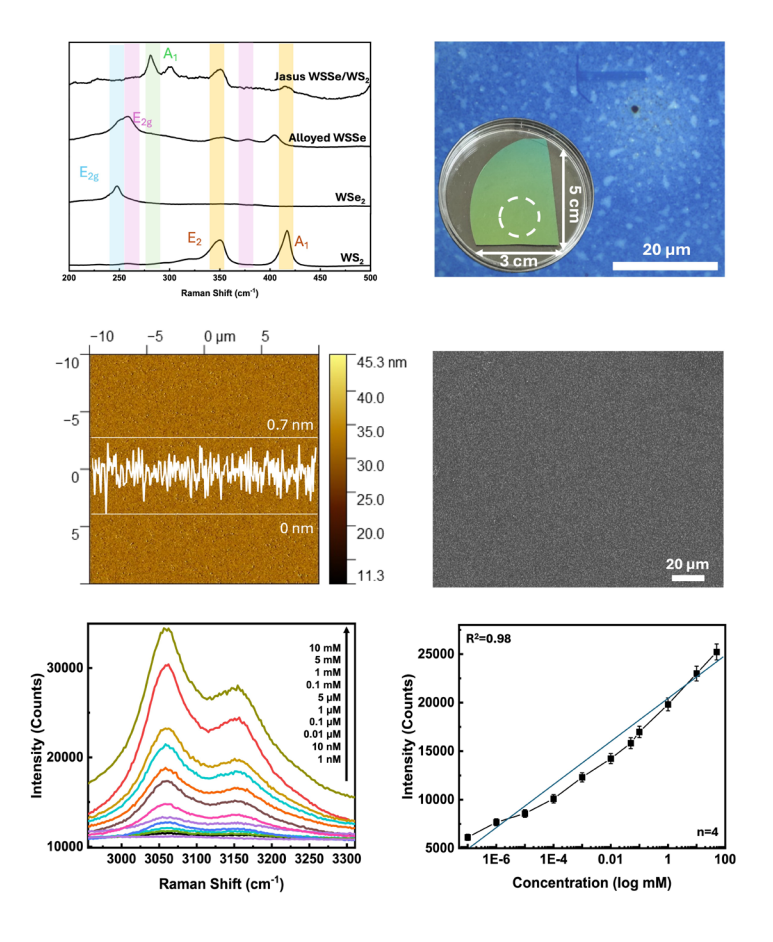
▲ Figure 1: Overview of Al-driven robotic optics lab. (a) Features: Al experimentation, remote operation, reproducible designs. (b) Architecture: Al control, vision, feedback, robotic arm, optical setup. (c) Physical setup: robot arm on optical breadboard.

A Novel SERS-Based Strategy for Rapid and Sensitive Detection of NRR Products Using Janus WSSe/WS2 Heterostructures

Y.-R. Peng, T. Zhang, T. H. Yang, S.-Y. Tang, S.-M. He, J. Kong Sponsorship: US Army Research Office grant number W911NF2210023, US Army Research Office through the Institute for Soldier Nanotechnologies at MIT, under cooperative agreement No. W911NF-18-2-0048.

Ammonia is a critical feedstock in many everyday products and is considered a crucial energy carrier in the context of the energy transition. Electrochemical nitrogen reduction reaction (NRR) under ambient conditions offers a sustainable alternative to the energy-intensive Haber-Bosch process. However, conventional NRR product detection methods require complex sample preparation and long analysis times. Here, we demonstrate a novel surface-enhanced Raman spectroscopy (SERS) platform based on Janus WSSe/WS2 heterostructures for rapid and sensitive detection

of NRR products. The asymmetric structure, featuring an intrinsic out-of-plane electric field and optimized surface chemistry, enables superior SERS performance with an enhancement factor of 10^6. This platform achieves rapid detection of ammonia with concentrations ranging from 1nM to 10mM, demonstrating excellent sensitivity and stability. This work provides a new strategy for rapid NRR product detection and demonstrates the potential of engineered Janus TMD heterostructures for molecular sensing applications.



▲ Figure 1: (Left) Characterization of a Janus WSSe/WS2-based SERS platform. (Right) Raman enhancement performance with varying NH4Cl concentrations and corresponding calibration curve.

Spatially and Spectrally Resolved Electric Field Inhomogeneity in Colloidal Cd-Free QD-LEDs

S. Srinivasan, R. Zhang, M. Dillender, T. Nguyen, M.Laitz, T. Kim, M. Bawendi, V. Bulović Sponsorship: Samsung Semiconductor Co.

Colloidal quantum dots (QDs) are solution-processable emitters with high quantum efficiencies and tunable emission wavelengths. They have emerged as promising materials for electronic displays, solid-state lighting, and optical communication. The demand for QD-based display technologies has necessitated the development of environmentally-benign QD compositions with similar optical properties to high-performing, but toxic, heavy-metal-containing QDs. Using time-resolved confocal micro-photoluminescence and micro-electroluminescence mapping under an applied electric field, we observe direct evidence of inhomogeneity in QD response to the electric field for InP/ZnSe/ ZnS quantum dot light emitting diodes (QD-LEDs). By applying a negative bias across the diode while photo-exciting the QDs, the steady-state and time-resolved exciton dynamics are modulated, resulting in photolu-

minescence (PL) quenching and a decrease in average exciton lifetime. Under confocal micro-PL mapping, intensity hotspots imaged in the QD thin film are found to be less-reactive to the applied electric field, resulting in spatial inhomogeneity in PL quenching after the application of the electric field. These same regions also exhibit limited electroluminescence. We thus hypothesize that the thicker regions of the QD film screen the effective electric field experienced by the dots in that region, leading to limited field-induced modulation. Subsequently, we posit that under positive bias, the same regions that are unresponsive under negative bias also do not contribute to charge injection and electroluminescence, leading to increased field exposure and aging in the surrounding QDs. This work provides a possible mechanism for the accelerated operational lifetime decays observed for InP/ZnSe/ZnS QD-LEDs.

Power Devices & Circuits

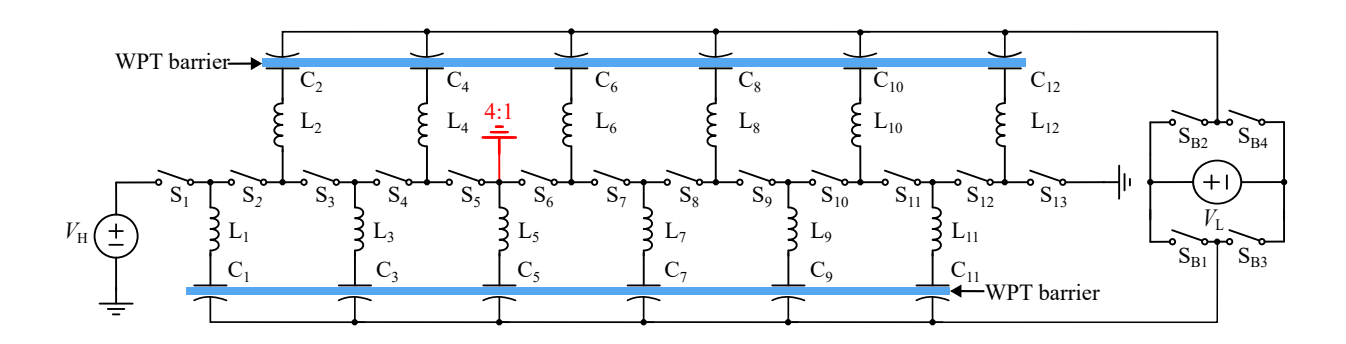
| A Hybrid Switched Capacitor Converter Enabling Capacitive-Based Wireless Power Transfer for Battery Charging Applications | 147 |
|--|-----|
| Soft-Switched Pulsed Bias Plasma Supply System | |
| Review of Piezoelectric-Based Power Conversion | |
| Specific Power Increases in DC-DC Power Converters for Electroaerodynamic Aircraft | 145 |
| TCAD Simulations to Explore Thermal Solutions for GaN-on-Silicon HEMTs | 146 |
| High Performance Scaled p-GaN-Gate HEMTs for Next Generation Medium-Voltage Power Converters | 147 |
| Design of Vertical AIN-Channel Power Transistors | 148 |
| The Analysis and Design of Resonant Capacitively-Isolated Cockcroft-Walton Converter | 149 |

A Hybrid Switched Capacitor Converter Enabling Capacitive-Based Wireless Power Transfer for Battery Charging Applications

J. Sund, S. Coday

Wireless power transfer is emerging for applications such as autonomous drones, electric vehicles, biomedical implants, and phone charging, where wired charging is inconvenient or impractical. This work investigates the feasibility of employing hybrid switched capacitor converters in wireless battery charging applications to decrease passive component sizing and switch

stress. A capacitively-isolated hybrid Dickson converter designed for use in low-power volume-constrained wireless power transfer applications is presented. The converter analysis, operation and design are detailed. Finally, a hardware prototype is presented, and experimental results validate wireless power transfer, across varying load and gap distances.



▲ Figure 1: Capacitively-isolated 12:1 hybrid Dickson converter schematic with WPT barrier shown. The ground connection (red) at the node between S_5 and S_6 converts the schematic to the 4:1 capacitively-isolated hybrid Dickson converter when S_6 – S_{13} , L_5 – L_{12} , and C_5 – C_{12} are omitted.

Soft-Switched Pulsed Bias Plasma Supply System

J. Estrin, A. Jurkov, D. J. Perreault Sponsorship: MKS Instruments, Inc.

Radio Frequency (RF) generators play a crucial role in plasma-enhanced semiconductor manufacturing, particularly as sources of bias voltage. Employing pulsed waveforms as bias voltage sources offers significant improvements in manufacturing precision. However, producing these waveforms is challenging due to the need for high voltages (in the kV range), high frequencies (hundreds of kHz to low MHz), precise timing, and broadband frequency content. Traditional methods to generate these waveforms are constrained by semiconductor voltage ratings, resulting in either low-voltage outputs or complex circuits to achieve higher pulse voltages.

This work introduces a simple and compact method for generating pulsed bias voltages for

plasma processing, enabling reduced loss compared to the more complex systems previously described in the literature. The approach synthesizes the pulsed waveform at a low, convenient voltage and then uses an auto-transformer to step up the voltage to the desired level. A coaxial-cable-based transformer with low leakage inductance has been developed to provide scaling with sufficient fidelity across a wide frequency range. Zero voltage switching (ZVS) is achieved on all devices, ensuring low-loss operation. The proposed system is validated through a lab bench prototype that generates pulses of 2.1 kV at 400 kHz. The proposed system further offers both adjustable pulse duty ratio and slew rate, providing enhanced control and versatility for various applications.

Review of Piezoelectric-Based Power Conversion

D. T. Brown, A. K. Jackson, J. H. Lang, D. J. Perreault Sponsorship: Texas Instruments, MIT SuperUROP

Power electronics are critical components of many electric systems. For example, power converters can be found in anything from consumer electronics to renewable energy generation. New applications demand smaller, lighter, and more efficient power converters. However, scaling down these parameters is often bottlenecked by magnetic energy storage elements: not only are they typically the largest element on the circuit, but they are also the least efficient at small volumes. Piezoelectric resonators are a promising alternative energy storage device. Instead of storing energy

in a magnetic field, these components store energy in mechanical vibrations. Critically, piezoelectric resonators do not suffer from the same limitations as magnetics do at small scales. Piezoelectric-resonator-based converters can achieve high-efficiency behaviors such as zero-voltage switching and capacitor soft-charging, both without the use of magnetics. In general, utilizing piezoelectric resonators for power conversion enables high power density, high efficiency and favorable scaling properties.

Specific Power Increases in DC-DC Power Converters for Electroaerodynamic Aircraft

M. Shevgaonkar Sponsorship: NASA NIAC Phase 2 (80HQTR23NOA01-23NIAC-A2)

Electroaerodynamic (EAD) propulsion is a novel form of propulsion that has no moving parts and is almost completely silent. Aircraft powered by EAD propulsion have the potential to perform nearly silent package delivery and surveillance missions. A major component of an EAD aircraft is the high voltage gain DC-DC conver er required to drive the high voltage thruster array from a lithium-ion energy source. The endurance of the aircraft is heavily dependent on the efficiency and specific power of the converter. The aim of this research is to design and implement a converter with specific power improvements over the last generation of EAD power conversion [1] designed at MIT. This can be accomplished by utilizing magnetics integration and cooling techniques as well as by changing high lev-

el parameters such as power level and output voltage. Magnetics integration involves consolidating several discrete magnetic structures into a single structure that is lighter in weight and more compact. Magnetics cooling techniques involve designing the magnetic structure for effective heat transfer to a forced convection parallel plate heat sink. Modeling suggests that magnetics integration and cooling combined with a higher power level and lower output voltage can result in an increase of specific power from 1.15 kW/kg [1] to nearly 3 kW/kg while maintaining 85% efficiency. Ongoing improvements in the thruster [3] and airframe combined with the aforementioned specific power increases in the converter would enable an endurance increase from from 90 seconds [2] to roughly 10 minutes.

Y. He and D. J. Perreault, "Lightweight High-Voltage Power Converters for Electroaerodynamic Propulsion," in IEEE J. of Emerging and Selected Topics in Industrial Electronics, vol. 2, no. 4, pp. 453-463, Oct. 2021, doi: 10.1109/JESTIE.2021.3087950.

N. Gomez-Vega and S. R. H. Barrett, "Order-of-Magnitude Improvement in Electroaerodynamic Thrust Density with Multistaged Ducted Thrusters", AIAA J. 2024 62:4, 1342-1353

[•] Xu, H., He, Y., Strobel, K.L. et al. "Flight of an Aeroplane with Solid-state Propulsion," Nature 563, 532–535 (2018). https://doi.org/10.1038/s41586-018-0707-9

TCAD Simulations to Explore Thermal Solutions for GaN-on-Silicon HEMTs

D. Erus, J. Niroula, P. Yadav, T. Palacios

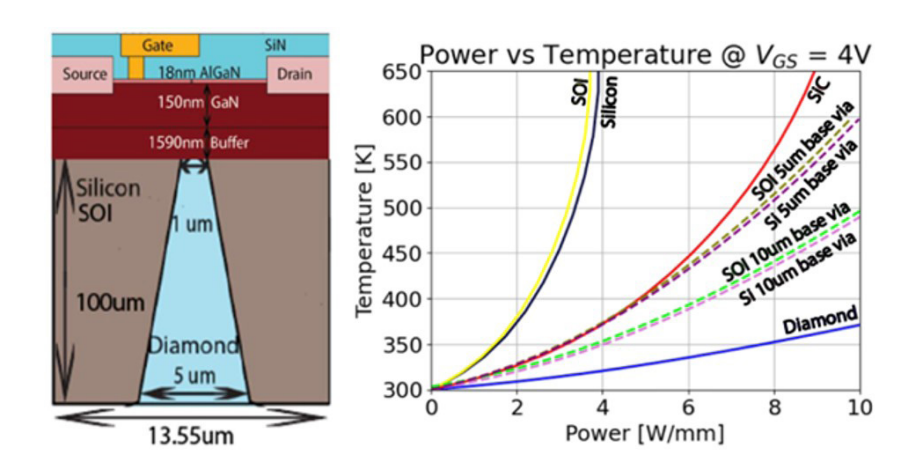
Sponsorship: Center 7 SUPREME: SUPeRior Energy-efficient Materials and dEvices, one of the seven centers in JUMP 2.0, a Semiconductor Research Corporation (SRC) program sponsored by Defense Advanced Research Projects Agency (DARPA) under the award no. 145105-21913.

The wide bandgap and large breakdown voltage of GaN makes GaN HEMTs a key element for the next generation of high-power and high-frequency electronics. Silicon (Si) based substrates allow wafer scaling to 8-12" wafers and the use of state-of-the-art fabrication tools. However, they make thermal management more difficult compared to more commonly used silicon carbide (SiC) substrate.

Thermal management is crucial because the large power density in GaN HEMTs induces extreme self-heating in their conducting channel which leads

to reduced current and device degradation. To fully leverage the benefits of Si-based substrates, this work uses TCAD simulations to explore thermal solutions that reduce the peak temperature of GaN-on-Si HEMTs to that of GaN-on-SiC HEMTs.

The simulations are calibrated using transferlength-method and Hall measurements of fabricated GaN-on-Si HEMTs. Explored solutions include strategically incorporating diamond vias into Si substrate to enhance heat dissipation.



▲ Figure 1: (a) Simulated structure with conical diamond via (not to scale) and (b) Power vs. Temperature curves of GaN HEMTs with various substrates. Shows that the diamond via reduces the peak temperature of GaN-on-Si ∼65% to a lower value than GaN-on-SiC.

A. Garcia Coleto, M. Notaros, and J. Notaros, "Integrated Liquid-Crystal-Based Modulators: Packaging Processes and Evaluation Techniques," 2023 IEEE Photonics Conference (IPC), pp. 1-2, 2023.

M. Notaros, A. Garcia Coleto, M. Raval, and J. Notaros, "Integrated Liquid-crystal-based Variable-tap Devices for Visible-light Amplitude Modulation," Opt. Lett. vol. 49, pp. 1041-1044, 2024.

M. Notaros, T. Dyer, M. Raval, C. Baiocco, J. Notaros, and M. R. Watts, "Integrated Visible-light Liquid-crystal-based Phase Modulators," Opt. Express vol. 30, pp. 13790-13801, 2022.

High Performance Scaled p-GaN-Gate HEMTs for Next Generation Medium-Voltage Power Converters

P. Darmawi-Iskandar, J. Niroula, Q. Xie, J. Hsia, C. R. Neve, J. Strate, T. Palacios Sponsorship: Samsung Electronics Co., Ltd. (033517-00001), National Defense Science and Engineering Graduate Fellowship

With the increasing prevalence of artificial intelligence, cloud computing, and internet of things, data centers consume 2% of the world's electricity, a number which is predicted to double by 2026. Key to the efficiency of powering these data centers are high speed and low on-resistance medium-voltage power switches (e.g. for use in 48V-12V DC-DC converters). P-GaN-gate high electron mobility transistors (HEMT) are a promising candidate for these switches due to their high breakdown voltage, high switching speed, low on-resistance, and normally-off operation. However, while >650V p-GaN-gate HEMT power switches have been heavily researched and are already commercially available, not much work has been done exploring the potential of p-GaN-gate HEMTs for low-medium voltage applications (10-100 V).

In this work we demonstrate a scaled p-GaN/ $Al_{0.2}GaN/GaN$ (80/15/200 nm) HEMT with a p-GaN Mg doping of $3x10^{19}$ cm₋₃ grown on an 8" Si substrate by SOITEC. To reduce on-resistance and improve the maximum current density, we employ a self-aligned

Schottky Tungsten gate first process. Devices with L_C/ L_{SD}/L_{GD} = 600/1300/370 nm demonstrated a maximum drain current of 1.07 A/mm, an on-off current ratio exceeding 1010, and a threshold voltage of 0.45 V. Furthermore, these devices exhibit on-resistances as low as 1.6 Ω ·mm and breakdown voltages exceeding 125 V which make them highly promising for use as medium-voltage power switches. To the best of the authors' knowledge, the demonstrated devices have the highest Baliga figure of merit (0.3 GW/cm²) of all medium-voltage (<200V) p-GaN-gate HEMTs reported in the literature. Compared to the current state-of-theart technology for medium voltage power switches, Si LDMOS, the demonstrated device demonstrates a greater than order-of-magnitude improvement in the specific on-resistance at the given breakdown voltage. This work demonstrates that replacing Si LDMOS switches with p-GaN-Gate HEMTs serves to greatly improve the efficiency of medium-voltage power converters.

Design of Vertical AIN-Channel Power Transistors

Z. Zhu, H. Pal, T. Palacios Sponsorship: Knut and Alice Wallenberg Foundation

As an ultrawide bandgap (UWBG) semiconductor, aluminum nitride (AlN) is a promising candidate for next-generation high-voltage electronic devices due to its remarkably large breakdown field of 11-15 MV/ cm. Moreover, AlN exhibits higher bulk electron mobility compared to other UWBG materials like AlGaN and Ga₂O₃. As a result, Baliga's figure of merit is over 10 times higher in AlN than in conventional wide-bandgap materials such as GaN and SiC. However, AlN faces challenges to achieve high carrier concentration through doping due to the large ionization energy of donors. Forming ohmic contacts is also difficult, as low electron affinity and Fermi level pinning near the charge neutrality level prevent reduction of the potential barrier at the metal/AlN interface. These factors limit the development of AlN-based power switches with high current density.

Here, we propose a heterostructure design of vertical AlN-channel fin field-effect transistors

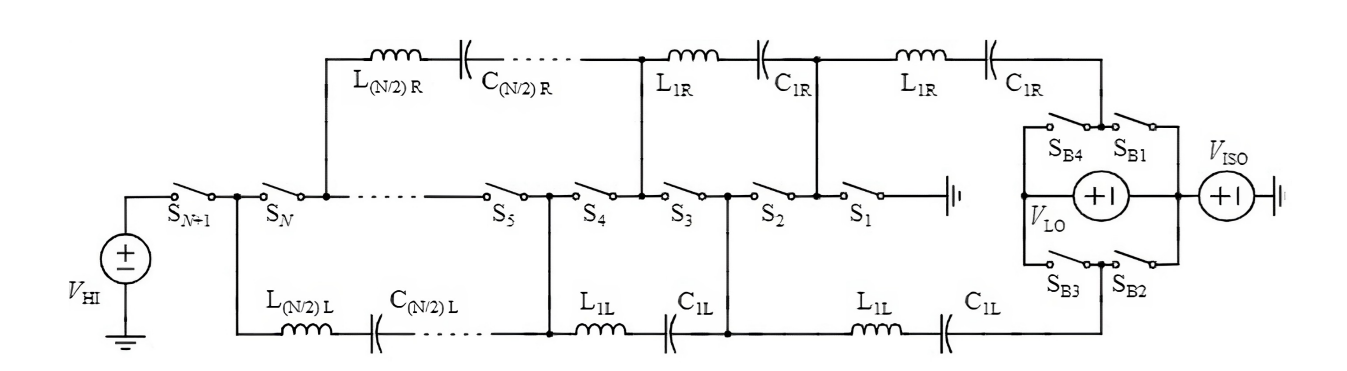
(FinFETs) on a sapphire substrate. A graded Al, Ga, N layer on both sides of the AlN channel serves as the source and drain, respectively. Strong polarization at the Al, Ga, N/AlN interface and within the graded layer forms a three-dimensional electron gas (3DEG), creating a polarization-induced doping region. This leads to an increased carrier concentration in the source and drain access region without compromising mobility from impurity doping, effectively reducing the on-resistance. Technology-Computer-Aided-Design (TCAD) simulation suggests that this device structure could achieve high on-current density above 100 mA/ mm at source-drain bias (V_{DS}) of 5 V, approximately three orders of magnitude higher than state-of-the-art lateral AlN transistors. These preliminary simulation results indicate that this vertical heterostructure device architecture may overcome the current obstacles in AlN-based power switches.

The Analysis and Design of Resonant Capacitively-Isolated Cockcroft-Walton Converter

E. Rabenold, R. Jerez, S. Coday

Hybrid switched-capacitor converters have been shown to be competitive with traditional magnetics-based converters in both efficiency and passive component volume due to their utilization of energy-dense capacitors for energy processing. However, one important feature that is yet underdeveloped in hybrid switched-capacitor converters is isolation between the input and output voltages, which is a critical feature for performance and safety. Traditional implementations of galvanic isolation employ transformers to create the isolation barrier. However, transformers are costly in both component volume and weight. In applications where passive volume is a key design con-

straint, the dielectric material of capacitors may instead be used to achieve isolation. This work proposes the introduction of a capacitor-based isolation barrier into the Cockcroft Walton converter to support isolated power transfer in applications that require extreme conversion ratios and output regulation. Generalized equations for mid-range flying capacitor voltages and switch voltages for converters of even level count are detailed. Experimental results for a 6:1 version of the resonant capacitively-isolated Cockcroft Walton are shared, and the viability of capacitive isolation in this topology is demonstrated.



▲ Figure 1: Schematic of an N-level capacitively-isolated Cockroft-Walton converter.

Quantum Science & Engineering

| Topological Bands and Correlated States in Helical Trilayer Graphene | 151 |
|--|-----|
| Fizeau Drag in 3D Dirac Semimetals Enables Tunable Nonreciprocal Energy Transport | 152 |
| Strain Tuning of Individual Telecom Color Centers in Reconfigurable Silicon Photonics | 153 |
| Strong-coupling Theory of Single-photon Detection in Superconducting Nanowires | 154 |
| Development of TiN Through-Silicon Vias for Superconducting Qubits | 155 |
| Nanoelectromechanical Cantilever Waveguide Diagnosis via Visible Spectral Domain Optical Coherence Tomography | 156 |
| Q-Pilot: Field Programmable Qubit Array Compilation with Flying Ancillas | 157 |
| Electron Energy Loss Spectroscopy of 2D Materials in a Scanning Electron Microscope | 158 |
| Diverse Impacts of Spin-Orbit Coupling on Superconductivity in Rhombohedral Graphene | 159 |
| Characterization and Comparison of Energy Relaxation in Planar Fluxonium Qubits | 160 |
| Quantum-Secure Multiparty Deep Learning in Optical Networks | 161 |
| Spectroscopy Signatures of Electron Correlations in a Trilayer Graphene/hBN Moiré Superlattice | 162 |
| Spectral Methods for Modeling Non-equilibrium Superconductivity | 163 |

Topological Bands and Correlated States in Helical Trilayer Graphene

L.-Q. Xia, S. C. de la Barrera, A. Uri, A. Sharpe, Y. H. Kwan, Z. Zhu, K. Watanabe, T. Taniguchi, D. Goldhaber-Gordon, L. Fu, T. Devakul, P. Jarillo-Herrero

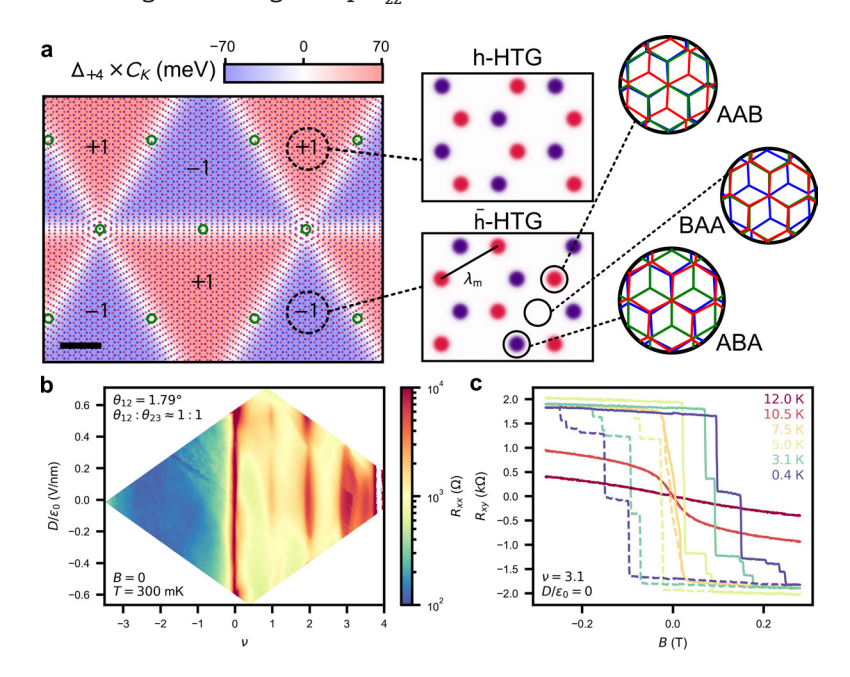
Sponsorship: Army Research Office, NSF, Gordon and Betty Moore Foundation

The intrinsic anomalous Hall effect (AHE) indicates nonzero Berry curvature of electronic wave-functions in solids and spontaneous time-reversal symmetry breaking. These conditions can be realized in two-dimensional systems with broken xy-inversion symmetry (C_{2z}) that host flat electronic bands. In recent years, moiré materials, systems with moiré patterns due to lattice mismatch, have emerged as a powerful platform for exploring the intriguing interplay between non-trivial topology and strong electronic correlations. To date, however, the majority of research has focused on structures with a single moiré pattern, while introducing multiple moiré patterns in a single structure could provide new degrees of freedom for engineering and understanding novel quantum phenomena.

In this work, we introduce helical trilayer graphene (HTG): three graphene layers, each twisted in sequence by the same angle. Unlike alternating-twist trilayer graphene, this results in two moiré patterns with different orientations. Although HTG is globally C_{22} -

symmetric, surprisingly, we observe clear signatures of topological bands. Using magnetotransport measurements, we uncover a robust phase diagram of correlated and magnetic states at a magic angle, $\theta_{\rm m} \approx 1.8^{\circ}$. We explain our observations in terms of lattice relaxation that leads to large periodic domains in which C_{2z} is broken on the moiré scale. Each domain harbors flat topological bands with valley-contrasting Chern numbers $\pm (1, -2)$. We find correlated states at integer electron fillings per moiré unit cell $\nu = 1,2,3$ and fractional fillings 2/3,7/2, with the AHE arising at $\nu = 1,3$ and 2/3,7/2. Finally, at $\nu = 1$, the absence of an AHE beyond a critical electric displacement field indicates a topological phase transition.

We establish HTG as an important platform that realizes ideal conditions for exploring strongly interacting topological phases and, due to its emergent moiré-scale symmetries, demonstrates a novel way to engineer topology in a multi-moiré system.



▲ Figure 1: a. Structure of HTG considering lattice relaxation. Left, middle, and right panels show structures at supermoiré, moiré, and atomic scales, respectively. b. Longitudinal resistance of magic-angle HTG, showing correlated states at integer fillings. c. Hall resistance measured around filling v=3 when sweeping the magnetic field, demonstrating AHE.

[•] Xia, L.-Q., de la Barrera, S.C., Uri, A., Sharpe, A., Kwan, Y.H., Zhu, Z., Watanabe, K., Tanigu-chi, T., et al. "Topological Bands and Correlated States in Helical Trilayer Graphene," *Nature Physics*, vol. 21, pp. 239-244, 2025.

[•] Devakul, T., Ledwith, P.J., Xia, L.-Q., Uri, A., de la Barrera, S.C., Jarillo-Herrero, P. and Fu, L., "Magic-angle Helical Trilayer Graphene," Science Advances, vol. 9, no. 36, p. eadi6063, 2023.

Fizeau Drag in 3D Dirac Semimetals Enables Tunable Nonreciprocal Energy Transport

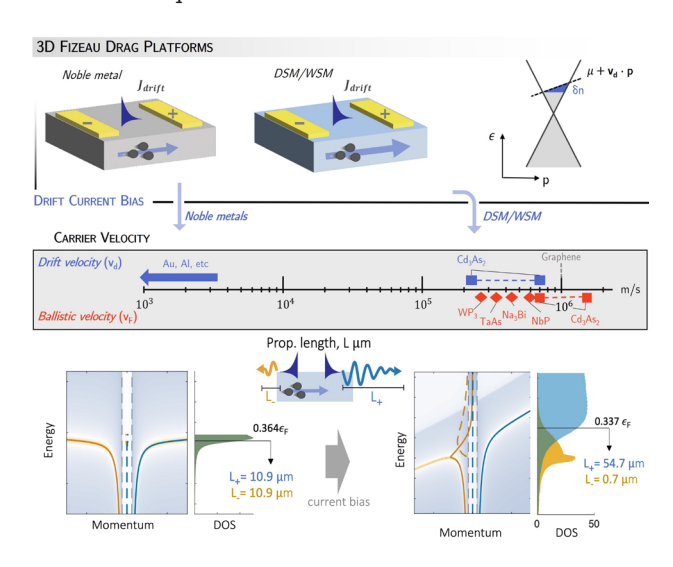
M. Blevins, H. Gold, S. Pajovic, A. Mukherjee, S. V. Boriskina Sponsorship: ARO-Multidisciplinary University Research Initiative program

In nonreciprocal optical systems, light behaves differently depending on the direction it travels. This phenomenon breaks the principle of Lorentz reciprocity and can be leveraged to eliminate backscattering noise and achieve unidirectional energy transport, enabling optical isolators and efficient light energy conversion systems. However, materials that exhibit strong magnetic or nonlinear responses necessary to achieve non-reciprocal light transport are rare. Magnetic fields cause interference with other on-chip components and complicate device integration. Therefore, there is an unmet need for alternative external stimuli that are easy to implement in situ.

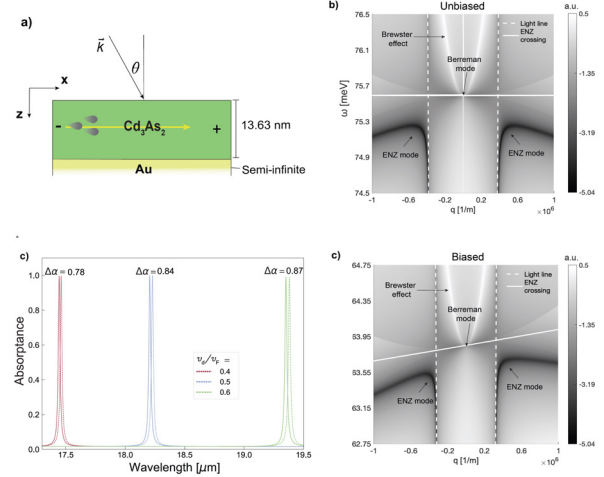
We propose to meet this need by using plasmon Fizeau drag, the phenomenon in which moving charge carriers impart either a dragging or an accelerating force on surface plasmon polariton waves. Plasmon Fizeau drag can induce nonreciprocal surface modes and enable one-way energy transport, but--similar to the Doppler shift effect for propagating light waves emitted from objects moving at relativistic velocities--requires relativistic electron drift velocities

to yield appreciable contrast between the dispersion characteristics of co-propagating and counterpropagating modes. The high electron drift and Fermi velocities in three-dimensional (3D) Dirac materials make them ideal candidates for the effect. However, both the theory of the Fizeau drag effect and its experimental demonstrations in these materials have been missing.

We developed a semiclassical theory of Fizeau drag in current-biased 3D Weyl and Dirac semimetals (W/DSMs), both under local and non-local approximation and with dissipative losses. We predict that under practical assumptions for loss, Fizeau drag in the DSM ${\rm Cd_3As_2}$ opens windows of pseudo-unidirectional transport of surface plasmon polariton modes (Figure 1). We illustrate the unique performance advantage of this dynamic mechanism of inducing nonreciprocity by designing a flat, sub-wavelength-thin infrared absorber with 100% peak absorptance, a high nonreciprocal absorptance contrast of ~87%, and a high in-situ spectral tunability (Figure 2).



▲ Figure 1: a) Plasmon Fizeau drag in bulk W/DSMs is enabled by their high carrier velocity. Nonreciprocal surface plasmon dispersion under current bias is plotted along-side corresponding photon density of states, associated with co-propagating (blue) vs. counter-propagating (yellow) modes.



▲ Figure 2: (a) Planar nonreciprocal absorber comprising 13.63-nm-thin film of Cd_3As_2 on top of Au mirror. (b,c) Dispersion characteristics of optical modes become nonreciprocal under direct current bias. (d) Resonant absorptance spectra for opposite angles of incidence exhibit nonreciprocity (peak splitting) and broadband tunability (peak shift).

- S. V. Boriskina, M. Blevins, and S. Pajovic, "The Nonreciprocal Adventures of Light," Optics and Photonics News, vol. 33, no. 9, pp. 46-53, 2022, [Link]
- M. Blevins and S. V. Boriskina, "Plasmon Fizeau Drag in 3D Dirac and Weyl Semi-metals," ACS Photonics, vol. 11, no. 2, pp. 537–549, 2024.
- H. Gold, M. Blevins, S. Pajovic, A. Mukherjee, and S. V. Boriskina, "Dynamically-tunable Nonreciprocal Epsilon-near-zero Photonic Platform Enabled by Current-biased Dirac Semimetals," Optical Materials Express, in press, 2025. DOI.org/10.1364/OME.559903

Strain Tuning of Individual Telecom Color Centers in Reconfigurable Silicon Photonics

A. Buzzi, C. Papon, M. Pirro, O. Hooybergs, H. Raniwala, V. Saggio, C. Errando-Herranz, D. R. Englund Sponsorship: NSF QuanNeCQT Grant No. 2134891

Color centers in silicon, such as G and T centers, have gained significant attention as potential candidates for quantum information processing, particularly due to their compatibility with established silicon fabrication techniques and their telecom wavelength operation. Despite their promise, the scalability of such systems depends on the ability to tune single emitters to identical frequencies, enabling multiphoton interference. Although frequency tuning of ensembles has been shown, the controllable and reversible tuning of individual color centers in silicon has not been demonstrated.

In this work, we present a waveguide-integrated device that leverages MEMS photonics to achieve controlled strain tuning of a single G center's emission frequency. By applying a 35 V driving voltage, we demonstrate a tuning range of up to 400 pm. Additionally, we compare these results to a piezospectroscopic model, correlating the tuning behavior with the emitter's position within the waveguide. This milestone is crucial for advancing silicon color center technology, potentially enabling the development of quantum memories and entangling gates for quantum communication and computing.

Strong-coupling Theory of Single-photon Detection in Superconducting Nanowires

A. Simon, R. Foster, E. Batson, M. Sahoo, C. Heil, K. K. Berggren Sponsorship: NSF GRFP and MIT Vanu Bose Presidential fellowship programs, Alan McWhorter fellowship, DARPA DSO

Superconducting nanowire single-photon detectors (SNSPDs) are the preferred technology for single-photon detection in the visible and near-infrared wavelengths. By optimizing design and material properties, SNSPDs have achieved near-unity single-photon detection efficiencies, ultra-low dark count rates, and jitter times of less than 3 ps. However, many applications, including dark matter search, biomedical imaging, and quantum networks, require an increase in the operating temperature or wavelength sensitivity range relative to the current state-of-the-art, without sacrificing detection efficiency or other relevant metrics. To enable these advances, we require a thorough understanding of the detection mechanism and its relation to material parameters to guide the search for new material platforms and device engineering for improved SNSPD

performance. However, though its importance is clear, only limited prior work has explored the role of the microscopic quasiparticle and phonon dynamics in the detection mechanism of SNSPDs. Likewise, no study has investigated the effect of the frequency-dependent electron-phonon coupling on detection efficiency and wavelength sensitivity, despite its importance in describing superconductivity in strong coupling superconductors such as niobium nitride. In this work, we develop a theory of SNSPD detection, generalized to the case of strong coupling superconductors, which is suitable to describe SNSPD detection in conventional superconductors. This work provides a theoretical framework to enable the study and exploration of new materials and device engineering for improved performance.

Development of TiN Through-Silicon Vias for Superconducting Qubits

G. D. Cutter, F. Bijarbooneh, A. Goswami, W. D. Oliver Sponsorship: National Science Foundation Graduate Research Fellowship under Grant No. (000885616).

Superconducting qubits are a promising platform to realize scalable fault-tolerant quantum computers. However, current architectures use mostly planar elements that make dense integration challenging. The incorporation of non-planar elements, such as through silicon vias (TSVs) and flip-chip bonding, can ease geometric constraints on signal routing and enable the fabrication of such densely integrated large-scale quantum processors. TSVs have been demonstrated to reduce spurious chip modes and can also be used to fabricate novel circuit elements, such as compact qubits and filters. In this work, we show our progress toward fabri-

cating wafer-scale superconducting Titanium Nitride (TiN) TSVs and integrating them into multi-qubit devices. First, we show the fabrication of TSVs on 6" Si wafers using a dry etching (Bosch) technique and characterize the TSV sidewall angle and sidewall smoothness. Next, we explore atomic layer deposition (ALD) as a technique to coat the TSV sidewalls with superconducting TiN. We further characterize the critical temperature of the ALD-deposited TiN on the planar surface and inside the TSV sidewalls. Preliminary electrical data of the TSVs as well as future directions of incorporating them into flip-chip architectures will be discussed.

Nanoelectromechanical Cantilever Waveguide Diagnosis via Visible Spectral Domain Optical Coherence Tomography

Y. M. Goh, C. Li, J. Fujimoto, D. R. Englund Sponsorship: Department of Energy (DOE) Quantum Systems Accelerator; MITRE

We present a method for characterizing optical losses in a NEMS-based photonic integrated circuit (PIC) platform designed for efficient photon routing between free space and on-chip photonics. The nitride waveguide is oxide-cladded and suspended on an aluminum nitride (AlN) piezoelectric cantilever, which curls upwards due to intrinsic stress gradient in the layered structure. Operating the device at resonant frequencies enables 2D beam steering and high-speed spot array control. Furthermore, scalable integration of on-chip modulators positions this platform as a critical component for development of quantum repeater networks and cluster state generation. While miniaturized projection capabilities have been demonstrated with this device, optical efficiency, particularly in the complete transfer of amplitude and phase information, remains a bottleneck for quantum information applications involving single-photon level signals. A key source of loss is imperfect fabrication in the initial prototyping stages. Specifically, scattering has been observed at periodic crossbar etch points, which are designed to mod-

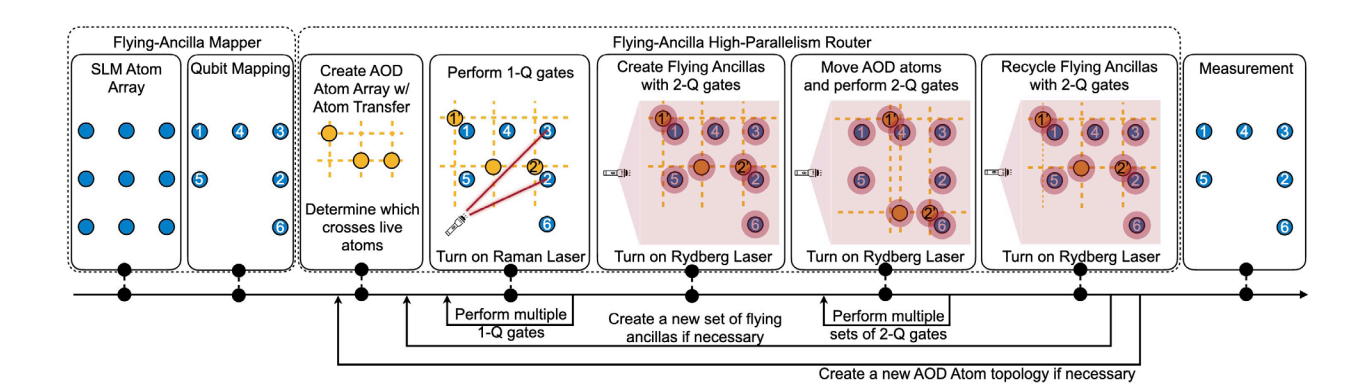
ulate the waveguide's stiffness and refractive index. To address these issues, we employ Spectral Domain Optical Coherence Tomography (SD-OCT), a non-invasive, high-resolution technique, to characterize and spatially resolve scattering and loss features within the waveguide. By employing a scannable delay line in the reference arm of the SD-OCT setup, we can probe the device with micrometer-level axial resolution over an arbitrary imaging depth by stitching together multiple spectrographs. Our experiment configuration allows us to distinguish between continuous loss and discrete scattering events within the waveguide, as well as scattering from waveguide input and termination ends. This work advances techniques for non-invasive waveguide loss characterization and supports the development of programmable photonic platforms for quantum networking applications. Efficient photon routing, fast qubit addressing, and scalable integration of on-chip modulators position this platform as a critical component for future quantum communication protocols.

Q-Pilot: Field Programmable Qubit Array Compilation with Flying Ancillas

H. Wang, B. Tan, P. Liu, Y. Liu, J. Gu, J. Cong, S. Han Sponsorship: NSF

Neutral atom arrays have become a promising platform for quantum computing, especially the field programmable qubit array. The qubit movement ability allows dynamic alterations in qubit connectivity during runtime, which can reduce the cost of executing long-range gates. However, this added flexibility introduces new challenges in compilation. We propose to map all data qubits to fixed atoms while utilizing movable atoms to route for 2-qubit gates between data qubits. Coined flying ancillas, these mobile atoms function as ancilla qubits, dynamically generated and recycled during

execution. We present Q-Pilot, a scalable compiler for FPQA employing flying ancillas to maximize circuit parallelism. For two important quantum applications, quantum simulation and the Quantum Approximate Optimization Algorithm, we devise domain-specific routing strategies. In comparison to alternative technologies such as superconducting devices or fixed atom arrays, Q-Pilot effectively harnesses the flexibility of FPQA, achieving reductions of 1.4x, 27.7x, and 6.3x in circuit depth for 100-qubit random, quantum simulation, and QAOA circuits, respectively.



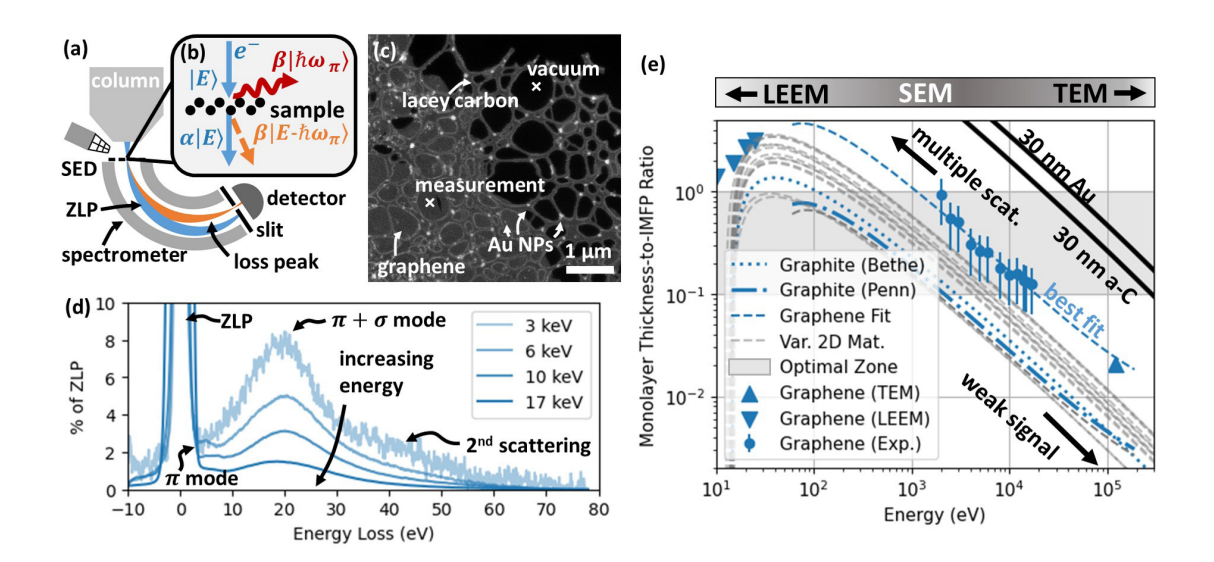
▲ Figure 1: The flowchart of the FPQA compilation framework.

Electron Energy Loss Spectroscopy of 2D Materials in a Scanning Electron Microscope

J. W. Simonaitis, J. A. Alongi, B. Slayton, W. P. Putnam, K. K. Berggren, P. D. Keathley Sponsorship: Department of Energy (DE-SC0022054), National Science Foundation (2110535)

This work demonstrates electron energy loss spectroscopy (EELS) of 2D materials in a 1-30 keV electron microscope, observing 50-times stronger electron-matter coupling relative to 125 keV transmission electron microscopes, which are historically used for such experiments. We observe for the first time that the universal curve relating beam energy to scattering holds for the transition from bulk graphite to graphene, albeit with a scale factor to account for this transition. We calculate

that optimal coupling for most 2D materials and optical nanostructures falls in energy range of scanning electron microscopes, concluding that the spectroscopy of such systems will greatly benefit from use of this previously unexplored energy regime. Specifically, we highlight ultrafast EELS, for this application, which could stand to greatly benefit from the order-of-magnitude performance to resolve previously unobservable ultrafast material dynamics.



▲ Figure 1: Rendering of our experiment. (a) Schematic of experiment, where after interaction (see (b)), measure the beam energy. (c) SEM micrograph of our sample. (d) graphene loss spectrum at various energies. (e) Plot of electron scattering intensity versus energy.

Diverse Impacts of Spin-Orbit Coupling on Superconductivity in Rhombohedral Graphene

J. Yang, X. Shi, S. Ye, C. Yoon, Z. Lu, V. Kakani, T. Han, J. Seo, L. Shi, K. Watanabe, T. Taniguchi, F. Zhang, L. Ju Sponsorship: NSF grant DMR-2414725 and DMR-2225925

Spin-orbit coupling (SOC) has played an important role in many topological and correlated electron materials. In graphene-based systems, SOC induced by transition metal dichalcogenide (TMD) at proximity was shown to drive topological states and strengthen superconductivity, the combination of which was proposed as a viable approach to engineer non-abelian quasiparticles for topological quantum computation. In particular, rhombohedral multilayer graphene with layer number N≥3 is a robust platform of electron topology, exhibiting both integer & fractional quantum anomalous Hall effects. However, superconductivity and the role of SOC in such systems remain largely unexplored. Here we report electron transport measurements of TMD-proximitized rhombohedral trilayer graphene (RTG). We observed a new hole-doped superconducting state SC4 with a transition temperature Tc of 230 mK. On the electron-doped side, we identified a new isospin-symmetry breaking three-quarter-metal (TQM) phase. Near this three-quarter-metal state, the state SC3, very weak in bare RTG, is fully developed into a superconducting state at 110 mK. Both SC3 and SC4 states reside at the phase boundaries between different isospin-symmetry-breaking states, and their observations are aligned with the existing understanding that SOC enhances graphene superconductivity. Surprisingly, the original superconducting state SC1 in bare RTG is strongly suppressed in the presence of TMD, and we cannot find it down to 40 mK— opposite to the effect of SOC on all other graphene superconductivities. Our observations form the basis of exploring superconductivity and non-Abelian quasiparticles in rhombohedral graphene devices, and provide experimental evidence that challenges the understanding of the impacts of SOC on graphene superconductivity.

Characterization and Comparison of Energy Relaxation in Planar Fluxonium Qubits

K. Azar, M. T. Randeria, R. DePencier Piñero, J. M. Gertler, L. Ateshian, H. Zhang, J. An, F. Contipelli, M. Gingras, K. Grossklaus, M. Hays, T. M. Hazard, D. K. Kim, J. Kim, B. M. Niedzielski, I. T. Rosen, H. Stickler, K. L. Tiwari, J. A. Grover, J. L. Yoder, M. E. Schwartz, W. D. Oliver, K. Serniak Sponsorship: Air Force Contract No. FA8702-15-D-0001

Fluxonium superconducting qubits have demonstrated high coherence times and high single and two qubit gate fidelities, making them a promising building block for superconducting quantum processors. In this work, we characterize the energy relaxation times T1 of multiple fluxonium qubits across their tunable frequency range in order to assess the dominant contributors to decoherence. Of the mechanisms considered, a circuit-based model for capacitive loss best captures the trends in the data over the majority of the tuning range. Motivated by this, we also consider modifications to this model accounting for a frequency-dependent effective capacitive quality factor. Furthermore, we use this analysis to bound the contributions of various other loss mechanisms. Finally, we utilize a composite model to compare these loss mechanisms on equal footing across individual qubits, and compare qubits fabricated with different materials processing techniques.

Quantum-Secure Multiparty Deep Learning in Optical Networks

K. Sulimany, S. K. Vadlamani, R. Hamerly, P. Iyengar, D. R. Englund Sponsorship: Israeli Council for Higher Education and the Zuckerman STEM Leadership Program, DARPA QuANET program (HR001124C0405)

Secure multiparty computation for deep learning has become a critical challenge as computational workloads are increasingly offloaded to cloud servers, leading to security vulnerabilities. We introduce a quantum-secure protocol using a coherent linear algebra engine based on the quantum properties of light, enabling privacy-preserving multiparty deep learning. We provide a security analysis relying on quantum information theorems to rigorously bound information leakage of both neural network weights and client data.

Applied to the MNIST classification benchmark, our approach achieves over 96% accuracy, setting information leakage upper bounds of 0.1 bits per weight symbol and 0.01 bits per data symbol. Our protocol offers information-theoretic security, unlike classical encryption methods that are dependent on computational complexity. Furthermore, the adaptation of classical encryption methods to machine learning is currently limited due to their computational overhead, which restricts their practical deployment in secure cloud-based inference.

Our protocol achieves physical layer security through an optical matrix-vector multiplication scheme that provides a scalable and efficient solution for real-world deployment. While previous studies have focused on optical AI accelerators to achieve energy-efficient, high-throughput computation, and reduced latency, we leverage optical networks and standard telecommunication components for secure multiparty computation. This work extends the application of optical processors to quantum cryptographic protocols, enabling data security within deep learning tasks.

This advancement paves the way for secure cloudbased artificial intelligence systems with applications in sensitive domains such as healthcare, finance, and more. By integrating a photonic computation architecture, our protocol provides a unique approach to preserving data confidentiality while maintaining strong performance in machine learning.

Spectroscopy Signatures of Electron Correlations in a Trilayer Graphene/hBN Moiré Superlattice

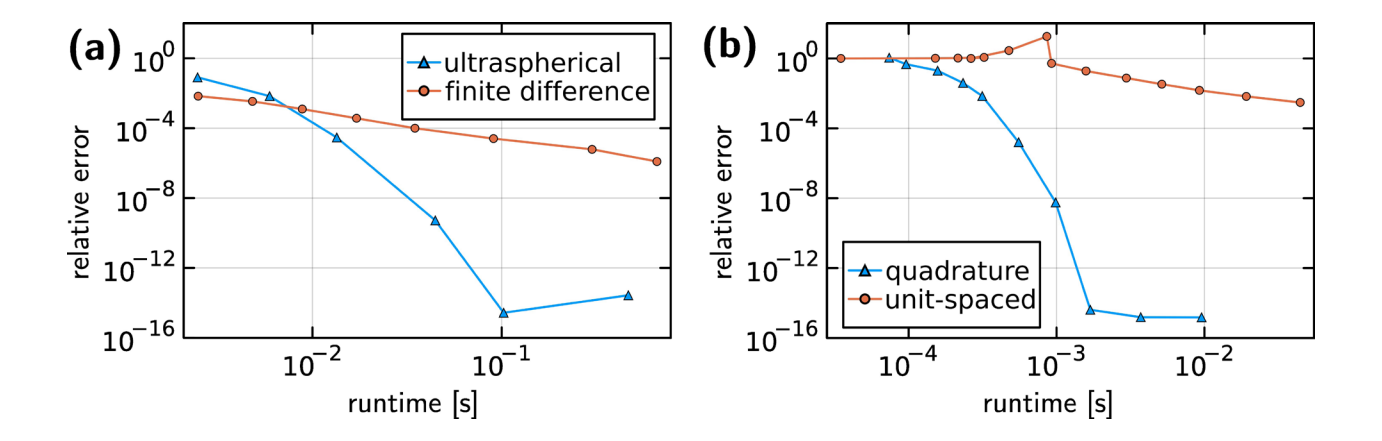
J. Yang, P. Liong, S. Ye, Z. Lu, T. Han, J. Seo, L. Shi, K. Watanabe, T. Taniguchi, L. Ju Sponsorship: STC Center for Integrated Quantum Materials, NSF grant no. DMR1231319

ABC-stacked trilayer graphene/hexagonal boron nitride moiré superlattice (TLG/hBN) has emerged as a playground for correlated electron physics. We report spectroscopy measurements of dual-gated TLG/ hBN using Fourier transform infrared photocurrent spectroscopy. We observed a strong optical transition between moiré minibands that narrows continuously as a bandgap is opened by gating, indicating a reduction of the single-particle bandwidth. At half-filling of the valence flat band, a broad absorption peak emerges at ~18 milli-electron volts, indicating direct optical excitation across an emerging Mott gap. Similar photocurrent spectra are observed in two other correlated insulating states at quarter- and half-filling of the first conduction band. Our findings provide key parameters of the Hubbard model for the understanding of electron correlation in TLG/hBN.

Spectral Methods for Modeling Non-equilibrium Superconductivity

R. Foster, A. Simon, K. K. Berggren Sponsorship: Alan McWhorter Fellowship, NSF GRFP and MIT Vanu Bose Presidential Fellowship Programs, DARPA DSO

The Usadel equations describe electron correlations in dirty superconductors, where the mean free path is much shorter than the coherence length [1]. This is useful for modeling the microscopic physics of photon absorption in superconducting nanowire single photon detectors (SNSPDs). In this work, we solve the Matsubara formulation of the Usadel equations with a Newton-Krylov method. The differential equation is discretized with an ultraspherical spectral method [2], and the infinite Matsubara sum is evaluated with a spectrally-accurate summation quadrature technique [3].



▲ Figure 1: (a) Comparison of ultraspherical and finite difference methods for spatial discretization. (b) Comparison of quadrature and unit-spaced methods for Matsubara sum evaluation.

RESEARCH ABSTRACTS: VOLUME II

Materials Synthesis & Characterization

| Defect-free Epitaxial Growth of GaAs on Silicon via Nanopatterning | 165 |
|--|-----|
| Defect Complexes in CrSBr Revealed through Electron Microscopy and Deep Learning | 166 |
| Twist Disorder in tWSe ₂ : Insights from Lateral Force Microscopy | 167 |
| Stress, Strain, and Temperature Tunability of 2D Metal Thiophosphate Materials Probed via | |
| Defect-induced Photoluminescence, X-ray, and Raman Spectroscopies | 168 |
| Electron Microscopy Studies of the Mechanisms of Epitaxial Titanium Oxide Growth on Graphene | 169 |
| Seeding Promoter Effect on Metal Organic Chemical Vapor Deposition Synthesized Molybdenum Disulfide | 170 |
| Metal-Organic Chemical Vapor Deposition-based Synthesis of p-type Tungsten Diselenide | 171 |
| Fabrication of Å-Scale Graphene Pores for Efficient Isomer and Ionic Separation | 172 |
| Mechanocaloric Polymer Discovery and Multi-Scale Engineering for Green HVAC Technologies | 173 |
| X-ray Induced Relaxation of Nickel and Nickel-based Nanoparticles on Silicon | 174 |
| Material Characterization of Niobium Nitride Sputtered Thin Films for SNSPDs | 175 |
| Uncovering Origins of Poor Photoluminescence Quantum Yield in 2D Hybrid Metal | |
| Organic Chalcogenolates (MOCs) | 176 |
| Group-IV-based Nanostructure Materials for Quantum Computing and Photonics | 177 |
| Electric Field Tunable Chern Insulators in Tetralayer Rhombohedral Graphene | 178 |
| Investigation of Novel Atomic Layer Deposited Dielectric Films for High Frequency, | |
| High Temperature Gallium Nitride Electronics | 179 |
| Hybrid Deposition Process of Perovskite Photovoltaics | 180 |
| Characterization of Interface-Driven Wake-Up and Fatigue of Ferroelectric ${ m Hf_{0.5}Zr_{0.5}O_2}$ | |
| for Non-Volatile Memory Applications | 181 |
| Semi-transparent Perovskite Solar Cells | 182 |
| Synthesis of Mixed Dimensional Perovskite Heterostructures | 183 |
| Selective Area Epitaxy of Defect-free III-V Layers on Silicon via Graphene Nanoholes | 184 |
| Densification of Vertically Aligned Boron Nitride Nanotubes via Biaxial Mechanical Compression | 185 |
| Artificial Intelligence-Assisted Synthesis and Integration Optimization of 2D Materials | 186 |

Defect-free Epitaxial Growth of GaAs on Silicon via Nanopatterning

C. Chen, K. Lu, D. Kwon, N. Han, J. Kim, F. M. Ross Sponsorship: Defense Advanced Research Projects Agency

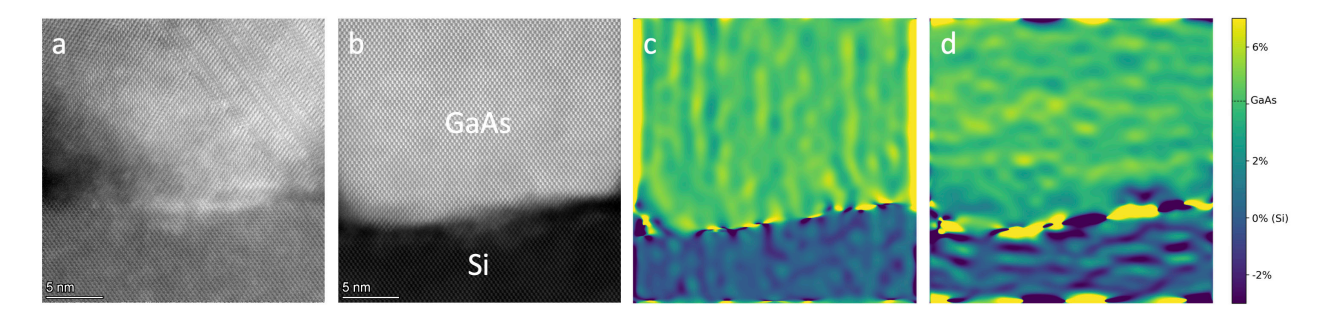
The advancement of semiconductor technology demands integrating the traditional microelectronic material, Si, with materials that can enhance the performance of devices, e.g., by improving speed. III-V semiconductors like GaAs, with their superior electron mobility, are promising for next-generation transistors. However, when growing GaAs on Si, the difference in atomic spacing between their lattices leads to the formation of interfacial defects that degrade device performance.

To overcome this, we grow GaAs on Si in confined areas, over which the lattice mismatch is small enough that interfacial defects don't form; an array of GaAs islands grows on Si. However, as we continue growing the islands up to coalescence, the contact area between GaAs and Si increases, and interfacial defects form. We thus pattern an interlayer on the Si before GaAs deposition, so that the GaAs and Si only make direct contact through small holes in the interlayer. The GaAs then grows across the interlayer. By optimizing the interlayer, this process of island formation followed

by GaAs lateral epitaxial overgrowth lead to defectfree interfaces in a process compatible with standard Si technology.

Measurements of the island and interface structure obtained using scanning transmission electron microscopy (STEM) guide our growth optimization. We use the Thermo Fisher Scientific Themis Z and prepare samples with the FEI Helios 600, both housed in Characterization.nano, to directly visualize atomic arrangements, identify defects such as dislocations and stacking faults (shown in Figure 1a), and map the local strain distribution (Figure 1b-d). Remarkably, geometric phase analysis of high-resolution STEM images reveals that GaAs nuclei can be fully relaxed, despite the lattice mismatch.

By leveraging advanced STEM characterization techniques, we are refining growth strategies to minimize defect formation. These findings open a new path toward integrating III-V materials on Si, so we may realize high-speed, energy-efficient semiconductor devices for future electronics.



▲ Figure 1: STEM images and geometric phase analysis of GaAs on Si. (a) Misaligned region showing polycrystallinity and stacking faults. (b) Defect-free single-crystalline GaAs. (c,d) Strain maps showing full relaxation of the GaAs nucleus in x- and y-directions.

[•] S. H. Bae, K. Lu, Y. Han, S. Kim, K. Qiao, C. Choi, Y. Nie, H. Kim, et al., "Graphene-assisted Spontaneous Relaxation Towards Dislocation-free Heteroepitaxy," *Nature Nanotechnology*, vol. 15, pp. 272–276, 2020. DOI: 10.1038/s41565-020-0633-5

H. Kim, S. Lee, J. Shin, M. Zhu, M. Akl, K. Lu, N. M. Han, Y. Baek, et al., "Graphene Nanopattern as a Universal Epitaxy Platform for Single-Crystal Membrane Production and Defect Reduction," Nature Nanotechnology, vol. 17, pp. 1054–1059, 2022. DOI: 10.1038/s41565-022-01200-6

Defect Complexes in CrSBr Revealed through Electron Microscopy and Deep Learning

M. Weile, S. Grytsiuk, A. Penn, D. G. Chica, X. Roy, K. Mosina, Z. Sofer, J. Schiøtz, S. Helveg, M. Rösner, F. M. Ross, J. Klein

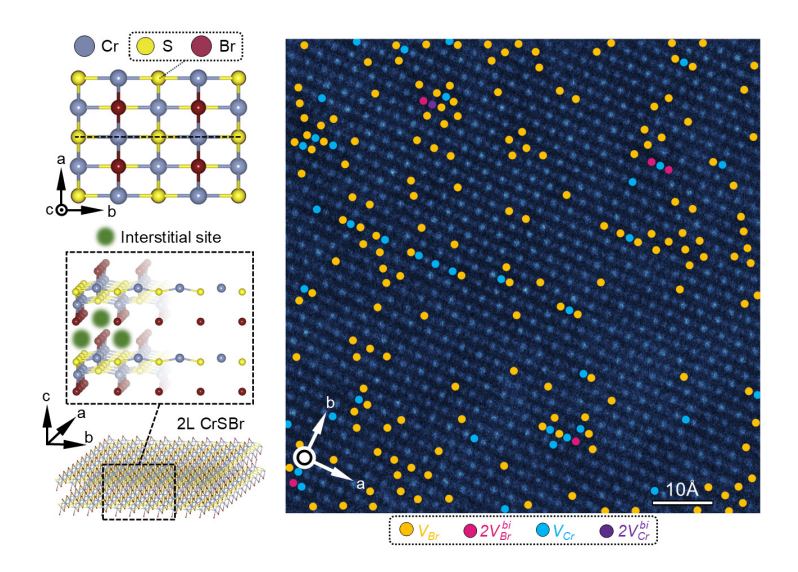
Atomic-scale defects influence the functional properties of layered materials. In this work, we present a comprehensive defect analysis in bilayer CrSBr, a magnetic quasi-1D van der Waals semiconductor of FeO-Cl-type symmetry, using a combination of atomic-resolution scanning transmission electron microscopy (STEM), deep learning, and ab-initio calculations.

To overcome beam sensitivity and low signal-to-noise ratios in bilayer CrSBr, we employ a low-dose STEM imaging approach combined with a custom machine learning pipeline for automated detection, classification, and statistical averaging of point defects. This workflow enables the identification of a diverse set of defect types, including single and stacked vacancy defects, interstitial Cr and Br vacancy defect complexes ($V_{\rm Cr}$ + Crint), Cr-Br vacancy complexes ($V_{\rm Cr}$ + $V_{\rm Br}$), and extended defect lines aligned along the crystallographic a-direction. These features are often difficult to resolve using traditional methods but

become visible through ML-assisted averaging across many images.

First-principle simulations support the experimental findings and provide insight into defect formation energies, structural relaxation, and electronic localization. Interstitial Cr defect complexes are shown to introduce highly localized in-gap electronic states with reduced dimensionality. These states are predicted to be optically active and magnetically tunable, offering potential for use in quantum light emitters, defect-based memory elements, or spintronic logic.

The methodology developed here is broadly applicable to other layered systems with limited defect visibility and motivates using STEM for targeted atomic-scale engineering of magnetic semiconductors. The insights gained here can be extended to over 20 related materials in the transition metal oxyhalide and chalcogenide halide families of FeOCl structural type.



▲ Figure 1: Schematic illustration of bilayer CrSBr. High-angle Annular Dark-field-STEM image with overlaid vacancy defects detected by deep convolutional neural networks.

- M. Weile, S. Grytsiuk, A. Penn, D. G. Chica, X. Roy, K. Mosina, Z. Sofer, J. Schiøtz, S. Helveg, M. Rösner, F. M. Ross, and J. Klein, "Defect Complexes in CrSBr Revealed through Electron Microscopy and Deep Learning," *Physical Review X*, vol. 15, p. 021080, 2025.
- J. Klein, T. Pham, J. D. Thomsen, J. B. Curtis, T. Denneulin, M. Lorke, M. Florian, A. Steinhoff, R. A. Wiscons, J. Luxa, Z. Sofer, F. Jahnke, P. Narang, and F. M. Ross, "Control of Structure and Spin Texture in the van der Waals Layered Magnet CrSBr," *Nature Communications*, vol. 13, p. 5420, 2022.
- K. Torres, A. Kuc, L. Maschio, T. Pham, K. Reidy, L. Dekanovsky, Z. Sofer, F. M. Ross, and J. Klein, "Probing Defects and Spin-Phonon Coupling in CrSBr via Resonant Raman Scattering," Adv. Funct. Mat., vol. 33, p. 2211366, 2023.

Twist Disorder in tWSe2: Insights from Lateral Force Microscopy

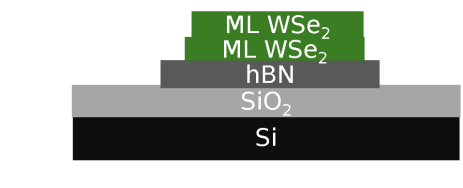
N.-L. Bathen, R. Dana, J. Klein, F. M. Ross, U. Wurstbauer Sponsorship: NSF

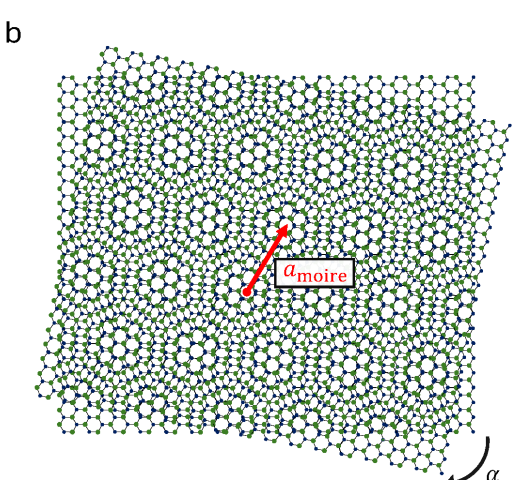
Twisted bilayers of transition metal dichalcogenides (TMDs) form moiré superlattices and host electronic minibands, enabling the exploration of Mott-Hubbard physics and correlated quantum phases. These systems are typically fabricated by stacking van der Waals materials (Figure 1a) with a slight twist mismatch, creating a long-range moiré periodicity determined by the twist angle, as illustrated in Figure 1b. While previous scanning probe microscopy studies have shown that local strain and atomic relaxation can cause real-space variations in the moiré wavelength, these effects have not been systematically analyzed over micrometer-scale

distances or across a broad range of twist angles. Such variations are expected to significantly influence optical experiments conducted in our labs.

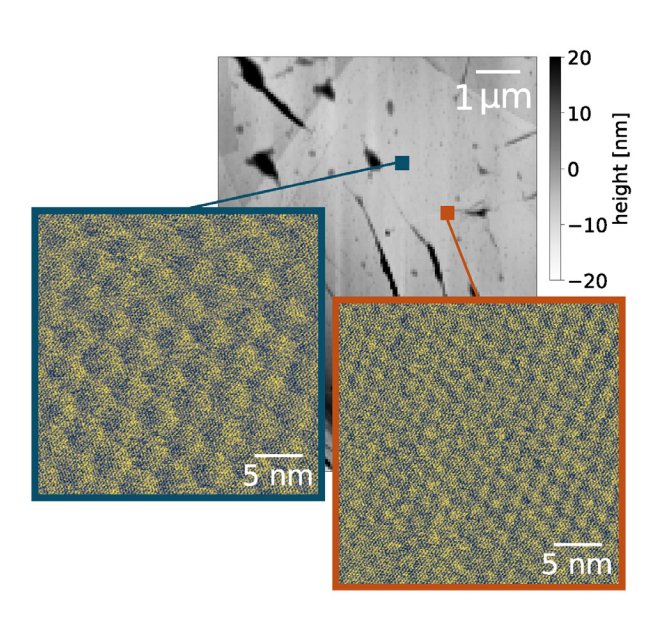
Here, we use lateral force microscopy (LFM) mode to map the moiré lattice and relocate individual scans within a topographic map of the sample. Thus twist disorder can be visualized, as shown for two positions on the sample in Figure 2. The results reveal twist angle variations of up to several degrees within micrometerscale distances. This analysis enables identification of homogeneous regions where optical and transport experiments can be reliably performed.

а





▲ Figure 1: Sketch of investigated material system. (a) Stacking order of individual van der Waals materials. (b) Schematic sketch of two static hexagonal lattices with two atomic basis rotated in respect to each other, forming moiré lattice.



▲ Figure 2: Height trace of investigated sample with relocated LFM scans, revealing moiré lattice at two individual positions on sample.

- S. Shabani, et al., "Deep Moiré Potentials In Twisted Transition Metal Dichalcogenide Bilayers," Nat. Phys., vol. 17, pp. 720–725, 2021.
- N. Saigal, et al., "Collective Charge Excitations between Moiré Minibands in Twisted WSe₂ Bilayers Probed with Resonant Inelastic Light Scattering," Phys. Rev. Lett., vol, 133, p. 046902, 2024.

Stress, Strain, and Temperature Tunability of 2D Metal Thiophosphate Materials Probed via Defect-induced Photoluminescence, X-ray, and Raman Spectroscopies

A. Mukherjee, S. V. Boriskina

Sponsorship: ARO-Multidisciplinary University Research Initiatives program, MIT International Science and Technology Initiatives-Poland Seed Fund, MIT-Monterrey Technology Program

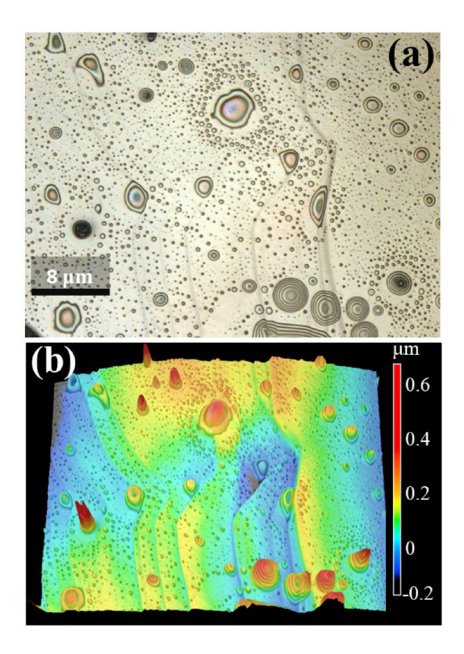
Metal thiophosphates (MTPs) are a new family of intermediate-bandgap (1.3–3.5 eV) two-dimensional (2D) materials that exhibit diverse electronic, magnetic, and nonlinear optical properties and show promise for applications in energy harvesting, storage, and photo-detection. These properties are strongly influenced by the transition metal element within the MPTs.

Sulfur vacancies and other defects in MTPs allow defect-state-to-valence-band transitions leading to visible light emission at sub-band gap energies. Photoluminescence (PL) measurements under a variety of external stimuli can shed light on the structural and electronic properties evolution in these materials and reveal material candidates to achieve high tunability or high stability under extreme conditions.

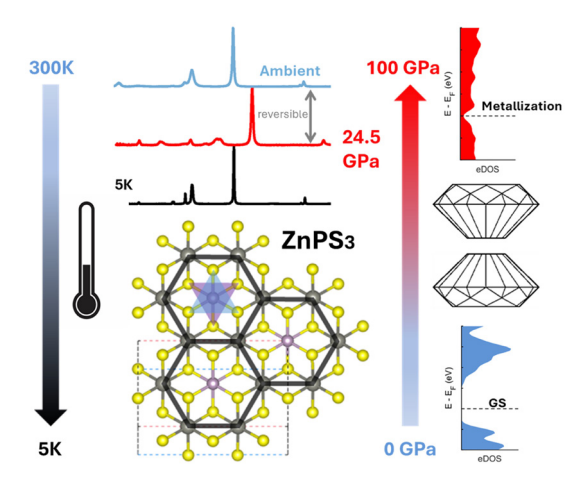
In collaboration with the Institute of Physics in Warsaw, the US Air Force Research Lab, and Technology de Monterrey, we showed experimentally that defect-mediated PL in AgScP₂S₆ can be enhanced and spectrally shaped by structural defects in the material (Figure 1). These defects form during material growth, originating from dislocations buried under surface planes, and exhibit varying thickness and

inhomogeneous localized strain distribution. Our data also show that PL can be further enhanced and tuned via thermal annealing, which increases the density of sulfur vacancies, and by temperature-induced strain gradients.

In turn, zinc phosphorus trisulfide (ZnPS₂), demonstrated remarkable structural stability under extreme pressures and cryogenic temperatures (Figure 2). PL measurements and Raman spectroscopy revealed a fully reversible pressure-induced phase transition starting at ~7 GPa, after which ZnPS3 demonstrates stability up to 24.5 GPa. Ab-initio density functional theory (DFT) calculations support these observations and predict a semiconductor-to-semimetal transition at 100 GPa. Cryogenic X-ray diffraction measurements revealed that ZnPS3 has a high mean thermal expansion coefficient of about 4.4 × 10⁻⁵ K⁻¹, among the highest reported for 2D materials. This unique combination of tunable electronic properties under low pressure and high thermal sensitivity makes ZnPS₂ a strong candidate for sensing applications in extreme environments.



 \blacktriangle Figure 1: (a) Morphology of an AgScP₂S₆ crystallite under optical microscope, which reveals multiple structural defects. (b) 3D height profile reconstruction using laser scanning confocal microscopy.



 \blacktriangle Figure 2: ZnPS $_3$ undergoes reversible pressure-induced phase transition, followed by semiconductor-to-semimetal transition at 100 GPa. It exhibits defect-assisted emission, large Grüneisen parameter at cryogenic temperatures, and high thermal expansion coefficient of approximately $4.4\times10^{-5}~\text{K}^{-1}.$

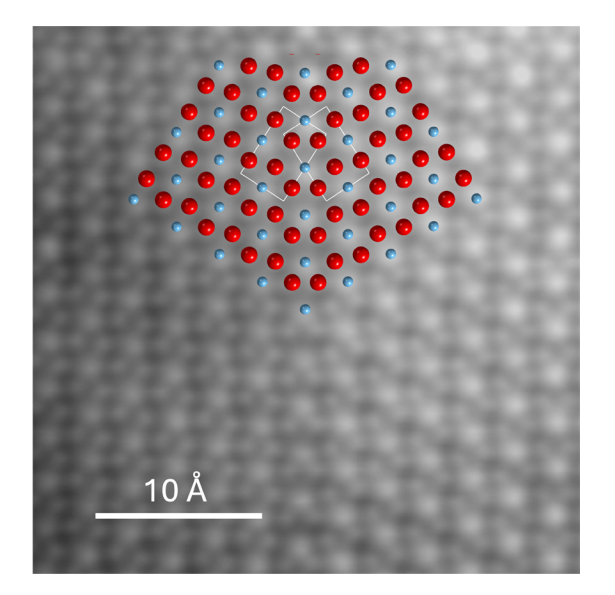
Electron Microscopy Studies of the Mechanisms of Epitaxial Titanium Oxide Growth on Graphene

P. Knight, F. M. Ross

The pressing need to reduce the energy used in computation is driving the creation of new designs for transistors and other computing architectures with reduced energy consumption. One promising concept is to use two-dimensional (2D) van der Waals materials as channel materials in transistor designs, which can be scaled to the atomically thin limit while avoiding short channel effects, thus minimizing static power consumption. Energy savings will also come from innovations in dielectric materials: for example, ferroelectric gate stacks that contain crystalline HfO₂ and ZrO₃ have recently been shown to exhibit "negative capacitance" effects that allow lower operating voltages by enabling a steeper switching transition between "on" and "off" states than is possible with conventional microelectronic materials. However, integrating any new material into advanced device designs faces the constraints of materials science and engineering. Here we need to create stacks of materials that include 2D layers with well-defined crystal structures and crystal orientations, perfect interfaces, and minimal defects. These problems are particularly challenging in the context of

incorporating 2D materials into devices because of the known difficulties in nucleating 3D materials on van der Waals surfaces.

We quantify oxidation transformations on 2D materials of Ti-group metal oxides, all of which are of interest as next-generation dielectric materials. We aim for the self-assembly of an epitaxial metal layer, followed by oxidation of the metal via a series of epitaxial suboxides to form a fully oxidized phase. We use the Themis Z-STEM in MIT.nano to study the strain and defects within these oxide phases to better understand the effect of those defects on the dielectric properties of the material. Figure 1 shows an example visualizing the arrangement of Ti atoms (bright) and O atoms (less bright) in rutile TiO₂ at a twin boundary. We anticipate that polarization at these kinds of defects could enable use of Ti oxides as dielectric layers in devices. Our ongoing studies aim to extend understanding of nucleation and growth of epitaxial Ti oxides, which defects result, and what influence these defects will have on electronic device performance.



◄ Figure 1: (a) Morphology of an AgScP₂S₆ crystallite under optical microscope, which reveals multiple structural defects. (b) 3D height profile reconstruction using laser scanning confocal microscopy.

FURTHER READING

 P. J. Knight, K. Reidy, A. Penn, A. Foucher, and F. M. Ross, "In-situ Phase Transformations of 3D Nanoislands on 2D Materials in the Ti-Graphene System," presented at Materials Research Society Fall Meeting, Boston, MA, 2024.

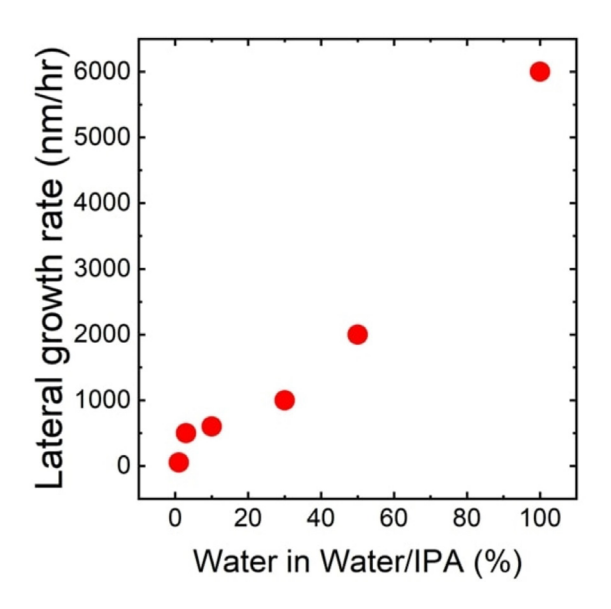
Seeding Promoter Effect on Metal Organic Chemical Vapor Deposition Synthesized Molybdenum Disulfide

Y. Jiao, J. Zhu, T. Palacios Sponsorship: Center for Heterogeneous Integration of Micro Electronic Systems (JUMP 2.0)

Two-dimensional (2D) transition metal dichalcogenide (TMD) materials are promising for the next generation electronics thanks to their excellent electronic and photonic properties. Metal organic chemical vapor deposition (MOCVD) can provide excellent uniformity and quality. Seeding promoters, such as sodium chloride (NaCl), have been reported to have significant improvement in the MOCVD growth rate and quality of molybdenum disulfide (MoS₂). Understanding the effect of seeding promoters can benefit overcoming lim-

itations of the large-scale fabrication of 2D electronics.

Here, we quantitatively investigate the concentration dependence of seeding density, and flake quality. We also demonstrate material uniformity across the 200 mm platform and a boost in the average mobility to above 75 cm 2 /(V·s). This effort has provided insight into the fundamental growth mechanism and heterogeneous integration of TMD material with complementary-metal-oxide-semiconductor (CMOS) technology.



▲ Figure 1: Lateral growth rate change based on NaCl concentration in the saturated water: IPA solution.

Metal-Organic Chemical Vapor Deposition-based Synthesis of P-type Tungsten Diselenide

S. Chakravarthi, H. W. Lee, Y. Jiao, X. Zheng, J. Zhu, J. Kong, T. Palacios Sponsorship: Intel

Two-dimensional(2D) materials with their high mobility, excellent gate electrostatic control, and atomically thin nature have emerged as promising channel materials for highly-scaled, energy-efficient electronics. However, most of the previous research focuses on n-type semiconductors, e.g., molybdenum disulfide (MoS_2). P-type 2D materials, e.g., tungsten diselenide (WSe_2), possess equal importance in constituting the complementary electronics circuits, but both the material synthesis and electrical characterizations are less developed.

In this work, using metal-organic chemical vapor deposition (MOCVD), the impact of precursor concentration, seeding promoter, carrier gas and forming gas (H₂) flow on WSe₂ synthesis are systematically discussed, providing insights for obtaining higher-quality materials. Comprehensive material and device characterizations are carried out to evaluate the quality of as-grown WSe₂. This paves the way for our future research on scaling up the material synthesis system to 8" wafer-scale and enabling direct integration of 2D WSe₂ on silicon complementary-metal-oxide-semiconductor (CMOS) circuits.

FURTHER READING

[•] J. Zhu, J. Park, S. A. Vitale, et al., "Low Thermal Budget Synthesis of Monolayer Molybdenum Disulfide for Silicon Back-end-of-line Integration on 200 mm Platform," Nat. Nanotechnol. 18, 456-463 (2023).

Fabrication of A-Scale Graphene Pores for Efficient Isomer and Ionic Separation

D. R. Chen, T. Zhang, S. M. He, Z Wang, C. Cheng, J. Wang, J. Kong Sponsorship: NSTC Graduate Students Study Abroad Program (113-2917-I-002-050)

Å-scale pores in monolayer graphene provide spatial confinement for small particles of various sizes, showing great potential in separation science, such as isomer and ionic separation. Conventional top-down methods for fabricating A-scale pores with high density and uniformity often lack atomistic precision, resulting in large, non-selective pores that cause leakage and reduced selectivity. We previously demonstrated a Cu-ion-sputtering cascade compression approach in Nature that addresses the problem that minimizes the tail-end of the pore size distribution while enhancing pore density. Despite this, it remains challenging to repeatably achieve precise, uniform nanopores for designed separation applications due to the uncontrollable number of Cu ions. Here, we utilize Ar, which delivery is better controlled through a mass flow

controller, as an ion source to enhance the reliability of in-situ pore fabrication. By applying voltage within the CVD chamber, Ar gas is ionized into Ar ions through a gas-phase electrochemical reaction and sputters carbon atoms out to create Å-scale pores. As a result, a repeatable production of sub-nanometer pores is implemented by such Ar-cascaded compression, verified by Raman spectroscopy and Conducting-AFM. The resulting Å-scale porous graphene film exhibits remarkable ion-ion selectivity along with high permeance. We plan to collect more data to further verify the repeatability for as-synthesized samples as separation films.

We hope the findings pave the way for Å-scale porous graphene, leading to future sustainable separation technologies.

Mechanocaloric Polymer Discovery and Multi-Scale Engineering for Green HVAC Technologies

D. Xu, H. Gold, T. Yu, S. V. Boriskina Sponsorship: SUSTech and ONR Global, MathWorks MechE Graduate Fellowship, NDSEG and PEM Graduate Fellowships

Residential thermal management (heating and refrigeration) is one of the most energy-intensive technology sectors, with space cooling alone accounting for nearly 16% of global electricity consumption in the buildings sector in 2021. The direct CO2 emissions from space and water heating reached a record high of 2.5 G tons in the same year. Solid-state cooling technologies offer a sustainable alternative to conventional HVAC systems, providing opportunities for enhanced energy efficiency and reduced environmental impact.

This work focuses on the AI-driven discovery, testing, and optimization of mechanocaloric (mC) polymers. We use a combination of ab-initio density functional theory and machine-learning surrogate model development to identify most promising polymers and co-polymers for mC applications, a molecular dynamics simulations to evaluate realistic material performance under mechanical deformations, followed by experimental verification

and optimization of the most promising materials. Our experimental results show that some of the new materials identified through our discovery pipeline exhibit strong performance, achieving temperature changes exceeding 5 °C under uniaxial strain and up to 20 °C under twisting deformation. Additionally, they exhibit a high coefficient of performance, low actuation stress, and a competitive cost-to-performance ratio, showing promise for scalable applications. Finally, we use macroscopic finite-element mechanical modeling to study the impact of larger-scale structural features, such as fiber plying, braiding and knotting on improving the material performance and fatigue resistance.

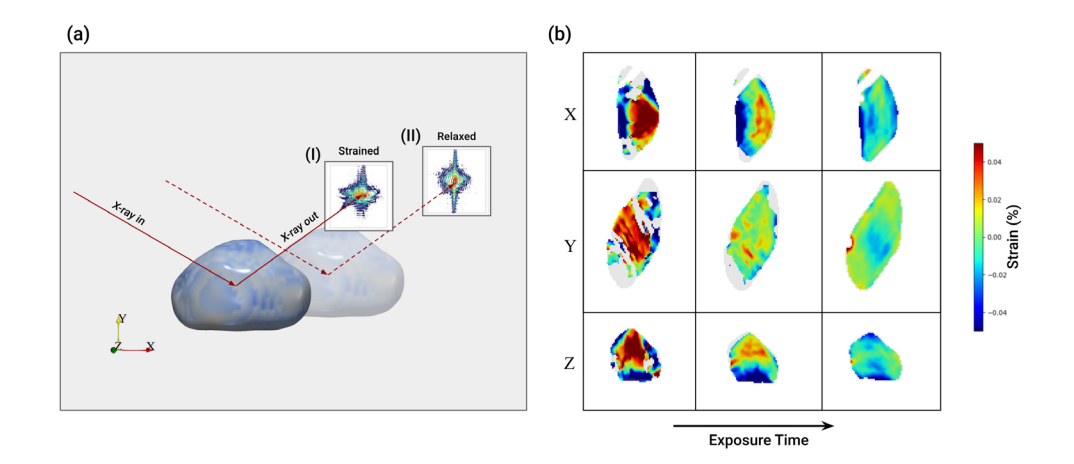
Through this multi-scale optimization and testing pipeline, we aim to accelerate the development of durable, high-performance mC materials for scalable and sustainable solid-state cooling and heating technologies.

X-ray Induced Relaxation of Nickel and Nickel-based Nanoparticles on Silicon

R. Hultquist, D. Simonne, E. Jossou Sponsorship: MathWorks Fellowship, Startup

Nickel and Nickel-Cobalt single crystals are model systems for studying the effects of radiation and corrosion in Light Water Reactor cooling components. While bulk alloys are used in full-scale systems, nanoparticle analogues can accelerate the research and development of bulk materials for use in extreme environments. Their morphologies, formed by dewetting, distinguish them from their bulk forms and influence local mechanical and chemical properties. Utilizing coherent X-rays to resolve strain and defects, Bragg Coherent Diffraction Imaging (BCDI) enables deep insight into single crystal

models. In this work, we demonstrate that coherent X-rays can be used to relax highly strained Nickel alloy single crystals on Silicon. Furthermore, we use atomistic density functional theory calculations to show how photo-assisted modulation of charge density at the interface leads to the observed relaxation. Understanding and controlling heteroepitaxy with coherent X-rays will provide deeper insight into the physical chemistry of heterointerfaces while also promoting the use of BCDI to characterize complex models of materials in extreme environments.



▲ Figure 1: (a): Schematic of crystal in initial state (I) and final state (II) with detected diffraction pattern showing changes from highly strained to relaxed state. (b): Crystal cross sections along X, Y and Z directions showing time dependent strain field relaxation under the influence of X-rays.

Material Characterization of Niobium Nitride Sputtered Thin Films for SNSPDs

F. Incalza, D. J. Paul, M. Castellani, O. Medeiros, E. Batson, K. K. Berggren Sponsorship: Darpa Program

Niobium Nitride (NbN) superconducting thin films have garnered significant interest for applications in superconducting electronics, quantum computation, and superconducting nanowire single-photon detectors (SNSPDs). SNSPD performance is highly dependent on the superconducting properties of NbN films, which are primarily determined by the film's microstructure and the substrate on which it is grown. A detailed understanding of the crystallographic structure and chemistry of NbN is essential for evaluating and optimizing device performance. Variations in the phononic spectrum, affected by whether the films are crystalline or polycrystalline, can lead to significant differences in SNSPD characteristics, including thermal conductance, detection efficiency, switching current, depairing current, critical temperature, and diffusion coefficients. This insight enables a direct relationship between crystal structure and device performance, guiding the optimization of NbN-based devices.

In this work, NbN thin films were deposited using sputtering techniques on sapphire, thermally oxidized silicon, and magnesium oxide substrates. The deposition process was analyzed and optimized based on the substrate type. Material and superconducting properties were examined using various techniques, including XRD, XPS, EBSD, ellipsometry, MPMS, and TEM. The critical temperature, crystal structure and orientation, grain dimensions, and optical properties were analyzed and compared across films, with each set of properties related to the achievable device characteristics. Using high-temperature (800 °C) sputtering, we achieved high-quality epitaxial NbN thin films on sapphire, with a critical temperature reaching the bulk value of 16 K, and compared their properties with those of films deposited on other substrates.

Uncovering Origins of Poor Photoluminescence Quantum Yield in 2D Hybrid Metal Organic Chalcogenolates (MOCs)

N. J. Samulewicz, W. S. Lee, W. A. Tisdale Sponsorship: NSF Graduate Research Fellowship, U.S Army Research Office Award

Innovations in blue emitting semiconductors and widespread adoption of light emitting diodes (LEDs) in recent years have drastically reduced global energy consumption associated with lighting. While this reduction is monumental, production and other energy intensive processes associated with LED lighting still contribute significant yearly CO2 emissions. To reach future sustainability targets, advancements in light emission are essential, driving research interest towards novel materials – particularly ones with more sustainable synthesis pathways.

Our lab investigates metal organic chalcogenolates (MOCs) – novel 2D van der Waals stacking hybrid semiconductors with strong exciton binding energies, in-plane anisotropy, and direct bandgap. Amongst others, these properties make MOCs suitable candidates for applications as LEDs, excitonic switches, and other optoelectronics. Importantly, high-quality millimeter scale single crystals are synthesizable through a simple, ambient single-

phase reaction. Covalent intralayer bonding in MOCs bolsters strong environmentally stability and enables property tuning through various functionalizations. Among them, mithrene, [AgSePh]oo, is of particular interest due to its narrow blue luminescence. However, nonradiative recombination dominates excited state dynamics, limiting its potential to revolutionize future optoelectronics. This work details efforts to uncover the origins of the low photoluminescence quantum yield in mithrene through spectroscopic analysis of defects, physical structure, and brighter MOC variants. Emission is highly impacted by defects, yet impervious to simpler defect-mitigation strategies, forcing exploration of more novel passivation techniques. Despite interest in mithrene's sharp blue emission, future viability of this material class to promote sustainable energy consumption is most dependent on the efficiency of light emission, and is necessary to pursue improvements in both performance and understanding.

Group-IV-based Nanostructure Materials for Quantum Computing and Photonics

S. Ben-David, S. P. Ramanandan, N. Amador-Mendez, A. Rudra, A. Fontcuberta i Morral Sponsorship: NCCR SPIN, SNSF SUGAR, Fulbright/Swiss Government Open Research Award

Group-IV semiconductors (Si, Ge, Sn) are key materials for nanoelectronics and show promise for quantum devices. While Si remains the most widely used semiconductor, Ge and GeSn draw interest due to their inherently higher electron and hole mobility. This work explores methods to realize Ge- and GeSn-based nanostructures.

Ge nanowires (NWs) offer a versatile platform for exploring quantum transport phenomena as the 1D charge confinement enables spin-based qubit logic. Despite these convenient properties, NW scalability remains a major challenge. Selective area epitaxy (SAE) offers a scalable solution for achieving horizontal NWs on device substrates. In this work, we advance the SAE of Ge NWs by growing the Ge in a Si V-groove nanomembrane (NM) instead of holes on a planar substrate. This approach confines the NWs fully within the Si V-groove, eliminating the direct interface between the Ge and SiO2 dielectric mask that hinders NW spin-qubit functionality. We present the

fabrication of the Si V-groove NM and the temporal evolution of the Ge NW growth using SEM, AFM, and cross-section TEM.

The incorporation of Si V-groove NMs enables precise confinement of Ge nanowires for scalable quantum devices while addressing limitations in spinqubit functionality. Nonetheless, the indirect bandgap of Ge restricts use in optoelectronics, which can be overcome by leveraging GeSn alloys with direct bandgap properties. GeSn can be monolithically integrated into Si photonics to act as a NIR emitter. We present a novel approach to realize GeSn nanostructures with Sn contents beyond the solubility limit (1%at) via flash annealing. We show the top-down fabrication of GeSn nanostructures and the material properties evaluated using XRD, AFM, Raman spectroscopy, and TEM. Future work focuses on integrating Ge and GeSn nanostructures into optoelectronic platforms to enhance device functionality and scalability.

Electric Field Tunable Chern Insulators in Tetralayer Rhombohedral Graphene

S. Ye, T. Han, Z. Lu, Y. Yao, J. Yang, J. Seo, L. Ju Sponsorship: NSF Grant

Rhombohedral graphene, characterized by its unique stacking order and flat electronic bands, has emerged as a versatile platform for exploring correlated and topological phenomena. The rhombohedral tetralayer graphene/hBN moiré system has been proposed to host novel superconductivity and topological phases, including the chiral superconductivity and quantum anomalous Hall effect. In this work, we present DC electrical transport measurements in a rhombohedral tetralayer graphene/hBN moiré superlattice. We observed electric-field-induced topological phase transitions of Chern insulators, with the Chern number tunable by displacement field from C=3 to C=4 at the

first hole filling of the superlattice. Magnetic hysteresis measurements revealed that these states emerge at extremely low magnetic fields (B=0.1) and exhibit perfect quantization. While the C=4 state aligns with previous prediction and observation of a quantum anomalous Hall state, the C=3 state observed at lower displacement fields is unexpected. Additionally, we identified another C=3 state at filling nu = -2. These findings enrich the topological landscape of this intriguing system. Combined with its unique superconducting properties, rhombohedral multilayer graphene is a promising platform for studying and engineering novel quantum phases of matter.

Investigation of Novel Atomic Layer Deposited Dielectric Films for High Frequency, High Temperature Gallium Nitride Electronics

J. Kang, J. Niroula, T. Palacios Sponsorship: AFOSR, SRC Jump 2.0 SUPREME Center

High temperature rated electronics are used in various ways such as hypersonic aircrafts, deep well oil drilling, and exploring Venus. Unfortunately, traditional silicon (Si) devices cannot operate above 250°C due to fundamental limits on its intrinsic carrier concentration. Therefore, semiconductors like silicon carbide (SiC) and gallium nitride (GaN) are more suitable to use for high temperatures because of their wide-band gap and negligible carrier thermal generation at temperatures around 500°C. Currently, plasma enhanced chemical vapor deposition (PECVD) silicon nitride (SiN) is the current state of the art in GaN passivation, but for high frequency devices, thin (<25 nm) passivation layers are needed to minimize parasitic capacitances. Thus, for next generation passivation layers, using Atomic Layer

Deposition (ALD) is the preferred deposition method on these devices as ALD allows for atomically precise control of very thin, high quality dielectric layers.

In this project, we investigate the electrical properties of ALD deposited Ga2O3, AlN, and Al2O3 as future passivation layers for next generation GaN devices. This is done through high temperature (25-300°C) electrical characterization of metal-insulatormetal (MIM) capacitors as well as through current collapse measurements of these films on GaN high electron mobility transistors (HEMTs). ALD grown films provide excellent passivation for silicon surfaces as they exhibit high breakdown voltage, low leakage current, and better thermal conductivity.

Hybrid Deposition Process of Perovskite Photovoltaics

T. Kadosh Zhitomirsky, K. Yang, S. Srinivasan, W.J. Hsu, E. Pettit, R. J. Holmes, H. L. Tuller, V. Bulović Sponsorship: U.S. Department of Energy

Halide perovskites have demonstrated remarkably high solar to electrical energy conversion efficiencies and are therefore of great interest for rapid commercialization. Currently, popular fabrication processes involve the hazardous solvent DMF, which is required to dissolve the lead based precursors, such as PbI2. These fabrication routes cannot be readily up-scaled as required. Vapor Transport Deposition (VTD) is an alternative, low-cost manufacturing technique that has been proven before for other solar cell materials.

VTD base process bypasses some solvent related challenges, namely uniform coverage of large areas, chemical compatibility, and toxicity. As a low-cost alternative to thermal evaporation, VTD has the potential to deposit organic and inorganic perovskite precursor materials either sequentially or via co-deposition. Furthermore, VTD potentially

offers higher tunability of deposition parameters, to enable film growth with improved composition and microstructure control. In this work, we demonstrate harnessing VTD to deposit the inorganic precursor lead iodide. By that we can eliminate the use of the toxic solvent DMF, and replace it by isopropanol which is considered 40 times less toxic.

We are currently working with a custom-made VTD system, with which we achieved champion FAPI and MAPI cells of 12% power conversion efficiency. We report our progress in investigating the influence of underlying layer, substrate and sublimation temperatures, chamber pressure and flow rate ratios on the morphology and stoichiometry of the forming perovskite film, and in turn, its photo-active and electronic properties.

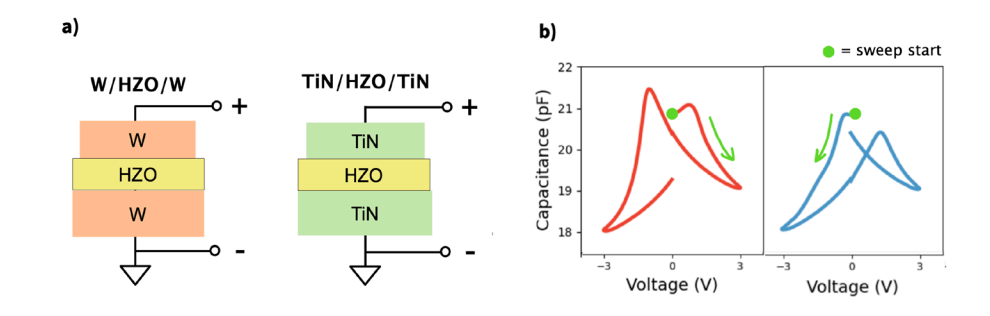
Characterization of Interface-Driven Wake-Up and Fatigue of Ferroelectric $Hf_{0.5}Zr_{0.5}O_2$ for Non-Volatile Memory Applications

T. E. Espedal, Y. Shao, E. R. Borujeny, J. A. del Alamo Sponsorship: MIT UROP, Intel Corporation, Semiconductor Research Corporation

Ferroelectric (FE) memory based on CMOS-compatible ${\rm Hf_{0.5}Zr_{0.5}O_2}$ (HZO) has emerged as an NVM technology may provide low-voltage operation, fast switching, long data retention, and high device endurance. Plasma-Enhanced ALD has shown enhanced HZO film quality, potentially improving memory. However, certain metal-FE-metal (MFM) capacitive structures show premature breakdown. Endurance characterization shows asymmetric wake-up, indicating unique physics at either metal-HZO interface.

We identify the asymmetric electrical characteristics of W/HZO and TiN/HZO devices that emerge with device cycling. Consistent symmetry patterns across pulsed I-V, DC I-V and C-V measurements indicate interfacial phenomena that eventually lead to device breakdown.

In this work, we show that interface physics are a critical aspect of MFM device endurance: specifically, process conditions and electrode metal are important in realizing high-endurance HZO films and thereby potential NVM applications.

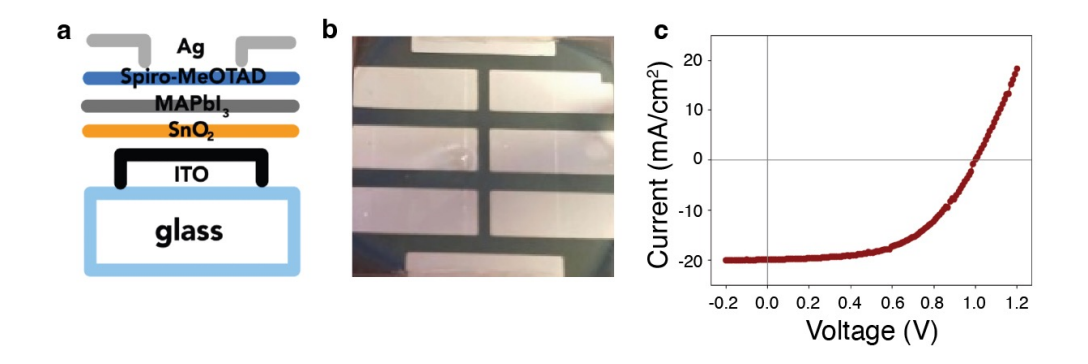


▲ Figure 1: a) Schematic of MFM structures. b) The observed W/HZO C-V characteristic is invariant to sweep direction reversal, indicating device asymmetry.

Semi-transparent Perovskite Solar Cells

E. Delarosa, K. Jander, V. Sandrapaty, F. Shangguan, R. Zhang, T. K. Zhitomirsky Sponsorship: MIT EECS, 6.2540 class

With growing global energy demands, renewable energy sources like solar are more critical than ever. Designing solar cells with a formfactor that allows their ubiquitous integration into the buildings, including windows as energy generating surfaces, can expand access to solar energy. Perovskite solar cells are especially promising due to their high efficiency and thin-film design which can facilitate their manufacturing, enable semi-transparency, and light weight. In this work, we designed and fabricated perovskite solar cells with efficiency as high as 10.7%, and investigated the transparency-efficiency tradeoff in these devices.



▲ Figure 1: a) Schematic illustration of the designed perovskite solar cell. b) Top-view photo of an example fabricated solar cell. c) Example I-V characteristic of a fabricated solar cell with 10.7% efficiency.

Synthesis of Mixed Dimensional Perovskite Heterostructures

M. Chattoraj, S. Saris, E. K. Price, W. A. Tisdale

Continued advancements in the synthesis and application of nanomaterials dictate the need for well-developed analysis frameworks that fully capture the fundamentals behind their interactions. Förster theory accurately describes the transfer of excitons between molecules. However, this framework has repeatedly failed to quantitatively predict energy transfer rates between semiconducting nanomaterials, particularly in heterostructure systems that combine nanomaterials of different composition and dimensionality. The shortcomings of Förster theory are exacerbated in the case of lead halide perovskites, offering an optimal

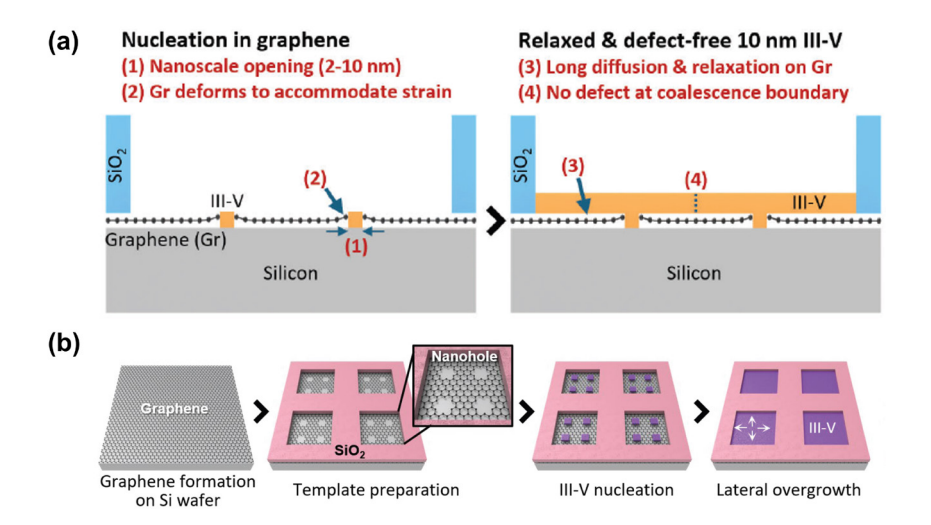
platform for pushing past the limits of current energy transfer models. Here, we synthesize mixed dimensional perovskite heterostructures and set the stage for studying energy transfer in these systems using time resolved photoluminescence spectroscopy. We focus on heterostructures combining spheroidal CsPbBr3 quantum dots and two dimensional hybrid organic inorganic perovskite crystals, and aim to contribute to a deeper, quantitative understanding of energy transfer mechanisms in novel nanomaterials, which will inform the design of optoelectronic devices with nanomaterial interfaces.

Selective Area Epitaxy of Defect-free III-V Layers on Silicon via Graphene Nanoholes

N. M. Han, K. Lu, D. A. Kwon, J. Kim Sponsorship: DARPA M-STUDIO (HR001124S0019--FP-006)

The integration of III-V semiconductors on silicon is a boon for electronic and optoelectronic devices due to their high electron mobility and direct bandgaps. However, their large lattice mismatch often leads to high dislocation densities, severely impacting performance. Standard techniques like graded-buffer layers, epitaxial lateral overgrowth, and aspect ratio trapping have shown limited success, and pseudomorphic growth, while dislocation-free, can result in interface roughening and mobility loss in thin channels.

To address this, I developed a graphene-assisted epitaxy method to achieve dislocation-free III-V growth on silicon. Here, graphene is grown on the silicon surface with nanoholes that expose nucleation sites for III-V growth, while lateral overgrowth over the graphene-covered surface facilitates strain relaxation. This scalable, CMOS-compatible method enables high-quality III-V material integration on silicon for next-generation electronic and optoelectronic devices.



▲ Figure 1: Schematic of the (a) mechanisms and (b) process of graphene-assisted epitaxy to achieve defect-free III-V films on Silicon.

184

Densification of Vertically Aligned Boron Nitride Nanotubes via Biaxial Mechanical Compression

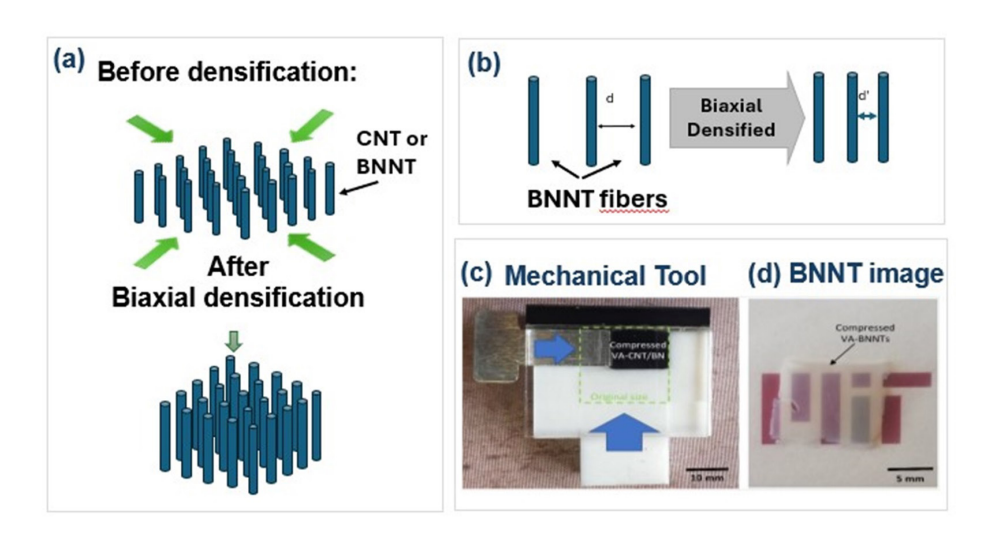
S. Sharma, A. R. C. Neto, M. Rogers, L. Acauan, B. L. Wardle Sponsorship: NECST consortium

Boron nitride nanotubes (BNNTs) have garnered significant interest due to their one-dimensional structure, piezoelectric properties, superior chemical, and thermal stabilities. All these attributes make BNNTs highly versatile, supporting diverse applications ranging from structural reinforcement to energy storage [1]. However, the synthesized vertically aligned BNNTs have a low volume fraction of around ~1% [2], which can limit their use in applications like piezoelectric sensor/actuators [3]. In this work, we demonstrate a biaxial densification technique, previously applied to VA-CNTs [4], that increases the volume fraction of VA-BNNTs by a factor of four.

In this study, the BNNTs were synthesized by coating VA-CNTs with hexagonal boron nitride (VA-CNT/BN), followed by thermal oxidation to remove

the CNT scaffold [2]. The work compares three different routes for densifying VA-BNNTs: (1) biaxially densifying the VA-BNNTs directly; (2) biaxially densifying the VA-CNT/BN and posteriorly removing the VA-CNT scaffold; and (3) coating the pre-densified VA-CNTs with BN and subsequently removing the VA-CNT scaffold.

Our results show that method (3) produces a poor BN coating on the CNTs, while method (1) leads to a nonuniformly densified VA-BNNT structure that breaks easily when the densifying forces are released. In contrast, method (2) achieves a uniformly densified VA-BNNT structure after removal of the CNT scaffold. These findings suggest that further densification is feasible with this approach, enabling applications that require a high-volume fraction of BNNTs.



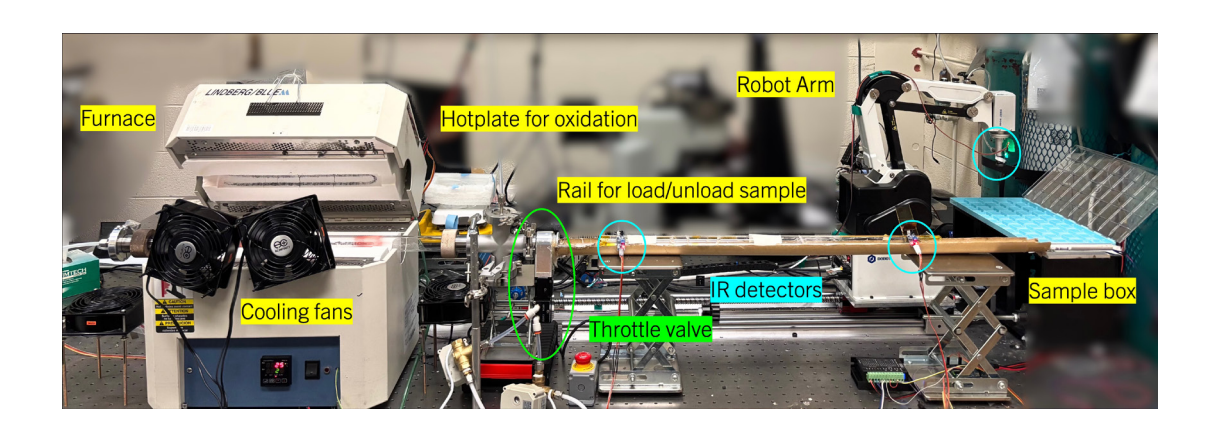
▲ Figure 1: (a,b) Schematic of the biaxial mechanical densification process, (c) Mechanical tool used for compressing VA-CNT compressed, and (d) image of bi-axially compressed VA-BNNT after CNT removal.

Artificial Intelligence-Assisted Synthesis and Integration Optimization of 2D Materials

Z. Wang, S. He, A. Lu, J. Wang, J. Kong Sponsorship: The Semiconductor Research Corporation Center 7 in JUMP 2.0 $\,$

Chemical vapor deposition (CVD) has developed to be the most efficient and scalable synthesis method for various two-dimensional materials, which hold great promise for advancing the semiconductor technology. However, manual process execution in the CVD synthesis is both time-consuming and labor-intensive. Here, we propose an autonomous CVD system that integrates AI and automation for increased efficiency and high-throughput. To demonstrate this idea, we have built an autonomous graphene CVD system, incorporating stationary robots and automated synthesis. This system can control all the growth parameters including

temperature, gas flow, pressure, through input parameters, and handle samples with a robot arm. This autonomous CVD system has the capacity to process up to 50 sets of different growth parameters and synthesize continuously without any manual operation. We have tested the stability of this system with 50 graphene growths within a time period of two weeks, which shows high reproducibility and stability. Enabled by this fully automated system, we plan to incorporate AI into recipe optimization and explore different parameters space of graphene synthesis.



▲ Figure 1: Photograph of the autonomous CVD system for graphene, consists of automated furnace (on the left) and robotic arm for sample handling (on the right).

In-situ Microscopy / Dynamic Processes

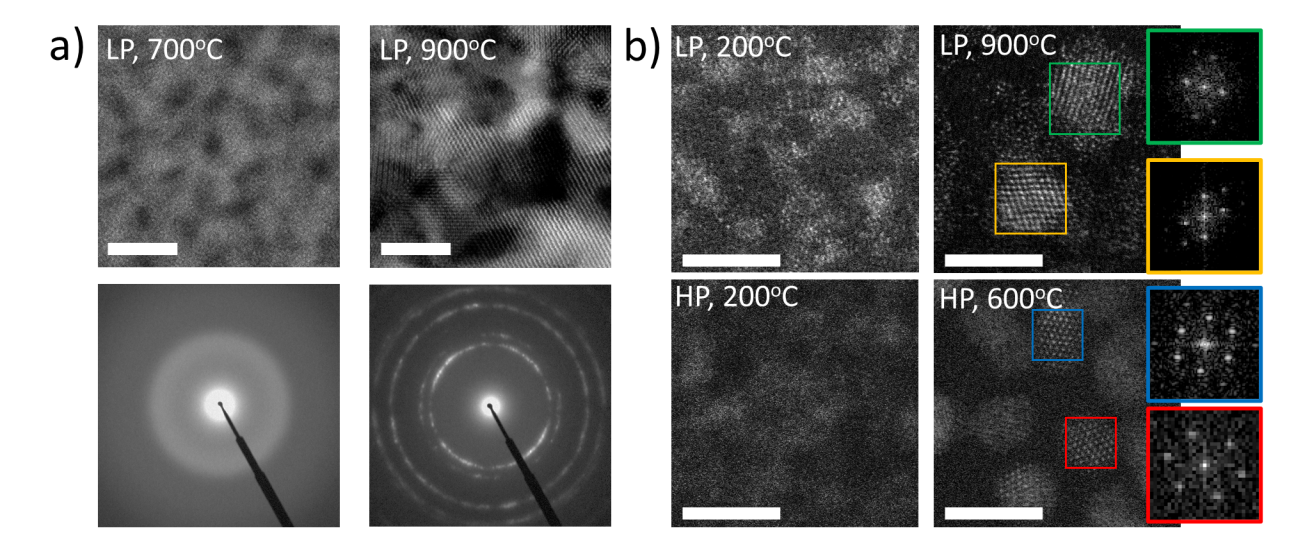
| In-situ Oxidation in Environmental Transmission Electron Microscopy for Engineering | |
|--|-----|
| Dielectric/2D Semiconductor Interfaces | 188 |
| Anisotropic 2D van der Waals Magnets Hosting 1D Spin Chains | 189 |
| Observing Nanoscale Transformations between Quicklime and Slaked Lime in an | |
| Environmental Transmission Electron Microscope | 190 |
| Revealing Metal Redox Pathways up to Ambient Pressure via in-situ Transmission Electron Microscopy | 191 |

In-situ Oxidation in Environmental Transmission Electron Microscopy for Engineering Dielectric/2D Semiconductor Interfaces

R. Kothari, Z. Liu, H. Wu, P. J. Knight, P. Miller, R. Jaramillo, F. M. Ross

Two-dimensional (2D) semiconductors have emerged as an exciting and promising opportunity to expand electronics beyond the capabilities of silicon. They offer high mobility in the ultrathin limit and can be used as components in sensors or flexible electronics. One key challenge is the integration of 2D semiconductors, such as molybdenum disulfide (MoS₂), with the high-performance dielectrics used to separate the semiconducting channel from the metal gate in field-effect transistors. As a strategy to create high-quality semiconductor/ dielectric interfaces, we use crystalline, epitaxial hafnium oxide (HfO2) as a seed layer on which we deposit hafnium-based oxides by atomic layer deposition (ALD), a scaled technology in silicon electronics. To optimize this strategy, we need to understand both (1) the initial oxidation of Hf metal and (2) the crystallization of Hf-based ALD oxides. We use the Hitachi HF5000 Environmental S/TEM at Characterization.

nano (ETEM) to perform these experiments. Figure 1a shows the crystallization of a sputtered Hf film on the thin silicon nitride (SiNx) membrane of an ETEM chip in response to temperature. Future work will probe this transformation for Hf on MoS₂. Figure 1b shows the crystallization of Hf-zirconium oxide (HZO) from an initially amorphous state. The HZO de-wets from the SiNx membrane and crystallizes in response to heating. Our past experiments could be carried out only at low oxygen pressures (10-7 atm), but recent improvements to the ETEM allow up to atmospheric pressures to be maintained during imaging, where similar HZO films were observed to crystallize at lower temperatures. We are also exploring the use of a TiN base layer to improve ALD adhesion and better replicate other studies of HZO's ferroelectric properties and structural modifications during switching.



 \blacktriangle Figure 1: (a) Crystallization of HfO $_2$ formed from 15-nm sputtered Hf metal at low O $_2$ pressure (LP, 10⁻⁷ atm). Top-HAADF STEM, bottom-TEM diffraction; (b) HAADF STEM of ALD HZO at LP and HP O $_2$ (1 atm) before and after crystallization in response to heating. Insets show FFTs of corresponding regions, consistent with monoclinic and orthorhombic phases. All scale bars are 5 nm.

FURTHER READING

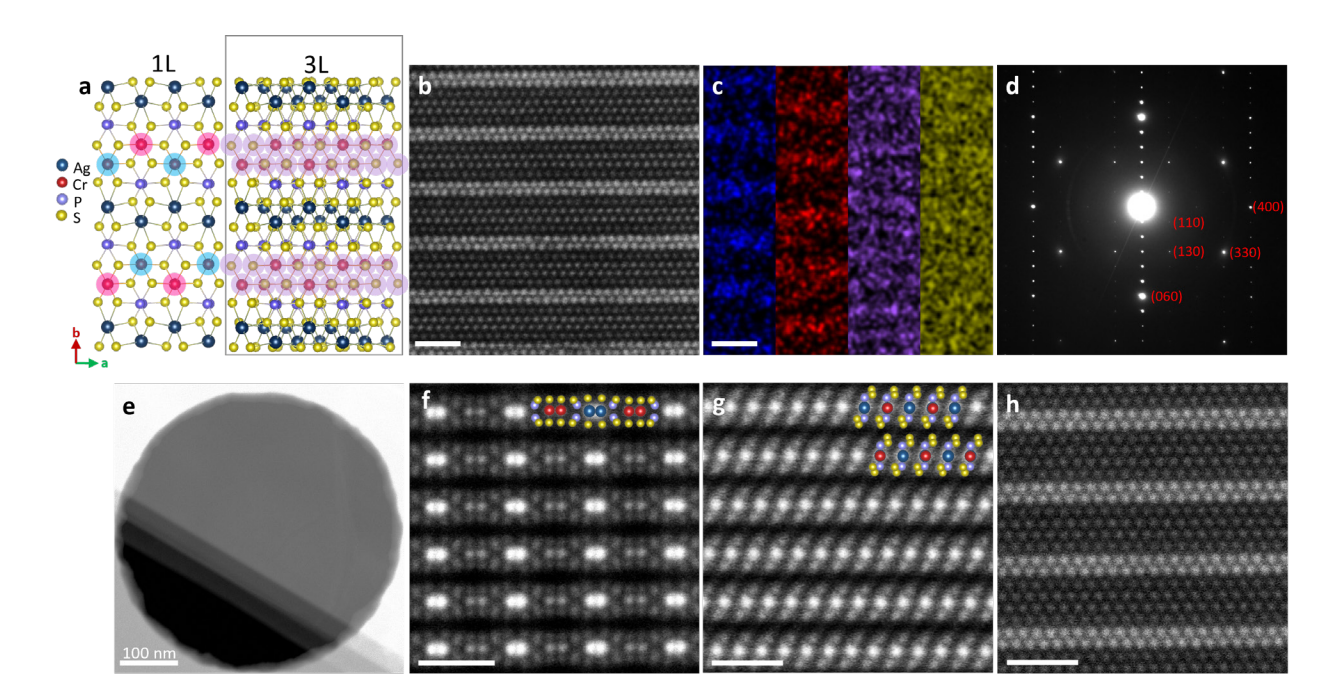
- A. Pannone, A. Raj, H. Ravichandran, et al., "Robust Chemical Analysis with Graphene Chemosensors and Machine Learning," Nature, vol. 634, pp. 572–578, 2024. DOI.org/10.1038/s41586-024-08003-w
- A. K. Katiyar, A. T. Hoang, D. Xu, et al., "2D Materials in Flexible Electronics: Recent Advances and Future Prospectives," Chemical Reviews, vol. 124, pp. 318–419, 2024. DOI.org/10.1021/acs.chemrev.3c00302
- Z. Liu, Q. Mao, V. Kamboj, et al., "Epitaxial Formation of Ultrathin HfO₂ on Graphene by Sequential Oxidation," arXiv 2504.11693, 2025. DOI. org/10.48550/arXiv.2504.11693

Anisotropic 2D van der Waals Magnets Hosting 1D Spin Chains

E. Park, J. P. Philbin, H. Chi, J. J. Sanchez, C. Occhialini, G. Varnavides, J. B. Curtis, Z. Song, J. Klein, J. D. Thomsen, M. G. Han, A. C. Foucher, K. Mosina, D. Kumawat, N. Gonzalez-Yepez, Y. Zhu, Z. Sofer, R. Comin, J. S. Moodera, P. Narang, F. M. Ross Sponsorship: MathWorks, Department of Energy BES QIS Program, ARO Multidisciplinary University Research Initiative

The exploration of one-dimensional (1D) magnetism, frequently portrayed as spin chains, constitutes an actively pursued research field that illuminates fundamental principles in many-body problems and applications in magnonics and spintronics. The inherent reduction in dimensionality often leads to robust spin fluctuations, impacting magnetic ordering and resulting in novel magnetic phenomena. Here, we explore structural, magnetic, and optical properties of highly anisotropic two-dimensional (2D) van der Waals antiferromagnets that uniquely host spin chains. First-princi-

ples calculations reveal that the weakest interaction is interchain, essentially leading to 1D magnetic behavior in each layer. With the additional degree of freedom arising from its anisotropic structure, we engineer the structure by alloying, varying the 1D spin chain length using electron beam irradiation, or twisting for localized patterning, and calculate spin textures, predicting robust stability of the antiferromagnetic ordering. Comparing them with other spin chain magnets, we anticipate these materials to bring fresh perspectives on harvesting low-dimensional magnetism.



 \blacktriangle Figure 1: STEM structural characterization of 2D van der Waals magnets with 1D magnetic chains.a) Schematic of structure of AgCrP₂S₆ shown for monolayer (1L) and tri-layer (3L). Zig-zag chains of Cr atoms are highlighted in blue (spin up) and pink (spin down) for 1L and purple for 3L. b) Plan view STEM image of AgCrP2S6. c) EDS map of AgCrP₂S₆ with Ag, Cr, P, and S indicated in blue, red, purple, and yellow, respectively. d) Diffraction pattern corresponding to area shown in b. e) Low magnification STEM image showing different layer numbers of flake. f-g) STEM images of the cross sections in crystallographic a and b directions, respectively, with atomic structures overlaid. h) Plan view STEM image of AgVP₂S₆. Scale bars in b, c, f-h, 1 nm.

FURTHER READING

E. Park et al., "Anisotropic 2D van der Waals Magnets Hosting 1D Spin Chains," Advanced Materials, vol. 36, p. 2401534, 2024.

Observing Nanoscale Transformations between Quicklime and Slaked Lime in an Environmental Transmission Electron Microscope

E. Vaserman, H. Wu, F. M. Ross, A. Masic

Quicklime (CaO) and slaked lime (Ca(OH)₂) are among the oldest material systems used by humans for construction, with a history spanning over 9,000 years. Today, the lime cycle (transformation between calcium carbonate (CaCO₃), CaO, and Ca(OH)₂) plays vital roles in modern construction sustainability, carbon sequestration, and various other industrial applications. Quicklime reacts exothermically with water to form slaked lime, which can reversibly decompose back to CaO and water upon heating. This CaO-Ca(OH)₂ cycle is fundamental to thermochemical energy storage technology and strongly influences the mechanical strength, durability, and carbonation behavior of ordinary Portland cement (OPC) and lime-based mortars and concretes. Although lime hydration and dehydration have been studied for centuries, the nanoscale mechanisms underlying these transformations remain poorly understood. In particular, the effect of environmental factors such as humidity and temperature on the hydration kinetics and the resulting morphology, microstructure, and porosity of slaked lime is not fully characterized.

In this work, we study the transformation between quicklime and slaked lime at the nanoscale using Characterization.nano's Hitachi HF5000-IS Environmental Transmission Electron Microscope (ETEM). In addition to conventional transmitted electron signals, the ETEM is equipped with a secondary electron (SE) detector, enabling simultaneous SE imaging of surface morphology evolution during the lime reactions. We observe the transformation of platelike Ca(OH), into stacked CaO nanoparticles in vacuum at different temperatures (Figure 1a), followed by their "fusion" back into Ca(OH)2 under varying water vapor pressures (Figure 1b). Interestingly, during dehydration, some Ca(OH)₂ nanoplates appear to expand, possibly driven by internal steam pressure accumulation. Our atomic-resolution SE results also reveal the formation of edge dislocations in newly formed CaO (Figure 1c). These new insights are important for understanding the long-term durability of historical lime-based materials and modern OPC-based cements and will guide the design of next-generation cementitious systems.

a Dehydration of slaked lime in vacuum C Atomic-resolution SE imaging of quicklime b Hydration of quicklime in water vapor 0 min 60 min 20 nm

 \blacktriangle Figure 1: SE images showing morphological evolution of lime during (a) Ca(OH)₂ dehydration in vacuum and (b) rehydration of the resulting CaO under water vapor. (c) Atomic-resolution SE image of CaO acquired in vacuum at 650 °C.

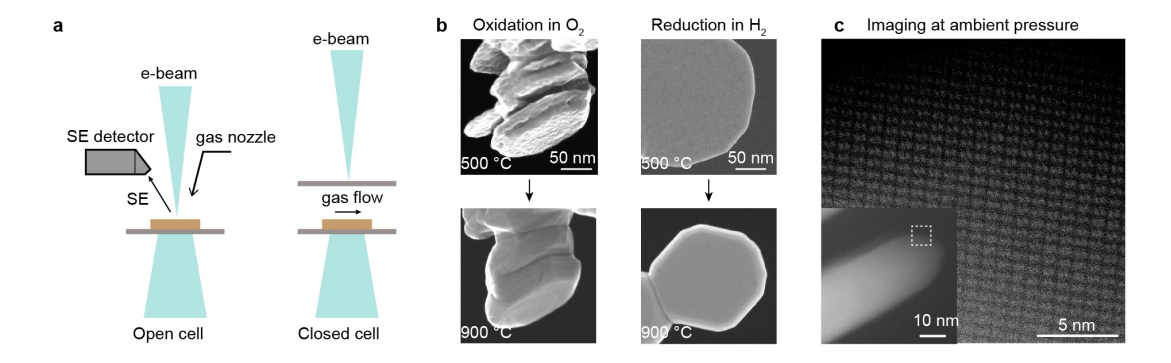
Revealing Metal Redox Pathways up to Ambient Pressure via in-situ Transmission Electron Microscopy

H. Wu, F. M. Ross

Sponsorship: Center for Entrepreneurship Development and Incubation, Seagate

Metal redox reactions are ubiquitous in nature (e.g., geological processes) and industrial applications. Understanding how materials evolve in morphology and structure at the nanoscale during such reactions in gaseous environments is critical for advancing catalysis, energy storage, and semiconductor technologies. Advances in transmission electron microscopy (TEM), microfabrication, and microelectromechanical systems have enabled the direct exposure of samples to a controlled gas environment at elevated temperatures within the microscope column. Gas can be introduced at low pressures (up to tens of millibars) using differential pumping or confined between two thin silicon nitride membranes in a closed-cell specimen holder (up to ambient pressure). Both approaches have proven effective in revealing atomistic mechanisms governing metal redox reactions. However, the effects of gas pressure on kinetic phase transformation pathways, particularly on transient surface morphological evolution during redox reactions, remain poorly understood.

In this project, we investigate metal redox reactions in various gaseous environments across different pressures using Characterization.nano's Hitachi HF5000-IS environmental TEM (ETEM) with a secondary electron (SE) detector. We visualize redox reactions occurring in a range of metal and alloys (Fe-, Zn- and Ni-based alloys) under gases, including H2, O2, methanol, and water vapor, up to ambient pressure. These experiments demonstrate that atomic resolution can be obtained under ambient pressure conditions and enable us to identify several transient phase transformation pathways during the early stages of oxidation and reduction of metals. The simultaneous SE imaging enabled us to understand the surface morphological changes taking place during these reactions, including the removal of surface ligand layers and the development of surface faceting. We anticipate that these advances will broaden the application of in-situ gas phase TEM for studying dynamic material process.



▲ Figure 1: (a) Schematics of setups for gas-phase TEM imaging. (b) SE images showing the morphological evolution of magnetite oxidation in O_2 (left) and hematite reduction in H_2 (right). (c) Atomic-resolution image of magnetite in O_2 at ambient pressure.

Immersive Simulation, Design, and Visualization

| Motion | Capture within | Space+Dance+Dig | tal | 193 |
|--------|----------------|-----------------|-----|-----|
| | | | | |

Motion Capture within Space+Dance+Digital

A. Akinleye Sponsorship: National Endowment for the Arts

Space+Dance+Digital (S+D2) is an immersive augmented reality (AR) dance-research platform utilizing motion capture technology in MIT.nano Immersion Lab. At the core of the project is a novel use of motion capture that uses the captured dataset to manipulate an aesthetic immersive four-dimensional (4D) space, accessed via AR.

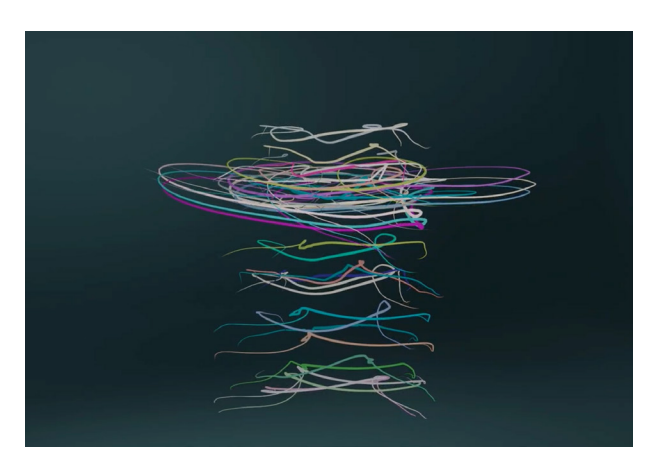
Position data from a minimal set of specific anatomical markers is used to capture spatial-temporal movement trajectories and relational patterns intentionally generated across the dancer's moving body. During motion capture, the dancer performs choreographed sequences to manipulate how the individual tracking markers interact and combine in the resulting dataset.

The data, visualized as trails of color, is overlaid and move through the digital space around the AR user, slowing dance's ephemerality into a lingering archive of path-ways and color. The AR user can move into the assemblage of trails, effectively moving with and within the unseen form of the dancer.

The AR user can generate temporary motion trails using hand tracking, enabling real-time responses to the choreography. This interaction invites users

to co-create the spatiality around them through an embodied dialogue with the digital environment. A networked, two-user application allows participants in different geographic locations to enter the AR choreography simultaneously. Each can see the other's hand trails in re-al-time. By engaging with the spatial logic created by the choreography, users can dance together, co-creating a spatial experience despite their separate physical circumstances. S+D2 is being further developed for occupational therapy and somatic-reconnection-focused applications in hospitals and prisons.

S+D2 approach utilizes motion capture as a tool for spatial-temporal co-creation, addressing the moving body as an assembled environment that seamlessly extends into larger assemblages. The project demonstrates how motion capture, when imagined as generative rather than representative, can support immersive, embodied intra-action. We continue to address our primary research questions: What does it mean for dance to take advantage of the physical boundary crossing of digital space? Can dance+digital contribute to new ways of artistic and political togetherness?



▲ Figure 1: Motion capture data rendered as 2D spatial trajectories. Each line represents path of specific anatomical marker over time, abstracting dancer's form and preserving dynamic qualities of movement.



▲ Figure 2: View from within AR experience, showing choreographic motion trails overlaid on user's physical environment. User's hand-tracked responses generate additional trails, enabling real-time interaction and spatial co-creation across locations.

FURTHER READING

- K. Barad, "Meeting the Universe Halfway: Quantum Physics and the Entanglement of Matter and Meaning," Durham, NC: Duke Univ. Press, 2007.
- T. Ingold, "The Perception of the Environment: Essays on Livelihood, Dwelling and Skill," London: Routledge, 2000.

Research Centers

| Center for Integrated Circuits and Systems | 195 |
|--|-----|
| MIT/MTL Center for Graphene Devices and 2-D Systems | 196 |
| The MIT Medical Electronic Device Realization Center | 197 |
| MIT Program on Advanced Display Technology | 198 |
| The MIT AI Hardware Program | 199 |
| Waves, Bits & Molecules Laboratory | 200 |

Center for Integrated Circuits and Systems

Professor Ruonan Han, Director

The Center for Integrated Circuits and Systems (CICS) at MIT, established in 1998, is an industrial consortium created to promote new research initiatives in circuits and systems design, as well as to promote a tighter technical relationship between MIT's research and relevant industry. Eight faculty members participate in the CICS: Director Ruonan Han, Hae-Seung (Harry) Lee, Anantha Chandrakasan, Song Han, David Perreault, Negar Reiskarimian, Charles Sodini, and Vivienne Sze.

CICS investigates circuits and systems for a wide range of applications, including artificial intelligence, wireless/wireline communication, sensing, security, biomedicine, power conversion, quantum information, among others.

We strongly believe in the synergistic relationship between industry and academia, especially in practical research areas of integrated circuits and systems. CICS is designed to be the conduit for such synergy.

CICS's research portfolio includes all research projects that the eight participating faculty members conduct, regardless of source(s) of funding, with a few exceptions.

Technical interaction between industry and MIT

researchers occurs on both a broad and individual level. Since its inception, CICS recognized the importance of holding technical meetings to facilitate communication among MIT faculty, students, and industry. We hold two full-day technical meetings per year open to CICS faculty, students, and representatives from participating companies. Throughout each meeting, faculty and students present their research, often presenting early concepts, designs, and results that have not been published yet. The participants then offer valuable technical feedback, as well as suggestions for future research. The meeting also serves as a valuable networking event for both participants and students. Closer technical interaction between MIT researchers and industry takes place through the projects of particular interest to participating companies. Companies may invite students to give onsite presentations, or they may offer students summer employment. Additionally, companies may send visiting scholars to MIT or create a separate research contract for more focused research for their particular interest. The result is truly synergistic, and it will have a lasting impact on the field of integrated circuits and systems.

MIT/MTL Center for Graphene Devices and 2-D Systems

Professor Tomás Palacios, Director

The MIT/MTL Center for Graphene Devices and 2-D Systems (MIT-CG) brings together MIT researchers and industrial partners to advance the science and engineering of graphene and other two-dimensional (2-D) materials.

Two-dimensional materials are revolutionizing electronics, mechanical and chemical engineering, physics and many other disciplines thanks to their extreme properties. These materials are the lightest, thinnest, strongest materials we know of. At the same time that they have extremely rich electronic and chemical properties. MIT has been leading research on the science and engineering of 2-D materials for more than 40 years. Since 2011, the MIT/MTL Center for Graphene Devices and 2-D Systems (MIT-CG) has played a key role in coordinating most of the work going on at MIT on these new materials, and in bringing together MIT faculty and students, with leading companies and government agencies interested in taking these materials from a science wonder to an engineering reality.

Specifically, the Center explores advanced

technologies and strategies that enable 2-D materials, devices, and systems to provide discriminating or breakthrough capabilities for a variety of system applications ranging from energy generation/storage and smart fabrics and materials to optoelectronics, RF communications, and sensing. In all these applications, the MIT-CG supports the development of the science, technology, tools, and analysis for the creation of a vision for the future of new systems enabled by 2-D materials.

Some of the many benefits of the Center's membership include complimentary attendance to meetings, industry focus days, and live webcasting of seminars related to the main research directions of the Center. Our industrial members also gain access to a resume book that connects students with potential employers, as well as access to timely white papers on key issues regarding the challenges and opportunities of these new technologies. There are also numerous opportunities to collaborate with leading researchers on projects that address some of today's challenges for these materials, devices, and systems.

The MIT Medical Electronic Device Realization Center

Professor Charles Sodini, Co-Director Professor Thomas Heldt, Co-Director

The vision of the MIT Medical Electronic Device Realization Center (MEDRC) is to revolutionize medical diagnostics and treatments by bringing health care directly to the individual and to create enabling technology for the future information-driven healthcare system. This vision will, in turn, transform the medical electronic device industry. Specific areas that show promise are wearable or minimally invasive monitoring devices, medical imaging, portable laboratory instrumentation, and the data communication and associated analysis and reasoning algorithms.

Rapid innovation in miniaturization, mobility, and connectivity will revolutionize medical diagnostics and treatments, bringing health care directly to the individual. Continuous monitoring of physiological markers will place capability for the early detection and prevention of disease in the hands of the consumer, shifting to a paradigm of maintaining wellness rather than treating sickness. Just as the personal computer revolution has brought computation to the individual, this revolution in personalized medicine will bring the hospital lab and the physician to the home and to the site of emergency situations. From at-home cholesterol monitors that can adjust treatment plans, to cell phoneenabled blood labs, these system solutions containing state-of-the-art sensors, electronics, and computation will radically change our approach to health care. This new generation of medical systems holds the promise of delivering better quality health care while reducing medical costs.

The revolution in personalized medicine is rooted in fundamental research in microelectronics from materials to sensors, to circuit and system design. This approach has already fueled the semiconductor industry to transform society over the last four decades. It provided the key technologies to continuously increase performance while constantly lowering cost for computation, communication, and consumer electronics. The processing power of current smart phones, for example, allows for sophisticated signal processing to extract information from this sensor data. Data analytics can combine this information with other patient data and medical records to produce actionable information customized to the patient's needs. The aging population, soaring healthcare costs, and the need for improved healthcare in developing nations are the driving force for the next semiconductor industry's societal transformation, Medical Electronic Devices.

The successful realization of such a vision also demands innovations in the usability and productivity of medical devices, and new technologies and approaches to manufacturing devices. Information technology is a critical component of the intelligence that will enhance the usability of devices; real-time image and signal processing combined with intelligent computer systems will enhance the practitioners' diagnostic intuition. Our research is at the intersection of Design, Healthcare, and Information Technology innovation. We perform fundamental and applied research in the design, manufacture, and use of medical electronic devices and create enabling technology for the future information-driven healthcare system.

The MEDRC has established a partnership between microelectronics companies, medical device companies, medical professionals at Boston-area hospitals, and MIT to collaboratively achieve needed radical changes in medical device architectures, enabling continuous monitoring of physiological parameters such as cardiac vital signs, intracranial pressure, and cerebral blood flow velocity. A visiting scientist from a project's sponsoring company is present at MIT. Ultimately this individual is the champion that helps translate the technology back to the company for commercialization and provide the industrial viewpoint in the realization of the technology. MEDRC projects have the advantage of insight from the technology arena, the medical arena, and the business arena, thus significantly increasing the chances that the devices will fulfill a real and broad healthcare need as well as be profitable for companies supplying the solutions. With a new trend toward increased healthcare quality, disease prevention, and cost-effectiveness, such a comprehensive perspective is crucial.

In addition to the strong relationship with MTL, MEDRC is associated with MIT's Institute for Medical Engineering and Science (IMES) that is charged to serve as a focal point for researchers with medical interest across MIT. MEDRC has been able to create strong connections with the medical device and microelectronics industry, venture-funded startups, and the Boston medical community. With the support of MTL and IMES, MEDRC serves as the catalyst for the deployment of medical devices that will reduce the cost of healthcare in both the developed and developing world.

MIT Program on Advanced Display Technology

Professor Jeehwan Kim, Director

The MIT Program on Advanced Display Technology, launched under the Microsystems Technology Laboratories (MTL), is an interdisciplinary initiative that brings together MIT faculty, students, and industry partners to advance the frontiers of next-generation display systems. The program was established with the goal of fostering deep collaboration between academic research and industrial innovation in the rapidly evolving display field.

A core focus of the program is on future-oriented display technologies, particularly those that will define the next generation of augmented and virtual reality (AR/VR) systems. The program brings together researchers who are working across the full stack of display innovation from backplanes and light-emitting devices to color converters and advanced optics. By addressing each of these critical components, the program aims to enable compact, efficient, and high-resolution displays tailored for emerging applications.

The program began in April 2024 with an internal workshop at MIT, which served as a kick-off for building a collaborative research community around cuttingedge display technology. Since then, the program

has organized two major workshops that brought together a diverse group of participants, including major technology companies including Samsung, Meta, Apple, and Google and emerging startups. These workshops created a platform for exchanging early-stage ideas, sharing technical progress, and exploring new avenues of collaboration.

A key focus of the program is to facilitate meaningful interactions between MIT researchers and industry stakeholders. Through presentations, discussions, and networking opportunities, the workshops have enabled companies to learn about ongoing research at MIT and engage with students and faculty working at the forefront of display innovation. In several cases, these interactions have led to follow-up meetings, exploratory collaborations, and sponsored research engagements.

By connecting MIT's research strengths with industry's technological needs and long-term vision, the MIT Program on Advanced Display Technology continues to grow as a hub for innovation, collaboration, and the future of display science and engineering.

The MIT AI Hardware Program

Professor Jesús del Alamo, Co-Director Professor Aude Oliva, Co-Director

The MIT AI Hardware Program is an academia-industry initiative advancing energy-efficient computing systems for cloud and edge AI. Co-led by Jesús del Alamo and Aude Oliva, and chaired by Anantha Chandrakasan, the program connects MIT researchers with industry partners to develop AI hardware innovations across the entire computing stack—from materials and circuits to algorithms and software.

The program encompasses a wide range of topics including analog neural networks, monolithic-3D AI systems, neuromorphic computing, secure edge AI, photonic neural networks, and quantum AI. Leveraging MIT.nano, the program supports cutting-edge, use-inspired research and collaborative projects on topics such as energy-efficient analog neural accelerators, inmemory computing, and TinyML for mobile devices.

The MIT AI Hardware Program strongly values synergistic academia-industry engagement. Technical interaction is facilitated through regular in-person and virtual meetings, including a biannual Spring Symposium and Fall Research Update. Corporate members receive access to a private portal with research updates, papers, and curated seminars. Additional benefits include event invitations, recruiting opportunities, and eligibility to send visiting scientists to MIT.

Through this partnership model, the program drives impactful innovation in AI hardware and fosters meaningful collaboration between MIT researchers and leading technology companies.

Waves, Bits & Molecules Laboratory

Ahmad Bahai, Co-Director Tomás Palacios, Co-Director Alex Shalek, Co-Director

The Waves, Bits & Molecules Laboratory is envisioned as a world-class Health Science & Semiconductor innovation space and multidisciplinary program leveraging innovation in semiconductor technology, machine learning, biochemistry, and material science towards a future of true personalized healthcare. It provides a flexible, open-access prototyping environment where researchers and students from diverse disciplines can rapidly iterate hardware and systems spanning biosensing, signal processing, microfluidics, and edge AI.

The lab supports joint projects that blend molecular systems with digital and analog circuitry-

fostering convergence at the intersection of technology, life science, and computation. To support this mission, the Waves, Bits & Molecules Laboratory has begun acquiring specialized equipment for optoacoustic imaging, magnetic sensing, microfluidic platforms, and physiological phantoms. As an incubator for early-stage translational research, the Waves, Bits & Molecules Laboratory advances MTL's mission of integrating waves (RF and optics), bits (information processing), and molecules (biological and chemical interfaces) to address critical health and technology challenges.

Faculty Profiles

| Anuradha M. Agarwal | 202 |
|--------------------------------|-----|
| Marc A. Baldo | 203 |
| George Barbastathis | 204 |
| Karl K. Berggren | 205 |
| Duane S. Boning | 206 |
| Svetlana V. Boriskina | 207 |
| Edward S. Boyden | 208 |
| Vladimir Bulović | 209 |
| Joseph Casamento | 210 |
| Anantha P. Chandrakasan | 211 |
| Yufeng (Kevin) Chen | 212 |
| Samantha Coday | 213 |
| Riccardo Comin | 214 |
| Jesús A. del Alamo | 215 |
| Catherine L. Drennan | 216 |
| Jongyoon Han | 217 |
| Ruonan Han | 218 |
| Song Han | 219 |
| Juejun (JJ) Hu | 220 |
| Qing Hu | 221 |
| Rafael Jaramillo | 222 |
| Long Ju | 223 |
| Philip "Donnie" Keathley | 224 |
| Jeehwan Kim | 225 |
| Jeffrey H. Lang | 226 |
| Hae-Seung Lee | 227 |
| Mingda Li | 228 |
| Luqiao Liu | 229 |
| Scott R. Manalis | 230 |
| Farnaz Niroui | 231 |
| Jelena Notaros | 232 |
| William D. Oliver | 233 |
| Tomás Palacios | 234 |
| Carlos M. Portela | 235 |
| Negar Reiskarimian | 236 |
| Charles G. Sodini | 237 |
| Vivienne Sze | 238 |
| Frances M. Ross | 239 |
| Luis Fernando Velásquez-García | 240 |

Anuradha M. Agarwal

Principal Research Scientist Materials Research Laboratory Leader

FUTUR-IC: Sustainable Microchip Manufacturing

LEAP: Lab for Education and Application Prototypes Electronic Photonic Packaging/ Heterogenous Integration

Sustainable materials and device designs for microchip manufacturing and use; Planar, integrated, Si-CMOS-compatible microphotonics platform for on-chip MIR hyperspectral imaging and chem-bio sensing applications; radiation effects on silicon microphotonics; non-linear materials and devices; aerosol detection; mid-infrared detectors, electronic-photonic packaging; heterogenous integration.

Rm. 13-4126 | 617-253-5302 | anu @ mit.edu

VISITORS/SUMMER STUDENTS/UROPS

Christian Duessel, Department of Materials Science and Engineering UROP Kajari Dutta, Visiting Faculty, Amity Institute of Applied Sciences, Kolkata, India Neal Haldar, DMSE MICRO UROP, University of California Berkeley

GRADUATE STUDENTS

Katherine Stoll, DMSE Drew Weninger, DMSE

SELECTED PUBLICATIONS

D. Weninger, S. Serna, A. Jain, L. Kimerling, and A. Agarwal, "High Density Vertical Optical Interconnects for Passive Assembly," *Optics Express*, Vol. 31, No. 2, Pages 2816-2832, Optica Publishing Group, 2023.

L. Neim, A. Yovanovich, J. Bartholomew, V. Deenadayalan, M. Ciminelli, T. Palone, M. van Niekerk, M. Song, A. Nauriyal, J. Notaros, S. S. Otálvaro, J. Cardenas, T. Brown, A. M. Agarwal, S. Saini, and S. F. Preble, "Hands-On Photonic Education Kits: Empowering the Integrated Photonics Workforce Through Practical Training," *Applied Optics* Vol. 62, Issue 31, Pages H24-H32, 2023.

M. Kang, B.-U. Sohn, Q. Du, D. Ma, R. Pujari, L. Sisken, C. Blanco, C. Goncalves, C. Arias, A. Zachariou, A. Yadav, P. E. Lynch, J. Lee, S. Novak, C. M Schwarz, I. Luzinov, J. Hu, A. M. Agarwal, D. T. H. Tan, and K. A. Richardson, "Self-healing Mechanisms for Ge–Sb–S Chalcogenide Glasses Upon Gamma Irradiation," *MRS Bulletin*, Pages 1-9, Springer International Publishing, 2024.

L. Ranno, J. X. B. Sia, C. Popescu, D. Weninger, S. Serna, S. Yu, L. C. Kimerling, A. Agarwal, T. Gu, and J. Hu, "Highly Efficient Fiber to Si Waveguide Free-form Coupler for Foundry-scale Silicon Photonics," *Photonics Research*, Vol. 12, Issue 5, Pages 1055-1066, Optica Publishing Group, 2024.

M. Kang, R. Sharma, C. Blanco, D. Wiedeman, Q. Altemose, P. E. Lynch, G. B. J. Sop Tagne, Y. Zhang, M. Y. Shalaginov, C.-C. Popescu, B. M. Triplett, C. Rivero-Baleine, C. M. Schwarz, A. M. Agarwal, T. Gu, J. Hu, and K. A. Richardson, "Solutionderived Ge-Sb-Se-Te phase-change chalcogenide films," *Scientific Reports*, Vol. 14, Issue 1, Pages 18151, 2024, Nature Publishing Group.

Marc A. Baldo

Director, Research Laboratory of Electronics
Dugald C. Jackson Professor
Department of Electrical Engineering & Computer Science

Spin and Excitonic Electronics Group: organic & molecular electronics, LEDs and solar cells, spintronics.

36-419 | 617-452-1532 | baldo @ mit . edu

POSTDOCTORAL ASSOCIATES

Tomi Baikie, RLE Kangmin Lee, RLE

GRADUATE STUDENTS

Dooyong Koh, EECS Aaron Li, Chemistry Narumi Nagaya, ChemE Oliver Nix, Chemistry Jaekang Song, EECS Janet Wang, EECS Jong Woong Park, EECS

SUPPORT STAFF

Catherine Bourgeois, Admin. Support Services Manager

SELECTED PUBLICATIONS

D. Koh, Q. Wang, B. C. McGoldrick, C.-T. Chou, L. Liu, and M. A. Baldo, "Closed Loop Superparamagnetic Tunnel Junctions for Reliable True Randomness and Generative Artificial Intelligence," *Nano Letts.*, 2025. [Link]

N. Nagaya, K. Lee, C. F. Perkinson, A. Li, Y. Lee, X. Zhong, S. Lee, L. P. Weisburn, J. Z. Wang, T. K. Baikie, M. G. Bawendi, T. Van Voorhis, W. A. Tisdale, A. Kahn, K. Seo, and M. A. Baldo, "Exciton Fission Enhanced Silicon Solar Cell," *Joule*, 2025. [Link]

N. Nagaya, A. Alexiu, C. F. Perkinson, O. M. Nix, D. Koh, M. G. Bawendi, W. A. Tisdale, T. Van Voorhis, and M. A. Baldo, "Triplet Exciton Sensitization of Silicon Mediated by Defect States in Hafnium Oxynitride," *Adv. Mater.*, 2024. [Link]

D. Koh, Q. Wang, B. C. McGoldrick, C.-T. Chou, L. Liu, and M. A. Baldo, "Closed Loop Superparamagnetic Tunnel Junctions for Reliable True Randomness and Generative Artificial Intelligence," *Nano Lett.* 2025, 25, 10, 3799–3806. [Link]

George Barbastathis

Professor of Mechanical Engineering Department of Mechanical Engineering Computational imaging and inverse problems; optical system design; machine learning and optimization for physical systems; digital holography; optical neural networks.

Rm. 3-461C | 617-253-1960 | gbarb @ mit . edu

POSTDOCTORAL ASSOCIATES

Nischita Kaza, MechE Yi Wei, MechE

GRADUATE STUDENTS

Yancheng (Sparrow) Tian, MechE Difei Zhang, EECS

SUPPORT STAFF

Derek Doung, Administrative Assistant

SELECTED PUBLICATIONS

Q. Zhang, H. Yue, N. Liu, D. Xu, R. Zhou, L. Cao, and G. Barbastathis, "Decorrelation in Complex Wave Scattering," *arXiv*:2504.11330, Apr. 2025.

T. Pham, A. Boquet-Pujadas, S. Mondal, M. Unser, and G. Barbastathis, "Deep-prior Odes Augment Fluorescence Imaging with Chemical Sensors," *Nature Communications*, 15(1):9172, Oct. 2024.

Q. Zhang, A. Pandit, Z. Liu, Z. Guo, S. Muddu, Y. YiWei, D. Pereg, N. Nazemifard, C. Papageorgiou, Y. Yang, W. Tang, R. D. Braatz, A. S. Myerson, and G. Barbastathis, "Non-invasive Estimation of the Powder Size Distribution from a Single Speckle Image," *Light: Science & Applications*, 13(1):200, Aug. 2024.

Karl K. Berggren

Faculty Head, Electrical Engineering
Joseph F. and Nancy P. Keithley Professor in EE
Department of Electrical Engineering & Computer Science

Methods of nanofabrication, especially applied to superconductive quantum circuits, photodetectors, high-speed superconductive electronics, and energy systems.

Rm. 38-219 | 617-324-0272 | berggren @ mit . edu

CO-GROUP LEADER/ PRINCIPAL RESEARCH SCIENTIST

Donald Keathley, RLE

RESEARCH SCIENTIST

Sang-Hoon Nam, RLE

POSTDOCTORAL ASSOCIATES

Gian Luca Dolso, RLE Felix Ritzkowski, RLE

GRADUATE STUDENTS

Joseph Alongi, EECS
Emma Batson, EECS, NSF Fellow
Adina Bechhofer, EECS
Camron Blackburn, MAS (co-supervised with N.
Gershenfeld)
Matteo Castellani, EECS
Reed Foster, EECS, NDSEG Fellow

Reed Foster, EECS, NDSEG Fellow
Evan Golden, EECS, Lincoln Lab Fellow
Francesca Incalza, EECS
Ben Mazur, EECS, NDSEG Fellow
Owen Medeiros, EECS
Dip Joti Paul, EECS
Malick Sere, EECS
Alejandro Simon, EECS
John Simonaitis, EECS

UNDERGRADUATE STUDENTS

Hanson Nguyen, MSRP Joshua Piety, EECS James Shi, EECS Pavan Yeddanapudi, EECS Andi Qu, EECS Eric Zhan, EECS Amy Chen, EECS

VISITORS

Giorgia Ciuffarella, Polytechnic of Turin & École Polytechnique Fédérale de Lausanne Gabriel LeGuay, Federal Polytechnique School of

Davide Mondin, École Polytechnique Fédérale de Lausanne

SUPPORT STAFF

Dorothy Fleischer, Administrative Assistant Rinske Wijtmans Robinson, Administrative Assistant

SELECTED PUBLICATIONS

M. Castellani, O. Medeiros, A. Buzzi, R. A. Foster, M. Colangelo, and K. K. Berggren, "A Superconducting Full-wave Bridge Rectifier," *Nature Electronics*, pp. 1–9, May 2025. [Link]

M. Yeung *et al.*, "Bandwidth of Lightwave-Driven Electronic Response from Metallic Nanoantennas," *Nano Letts.*, vol. 25, no. 13, pp. 5250–5257, Apr. 2025. [Link]

L. C. Blackburn, A. Wynn, K. K. Berggren, and N. Gershenfeld, "A Compact Bit Serial Memory Cell for Adiabatic Quantum Flux Parametron Register Files," *IEEE Transactions on Applied Superconductivity*, pp. 1–5, Feb. 2025. [Link]

F. Ritzkowsky *et al.*, "On-chip Petahertz Electronics for Single-shot Phase Detection," *Nature Communications*, vol. 15, no. 1, pp. 1–8, Nov. 2024. [Link]

M. Yeung, L.-T. Chou, M. Turchetti, F. Ritzkowsky, K. K. Berggren, and P. D. Keathley, "Lightwave-electronic harmonic frequency mixing," *Science Advances*, vol. 10, no. 33, p. eadq0642, Aug. 2024. [Link]

M. Castellani *et al.*, "Nanocryotron ripple counter integrated with a superconducting nanowire single-photon detector for megapixel arrays," *Phys. Rev. Appl.*, vol. 22, no. 2, p. 024020, Aug. 2024. [Link]

A. Simon, R. Foster, O. Medeiros, M. Castellani, E. Batson, and K. K. Berggren, "Characterizing and Modeling the Influence of Geometry on the Performance of Superconducting Nanowire Cryotrons," *IEEE Transactions on Applied Superconductivity*, vol. 35, no. 5, pp. 1–5, Aug. 2024. [Link]

I. Charaev *et al.*, "Single-photon Detection Using Largescale High-temperature MgB2 Sensors at 20 K," *Nature Communications*, vol. 15, no. 1, p. 3973, May 2024. [Link]

M. Colangelo *et al.*, "Molybdenum Silicide Superconducting Nanowire Single-Photon Detectors on Lithium Niobate Waveguides," *ACS Photonics*, Jan. 2024. [Link]

Duane S. Boning

Vice Provost of International Activities
Clarence J. LeBel Professor of Electrical Engineering
Professor of Electrical Engineering & Computer Science,
Department of Electrical Engineering & Computer Science

Design for manufacturability of processes, devices, and circuits. Understanding and reduction of variation in semiconductor, photonics and MEMS manufacturing, emphasizing statistical, machine learning, and physical modeling of spatial and operating variation in circuits, devices, and manufacturing processes.

Rm. 39-415a | 617-253-0931 | boning @ mtl . mit . edu

VISITORS

Emmanuel Bender, MTL Research Affiliate

GRADUATE STUDENTS

Uttara Chakraborty, EECS (co-advised with C. V. Thompson)
Mohit Dighamber, EECS Zhengqi Gao, EECS
Rachel Harkavay, EECS and Sloan
Chih-Yu (Andrew) Lai, EECS
Carla Lorente, EECS and Sloan
Bonny Mahajan, EECS and Sloan
Rachel Owens, EECS
Jiahe Shi, EECS
Fan-Keng Sun, EECS
Yu-Cheng Wu, EECS

SUPPORT STAFF

Jami L. Mitchell, Project Coordinator

SELECTED PUBLICATIONS

Mark Zachary, EECS and Sloan

Z. Gao, X. Chen, Z. Zhang, U. Chakraborty, W. Bogaerts, and D. S. Boning, "Gradient-Based Power Efficient Functional Synthesis for Programmable Photonic Circuits," *J. of Lightwave Technology*, vol. 42, no. 17, pp. 5956-5965, Sept. 2024.

- Z. Gao, Z. Zhang, Z. He, J. Gu, D. Z. Pan, and D. S. Boning, "Selecting Robust Silicon Photonic Designs after Bayesian Optimization without Extra Simulations," *Optics Express*, vol. 32, no. 21, pp. 37585-37598, 2024. (Editor's Pick highlight)
- U. Chakraborty, D. S. Boning, and C. Thompson, "Bound-constrained Expectation Maximization for Failure Mode Identification in Weibull Competing-risks Device Reliability," *IEEE Trans. on Device and Material Reliability*, vol. 24, no. 4, pp. 556-670, Dec. 2024.
- P. Ma, H. Yang, Z. Gao, D. S. Boning, and J. Gu, "PIC2O-Sim: A Physics-Inspired Causality-Aware Dynamic Convolutional Neural Operator for Ultra-Fast Photonic Device FDTD Simulation," *arXiv:2406.17810*, Oct. 2024.
- S. Zheng, Z. Gao, F.-K. Sun, D. S. Boning, and M. Wong, "Improving Neural ODE Training with Temporal Adaptive Batch Normalization," *Advances in Neural Information Processing Systems (NeurIPS)*, Vancouver, Canada, Dec. 2024.

P. Ma, Z. Gao, A. Begovic, M. Zhang, H. Yang, H. Ren, R. Huang, D. Boning, and J. Gu, "BOSON-1: Understanding and Enabling Physically-Robust Photonic Inverse Design with Adaptive Variation-Aware Subspace Optimization," *Design, Automation & Test in Europe (DATE)*, Lyon, France, Apr. 2025. Also *arXiv*:2411.08210.

- Z. Gao, K. Zha, T. Zhang, Z, Xue, and D. S. Boning, "REG: Rectified Gradient Guidance for Conditional Diffusion Models," *International Conference on Machine Learning (ICML)*, July 2025. Also *arXiv:2501.18865*.
- Z. Gao, S. Vitillo, K. Joinson, and D. S. Boning, "Class-Conditional Vial Image Generation Using Diffusion Models for Enhanced Visual Inspection," *PDA Visual Inspection Forum 2025*, Raleigh, NC, Mar. 2025.
- P. Ma, Z. Gao, M. Zhang, H. Yang, M. Ren, R. Huang, D. Boning, and J. Gu, "MAPS: Multi-Fidelity AI-Augmented Photonic Simulation and Inverse Design Infrastructure," *arXiv:2503.01046*, Mar. 2025.
- F.-K. Sun, Y.-C. Wu, and D. S. Boning, "Simple Feedforward Neural Networks are Almost All You Need for Time Series Forecasting," *arXiv:2503.23621*, Mar. 2025.

Svetlana V. Boriskina

Director of Multifunctional Metamaterials (META) Lab Principal Research Scientist Department of Mechanical Engineering Multi-disciplinary research that blends photonics, opto-electronics, polymer physics, thermodynamics, and mechanics with the goal of advancing the fundamental understanding of materials and engineering infrared sensors, tunable photonic meta-materials, advanced fibers, and smart textiles.

Rm. 3-435B | 617-253-0079 | sborisk @ mit . edu

POSTDOCTORAL ASSOCIATES

Dr. Nataliia Fihurka, GMAF-Ukraine Program

Dr. Ricardo Flores, MechE

Dr. Most Kaniz Moriam, MechE

Dr. Carolina Orona Navar, MechE

Dr. Vivian Santamaria-Garcia, MechE

GRADUATE STUDENTS

Morgan Blevins, EECS
Hannah Gold, EECS
Amy Huynh, TPP
Xianglin Ji, MechE
Sangbin Lee, visiting student
Abhishek Mukherjee, EECS
Simo Pajovic, MechE
Mingyu Park, visiting student
Ikra Shuvo, MAS
Grace Smith, MechE
Duo Xu, MechE

SUPPORT STAFF

Khemjira Lockenwitz, Financial Officer

SELECTED PUBLICATIONS

S. Pajovic, Y. Tsurimaki, X. Qian, G. Chen, and S. V. Boriskina, "Nonreciprocal Reflection of Mid-infrared Light by Highly Doped InAs at Low Magnetic Fields," Opt. Express 33, 8661-8674, 2025.

R. V. B. Campos, F. E. A. Nogueira, J. P. C. do Nascimento, F. F. do Carmo, M. A. S. da Silva, S. P. Marcondes, A. C. Hernandes, S. V. Boriskina, L. M. Lozano, and A. S. B. Sombra, "High-Performance Piezoelectric Generator Based on a Monocrystalline LiNbO₃ Fiber," *Crystal Growth & Design*, 25 (3), 672-679, 2025.

C. M. Hartquist, B. Li, J. H. Zhang, G. Lv, J. Shin, S. V. Boriskina, G. Chen, X. Zhao, and S. Lin, "Reversible Twoway Tuning of Thermal Conductivity in an End-linked Star-shaped Thermoset," *Nature Communications* 15, 5590, 2024.

A. Mukherjee, D. Wlodarczyk, A. K. Somakumar, P. Sybilski, R. Siebenaller, M. A. Susner, A. Suchocki, and S. V. Boriskina, "Synergistic Effects of Defects and Strain on Photoluminescence in Van der Waals Layered Crystal," *Advanced Optical Materials*, 2400481, 2024.

O. Y. Long, S. Pajovic, C. Roques-Carmes, Y. Tsurimaki, N. Rivera, M. Soljačić, S. V. Boriskina, and S. Fan, "Nonreciprocal Scintillation Using One-dimensional Magneto-optical Photonic Crystals," *Phys. Rev. Applied* 22, 054062, 2024.

A. S. Ahteck, H. Gold, C. Cheng, R. Gu, A. Huynh, E. Scott, G. Goldstein, and S. V. Boriskina, "Generative AI for Textile Engineering: Blending Tradition and Functionality Through Lace," *An MIT Exploration of Generative AI*, DOI: 10.21428/e4baedd9.b3dfc1cf, Sept. 2024.

H. Gold, M. Blevins, S. Pajovic, A. Mukherjee, and S. V. Boriskina, "Dynamically-tunable Nonreciprocal Epsilonnear-zero Photonic Platform Enabled by Current-biased Dirac Semimetals," *Optical Materials Express*, in press, 2025. [Link]

A. Mukherjee, V. J. Santamaría-García, D. Wlodarczyk, A. K. Somakumar, P. Sybilski, R. Siebenaller, E. Rowe, S. Narayanan, L. M. Lozano-Sanchez, M. A. Susner, A. Suchocki, and S. V. Boriskina, "Thermal and Dimensional Stability of Photocatalytic Material ZnPS₃ Under Extreme Environmental Conditions," *Advanced Electronic Materials*, in press, 2025. [Link]

Edward S. Boyden

Y. Eva Tan Professor, Neurotechnology
Director of Center for Neurobiological Engineering, K Lisa Yang
Center for Bionics; Departments of Brain and Cognitive Sciences,
Media Arts and Sciences, and Biological Engineering
McGovern Institute, Yang Tan Collective, and HHMI

Research Areas and Special Interests: Developing, and applying, tools that enable the mapping of the molecules and wiring of the brain, the recording and control of its neural dynamics, the repair of its dysfunction, and the simulation of its computation.

Rm. 46-2171C | 617-324-3085 | edboyden @ mit . edu

RESEARCH SCIENTISTS AND TECHNICAL ASSOCIATES

Bobae An, McGovern
Ella Callahan, McGovern
Debarati Ghosh, McGovern
Konstantinos Kagias, McGovern
Yuki Kanazawa, McGovern
Jinyoung Kang, McGovern
Eung Chang Kim, McGovern
Yuechuan Lin, McGovern
Daniel Min, McGovern
Nava Shmoel David, McGovern
Giovanni Talei Franzesi, McGovern
Doug Weston, McGovern
Aimei Yang, McGovern
Eunah Yu, McGovern
Jian-Ping Zhao, McGovern

POSTDOCTORAL ASSOCIATES

Shahar Bracha, McGovern
Robert Hurt, McGovern
Kayla Kroning, McGovern
Yixi Liu, McGovern
Yangning Lu, McGovern
Daisong Pan, McGovern
Anubhav Sinha, McGovern
Sapna Sinha, McGovern
Michael Skuhersky, McGovern
Hui Sun, McGovern/EAPS
Corban Swain, McGovern
Panagiotis (Panos) Symvoulidis, McGovern
Zeguan Wang, McGovern
Guang Xu, McGovern
Yasu Xu, McGovern

GRADUATE STUDENTS

Nick Barry, MAS
Jeffrey Brown, EECS
Liyam Chitayat, CSBi
Davy Deng, HST
Isaak Freeman, MAS
Kettner Griswold, MAS
Jordan Harrod, HST
Helena Hu, BE
Andrew Kirjner, BCS
Camille Mitchell, BCS
William Niu, CSBi
Cipriano Romero, EECS
Evan Ruesch, BCS
Catherine Marin Della Santina. BE

Quilee Simeon, BCS Sara Tavana, McGovern Shiwei Wang, Chemistry Lige (Caroline) Zhang, MAS

SUPPORT STAFF

Ally Bassile-McCarthy, Administrative Assistant Macey Lavoie, Administrative Assistant Lisa Lieberson, Senior Administrative Assistant Fira Zainal, Financial Assistant

SELECTED PUBLICATIONS

T. W. Shin, H. Wang*, C. Zhang C*, B. An, Y. Lu, E. Zhang, X. Lu, E. D. Karagiannis, J. S. Kang, A. Emenari, P. Symvoulidis, S. Asano, L. Lin, E. K. Costa (IMAXT Grand Challenge Consortium), A. H. Marblestone, N. Kasthuri, L. H. Tsai, and E. S. Boyden, "Dense, Continuous Membrane Labeling and Expansion Microscopy Visualization of Ultrastructure in Tissues," *Nature Communications* 16(1):1579, 2025. (*, contributed equally)

X. Xiao*, A. Yang*, H. Zhang, D. Park, Y. Wang, B. Szabo, E. S. Boyden**, and K. D. Piatkevich**, "Engineering of Genetically Encoded Bright Near-Infrared Fluorescent Voltage Indicator," *International J. of Molecular Sciences* 26(4):1442, 2025. (*, contributed equally; **, co-corresponding)

J. Kang*, M. E. Schroeder*, Y. Lee, C. Kapoor, E. Yu, T. B. Tarr, K. Titterton, M. Zeng, D. Park, E. Niederst, D. Wei, G. Feng, and E. S. Boyden, "Multiplexed Expansion Revealing for Imaging Multiprotein Nanostructures in Healthy and Diseased Brain," *Nature Communications* 15(1):9722, 2024. (*, contributed equally)

S. Wang*, T. W. Shin*, H. B. Yoder II, R. B. McMillan, H. Su, Y. Liu, C. Zhang, K. S. Leung, P. Yin, L. L. Kiessling**, and E. S. Boyden**, "Single-shot 20-fold Expansion Microscopy," *Nature Methods*, doi:10.1038/s41592-024-02454-9, 2024. Online ahead of print. (*, equal contribution; **, co-corresponding authors)

Vladimir Bulović

MIT.nano Director

Fariborz Maseeh (1990) Professor of Emerging Technology Department of Electrical Engineering and Computer Science Physical properties of nanostructured materials and composite structures and their use in development of electronic, excitonic, optical, and nano-mechanical devices. Applications of nanostructures in large-scale technologies.

Rm. 13-3138 | 617-253-7012 | bulovic @ mit . edu

RESEARCH SCIENTISTS

Jeremiah Mwaura, RLE Annie Wang, RLE

POSTDOCTORAL ASSOCIATES

Benjia Dak Dou, RLE Jun Guan, RLE Jinchi Han, RLE Richard Swartwout. RLE

GRADUATE STUDENTS

Roberto Brenes, EECS, NSF Fellow
Tori Dang, EECS
Jamie Geng, EECS
Tamar Kadosh, DMSE
Madeliene Laitz, EECS, NSF Fellow
Brendan Motes, MEng
Mayuran Saravanapavanantham, EECS, NSF Fellow
Shreyas Srinivasan, Chemistry
Ella Wassweiler, EECS, NSF Fellow
Ruiqi Zhang, EECS
Karen Yang, EECS, McWhorter Fellow

SUPPORT STAFF

Samantha Farrell, Sr. Administrative Assistant Jay Sandlin, Research Support Associate

SELECTED PUBLICATIONS

E. L. Wassweiler, M. Sponseller, A. Osherov, J. Jean, M. G. Bawendi, and V, Bulović, "Metal Oxide Interlayers Enable Lower-Cost Electrodes in PbS QD Solar Cells," *ACS Applied Energy Materials* 6, 5646–5652 (2023).

M. Laitz, A. E. K. Kaplan, J. Deschamps, U. Barotov, A.H. Proppe, I. García-Benito, A. Osherov, G. Grancini, D.W. deQuilettes, K.A Nelson, M.G. Bawendi, and V. Bulović, "Uncovering Temperature-dependent Exciton-polariton Relaxation Mechanisms in Hybrid Organic-inorganic Perovskites," *Nature Communications* 14, 2426 (2023).

E. Pettit, W. J. Hsu, R. Holmes, R. Swartwout, E. Wassweiler, T. Kadosh, and V. Bulović, "Vapor Transport Deposition of Metal-Halide Perovskites for Photovoltaic Applications," *Bulletin of the American Physical Society* (2023).

M. Saravanapavanantham, J. Mwaura, and V. Bulović, "Printed Organic Photovoltaic Modules on Transferable Ultra-thin Substrates as Additive Power Sources," *Small Methods* 7, 2200940 (2023).

J. Shi, D. Yoo, F. Vidal-Codina, C. W. Baik, K. S. Cho, N. C. Nguyen, H. Utzat, J. Han, A. M. Lindenberg, V. Bulović, M. G. Bawendi, J. Peraire, S.-H. Oh, and K. A. Nelson, "A Room-temperature Polarization-sensitive CMOS Terahertz Camera Based on Quantum-dot-enhanced Terahertz-to-visible Photon Upconversion," *Nature Nanotechnology*, 17, 1288–1293 (2022).

J. Han, F. Niroui, J. H. Lang, and V. Bulović, "Scalable Self-Limiting Dielectrophoretic Trapping for Site-Selective Assembly of Nanoparticles," *Nano Letts.* 22, 8258-8265 (2022).

R. Brenes, D. W. deQuilettes, R. Swartwout, A. Y. Alsalloum, O. M. Bakr, and V. Bulović, "Mapping the Diffusion Tensor in Microstructured Perovskites," *arXiv preprint arXiv:2209.08684* (2022).

J. Han, M. Saravanapavanantham, M. R. Chua, J. H. Lang, and V. Bulović, "A versatile acoustically active surface based on piezoelectric microstructures," *Microsystems & Nanoengineering* 8, 55 (2022).

S. Xie, H. Zhu, M. Li, and V. Bulović, "Voltage-controlled reversible modulation of colloidal quantum dot thin film photoluminescence," *Applied Physics Letts.* 120, 211104 (2022).

R. Swartwout, R. Patidar, E. Belliveau, B. Dou, D. Beynon, P. Greenwood, N. Moody, D. deQuilettes, M. Bawendi, T. Watson, and V. Bulović, "Predicting Low Toxicity and Scalable Solvent Systems for High-Speed Roll-to-Roll Perovskite Manufacturing," *Solar RRL* 6, 2100567 (2022).

Joseph Casamento

Assistant Professor of Materials Science and Engineering Department of Materials Science and Engineering

Semiconducting materials and dielectrics, heterostructure design, thin film synthesis, and device fabrication. Specifically, a focus on non-equilibrium synthesis and plasma processing of nitride semiconductors and related materials; widely used in light-emitting diodes and lasers, RF transistor amplifiers, and acoustic devices.

Rm. 8-237 | 617-253-3315 | jac93 @ mit . edu

GRADUATE STUDENTS

Dadam Kang, DMSE Lois Talli, DMSE

SUPPORT STAFF

Neko Smith, Faculty Assistant

SELECTED PUBLICATIONS

Q. Tran, J. Hayden, J. Casamento, J. P. Maria, and T. N. Jackson, "Aluminum Boron Nitride Ferroelectric Field-Effect Transistors With ZnO Semiconductor Channel," *IEEE Transactions on Electron Devices*, 72: 3774, 2025.

C. Savant, T. S. Nguyen, K. Nomoto, S. Vishwakarma, S. Ma, A. Dhar, Y. S. Chen, J. Casamento, D. J. Smith, H. G. Xing, and D. Jena, "Epitaxial High-K Barrier AlBN/GaN HEMTs," *Applied Physics Letts.*, 126: 112906, 2025.

K. Nomoto, J. Casamento, T. S. Nguyen, L. Li, H. Lee, C. Savant, A. L. Hickman, T. Maeda, J. Encomendero, V. Gund, T. Vasen, S. Afroz, D. Hannan, J. C. M. Hwang, D. Jena, and H. G. Xing, "AlScN/GaN HEMTs With 4 A/mm On-Current and Maximum Oscillation Frequency >130 GHz," Applied Physics Express, 18: 016506, 2025.

C. H. Skidmore, R. J. Spurling, J. Hayden, S. M. Baksa, D. Behrendt, D. Goodling, J. L. Nordlander, A. Suceava, J. Casamento, B. Akkopru-Akgun, S. Calderon, I. Dabo, V. Gopalan, K. P. Kelley, A. M. Rappe, S. Trolier-McKinstry, E. C. Dickey, and J. P. Maria, "Proximity Ferroelectricity in Wurtzite Heterostructures," *Nature*, 637: 574, 2025.

K. Kang, J. A. Casamento, D. C. Shoemaker, Y. Song, E. Z. Ozdemir, N. S. McIlwaine, J. P. Maria, S. Choi, and S. E. Trolier-McKinstry, "Thermal Characterization of Ferroelectric $Al_{1-x}B_xN$ for Nonvolatile Memory," ACS Applied Materials & Interfaces, 16: 67921, 2024.

C. P. Savant, A. Verma, T. S. Nguyen, L. van Deurzen, Y. H. Chen, Z. He, S. S. Rezaie, J. Gollwitzer, B. Gregory, S. Sarker, J. Ruff, G. Khalsa, A. Singer, D. A. Muller, H. G. Xing, D. Jena, and J. Casamento, "Self-Activated Epitaxial Growth of ScN Films From Molecular Nitrogen at Low Temperatures," APL Materials, 12: 111108, 2024.

T. S. Nguyen, N. Pieczulewski, C. Savant, J. J. P. Cooper, J. Casamento, R. S. Goldman, D. A. Muller, H. G. Xing, and D. Jena, "Lattice-Matched Multiple Channel AlScN/GaN Heterostructures," *APL Materials*, 12: 101117, 2024.

C. Savant, V. Gund, K. Nomoto, T. Maeda, S. Jadhav, J. Lee, M. Ramesh, E. Kim, T. S. Nguyen, Y. H. Chen, J. Casamento, F. Rana, A. Lal, H. G. Xing, and D. Jena, "Ferroelectric AlBN Films by Molecular Beam Epitaxy," *Applied Physics Letts.*, 125: 072902, 2024.

Q. Tran, J. Hayden, J. Casamento, J. P. Maria, and T. N. Jackson, "Boron-Doped Aluminum Nitride Ferroelectric Field-Effect Transistors With ZnO Semiconductor Channel," *Device Research Conference (DRC)*, College Park, MD, pp. 1-2, 2024.

Anantha P. Chandrakasan

MIT Provost

Vannevar Bush Professor of Electrical Engineering & Computer Science
Department of Electrical Engineering and Computer Science

Design of digital integrated circuits and systems. Energy efficient implementation of signal processing, communication and medical systems. Circuit design with emerging technologies.

Rm. 38-107 | 617-258-7619 | anantha @ mit . edu

POSTDOCTORAL ASSOCIATES

Aya Amer, RLE

Peggie Dong, RLE (co-supervised with A. Belcher) Kyungmi Lee,RLE

Saransh Sharma, RLE (co-supervised with G. Traverso) Soyeon Um, RLE

GRADUATE STUDENTS

Aylin Baca, EECS (co-supervised with P. Anikeeva) Adam Gierlach, EECS (co-supervised with G. Traverso) Seoyoon Jang, EECS

Patricia Jastrzebska-Perfect (co-supervised with G. Traverso) Mingran Jia, EECS (co-supervised with R. Han) Jaehong Jung, EECS (co-supervised with R. Han) Dimple Kochar, EECS (co-supervised with H. Lee) Eunseok Lee, EECS (co-supervised with R. Han) Hyemin Stella Lee, EECS Woobean Lee, EECS Mohith Harish Manohara, EECS

Sarina Sabouri, EECS (co-supervised with N. Reiskarimian) Saebyeok Shin, EECS

Zoey (Zhiye) Song, EECS

So-Yoon Yang, EECS (co-supervised with G. Traverso)

VISITING SCIENTIST AND SCHOLARS

Ulkuhan Guler, WPI Daehyun Kwon, Samsung

SUPPORT STAFF

Katey Provost, Program/Project Coordinator

SELECTED PUBLICATIONS

S. Y. Yang, D. U. Yildirim, S. Sharma, D. Han, R. Mittal, H. Ellis, J. Jung, E. Lee, Y. Cai, G. Traverso, and A. P. Chandrakasan, "A Fully-Integrated Wireless Ingestible Drug Delivery Chip with Electrochemical Energy Harvesting and pH-Based MPPT," *IEEE Custom Integrated Circuits Conference (CICC)*, Boston, MA, Apr. 2025.

D. Han and A. P. Chandrakasan, "MEGA.mini: A Universal Generative AI Processor with a New Big/Little Core Architecture for NPU," *IEEE International Solid-State Circuits Conference (ISSCC)*, San Francisco, CA, Feb. 2025.

M. Ashok, S. Maji, X. Zhang, J. Cohn, and A. P. Chandrakasan, "Digital In-Memory Compute for Machine Learning Applications with Input and Model Security," *IEEE J. of Solid-State Circuits*, Feb. 2025.

K. Lee, M. Ashok, S. Maji, R. Agrawal, A. Joshi, M. Yan, J. Emer, and A. Chandrakasan, "Secure Machine Learning Hardware: Challenges and Progress [Feature]," *IEEE Circuits and Systems Magazine*, Feb. 2025.

A. G. Amer, M. Ashok, X. Zhang, J. Cohn, and A. P. Chandrakasan, "A 14-nm Energy-Efficient and Reconfigurable Analog Current-Domain In-Memory Compute SRAM Accelerator," 38th International Conference on VLSI Design and 23rd International Conference on Embedded Systems (VLSID), Bangalore, India, Jan. 2025.

D. V. Kochar, M. Ashok, and A. P. Chandrakasan, "A 0.75mm² 407 µW Real-Time Speech Audio Denoiser with Quantized Cascaded Redundant Convolutional Encoder-Decoder for Wearable IoT Devices," 38th International Conference on VLSI Design and 23rd International Conference on Embedded Systems (VLSID), IEEE, Jan. 2025.

Z. Ji, H. Wang, M. Wang, W. Khwa, M. Chang, S. Han, and A. P. Chandrakasan, "A Fully-Integrated Energy-Scalable Transformer Accelerator for Language Understanding on Edge Devices," *IEEE Open J. of the Solid-State Circuits Society*, Jan. 2025.

D. U. Yildirim, J. Jung, A. Elsakka, G. Moschetti, M. M. Lopez, J. Hansryd, T. Palacios, and A. P. Chandrakasan, "A 0.7 cm², 3.5 GHz, –31 dBm Sensitivity Battery-Free 5G Energy-Harvester Backscatterer with 20 s Cold-Start Wake-Up Time for IoT-Enabled Warehouses," *IEEE J. of Solid-State Circuits*, Nov. 2024.

A. G. Amer, G. Hills, G. Kyriazidis, A. P. Chandrakasan, and M. M. Shulaker, "Reconfigurable 3D Edge Sensing System of Carbon Nanotube Sensing and Silicon CMOS from a Commercial Manufacturing Facilities," *IEEE Workshop on Signal Processing Systems (SiPS)*, Nov. 2024.

V. Kochar, Dimple, et al., "LEDRO: LLM-Enhanced Design Space Reduction and Optimization for Analog Circuits," arXiv e-prints, Nov. 2024.

H. Huang, P. R. Chai, S. Lee, T. Kerssemakers, A. Imani, J. Chen, M. Heim, J. Y. Bo, A. Wentworth, F. T. Sanoudos-Dramaliotis, I. Ballinger, S. Maji, M. Murphy, A. Alexiev, G. H. Kang, N. Fabian, J. Jenkins, A. Pettinari, K. Ishida, J. Li, S. S. You, A. M. Hayward, A. Chandrakasan, and G. Traverso, "An Implantable System for Opioid Safety," *Device*, Aug. 2024.

Yufeng (Kevin) Chen

Director of Soft and Microrobotics Laboratory
Associate Professor of Electrical Engineering & Computer Science
Department of Electrical Engineering & Computer Science

Power electronics, biomimetic robotics, insect-scale robotics, intermediate Reynolds number fluid dynamics, unsteady aerodynamics, soft artificial muscles, electroactive polymer actuators.

Rm. 10-140H | 617-253-7351 | yufengc @ mit . edu

POSTDOCTORAL ASSOCIATE

Wedyan Babatain (co-advised), Media Lab

GRADUATE STUDENTS

Yi-Hsuan Hsiao, EECS Quang Phuc N. Kieu, EECS Suhan Kim, EECS Zhijian Ren, EECS

UNDERGRADUATE STUDENTS

Katrina Jander, EECS Meenakshi Singh, EECS

SUPPORT STAFF

Eliza Grisanti, Administrative Assistant

SELECTED PUBLICATIONS

S. Kim, Y. H. Hsiao, Z. Ren, J. Huang, and Y. Chen, "Acrobatics at the Insect Scale: A Durable, Precise, and Agile Micro–Aerial Robot," *Science Robotics*, vol. 10, no. 98, p. eadp4256, 2025.

Y. H. Hsiao, S. Bai, Z. Guan, S. Kim, Z. Ren, P. Chirarattananon, and Y. Chen, "Hybrid Locomotion at the Insect Scale: Combined Flying and Jumping for Enhanced Efficiency and Versatility," *Science Advances*, vol. 11, no. 15, p. eadu4474, 2025.

Y. H. Hsiao, W. T. Chen, Y. S. Chang, P. Agrawal, and Y. Chen, "Hovering Flight of Soft-Actuated Insect-Scale Micro Aerial Vehicles Using Deep Reinforcement Learning," in *Proc. IEEE 8th Int. Conf. Soft Robot. (RoboSoft)*, 2025.

Samantha Coday

Emanuel E. Landsman (1958) Career Development
Assistant Professor of Electrical Engineering & Computer Science
Department of Electrical Engineering & Computer Science

Design of lightweight and efficient power electronics utilizing capacitor-based converter topologies.

Rm. 10-140G | 617-253-3934 | coday @ mit . edu

GRADUATE STUDENTS

Qijia Li, EECS Ellie Rabenold, EECS Andre Rodriguez, EECS Jade Sund, EECS

SUPPORT STAFF

Eliza Grisanti, Administrative Assistant

SELECTED PUBLICATIONS

S. Coday, N. M. Ellis and R. C. N. Pilawa-Podgurski, "Modeling and Analysis of Shutdown Dynamics in Flying Capacitor Multilevel Converters," in *IEEE Transactions on Power Electronics*, vol. 39, no. 8, pp. 9150-9159, Aug. 2024, doi: 10.1109/TPEL.2023.3285741. [Link]

N. M. Ellis, N. C. Brooks, M. E. Blackwell, R. A. Abramson, S. Coday, and R. C. N. Pilawa-Podgurski, "A General Analysis of Resonant Switched-Capacitor Converters Using Peak Energy Storage and Switch Stress Including Ripple," in *IEEE Transactions on Power Electronics*, vol. 39, no. 7, pp. 8363-8383, Jul. 2024, doi:10.1109/TPEL.2023.3285745. [Link]

- E. Krause, S. Coday, L. Horowitz, and R. C. N. Pilawa-Podgurski, "An 840 V-to-120 V Radiation-Tolerant Flying Capacitor Multilevel Converter for Space Robotics," 2024 IEEE Energy Conversion Congress and Exposition (ECCE), Phoenix, AZ, USA, 2024, pp. 3479-3485, doi:10.1109/ECCE55643.2024.10861108. [Link]
- S. Coday et al., "Design and Implementation of a GaN-Based Composite Hybrid Switched-Capacitor DC-DC Converter for Space Applications," in *IEEE Open J. of Power Electronics*, vol. 6, pp. 150-161, 2025, doi: 10.1109/OJPEL.2024.3471670. [Link]
- E. Rabenold, R. Jerez, and S. Coday, "The Analysis and Design of a Resonant Capacitively-Isolated Cockcroft-Walton Converter," 2025 IEEE Applied Power Electronics Conference and Exposition (APEC), Atlanta, GA, USA, 2025, pp. 2249-2253, doi: 10.1109/APEC48143.2025.10977355. [Link]
- J. Sund and S. Coday, "A Hybrid Switched Capacitor Converter Enabling Capacitive-Based Wireless Power Transfer for Battery Charging Applications," 2025 IEEE Applied Power Electronics Conference and Exposition (APEC), Atlanta, GA, USA, 2025, pp. 971-977, doi: 10.1109/APEC48143.2025.10977546. [Link]

Riccardo Comin

Associate Professor Department of Physics Quantum solids, electronic systems with strong interactions, superconductors, multiferroics, topological materials, 2D magnets and devices. Thin film & bulk single crystal synthesis of transition metal-based compounds. Angle-resolved Photoemission Spectroscopy, optical and Raman spectroscopy, and Resonant X-ray scattering to probe electronic, magnetic, and optical properties.

Rm. 13-2153 | 617-253-7834 | rcomin@mit.edu

POSTDOCTORAL ASSOCIATES

Xiangyu Luo, Physics Dongjin Oh, Physics Dayne Sasaki, Physics

GRADUATE STUDENTS

Qian Song, DMSE Jiaruo Li, Physics Ahmet Kemal Demir, Physics Meg Shankar, Physics Sahaj Patel, Physics

UNDERGRADUATE STUDENT

Bella Torres, DMSE

SUPPORT STAFF

Gerry Miller, Administrative Assistant

SELECTED PUBLICATIONS

Q. Song, S. Stavric, P. Barone, A. Droghetti, D. S. Antonenko, J. W. F. Venderbos, C. A. Occhialini, B. Ilyas, E. Ergecen, N. Gedik, S.-W. Cheong, R. M. Fernandes, S. Picozzi, and R. Comin, "Electrical Switching of a P-wave Magnet," *Nature* 642, 64 (2025).

M. Kang, S. Kim, Y. Qian, P. M. Neves, L. Ye, J. Jung, D. Puntel, F. Mazzola, S. Fang, C. Jozwiak, A. Bostwick, E. Rotenberg, J. Fuji, I. Vobornik, J.-H. Park, J. G. Checkelsky, B.-J. Yang, R. Comin, "Measurements of the Quantum Geometric Tensor in Solids," *Nature Physics* 21, 110 (2025).

C. A. Occhialinit, Y. Tsengt, H. Elnaggar, Q. Song, M. Blei, S. A. Tongay, V. Bisogni, F. M. F. de Groot, J. Pelliciari, and R. Comin. "Nature of Excitons and Their Ligand-Mediated Delocalization in Nickel Dihalide Charge-Transfer Insulators," *Physical Review X* 14, 031007 (2024).

J. Wakefield†, M. Kang†, P. Neves†, D. Oh†, S. Fang, R. McTigue, S. Y. F. Zhao, T. N. Lamichhane, A. Chen, S. Lee, S. Park, J.-H. Park, C. Jozwiak, A. Bostwick, E. Rotenberg, A. Rajapitamahuni, E. Vescovo, J. L. McChesney, D. Graf, J. C. Palmstrom, T. Suzuki, M. Li, R. Comin, and J. G. Checkelsky, "Three-dimensional flat bands in pyrochlore metal CaNi₂," *Nature* 623, 301 (2023).

C. A. Occhialini, J. J. Sanchez, Q. Song, G. Fabbris, Y. Choi, J.-W. Kim, P. J. Ryan, and R. Comin, "Spontaneous orbital polarization in the nematic phase of FeSe," *Nature Materials* 22, 985 (2023).

L. G. Pimenta Martins, D. A. Ruiz-Tijerina, C. A. Occhialini, J.-H. Park, Q. Song, A.-Y. Lu, P. Venezuela, L. G. Cançado, M. S. C. Mazzoni, M. J. S. Matos, J. Kong, and R. Comin, "Pressure tuning of minibands in MoS2/WSe2 heterostructures revealed by moiré phonons," *Nature Nanotechnology* 18, 1147 (2023).

M. Kang, S. Fang, J. Yoo, B. R. Ortiz, Y. Oey, S. H. Ryu, J. Kim, C. Jozwiak, A. Bostwick, E. Rotenberg, E. Kaxiras, J. Checkelsky, S. D. Wilson, J.-H. Park, and R. Comin, "Charge order landscape and competition with superconductivity in kagome metals," *Nature Materials* 22, 186 (2023).

Q. Songt, C. A. Occhialinit, E. Ergeçent, B. Ilyast, D. Amoroso, P. Barone, J. Kapeghian, K. Watanabe, T. Taniguchi, A. S. Botana, S. Picozzi, N. Gedik, and R. Comin, "Evidence for a single-layer van der Waals multiferroic," *Nature* 602, 601 (2022).

M. Kang, S. Fang, J.-K. Kim, B. R. Ortiz, S. H. Ryu, J. Kim, J. Yoo, G. Sangiovanni, D. Di Sante, B.-G. Park, C. Jozwiak, A. Bostwick, E. Rotenberg, E. Kaxiras, S. D. Wilson, J.-H. Park†, and R. Comin†, "Twofold van Hove singularity and origin of charge order in topological kagome superconductor CsV₃Sb_s," *Nature Physics* 18, 301 (2022).

J. Pelliciari, S. Karakuzu, Q. Song, R. Arpaia, A. Nag, M. Rossi, J. Li, T. Yu, X. Chen, R. Peng, M. García-Fernández, A. C. Walters, Q. Wang, J. Zhao, G. Ghiringhelli, D. Feng, T. A. Maier, K.-J. Zhou, S. Johnston, and R. Comin, "Evolution of spin excitations from bulk to monolayer FeSe," *Nature Communications* 12, 3122 (2021).

J. Li, R. J. Green, Z. Zhang, R. Sutarto, J. T. Sadowski, Z. Zhu, G. Zhang, D. Zhou, Y. Sun, F. He, S. Ramanathan, and R. Comin, "Sudden Collapse of Magnetic Order in Oxygen-Deficient Nickelate Films," *Physical Review Letts.* 126, 187602 (2021).

M. Kang, S. Fang, L. Ye, H. C. Po, J. Denlinger, C. Jozwiak, A. Bostwick, E. Rotenberg, E. Kaxiras, J. G. Checkelsky, and R. Comin. Topological flat bands in frustrated kagome lattice CoSn," *Nature Communications* 11, 4004 (2020).

Jesús A. del Alamo

Donner Professor

Professor of Electrical Engineering epartment of Electrical Engineering & Computer Science

Nanometer-scale III-V compound semiconductor transistors for future digital, power, RF, microwave and millimeter wave applications. Reliability of compound semiconductor transistors. Diamond transistors. Ionic and ferroelectric non-volatile programmable Al synapses.

Rm. 38-246 | 617-253-4764 | alamo @ mit.edu

POSTDOCTORAL ASSOCIATES

Sapir Bitton, Fulbright Visiting Scholar Yanjie Shao, MTL

GRADUATE STUDENTS

Drew E. Buzzell, EECS Hyungeun Choi, EECS John C.-C. Huang, EECS Jungsoo Lee, EECS Aviram Massuda, EECS Dingyu Shen, EECS Arina Yu, EECS

UNDERGRADUATE STUDENT

Tyra E. Espedal, UROP

VISITING SCIENTISTS

Minsoo Kim, Samsung Electronics Ignacio Jiménez Gallo, Polytechnic University of Madrid Jesús Grajal de la Fuente, Polytechnic University of Madrid

SUPPORT STAFF

Elizabeth Kubicki. Administrative Assistant

SELECTED PUBLICATIONS

T. E. Espedal, Y. Shao, J. C.-C. Huang, E. R. Borujeny, D. A. Antoniadis, and J. A. del Alamo, "Frequency-Dependent Wake-Up in Ferroelectric $\mathrm{Hf_{0.5}Zr_{0.5}O_2}$ Devices," to be presented at 83rd IEEE Device Research Conf. (DRC), Durham, NC, Jun. 22–25, 2025.

M. Huang, L. Xu, J. A. del Alamo, J. Li, and B. Yildiz, "Nonlinear Ion Dynamics Enable Spike Timing Dependent Plasticity of Electrochemical Ionic Synapses," *Advanced Materials*, 2418484, 2025. DOI: 10.1002/adma.202418484.

Y. Shao, E. R. Borujeny, J. Navarro, J. C.-C. Huang, T. E. Espedal, D. A. Antoniadis, and J. A. del Alamo, "Domain-Level Ferroelectric Polarization Switching in Nanoscale Oxide-Channel Ferroelectric Field-Effect Transistors," *NanoLetts.*, vol. 25, pp. 3173–3179, 2025. DOI: 10.1021/acs. nanolett.4c05731.

T. Kim, J. A. del Alamo, and D. A. Antoniadis, "On the Imprint Mechanism of Thin-Film $\mathrm{Hf_{0.5}Zr_{0.5}O_2}$ Ferroelectrics," *IEEE Trans. Electron Devices*, vol. 71, no. 11, pp. 6620–6626, Nov. 2024.

Y. Shao, M. Pala, H. Tang, B. Wang, J. Li, D. Esseni, and J. A. del Alamo, "Realizing the Potential of Ultra-Scaled Tunneling Electronics Through Extreme Quantum Confinement," *Nature Electronics*, Nov. 4, 2024.

Y. Shao, J. C.-C. Huang, E. R. Borujeny, T. E. Espedal, D. A. Antoniadis, and J. A. del Alamo, "Highly-Scaled BEOL E-Mode Transistor and Discrete-Domain Ferroelectric Memory Platform Enabled by PEALD \ln_2O_3 ," in *Proc. IEEE Int. Electron Devices Meeting (IEDM)*, San Francisco, CA, Dec. 7–11, 2024.

T. E. Espedal, Y. Shao, E. R. Borujeny, and J. A. del Alamo, "Characterization of Ferroelectric Endurance in $\mathrm{Hf}_{0.5}\mathrm{Zr}_{0.5}\mathrm{O}_2$ Deposited by Plasma-Enhanced ALD Under Different Process Conditions," in *Proc. TECHCON* 2024, Austin, TX, Sep. 8–10, 2024.

Y. Shao, E. R. Borujeny, J. Navarro, J. C.-C. Huang, T. E. Espedal, D. A. Antoniadis, and J. A. del Alamo, "Discrete Domain Switching in Scaled Amorphous Metal-Oxide Channel Ferroelectric FETs," in *Proc. TECHCON* 2024, Austin, TX, Sep. 8–10, 2024.

M. Schwacke, P. Zguns, J. A. del Alamo, J. Li, and B. Yildiz, "Electrochemical Ionic Synapses with Mg²⁺ as the Working Ion," *Advanced Electronic Materials*, 2300577, 2024.

H. Roh, D.-H. Kim, Y. Cho, Y.-M. Jo, J. A. del Alamo, H. J. Kulik, M. Dinca, and A. Gumyusenge, "Robust Chemiresistive Behavior in Conductive Polymer/MOF Composites," *Advanced Materials*, 2312382, 2024.

Y. Shao, E. R. Borujeny, J. Navarro, J. C.-C. Huang, T. E. Espedal, D. A. Antoniadis, and J. A. del Alamo, "Discrete Domain Switching in Scaled Oxide-Channel Ferroelectric FETs," in *Proc. 82nd IEEE Device Research Conf. (DRC)*, College Park, MD, Jun. 23–26, 2024.

D. Buzzell, F. Kurnia, H. Chu, L. Kong, J. A. del Alamo, and J. L. M. Rupp, "Tailoring $\mathrm{Li_4Ti_5O_{12}}$ Thin-Film Carrier Kinetics Through Solid-Solution Doping for Battery and Memristor Applications," in *Proc. 24th Int. Conf. Solid State Ionics (SSI24)*, London, UK, Jul. 15–19, 2024.

Catherine L. Drennan

John and Dorothy Wilson Professor of Biochemistry Howard Hughes Medical Institute Professor and Investigator Structural Biology of Metalloproteins.

Rm. 68-680 | 617-253-5622 | cdrennan @ mit . edu

POSTDOCTORAL ASSOCIATES

Juan Carlos Caceres Vergara, Biology and HHMI Jayoh Hernandez, Biology Kelsey R. Miller-Brown, Biology Jared Paris, Biology and HHMI Ari Selzer, Biology and HHMI Dana Westmoreland, Biology Zhuangyu Zhao, Biology

GRADUATE STUDENTS

Dante M. Avalos, Harvard University Biophysics Andrew J. Dorfeuille, Chemistry Nina Greeley, Chemistry Christa N. Imrich, Chemistry Steve Xiaomeng Liu, Harvard University Chemistry Andrea N. Marcano-Delgado, Chemistry Sorin Srinivasa, Chemistry Naike Ye, Chemistry

SUPPORT STAFF

Rebekah Bjork, Lab Manager

SELECTED PUBLICATIONS

D. E. Westmoreland, P. R. Feliciano, G. Kang, C. Cui, A. Kim, J. Stubbe, D. G. Nocera, and C. L. Drennan, "2.6-Å Resolution Cryo-EM Structure of a Class Ia Ribonucleotide Reductase Trapped with Mechanism-based Inhibitor N_3 CDP," *Proc. Natl. Acad. Sci. U.S.A.* 121, 41, e2417157121, 2024.

A. Biester, D. A. Grahame, and C. L. Drennan, "Capturing a Methanogenic Carbon Monoxide Dehydrogenase/ Acetyl-CoA Synthase Complex via Cryogenic Electron Microscopy," *Proc. Natl. Acad. Sci. U.S.A.*121, 41, e2410995121, 2024.

M. A. Funk, C. M. Zimanyi, G. A. Andree, A. E. Hamilos, C. L. Drennan, "How ATP and dATP Act as Molecular Switches to Regulate Enzymatic Activity in the Prototypical Bacterial Class Ia Ribonucleotide Reductase," *Biochemistry* 63, 19, 2517-2531, 2024.

S. Adak, N. Ye, L. A. Calderone, M. Duan, W. Lubeck, R. J. B. Schäfer, A. L. Lukowski, K. N. Houk, M.-E. Pandelia, C. L. Drennan, and B. S. Moore, "Oxidative Rearrangement of Tryptophan to Indole Nitrile by a Single Diiron Enzyme" *Nat. Chem.* 16, 1989-1998, 2024.

Jongyoon Han

Professor of Electrical Engineering & Biological Engineering Department of Electrical Engineering & Computer Science Department of Biological Engineering BioMEMS, cell and molecular sorting, novel nanofluidic phenomena, biomolecule separation and pre-concentration, seawater desalination and water purification, bioprocessing, stem cells, engineering for cell therapy.

Rm. 36-841 | 617-253-2290 | jyhan @ mit . edu

RESEARCH SCIENTIST

Kerwin Keck, SMART Centre, Singapore

POSTDOCTORAL ASSOCIATES

Mingyang Cui, RLE Do Hyun Kim, RLE Yaoping Liu, SMART Centre, Singapore Daniel Roxby, SMART Centre, Singapore Yunfan Shi, RLE Yanmeng Yang, SMART Centre, Singapore

GRADUATE STUDENTS

Alexander Bevacqua, BE Hans Gaensbauer, EECS Yejin Park, EECS Jerome Tan, Singapore SMART Centre / NTU, Singapore Eric Wynne, EECS

RESEARCH ENGINEER

Nicholas Ng, SMART Centre, Singapore

SUPPORT STAFF

Arlene Wint, Administrative Assistant

SELECTED PUBLICATIONS

K. Z. Kwek, G. Llanora, K. Quek, C. R. Goh, N. Ng, J. Han, and K. T. Yeo, "Whole Blood Biophysical Immune Profiling of Newborn Infants Correlates with Immune Responses," *Pediatric Research*, DOI: 10.1038/s41390-025-03952-y, 2025.

H. Jeon and J. Han, "Microfluidics with Machine Learning for Biophysical Characterization of Cells," *Annual Review of Analytical Chemistry*, vol. 18, DOI: 10.1146/annurev-anchem-061622-025021, 2025.

X. Wu, J. J. R. Raymond, Y. Liu, A. J. Odematt, W.-X. Sin, D. B. L. Teo, M. Natarajan, I. C. Ng, M. E. Birnbaum, T. K. Lu, J. Han, S. L. Springs, and H. Yu, "Rapid Universal Detection of High-Risk and Low-Abundance Microbial Contaminations in CAR-T Cell Therapy," *Small Methods*, DOI: 10.1002/smtd.202500253, 2025.

H. Jeon, J. Yoon, and J. Han, "Membrane-Free Microplastic Removal Based on a Multiplexed Spiral Inertial Microfluidic System," *Separation and Purification Technology*, vol. 354, no. 5, p. 129113, 2025.

J. Tan, J. Chen, D. Roxby, W. H. Chooi, T. D. Nguyen, S. Y. Ng, J. Han, and S. Y. Chew, "Magnetic Resonance Relaxometry to Evaluate the Safety and Quality of Induced Pluripotent Stem Cell-Derived Spinal Cord Progenitor Cells," *Stem Cell Research & Therapy*, vol. 15, p. 465, 2024.

H. Gaensbauer, D. H. Park, A. Bevacqua, and J. Han, "Contact Free On-Line Monitoring of Bioreactor Cell Cultures with Magnetic Resonance Relaxometry," *Analytical Chemistry*, vol. 96, no. 49, pp. 19466–19472, 2024.

E. Wynne, J. Yoon, D. Park, M. Cui, C. Morris, J. Lee, Z. Wang, S. Yoon, and J. Han, "Regeneration of Spent Culture Media for Sustainable and Continuous mAb Production via Ion Concentration Polarization," *Biotechnology and Bioprocessing*, vol. 122, no. 2, pp. 373–381, 2024.

M. Kang, Y. Yang, H. Zhang, Y. Zhang, Y. Wu, V. Denslin, R. B. Othman, Z. Yang, and J. Han, "Comparative Analysis on Serum and Serum-Free Medium Cultured Mesenchymal Stem Cells for Cartilage Repair," *International J. of Molecular Sciences*, vol. 25, no. 19, p. 10627, 2024.

C. A. Tee, D. N. Roxby, R. Othman, V. Denslin, K. S. Bhat, Z. Yang, J. Han, L. Tucker-Kellogg, and L. A. Boyer, "Metabolic Modulation to Improve MSC Expansion and Therapeutic Potential for Articular Cartilage Repair," *Stem Cell Research & Therapy*, vol. 15, p. 308, 2024.

Y. Liu, J. J. Raymond, X. Wu, P. W. L. Chua, S. Y. H. Ling, C. C. Chan, C. Chan, J. X. Y. Loh, M. X. Y. Song, M. Y. Y. Ong, P. H. Ho, M. E. Mcbee, S. L. Springs, H. Yu, and J. Han, "Electrostatic Microfiltration (EM) Enriches and Recovers Viable Microorganisms at Low-Abundance in Large-Volume Samples and Enhances Downstream Detection," *Lab on a Chip*, vol. 24, pp. 4275–4287, 2024.

R. Lu, Y. Ang, K.-W. Cheung, K. Y. Quek, W.-X. Sin, E. Lee, S. L. Lim, L.-Y. L. Yung, M. Birnbaum, J. Han, L. F. Cheow, K. Z. Kwek, "iSECRETE: Integrating Microfluidics and DNA Proximity Amplification for Synchronous Single-Cell Activation and IFN- γ Secretion Profiling," *Advanced Science*, vol. 11, no. 40, p. 2309920, 2024.

H. Jeon, C. R. Perez, T. Kyung, M. E. Birnbaum, and J. Han, "Separation of Activated T Cells Using Multidimensional Double Spiral (MDDS) Inertial Microfluidics for High-Efficiency CAR T Cell Manufacturing," *Analytical Chemistry*, vol. 96, no. 26, pp. 10780–10790, 2024.

Ruonan Han

Associate Director of Microsystem Technology Laboratories (MTL)
Director of MTL Center of Integrated Circuits and Systems (CICS)
Professor, Department of Electrical Engineering & Computer Science

Integrated circuits and systems operating from RF to THz frequencies for sensing, communication, metrology, security and quantum applications.

Rm. 39-527A | 617-324-5281 | ruonan @ mit . edu

GRADUATE STUDENTS

Xibi Chen. EECS

Mingran Jia, EECS (co-advised with A. Chandrakasan) Jaehong Jung, EECS (co-advised with A.

Chandrakasan)

Eunseok Lee, EECS (co-advised with A. Chandrakasan) Tiffany Louie, EECS

Krishna Pochana, EECS

Daniel Sheen, EECS (co-advised with F. Lind at MIT Haystack Observatory)

Lejla Skelic, EECS

Pradyot Yadav, EECS (co-advised with T. Palacios)

Yan Xu, EECS

Jinchen Wang, EECS

SUPPORT STAFF

Ava Bowen, Administrative Assistant Elizabeth Kubicki, Administrative Assistant

SELECTED PUBLICATIONS

J. Jung, E. Lee, D. Han, J. Wang, A. Chandrakasan, and R. Han, "A 55.8-to-64.2GHz, $58.3 \mathrm{fs_{rms}}$ -Jitter, -250.2dB-FoM $_{\mathrm{J}}$ Fractional-N Cascaded PLL in 28nm CMOS," *IEEE VLSI Circuits Symposium*, Kyoto, Japan, Jun. 2025.

M. Jia, J. Wang, J. Jung, X. Chen, E. Lee, A. Chandrakasan, and R. Han, "A Fully Integrated 263-GHz Retro-Backscatter Circuit with 105° Reading Angle and 12-dB Conversion Loss," *IEEE Radio-Frequency Integrated Circuit Symposium (RFIC)*, San Francisco, CA, Jun. 2025.

- P. Yadav, J. Wang, D. Baig, J. Pastrana-Gonzales, J. Niroula, P. Darmawi-Isakandar, A. Islam, M. Bakir, R. Han, and T. Palacios, "3D-Millimeter Wave Integrated Circuit (3D-mmWIC): A Gold-Free 3D-Integration Platform for Scaled RF GaN-on-Si Dielets with Intel 16 Si CMOS," IEEE Radio-Frequency Integrated Circuit Symposium (RFIC), San Francisco, CA, Jun. 2025.
- J. Wang, D. Sheen, X. Chen, S. Nagle and R. Han, "A 232-260GHz CMOS Amplifier-Multiplier Chain with a Low-Cost, Matching-Sheet-Assisted Radiation Package and 11.1dBm Total Radiated Power," *IEEE Intl. Solid-State Circuit Conf. (ISSCC)*, San Francisco, CA, Feb. 2025.
- J. Wang, I. B. W. Harris, M. I. Ibrahim, D. Englund and R. Han, "A Bidirectional Wireless THz Datalink Designed to Maximize the Information-per-Heat Transfer to A Cryogenic Device," *Nature Electronics*, Mar. 2025.

- X. Chen, N. M. Monroe, G. C. Dogiamis, R. A. Stingel, P. Myers, and R. Han, "A 265-GHz CMOS Reflectarray with 98×98 Elements for 1°-Wide Beam Forming and High-Angular-Resolution Radar," *IEEE J. of Solid-State Circuits (JSSC)*, vol. 59, no. 11, Nov. 2024.
- L. Li, L. De Santis, I. Harris, K. Chen, I. Christen, M. Trusheim, Y. Song, Y. Gao, C. Errando-Herranz, J. Du, G. Clark, M. Ibrahim, G. Gilbert, R. Hanand D. Englund, "Heterogeneous Integration of Spin-Photon Interfaces with A CMOS Platform," *Nature*, 630, 70-76, 2024.
- X. Chen, N. M. Monroe, G. C. Dogiamis, R. A. Stingel, P. Myers, and R. Han, "A 265-GHz CMOS Reflectarray with 98×98 Elements for 1°-Wide Beam Forming and High-Angular-Resolution Radar," *IEEE J. of Solid-State Circuits (JSSC)*, 2024.
- E. Lee, M. I. W. Khan, X. Chen, U. Banerjee, N. Monroe, R. T. Yazicigil, R. Han, A. P. Chandrakasan, "A 1.54 mm², 264-GHz Wake-Up Receiver with Integrated Cryptographic Authentication for Ultra-Miniaturized Platforms," *IEEE J. of Solid-State Circuits (JSSC), CICC Special Issue*, vol. 59, no. 3, 2024.
- R. Han, "The Pursuit of Practical Applications of THz CMOS Chips," *IEEE Custom Integrated Circuit Conf. (CICC)*, Denver, CO, Apr. 2024. (Invited)
- J. Wang, I. Harris, X. Chen, D. Englund and R. Han, "A CMOS-Integrated Color Center Pulse-Sequence Control and Detection System," *IEEE Custom Integrated Circuit Conf. (CICC)*, Denver, CO, Apr. 2024.
- E. Lee, X. Chen, M. Ashok, J. Won, A. Chandrakasan and R. Han, "A Packageless Anti-Tampering Tag Utilizing Unclonable Sub-THz Wave Scattering at the Chip-Item Interface," *IEEE Intl. Solid-State Circuit Conf. (ISSCC)*, San Francisco, CA, Feb. 2024.

Song Han

Associate Professor

Department of Electrical Engineering & Computer Science

Machine learning, artificial intelligence, model compression, hardware acceleration

Rm. 38-344 | 617-253-0086 | songhan @ mit . edu

POSTDOCTORAL ASSOCIATE

Qinghao Hu, EECS

GRADUATE STUDENTS

Muyang Li, EECS Jiaming Tang, EECS Guangxuan Xiao, EECS Shang Yang, EECS Zhekai Zhang, EECS Zhuoyang Zhang, EECS

UNDERGRADUATE STUDENT

Shreya Chaudhury, EECS Maggie Liu, EECS

SUPPORT STAFF

Jami L. Mitchell, Project Coordinator

SELECTED PUBLICATIONS

S. Yang, J. Guo, H. Tang, Q. Hu, G. Xiao, J. Tang, Y. Lin, Z. Liu, Y. Lu, and S. Han, "LServe: Efficient Long-sequence LLM Serving with Unified Sparse Attention," Conference on Machine Learning and Systems 2025.

Y. Lin, H. Tang, S. Yang, Z. Zhang, G. Xiao, C. Gan, and S. Han, "QServe: W4A8KV4 Quantization and System Co-design for Efficient LLM Serving," *Conference on Machine Learning and Systems* 2025.

M. Li, Y. Lin, Z. Zhang, T. Cai, X. Li, J. Guo, E. Xie, C. Meng, J.-Y. Zhu, and S. Han, "SVDQuant: Absorbing Outliers by Low-Rank Components for 4-Bit Diffusion Models," *International Conference on Learning Representations (ICLR)* 2025.

H. Xi, H. Cai, L. Zhu, Y. Lu, K. Keutzer, J. Chen, and S. Han, "COAT: Compressing Optimizer States and Activation for Memory-Efficient FP8 Training," *International Conference on Learning Representations (ICLR)* 2025.

E. Xie, J. Chen, J. Chen, H. Cai, H. Tang, Y. Lin, Z. Zhang, M. Li, L. Zhu, L. Lu, and S. Han, "SANA: Efficient High-Resolution Image Synthesis with Linear Diffusion Transformers," *International Conference on Learning Representations (ICLR)* 2025.

G. Xiao, J. Tang, J. Zuo, J. Guo, S. Yang, H. Tang, Y. Fu, and S. Han, "DuoAttention: Efficient Long-Context LLM Inference with Retrieval and Streaming Heads," *International Conference on Learning Representations (ICLR)* 2025.

J. Chen, H. Cai, J. Chen, E. Xie, S. Yang, H. Tang, M. Li, Y. Lu, and S. Han, "Deep Compression Autoencoder for Efficient High-Resolution Diffusion Models," *International Conference on Learning Representations (ICLR)* 2025.

Y. Chen, F. Xue, D. Li, Q. Hu, L. Zhu, X. Li, Y. Fang, H. Tang, S. Yang, Z. Liu, E. He, H. Yin, P. Molchanov, J. Kautz, L. Fan, Y. Zhu, Y. Lu, and S. Han, "LongVILA: Scaling Long-Context Visual Language Models for Long Videos," *International Conference on Learning Representations (ICLR)*, 2025.

Y. Lin, Z. Zhang, and S. Han, "LEGO: Spatial Accelerator Generation and Optimization for Tensor Applications," 2025 IEEE International Symposium on High-Performance Computer Architecture (HPCA), 2025.

H. Tang, Y. Wu, S. Yang, E. Xie, J. Chen, J. Chen, Z. Zhang, H. Cai, Y. Lu, and S. Han, "HART: Efficient Visual Generation with Hybrid Autoregressive Transformer," *International Conference on Learning Representations (ICLR)* 2025.

Z. Liu, Z. Zhang, S. Khaki, S. Yang, H. Tang, C. Xu, K. Keutzer, and S. Han, "Sparse Refinement for Efficient High-Resolution Semantic Segmentation," *European Conference on Computer Vision (ECCV)* 2024.

X. Xiao, T. Yin, W. T. Freeman, F. Durand, and S. Han, "Fast-Composer: Tuning-Free Multi-Subject Image Generation with Localized Attention," *International J. of Computer Vision*, 2024.

Juejun (JJ) Hu

John F. Elliott Professor of Materials Science & Engineering Department of Materials Science & Engineering Integrated photonics, silicon photonics, optical metasurfaces.

Rm. 13-4054 | 302-766-3083 | hujuejun @ mit . edu

RESEARCH SCIENTISTS

Tian Gu, MRL Zhaoyi Li, DMSE

POSTDOCTORAL ASSOCIATES

Lamyaa Almehmadi, DMSE Rui Chen, DMSE June Sang Lee, DMSE Louis Martin, DMSE Lidan Zhang, DMSE

GRADUATE STUDENTS

Kaiyuan Chen, DMSE Cosmin Constantin-Popescu, DMSE Khoi Phuong Dao, DMSE Zhiping He, DMSE Brian Mills, DMSE Maarten Peters, DMSE Zhiping Xu, DMSE

SUPPORT STAFF

Sarah Ciriello. Administrative Assistant

SELECTED PUBLICATIONS

S. Yu, L. Ranno, Q. Du, S. Serna, C. McDonough, N. Fahrenkopf, T. Gu, and J. Hu, "Free-form Micro-optics Enabling Ultra-broadband Low-loss Fiber-to-chip Coupling," *Laser Photonics Rev.* 17, 2200025 (2023).

C. Ríos, Q. Du, Y. Zhang, C. Popescu, M. Shalaginov, P. Miller, C. Roberts, M. Kang, K. Richardson, T. Gu, S. Vitale, and J. Hu, "Ultra-Compact Nonvolatile Phase Shifter Based on Electrically Reprogrammable Transparent Phase Change Materials," *PhotoniX* 3, 26 (2022).

Y. Zhang, C. Fowler, J. Liang, B. Azhar, M. Shalaginov, S. Deckoff-Jones, S. An, J. Chou, C. Roberts, V. Liberman, M. Kang, C. Ríos, K. Richardson, C. Rivero-Baleine, T. Gu, H. Zhang, and J. Hu, "Electrically Reconfigurable Nonvolatile Metasurface Using Low-Loss Optical Phase Change Material," *Nat. Nanotechnology* 16, 661-666 (2021).

M. Shalaginov, S. An, Y. Zhang, F. Yang, P. Su, V. Liberman, J. Chou, C. Roberts, M. Kang, C. Ríos, Q. Du, C. Fowler, A. Agarwal, K. Richardson, C. Rivero-Baleine, H. Zhang, J. Hu, and T. Gu, "Reconfigurable All-dielectric Metalens with Diffraction Limited Performance," *Nat. Communications* 12, 1225 (2021).

M. Shalaginov, S. An, F. Yang, P. Su, D. Lyzwa, A. Agarwal, H. Zhang, J. Hu, and T. Gu, "Single-Element Diffraction-Limited Fisheye Metalens," *Nano Letts*. 20, 7429-7437(2020).

Y. Zhang, J. Chou, J. Li, H. Li, Q. Du, A. Yadav, S. Zhou, M. Shalaginov, Z. Fang, H. Zhong, C. Roberts, P. Robinson, B. Bohlin, C. Rios, H. Lin, M. Kang, T. Gu, J. Warner, V. Liber-man, K. Richardson, and J. Hu, "Broadband Transparent Optical Phase Change Materials for High-Performance Nonvolatile Photonics," *Nat. Communications* 10, 4279(2019).

Y. Zhang, Q. Du, C. Wang, T. Fakhrul, S. Liu, L. Deng, D. Huang, P. Pintus, J. Bowers, C. A. Ross, J. Hu, and L. Bi, "Monolithic Integration of Broadband Optical Isolators for Polarization-diverse Silicon Photonics," *Optica* 6, 473-478 (2019).

D. Kita, B. Miranda, D. Favela, D. Bono, J. Michon, H. Lin, T. Gu, and J. Hu, "High-performance and Scalable On-chip Digital Fourier Transform Spectroscopy," *Nat. Communications* 9, 4405 (2018).



Distinguished Professor
Department of Electrical Engineering & Computer Science

Rm. 36-465 | 617-253-1573 | qhu @ mit . edu

COLLABORATORS

Jianrong Gao, Delft University Kevin Lascola, Thorlabs John L. Reno, Sandia National Lab. Zbig Wasilewski, University of Waterloo Gerard Wysocki, Princeton University

GRADUATE STUDENTS

Andrew Paulsen, EECS

SUPPORT STAFF

Shayne Fernandes, Administrative Assistant

SELECTED PUBLICATIONS

Q. Hu, "Broadband LWIR frequency combs and traveling-wave THz amplifiers," International Quantum Cascade Lasers School and Workshop (IQCLSW2024), Ischia Island (Napoli), Italy, Aug. 25-30 (2024) (Invited)

J. R. G. Silva, C. K. Walker, C. Kulesa, A. Young, J. Gao, Q. Hu, J. Hesler, A. Emrich, P. Hartogh, W. M. Laauwen, G. D. Lange, and P. Roelfsema, "High-Resolution Receiver (HiRX) for the Single Aperture Large Telescope for Universe Studies (SALTUS)," *J. of Astronomical Telescopes, Instruments, and Systems*, 10, 042308 (2024).

G. Chin, C. M. Anderson, J. Bergner, N. Biver, G. L. Bjoraker, T. Cavalie, M. A. DiSanti, J. Gao, P. Hartogh, L. K. Harding, Q. Hu, D. Kim, C. Kulesa, G. De Lange, D. Leisawitz, R. C. Levy, A. W. Lichtenberger, D. P. Marrone, J. Najita, T. Newswander, G. H. Rieke, D. Rigopoulou, P. R. Roelsema, N. X. Roth, K. Schwarz, Y. Shirley, J. Spilker, A. A. Stark, F. Van Der Tak, Y. Takashima, A. Tielens, D. J. Willner, E. J. Wollack, S. Yates, E. Young, and C. K. Walker, "Single Aperture Large Telescope for Universe Studies (SALTUS): Science Overview," accepted for publication in *J. of Astronomical Telescopes, Instruments, and Systems*, 10, 042310 (2024).

T. Zeng, Y. Dikmelik, F. Xie, K. Lascola, D. Burghoff, and Q. Hu, "Ultrabroadband Air-dielectric Double-Chirped Mirrors for Laser Frequency Combs," in review, *Light: Science & Applications* (2025).

Rafael Jaramillo

Stavros and Matoula Salapatas Associate Professor Department of Materials Science and Engineering Developing compound semiconductors for application in photonics, microelectronics, communication, and energy conversion. Emphasis on chalcogenide thin film processing, including molecular beam epitaxy (MBE) and advanced characterization.

Rm. 13-5025 | 617-324-6871 | rjaramil @ mit.edu

POSTDOCTORAL ASSOCIATES

Zhenjing Liu, MRL
Olivia Schneble, DMSE
Graduate Students
Tao Cai, DMSE
Jessica Dong, DMSE
Jiahao Dong, DMSE
Rishabh Kothari, DMSE
Jack Van Sambeek, DMSE

K. Ye, I. Sadeghi, M. Xu, J. Van Sambeek, T. Cai, J. Dong, R. Kothari, J. M. LeBeau, and R. Jaramillo, "A Processing Route to Chalcogenide Perovskites Alloys with Tunable Band Gap via Anion Exchange," Advanced Functional Materials 34(44): 2405135, 2024.

SELECTED PUBLICATIONS

J. V. Sambeek, J. Dong, A. V. Ievlev, T. Cai, I. Sadeghi, and R. Jaramillo, "Electronic Mobility, Doping, and Defects in Epitaxial $BaZrS_3$ Chalcogenide Perovskite Thin Films," arXiv preprint arXiv:2505.16016, 2025.

Z. Liu, Q. Mao, V. Kamboj, R. Kothari, P. Miller, K. Reidy, A. C. T. van Duin, R. Jaramillo, and F. M. Ross, "Epitaxial Formation of Ultrathin HfO_2 on Graphene by Sequential Oxidation," arXiv preprint arXiv:2504.11693, 2025.

A. C. Foucher, W. Mortelmans, W. Bing, Z. Sofer, R. Jaramillo, and F. M. Ross, "Structural Changes in HfSe₂ and ZrSe₂ Thin Films with Various Oxidation Methods," *J. of Materials Chemistry C* 12(26): 9677–9684, 2024.

J. Dong and R. Jaramillo, "A Junction Photoconductive Semiconductor Switch (J-PCSS) in AlN With Sub-Band Gap Responsivity and Accelerated Turn-Off Speed," *IEEE Electron Device Letts*. 46(6): 916–919, 2025.

M. Xu, K. Ye, I. Sadeghi, R. Jaramillo, and J. M. LeBeau, "Atomic Structure of Self-Buffered BaZr(S,Se) $_3$ Epitaxial Thin Film Interfaces," *J. of Vacuum Science & Technology A* 42(6): 063207, 2024.

K. Ye, M. Menahem, T. Salzillo, F. Knoop, B. Zhao, S. Niu, O. Hellman, J. Ravichandran, R. Jaramillo, and O. Yaffe, "Differing Vibrational Properties of Halide and Chalcogenide Perovskite Semiconductors and Impact on Optoelectronic Performance," Physical Review Materials 8(8): 085402, 2024.

J. Dong and R. Jaramillo, "Modeling Defect-Level Switching for Nonlinear and Hysteretic Electronic Devices," *J. of Applied Physics* 135(22): 224501, 2024.

Long Ju

Lawrence and Sarah W. Biedenharn Career Development Assistant Professor of Science, Department of Physics

Two-dimensional materials, electrical properties, optical spectroscopy, opto-

Rm. 13-2005 | 617-253-4828 | long ju @ mit . edu

POSTDOCTORAL ASSOCIATES

Zhengguang Lu, Physics Wenhao Zheng, Physics

GRADUATE STUDENTS

Jixiang Yang, Physics Tonghang Han, Physics Junseok Seo, Physics Dasol Kim, Physics Shenyong Ye, DMSE Zacharia Hadjri, Physics

UNDERGRADUATE STUDENT

Emily Aitken, Physics Proyoga Liong, RLE

SUPPORT STAFF

Gerry Miller, Administrative Assistant

SELECTED PUBLICATIONS

T. Han, Z. Lu, Z. Hadjri, L. Shi, Z. Wu, W. Xu, Y. Yao, A. A. Cotton, O. S. Sedeh, H. Weldeyesus, J. Yang, J. Seo, S. Ye, M. Zhou, H. Liu, G. Shi, Z. Hua, K. Watanabe, T. Taniguchi, P. Xiong, D. M. Zumbühl, L. Fu, and L. Ju, "Signatures of Chiral Superconductivity in Rhombohedral Graphene," Nature (2025). [Link]

J. Yang, X. Shi, S. Ye, C. Yoon, Z. Lu, V. Kakani, T. Han, J. Seo, L. Shi, K. Watanabe, T. Taniguchi, F. Zhang, and L. Ju, "Diverse Impacts of Spin-Orbit Coupling on Superconductivity in Rhombohedral Graphene," Nature Materials (2025). [Link]

Lu, T. Han, Y. Yao, J. Yang, J. Seo, L. Shi, S. Ye, K. Watanabe, T. Taniguchi, and L. Ju, "Extended Quantum Anomalous Hall States in Graphene/hBN Moiré Superlattices," Nature 637: 1090-1095, 2025. [Link]

J. Seo, Z. Lu, S. Park, J. Yang, F. Xia, S. Ye, Y. Yao, T. Han, L. Shi, K. Watanabe, T. Taniguchi, A. Yacoby, and L. Ju, "On-Chip Terahertz Spectroscopy for Dual-Gated van der Waals Heterostructures at Cryogenic Temperatures," Nano Letts. 24(47): 15060-15067, 2024. [Link]

L. Ju, A. H. MacDonald, K. F. Mak, J. Shan, and X. Xu, "The Fractional Quantum Anomalous Hall Effect," Nature Reviews Materials 9: 455-459, 2024. [Link]

Z. Lu, T. Han, Y. Yao, A. P. Reddy, J. Yang, J. Seo, K. Watanabe, T. Taniguchi, L. Fu, and L. Ju, "Fractional Quantum Anomalous Hall Effect in Multilayer Graphene," Nature 626: 759-764, 2024. [Link]

T. Han, Z. Lu, Y. Yao, J. Yang, J. Seo, C. Yoon, K. Watanabe, T. Taniguchi, L. Fu, F. Zhang, and L. Ju, "Large Quantum Anomalous Hall Effect in Spin-Orbit Proximitized Rhombohedral Graphene," Science 384: 647-651, 2024. [Link]

T. Han, Z. Lu, G. Scuri, J. Sung, J. Wang, T. Han, K. Watanabe, T. Taniguchi, L. Fu, H. Park, and L. Ju, "Orbital Multiferroicity in Rhombohedral Graphene," Nature 623: 41-47, 2023. [Link]

T. Han, Z. Lu, G. Scuri, J. Sung, J. Wang, T. Han, K. Watanabe, T. Taniguchi, H. Park, and L. Ju, "Correlated Insulator and Chern Insulators in Pentalayer Rhombohedral Stacked Graphene," Nature Nanotechnology (2023). [Link]

J. Yang, G. Chen, T. Han, Q. Zhang, Y.-H. Zhang, L. Jiang, B. Lyu, et al., "Spectroscopy Signatures of Electron Correlations in a Trilayer Graphene/hBN Moiré Superlattice," Science 375(6586): 1295-1299, 2022.

T. Han, J. Yang, Q. Zhang, L. Wang, K. Watanabe, T. Taniguchi, P. L. McEuen, and L. Ju, "Accurate Measurement of the Gap of Graphene/hBN Moiré Superlattice Through Photocurrent Spectroscopy," Physical Review Letts. (2021).

L. Ju, L. Wang, T. Cao, T. Taniguchi, K. Watanabe, S. G. Louie, F. Rana, et al., "Tunable Excitons in Bilayer Graphene," Science 358(6365): 907–910, 2017.

L. Jiang, Z. Shi, B. Zeng, S. Wang, J.-H. Kang, T. Joshi, C. Jin, et al., "Soliton-Dependent Plasmon Reflection at Bilayer Graphene Domain Walls," Nature Materials 15(8): 840-844, 2016.

D. Wong, J. Velasco Jr., L. Ju, J. Lee, S. Kahn, H.-Z. Tsai, C. Germany, et al., "Characterization and Manipulation of Individual Defects in Insulating Hexagonal Boron Nitride Using Scanning Tunnelling Microscopy," Nature Nanotechnology 10(11): 949, 2015.

Philip "Donnie" Keathley

Principal Research Scientist
Co-Group Leader, QNN Group
Department of Electrical Engineering & Computer Science

Spans the areas of ultrafast optics, strong-field science, attosecond physics, nanophotonics, and plasmonics. At the Quantum Nanostructures and Nanofabrication group he develops petahertz electronics, nanoscale free-electron light sources, and radiation-hard nanoscale vacuum-electronics.

Rm. 36-293 | 617-324-67209 | pdkeat2 @ mit . edu

CO-GROUP LEADER/ PRINCIPAL RESEARCH SCIENTIST

Prof. Karl Berggren, RLE

RESEARCH SCIENTIST

Sang-Hoon Nam, RLE

POSTDOCTORAL ASSOCIATES

Gian Luca Dolso, RLE Felix Ritzkowski, RLE

GRADUATE STUDENTS

Joseph Alongi, EECS
Emma Batson, EECS, NSF Fellow
Adina Bechhofer, EECS
Camron Blackburn, MAS (co-supervised with N.
Gershenfeld)
Matteo Castellani, EECS

Reed Foster, EECS, NDSEG Fellow
Evan Golden, EECS, Lincoln Lab Fellow
Francesca Incalza, EECS
Ben Mazur, EECS, NDSEG Fellow
Owen Medeiros, EECS
Dip Joti Paul, EECS
Malick Sere, EECS
Alejandro Simon, EECS
John Simonaitis, EECS

UNDERGRADUATE STUDENTS

Hanson Nguyen, MSRP Joshua Piety, EECS James Shi, EECS Pavan Yeddanapudi, EECS Andi Qu, EECS Eric Zhan, EECS Amy Chen, EECS

VISITORS

Giorgia Ciuffarella, Polytechnic of Turin & École Polytechnique Fédérale de Lausanne Gabriel LeGuay, Federal Polytechnique School of Zurich

Davide Mondin, École Polytechnique Fédérale de Lausanne

SUPPORT STAFF

Dorothy Fleischer, Administrative Assistant Rinske Wijtmans Robinson, Administrative Assistant

SELECTED PUBLICATIONS

M. Castellani, O. Medeiros, A. Buzzi, R. A. Foster, M. Colangelo, and K. K. Berggren, "A Superconducting Full-wave Bridge Rectifier," *Nature Electronics*, pp. 1–9, May 2025. [Link]

M. Yeung *et al.*, "Bandwidth of Lightwave-Driven Electronic Response from Metallic Nanoantennas," *Nano Letts.*, vol. 25, no. 13, pp. 5250–5257, Apr. 2025. [Link]

L. C. Blackburn, A. Wynn, K. K. Berggren, and N. Gershenfeld, "A Compact Bit Serial Memory Cell for Adiabatic Quantum Flux Parametron Register Files," *IEEE Transactions on Applied Superconductivity*, pp. 1–5, Feb. 2025. [Link]

F. Ritzkowsky *et al.*, "On-chip Petahertz Electronics for Single-shot Phase Detection," *Nature Communications*, vol. 15, no. 1, pp. 1–8, Nov. 2024. [Link]

M. Yeung, L.-T. Chou, M. Turchetti, F. Ritzkowsky, K. K. Berggren, and P. D. Keathley, "Lightwave-electronic harmonic frequency mixing," *Science Advances*, vol. 10, no. 33, p. eadq0642, Aug. 2024. [Link]

M. Castellani *et al.*, "Nanocryotron ripple counter integrated with a superconducting nanowire single-photon detector for megapixel arrays," *Phys. Rev. Appl.*, vol. 22, no. 2, p. 024020, Aug. 2024. [Link]

A. Simon, R. Foster, O. Medeiros, M. Castellani, E. Batson, and K. K. Berggren, "Characterizing and Modeling the Influence of Geometry on the Performance of Superconducting Nanowire Cryotrons," *IEEE Transactions on Applied Superconductivity*, vol. 35, no. 5, pp. 1–5, Aug. 2024. [Link]

I. Charaev *et al.*, "Single-photon Detection Using Largescale High-temperature MgB2 Sensors at 20 K," *Nature Communications*, vol. 15, no. 1, p. 3973, May 2024. [Link]

M. Colangelo *et al.*, "Molybdenum Silicide Superconducting Nanowire Single-Photon Detectors on Lithium Niobate Waveguides," *ACS Photonics*, Jan. 2024. [Link]

Jeehwan Kim

Associate Professor of Materials Science and Engineering Principal Investigator of Research Laboratory of Electronics Department of Mechanical Engineering Remote epitaxy, Two-dimensional materials, 2D material-based layer transfer, III-V / III-N electronics, Complex oxides-based applications, Heterogeneous integration, Flexible electronics, Electronic skin, Sensor fusion, Neuromorphic computing.

Rm. 38-276 | 617-324-1948 | jeehwan @ mit . edu

POSTDOCTORAL ASSOCIATES

Ki Seok Kim, RLE
Sangho Lee, MechE
Jae Hwan Kim, MechE
Young Jin Yoo, RLE
Kuangye Lu, RLE
Jung-El Ryu, RLE
Seong Ho Cho, RLE
Atharva Sahasrabudhe, RLE
Yuxing Ren, RLE
Seokje Lee, RLE

GRADUATE STUDENTS

Chen Chang, DMSE Jin Feng, MechE Ne Myo Han, MechE Doa Kwon, MechE Kangkyu Kwon, MechE Doyoon Lee, DMSE Giho Lee, MechE Xinyuan Zhang, DMSE

SUPPORT STAFF

John Mayo, Administrative Assistant

SELECTED PUBLICATIONS

X. Zhang, O. Ericksen, S. Lee, M. Akl, M.-K. Song, H. Lan, P. Pal, et al., "Atomic Lift-Off of Epitaxial Membranes for Cooling-Free Infrared Detection," *Nature* 641: 95–105, 2025.

K. S. Kim, S. Seo†, J. Kwon, D. Lee, C. Kim, J.-E. Ryu, J. Kim, et al., "Growth-Based Monolithic 3D Integration of Single-Crystal 2D Semiconductors," *Nature* 636(8043): 615–621, 2024.

S. Lee, X. Zhang, P. Abdollahi, M. R. Barone, C. Dong, Y. J. Yoo, M.-K. Song, et al., "Route to Enhancing Remote Epitaxy of Perovskite Complex Oxide Thin Films," *ACS Nano* 18(45): 31225–31233, 2024.

S. Lee, M.-K. Song, X. Zhang, J. M. Suh, J.-E. Ryu, and J. Kim, "Mixed-Dimensional Integration of 3D-on-2D Heterostructures for Advanced Electronics," *Nano Letts.* 24(30): 9117–9128, 2024.

K. S. Kim, J. Kwon, H. Ryu, C. Kim, H. Kim, E.-K. Lee, D. Lee, et al., "The Future of Two-Dimensional Semiconductors Beyond Moore's Law," *Nature Nanotechnology* 19(7): 895–906, 2024.

K. Lu, J. Shim, K. S. Kim, S. W. Kim, and J. Kim, "2D Materials Can Unlock Single-Crystal-Based Monolithic 3D Integration," *Nature Electronics* 7(6): 416–418, 2024.

B.-I. Park, J. Kim, K. Lu, X. Zhang, S. Lee, J. M. Suh, D.-H. Kim, H. Kim, and J. Kim, "Remote Epitaxy: Fundamentals, Challenges, and Opportunities," *Nano Letts.* 24(10): 2939–2952, 2024.

Jeffrey H. Lang

Vitesse Professor of Electrical Engineering
Department of Electrical Engineering & Computer Science

Analysis, design, and control of electro-mechanical systems with application to traditional rotating machinery and variable-speed drives, micro/nano-scale (MEMS/NEMS) sensors and actuators, flexible structures, and the dual use of actuators as force and motion sensors.

Rm. 10-176 | 617-253-4687 | lang @ mit . edu

GRADUATE STUDENTS

Marco Andrade, EECS Tori Dang, EECS Alex Miller, Aero Astro William Nolan, EECS Oliver Rayner, EECS Emma Warzynek, EECS John Zhang, MechE Jackie Zheng, EECS

UNDERGRADUATE STUDENTS

George Jurgiel, EECS Otto Beal, EECS

SUPPORT STAFF

Eliza Grisante, Administrative Assistant Arlene Wint, Administrative Assistant

SELECTED PUBLICATIONS

J. Z. Zhang, H. G. Bhundiya, K. D. Overby, F. Royer, J. H. Lang, Z. C. Cordero, W. F. Moulder, S. K. Jeon, and M. J. Silver, "Electrostatically-actuated X-band Mesh Reflector with Bend-formed Support Structure," *AIAA J. of Spacecraft and Rockets*, Apr. 30, 2024.

M. M. Qasim, D. M. Otten, J. H. Lang, J. L. Kirtley, and D. J. Perreault, "Comparison of Inverter Topologies for High-Speed Motor Drive Applications," *IEEE Transactions on Power Electronics*. vol 39, 7404-7442. Jun. 2024.

E. F. Wawrzynek, J. Z. Zhang, I. Kymissis, E. S. Olson, H. H. Nakajima, and J. H. Lang, "A Piezoelectric Middle-ear Microphone for Cochlear Implants," *Hilton Head Workshop on Solid-State Sensors and Actuators*, Hilton Head, SC, Jun. 2-6, 2024.

E. F. Wawrzynek, J. Z. Zhang, I. Kymissis, E. S. Olson, J. H. Lang, and H. H. Nakajima, "Progress on an Implantable Microphone for Cochlear Implants," *Mechanics of Hearing*, Ann Arbor, MI, Jun. 8-14, 2024.

A. J. Yeiser, E. F. Wawrzynek, J. Z. Zhang, L. Graf, C. I. McHugh, I. Kymissis, E. S. Olson, J. H. Lang, and H. H. Nakajima, "The UmboMic: A PVDF Cantilever Microphone," *J. of Micromechanics and Microengineering*, Jun. 27, 2024.

S. Mohammadi, W. R. Brenner, J. L. Kirtley, and J. H. Lang, "An Actuator with Magnetic Restoration, Part I: Electromechanical Model and Identification," *IEEE Transactions* on Energy Conversion, vol 39, 4, 2529-2542, Dec. 2024.

S. Mohammadi, W. R. Brenner, J. L. Kirtley, and J. H. Lang, "An Actuator with Magnetic Restoration, Part II: Drive Circuit and Control Loops," *IEEE Transactions on Energy Conversion*, vol 39, 4, 2543-2558, Dec. 2024.

D. T. Brown, A. K. Jackson, J. H. Lang, and D. J. Perreault, "Isolated Piezoelectric-based Power Converter," *COMPEL*, Knoxville, TN, Jun. 22-26, 2025.

T. Dang, J. Han, Z. Wang, Z. Zheng, J. Kong, J. H. Lang, and V. Bulovic, "Low-voltage Electromechanical Switching Based On Low-Dimensional Materials," *International Conference on Solid-State Sensors, Actuators and Microsystems*, Orlando, FL, Jun. 29 – Jul. 3, 2025.

Hae-Seung Lee

ATSC Professor of Electrical Engineering & Computer Science Department of Electrical Engineering & Computer Science

Analog and Mixed-signal Integrated Circuits, with a Particular Emphasis in Data Conversion Circuits in scaled CMOS.

Rm. 39-521 | 617-253-5174 | hslee @ mtl . mit . edu

POSTDOCTORAL ASSOCIATE

Anand Chandrasekhar, EECS

GRADUATE STUDENTS

Mohamed Elsheikh, EECS William Hung, EECS Dimple Kochar, EECS Ana Pascual Lopez, EECS Isabella Romero Estevez, EECS

VISITING SCIENTISTS

Jaejin Jung, Samsung Electronics Jongmi Lee, Samsung Electronics

SUPPORT STAFF

Elizabeth Kubicki, Administrative Assistant

SELECTED PUBLICATIONS

R. Mittal, H. Shibata, S. Patil, E. Krommenhoek, P. Shrestha, G. Manganaro, A. Chandrakasan, and H.-S. Lee, "A 6.4-GS/s1-GHz BW Continuous-Time Pipelined ADC with Time-Interleaved sub-ADC-DAC Achieving 61.7-dB SNDR in 16-nm FinFET," *IEEE J. Solid-State Circuits*, Apr. 2024. [Link]

R. Ho, S. Fuller, H.-S. Lee, and M. Shulaker, "BioSensor Chip for Point-of-Care Diagnostics: Carbon Nanotube Sensing Platform for Bacterial Detection and Identification," *IEEE Trans. Nanotechnology*, pp. 281-285, 10.1109/TNANO.2024.3380997, Mar. 2024.

M. Ashok, R. Chen, T. Jeong, A. P. Chandrakasan, and H.-S. Lee, "Protecting the Mixed Signal Domain: Secure ADCs for Internet of Things Devices," accepted for publication in *Proceedings of IEEE*, 2025.

Associate Professor

Department of Nuclear Science and Engineering

POSTDOCTORAL ASSOCIATES

Chuliang Fu, NSE Michael Landry, NSE & Physics

GRADUATE STUDENTS

Denisse Cordova Carrizales, NSE Mouyang Cheng, CSE & DMSE Abhijatmedhi Chotrattanapituk, EECS Ryotaro Okabe, Chemistry Runbi Rha, NSE Phum Siriviboon, Physics

SUPPORT STAFF

Nick Farmer, Administrative Assistant

SELECTED PUBLICATIONS

N. T. Hung, R. Okabe, A. Chotrattanapituk, and M. Li, "Universal Ensemble-Embedding Graph Neural Network for Direct Prediction of Optical Spectra from Crystal Structures," *Advanced Materials*, vol. 36, no. 18, p. 2409175, 2024.

M. Mandal, A. Chotrattanapituk, K. Woller, L. J. Wu, H. Xu, N. T. Hung, N. Mao, R. Okabe, A. Boonkird, T. Nguyen, N. C. Drucker, X. M. Chen, T. Momiki, J. Li, J. Kong, Y. Zhu, and M. Li, "Precise Fermi-level engineering in a topological Weyl semimetal via fast ion implantation," *Applied Physics Reviews*, vol. 11, no. 2, p. 021429, 2024.

R. Okabe, A. Chotrattanapituk, A. Boonkird, N. Andrejevic, X. Fu, T. S. Jaakkola, Q. Song, T. Nguyen, N. C. Drucker, S. Mu, B. Liao, Y. Cheng, and M. Li, "Virtual Node Graph Neural Network for Full Phonon Prediction," *Nature Computational Science*, vol. 4, pp. 522–529, 2024.

M. Cheng, R. Okabe, A. Chotrattanapituk, and M. Li, "Machine Learning Detection of Majorana Zero Modes from Zero Bias Peak Measurements," *Matter*, vol. 7, no. 9, pp. 2507–2518, 2024.

R. Okabe, S. Xue, J. Vavrek, J. Yu, R. Pavlovsky, V. Negut, B. Quiter, J. Cates, T. Liu, B. Forget, S. Jegelka, G. Kohse, L.-W. Hu, and M. Li, "Tetris-inspired detector with neural network for radiation mapping," *Nature Communications*, vol. 15, p. 3061, 2024.

Luqiao Liu

Associate Professor of Electrical Engineering & Computer Science Department of Electrical Engineering & Computer Science

Spintronics; spin based logic and memory device for digital and neuromorphic computing; nanoscale magnetic material for information storage and microwave application; fabrication technique of magnetic nanodevices; spin related phenomena in semiconductor, topological insulator; magnetic dynamics, spin based quantum system.

Rm. 39-553A | 617-253-0019 | luqiao @ mit.edu

GRADUATE STUDENTS

Josh Chou, Physics Tudor Mocioi, EECS Youfu Qian, EECS Qiuyuan Wang, EECS

SUPPORT STAFF

Maria Markulis, Administrative Assistant

SELECTED PUBLICATIONS

Z. Hu, Z. He, Q. Wang, C.-T. Chou, J. T. Hou, and L. Liu, "Nonlinear Magnetic Sensing with Hybrid Nitrogen-Vacancy/Magnon Systems," *Nano Letts.* 24: 15731, 2024.

C.-T. Chou, S. Ghosh, B. C. McGoldrick, T. Nguyen, G. Gurung, E. Y. Tsymbal, M. Li, K. A. Mkhoyan, and L. Liu, "Large Spin Polarization from Symmetry-Breaking Antiferromagnets in Antiferromagnetic Tunnel Junctions," *Nature Communications* 15: 7840, 2024.

Z. He, C.-T. Chou, E. Park, A. C. Foucher, B. C. McGoldrick, Q. Wang, J. T. Hou, and L. Liu, "Magnetic Tunnel Junctions Featuring the Topological Weyl Semimetal Co₂MnGa," *Physical Review Applied* 22: 044024, 2024.

D. Koh, Q. Wang, B. C. McGoldrick, C.-T. Chou, L. Liu, and M. A. Baldo, "Closed Loop Superparamagnetic Tunnel Junctions for Reliable True Randomness and Generative Artificial Intelligence," *Nano Letts.* 25: 3799, 2025.

B. Khurana, A. C. Kaczmarek, C.-T. Chou, T. Su, K. Lasinger, T. Grossmark, D. C. Bono, L. Liu, and C. A. Ross, "Rare-Earth Iron Garnet Superlattices with Sub-Unit Cell Composition Modulation," *ACS Nano* 18: 35269, 2024.

Y. Fan, T. Fakhrul, J. T. Hou, C.-T. Chou, B. Khurana, Y. Tserkovnyak, L. Liu, and C. A. Ross, "Dynamically Tunable Magnon-Magnon Coupling in a Perpendicular Anisotropy Magnetic Garnet-Ferromagnet Bilayer," *Physical Review Letts.* 134: 126702, 2025.

Scott R. Manalis

David H. Koch Professor in Engineering Departments of Biological and Mechanical Engineering The development of novel instrumentation for cancer research.

Rm. 76-261 | 617-253-5039 | srm @ mit . edu

POSTDOCTORAL ASSOCIATES

Yanqi Wu, KI Jiaquan (Jason) Yu, KI Ye Zhang, KI

GRADUATE STUDENTS

Myra Dada, BE Sarah Duquette, BE Adam Langenbucher, CSB Felicia Rodriguez, BE Thomas Usherwood, HST Amy Zhang, HST

SUPPORT STAFF

Teemu Miettinen, Research Scientist Mariann Murray, Administrative Assistant

SELECTED PUBLICATIONS

B. Roller, C. Hellerschmied, Y. Wu, T. P. Miettinen, S. R. Manalis, M. F. Polz, "Single-cell Mass Distributions Reveal Simple Rules for Achieving Steady-state Growth," *mBio*, vol. 14, no. 5, pp. 01585-23, Oct. 2023.

A. B. Miller, A. Langenbucher, F. H. Rodriguez, L. Lin, C. Bray, S. Duquette, Y. Zhang, D. Goulet, A. A. Lane, D. M. Weinstock, M. T. Hemann, and S. R. Manalis, "Leukemia Circulation Kinetics Revealed Through Blood Exchange Method," *Communications Biology*, vol. 7, no. 483, Apr. 2024.

M. Diaz-Cuadros, T. P. Miettinen, D. Sheedy, C. M. Díaz-García, S. Gapon, A. Hubaud, G. Yellen, S. R. Manalis, W. Oldham, O. Pourquié, "Metabolic Regulation of Species-specific Developmental Rates," *Nature*, vol. 613, no. 7944, pp.550-557, Jul. 2023.

Farnaz Niroui

Associate Professor
Department of Electrical Engineering & Computer Science

Nanofabrication technologies at the few-nanometer-scale and for the emerging nanomaterials. Surfaces, interfaces and forces at the nanoscale. Active nanoscale devices with applications in molecular electronics, nanoelectromechanical systems, reconfigurable nanosystems for next-generation computing, sensing, and photonic quantum information processing.

Rm. 13-3005B | 617-324-7415 | fniroui @ mit.edu

GRADUATE STUDENTS

Shelly Ben-David, EECS
Maxwell Conte, DMSE
Teddy Hsieh, EECS, NSF Fellow
Hohyeon Kim, MechE
Peter Satterthwaite, EECS, NSF Fellow
Jinwoo Sim, EECS
Sarah Spector, EECS, NSF Fellow
Spencer (Weikun) Zhu, ChemE

UNDERGRADUATE STUDENTS

Srinidhi Venkatesh. EECS

SUPPORT STAFF

Phoebe Eboli, Administrative Assistant

SELECTED PUBLICATIONS

P. F. Satterthwaite, W. Zhu, P. Jastrzebska-Perfect, M. Tang, S. O. Spector, H. Gao, H. Kitadai, A. Lu, Q. Tan, S. Tang, Y. Chueh, C. Kuo, C. Lue, J. Kong, X. Ling, and F. Niroui, "Van der Waals Device Integration Beyond The Limits of van der Waals forces via Adhesive Matrix Transfer," *Nature Electronics*, vol. 7, pp. 17-28, 2024.

P. F. Satterthwaite, S. O. Spector, J. Song, and F. Niroui, "Direct van der Waals Integration of 2D Materials for High-performance Chemical Sensors," *Hilton Head Workshop*, 2024.

S. O. Spector, W. Zh, A. Quach, P. F. Satterthwaite, and F. Niroui, "Localized and Conformal Strain Engineering of 2D Materials for Scalable, Functional Devices," *Hilton Head Workshop*, 2024.

A. Sahasrabudhe, L. E. Rupprecht, S. Orguc, T. Khudiyev, T. Tanaka, J. Sands, W. Zhu, A. Tabet, M. Manthey, H. Allen, G. Loke, M. J. Antonini, D. Rosenfeld, J. Park, I. Garwood, W. Yan, F. Niroui, Y. Fink, A. Chandrakasan, D. V. Bohórquez, and P. Anikeeva, "Multifunctional microelectronic fibers enable wireless modulation of gut and brain neural circuits," *Nature Biotechnology*, vol. 42, no. 6, 892-904, 2024.

P. Jastrzebska-Perfect, W. Zhu, M. Saravanapavanantham, Z. Li, S. O. Spector, R. Brenes, P. F. Satterthwaite, R. Ram, and F. Niroui, "On-site growth of perovskite nanocrystal arrays for integrated nanodevices," *Nature Communications*, vol.14, no. 3883, 2023.

Jelena Notaros

Robert J. Shillman (1974) Career Development Associate Professor Department of Electrical Engineering & Computer Science Silicon photonics platforms, devices, and systems for applications including displays, sensing, communications, quantum, and biology.

Rm. 26-343 | 617-253-3073 | notaros @ mit . edu

GRADUATE STUDENTS

Sabrina Corsetti, EECS, MIT Locher Fellow & NSF Fellow Henry Crawford-Eng, EECS, MIT Locher Fellow & NSF Fellow

Daniel DeSantis, EECS, MIT Locher Fellow & NSF Fellow Andres Garcia, EECS, MIT SoE Mathworks Fellow Benjamin Mazur, EECS, NDSEG Fellow

UNDERGRADUATE STUDENT

Maria Schnuck, EECS

SUPPORT STAFF

Pearl Nelson-Greene, Administrative Assistant

SELECTED PUBLICATIONS

S. Corsetti, A. Hattori, E. R. Clements, F. W. Knollmann, M. Notaros, R. Swint, T. Sneh, P. T. Callahan, G. N. West, D. Kharas, T. Mahony, C. Bruzewicz, C. Sorace-Agaskar, R. McConnell, I. Chuang, J. Chiaverini, and J. Notaros, "Integrated-Photonics-Based Systems for Polarization-Gradient Cooling of Trapped Ions," *arXiv* 2411.06025.

E. Clements, F. W. Knollmann, S. Corsetti, Z. Li, A. Hattori, M. Notaros, R. Swint, T. Sneh, M. E. Kim, A. D. Leu, P. Callahan, T. Mahony, G. N. West, C. Sorace-Agaskar, D. Kharas, R. McConnell, C. D. Bruzewicz, I. L. Chuang, J. Notaros, and J. Chiaverini, "Sub-Doppler cooling of a trapped ion in a phase-stable polarization gradient," *arXiv* 2411.06026.

Y. Liu, C. Zhang, D. M. DeSantis, D. Hu, T. Meissner, J. Notaros, and J. Klamkin, "High-Resolution Arrayed Waveguide Grating-Assisted Passive Optical Phased Array for 2D Beam Steering," *Optics Express* 33(4), 7714-7722 (2025).

A. Garcia Coleto, M. Notaros, and J. Notaros, "Visible-Light Uniform and Unidirectional Grating-Based Antennas for Integrated Optical Phased Arrays," *Optics Express* 32(26), 46447-46466 (2024).

D. M. DeSantis, M. R. Torres, A. Garcia Coleto, B. M. Mazur, S. Corsetti, M. Notaros, and J. Notaros, "Spiral Integrated Optical Phased Arrays for Tunable Near-Field-Focusing Emission," *Optics Express* 32(25), 44567-44580 (2024).

T. Sneh, S. Corsetti, M. Notaros, K. Kikkeri, J. Voldman, and J. Notaros, "Optical Tweezing of Microparticles and Cells Using Silicon-Photonics-Based Optical Phased Arrays," *Nature Communications* 15, 8493 (2024).

D. M. DeSantis, B. M. Mazur, M. Notaros, and J. Notaros, "Multi-beam solid-state LiDAR using star-coupler-based optical phased arrays," *Optics Express* 32(21), 36656-36673 (2024).

S. Park, M. Notaros, A. Mohanty, D. Kim, J. Notaros, and S. Mouradian, "Technologies for Modulation of Visible Light and their Applications," *Progress in Quantum Electronics* 97, 100534 (2024). (Invited Review Paper)

S. Corsetti, M. Notaros, T. Sneh, A. Stafford, Z. Page, and J. Notaros, "Silicon-Photonics-Enabled Chip-Based 3D Printer," *Nature Light: Science & Applications* 13, 132 (2024). (Top Downloaded Paper)

M. Notaros, T. Dyer, A. Garcia Coleto, A. Hattori, K. Fealey, S. Kruger, and J. Notaros, "Mechanically-Flexible Wafer-Scale Integrated-Photonics Fabrication Platform," *Nature Scientific Reports* 14, 10623 (2024).

A. Hattori*, T. Sneh*, M. Notaros, S. Corsetti, P. T. Callahan, D. Kharas, T. Mahony, R. McConnell, J. Chiaverini, and J. Notaros, "Integrated Visible-Light Polarization Rotators and Splitters for Atomic Quantum Systems," *Optics Letts.* 49(7), 1794-1797 (2024). (*Equal Contributors)

M. Notaros, A. Garcia Coleto, M. Raval, and J. Notaros, "Integrated Liquid-Crystal-Based Variable-Tap Devices for Visible-Light Amplitude Modulation," *Optics Letts.* 49(4), 1041-1044 (2024).

S. M. Corsetti, A. Hattori, E. R. Clements, F. W. Knollmann, M. Notaros, R. Swint, T. Sneh, P. T. Callahan, G. N. West, D. Kharas, T. Mahony, C. Bruzewicz, C. Sorace-Agaskar, R. McConnell, I. Chuang, J. Chiaverini, and J. Notaros, "Integrated-Photonics-Based Devices and Systems for Polarization-Gradient Cooling of Trapped Ions," in *Proc. of Conference on Lasers and Electro-Optics (CLEO)* (OSA, 2025).

D. M. DeSantis, M. R. Torres, A. Garcia Coleto, B. M. Mazur, S. Corsetti, M. Notaros, and J. Notaros, "Spiral Integrated Optical Phased Arrays for Variable Near-Field Focusing Emission," in *Proc. of Conference on Lasers and Electro-Optics (CLEO)* (OSA, 2025).

A. Garcia Coleto, M. Notaros, and J. Notaros, "Design and Demonstration of Grating-Based Antennas for Visible-Light Integrated Optical Phased Arrays," in *Proc. of Conference on Lasers and Electro-Optics (CLEO)* (OSA, 2025).

William D. Oliver

Henry Ellis Warren (1894) Professor of EECS & Physics Director of Center for Quantum Engineering Associate Director of Research Laboratory of Electronics The materials growth, fabrication, design, measurement of superconducting qubits. The development of cryogenic packaging and control William electronics involving cryogenic CMOS and single-flux quantum digital logic.

Rm. 13-3050 | 617-258-6018 | william.oliver @ mit . edu

RESEARCH SCIENTISTS

Jeff Grover, RLE & CQE Kyle Serniak RLE, CQE & Lincoln Lab Joel I. J. Wang, RLE & CQE

POSTDOCTORAL ASSOCIATES

Réouven Assouly, RLE Farid Hassani Bijarbooneh, RLE Aranya Goswami, RLE Max Hays, RLE, IC Postdoc Fellow Daniel Rodan Legrain, RLE, Rafael del Pino Fellow Jorge Marques, RLE Doug Pinckney, RLE Ilan Rosen, RLE, IC Postdoc Fellow Holly Stemp, RLE Helin Zhang, RLE

GRADUATE STUDENTS

Vaishnavi Addala, EECS, DOE CSGF Fellow Aziza Almanakly, EECS, CBL Fellow Junyoung An, EECS, KFAS Fellow Lamia Ateshian, EECS, CQE Fellow Kate Azar. EECS Will Banner. EECS Cora Barrett, EECS, NSF Fellow Frederike Brockmeyer, EECS, Jacobs Presidential Fellow Shoumik Chowdhury, EECS, NSF Fellow Gabriel Cutter, EECS, NSF Fellow Qi (Andy) Ding, EECS Shantanu Jha, EECS, NSF Fellow Om Joshi. EECS Hanlim (Harry) Kang, EECS, KFAS Fellow Gyunghun (Hoon) Kim, EECS Junghyun Kim, EECS, KFAS Fellow Chris McNally, EECS Miguel Moreira, EECS Sarah Muschinske, EECS David Pahl, EECS Lukas Pahl, EECS David Rower, Physics Chia-Chin Tsai, DMSE, TGET Scholarship recipient Hung-Yu Tsao, EECS

UNDERGRADUATE STUDENTS

Beatriz Yankelevich, EECS, Hertz/ NSF Fellow

Sameia Zaman, EECS, SLB Faculty for the Future Fellow

Justin Chen, Physics Catherine Lowe, EECS Matan Yablon, Physics

VISITING STUDENTS

Anuj Aggarwal, Chalmers University of Technology Jonathan Knoll, ETH Zurich Melvin Mathews, ETH Zurich Mathis Moes, ETH Zurich Sein Park, POSTECH Alex Rommens, ETH Zurich

SUPPORT STAFF

Lenore Buck, Administrative Assistant Chihiro Watanabe, Program Administrator

SELECTED PUBLICATIONS

D. A. Rower, L. Ding, H. Zhang, M. Hays, J. An, P. M. Harrington, I. T. Rosen, J. M. Gertler, T. M. Hazard, B. M. Niedzielski, M.E. Schwartz, S. Gustavsson, K. Serniak, J. A. Grover, and W. D. Oliver, "Suppressing Counter-Rotating Errors for Fast Single-Qubit Gates with Fluxonium," PRX Quantum 5, 040342, Dec. 2024.

I.T. Rosen, S. Muschinske, C. N. Barrett, A. Chatterjee, M. Hays, M. A. DeMarco, A. H. Karamlou, D. A. Rower, R. Das, D. K. Kim, B. M. Niedzielski, M. Schuldt, K. Serniak, M. E. Schwartz, J. L. Yoder, J. A. Grover, and W. D. Oliver, "A Synthetic Magnetic Vector Potential in a 2D Superconducting Qubit Array," Nature Physics 20, 1881-1887, Oct. 2024.

B. Loer, P. M. Harrington, B. Archambault, E. Fuller, B. Pierson, I. Arnquist, K. Harouaka, T. D. Schlieder, D. K. Kim, A. J. Melville, B. M. Niedzielski, J. K. Yoder, K. Serniak, W. D. Oliver, J. L. Orrell, R. Bunker, B. A. VanDevender, and M. Warner, "Abatement of lonizing Radiation for Superconducting Quantum Devices," J. of Instrumentation 19, Po9001, Sep. 2024.

M. T. Randeria, T. M. Hazard, A. Di Paolo, K. Azar, M. Hays, L. Ding, J. An, M. Gingras, B. M. Niedzielski, H. Stickler, J. A. Grover, J. L. Yoder, M. E. Schwartz, W. D. Oliver, and K. Serniak, "Dephasing in Fluxonium Qubits from Coherent Quantum Phase Slips," PRX Quantum 5, 030341, Aug. 2024.

A. H. Karamlou, I. T. Rosen, S. E. Muschinske, C. N. Barrett, A. Di Paolo, L. Ding, P. M. Harrington, M. Hays, R. Das, D. K. Kim, B. M. Niedzielski, M. Schuldt, K. Serniak, M. E. Schwartz, J. L. Yoder, S. Gustavsson, Y. Yanay, J. A. Grover, and W.D. Oliver, "Probing entanglement in a 2D hard-core Bose-Hubbard lattice," Nature 629, 561-566, Apr. 2024.

Tomás Palacios

Director, Microsystems Technology Laboratories Clarence J. LeBel Professor Department of Electrical Engineering and Computer Science Design, fabrication, and characterization of novel electronic devices and systems based on wide bandgap semiconductors & two-dimensional (2-D) materials, polarization & bandgap engineering, transistors for high voltage, submm wave power & digital applications, sensors, heterogeneous integration and advanced packaging.

Rm. 39-567A | 617-324-2395 | tpalacios @ mit . edu

POSTDOCTORAL ASSOCIATES

John Niroula, MTL Jiadi Zhu, MTL Zhongyunshen Zhu, MTL

GRADUATE STUDENTS

Christian Lopez Angeles, EECS Joshua Park, EECS Joshua Perozek, EECS Hridibrata Pal, EECS Aditya Varma, EECS Ashley Goodnight, EECS Ayush Gupta, EECS Jung-Han (Sharon) Hsia, EECS Yixuan Jiao. EECS Hae Won Lee, EECS Kevin Limanta, EECS Cheng-Hsin Liu, EECS Christian Lopez Angeles, EECS Gillian Micale, DMSE Joshua Park, EECS Joshua Perozek, EECS Hridibrata Pal. EECS Srikrishna Chakravarthi, EECS Patrick Darmawi-Iskander, EECS Pradyot Yadav, EECS Aijia Yao, EECS

UNDERGRADUATE STUDENTS

Denis Eruz, SuperUROP Ellie M Bultena, UROP Erin W Zhang, UROP Franck Belemkoabga, SuperUROP Hasan Zeki Yildiz, UROP Jeewoo Kang, UROP Makar Kuznietsov, UROP Matthew A Taylor, UROP Rachel Jiang, UROP

VISITORS

Amadeo de Gracia, Universidad Politécnica de Madrid Ana Cremades, Universidad Complutense de Madrid Michal Prokop, Catalan Institute of Nanoscience and Nanotechnology, Barcelona, Spain Marisa Lopez-Vallejo, Professor, Universidad Politécnica de Madrid Sam Fuller, Analog Devices Ulrich Rohde, Rohde & Schwarz GmbH & Co. KG Yohei Suzuki. Murata

SUPPORT STAFF

Elizabeth Green, Sr. Administrative Assistant Preetha Kingsview, Project Coordinator

SELECTED PUBLICATIONS

- J. Würfl, T. Palacios, H. G. Xing, Y. Hao, and M. Schubert, "Special Topic on Wide- and Ultrawide-Bandgap Electronic Semi-Conductor Devices," *Applied Physics Letts.* 125(7), 2024.
- E. McVay, Z. Lu, A. Golden, L. Ju, and T. Palacios, "AB-Stacked Bilayer Graphene for Hyperspectral LWIR Imaging," *Unconventional Imaging, Sensing, and Adaptive Optics* 2024 13149: 1314902, Oct. 2024. (SPIE)
- T. Palacios, N. Chowdhury, and Q. Xie, "Semiconductor Device With Linear Capacitance," *U.S. Patent* 12,113,061, 2024. (Massachusetts Institute of Technology)
- D. U. Yildirim, J. Jung, A. Elsakka, G. Moschetti, M. M. Lopez, J. Hansryd, T. Palacios, and A. P. Chandrakasan, "A 0.7 cm², 3.5 GHz, –31 dBm Sensitivity Battery-Free 5G Energy-Harvester Backscatterer With 20 s Cold-Start Wake-Up Time for IoT-Enabled Warehouses," *IEEE J. of Solid-State Circuits*, 2024.
- J. Perozek and T. Palacios, "Self-Aligned Fabrication of Vertical, Fin-Based Structures," *J. of Vacuum Science & Technology B* 42(6), 2024.
- J. Zhu, A. Yao, P. Wu, Y. Jiao, J. H. Park, J. Jiang, T. H. Yang, A. S. Gupta, S. S. Cheema, J. Kong, and T. Palacios, "Enhancement-Mode Multichannel MoS₂ Transistor With Spacer Engineering and Design-Technology Co-Optimization Based on the 8" Platform," 2024 IEEE International Electron Devices Meeting (IEDM): 1–4, Dec. 2024. (IEEE)
- R. H. Palash, T. Hossain, B. Sikder, Q. Xie, V. Moroz, T. Palacios, and N. Chowdhury, "Performance Optimization of GaN Based Optically Triggered Transistors," 2024 IEEE International Electron Devices Meeting (IEDM): 1–4, Dec. 2024. (IEEE)
- J.-H. Hsia, J. A. Perozek, and T. Palacios, "First Demonstration of Optically-Controlled Vertical GaN FinFET for Power Applications," *IEEE Electron Device Letts.* 45(5): 774–777, May 2024. [Link]

Carlos M. Portela

Robert N. Noyce Career Development Chair Associate Professor Department of Mechanical Engineering (MechE) Institute for Soldier Nanotechnologies (ISN) Mechanics of materials, emphasis on architected materials, nanomechanics, in situ mechanical testing, extreme dynamic conditions, acoustic metamaterials, precision additive manufacturing

Rm. 1-304 | 617-715-2680 | cportela @ mit . edu

POSTDOCTORAL ASSOCIATES

Mohammad Charara, MechE, MIT Engineering Excellence Fellow Tiemo Pedergnana, MechE Jet Lem, MechE James U. Surjadi, MechE Lei Wu, MechE

GRADUATE STUDENTS

Thomas Butruille, MechE Andrew Chen, MechE Somayajulu Dhulipala, MechE Michael Espinal, MechE Rishi Komalapati, MechE Ayan Kumar, MechE Rachel Sun, MechE Ling Xu, MechE

SUPPORT STAFF

Janet Maslow. Administrative Assistant

SELECTED PUBLICATIONS

S. Dhulipala, C. M. Portela, "Curvature-guided Mechanics and Design of Spinodal and Shell-based Architected Materials," *J. Mech. Phys. Solids* 204 (2025) 106273. [Link]

J. U. Surjadi, B. F. G. Aymon, M. Carton, C. M. Portela, "Double-network-inspired Mechanical Metamaterials," *Nat. Mater.* (2025). [Link]

M. Perroni-Scharf, Z. Ferguson, T. Butruille, C. Portela, M. Konaković Luković, "Data-Efficient Discovery of Hyperelastic TPMS Metamaterials with Extreme Energy Dissipation," in: *Proc. Spec. Interest Group Comput. Graph. Interact. Tech. Conf. Conf. Pap.*, ACM, Vancouver BC Canada, 2025: pp. 1–12.

J. U. Surjadi, C. M. Portela, "Enabling Three-dimensional Architected Materials Across Length Scales and Timescales," *Nat. Mater.* (2025). [Link]

P. Serles, J. Yeo, M. Haché, P. G. Demingos, J. Kong, P. Kiefer, S. Dhulipala, B. Kumral, K. Jia, S. Yang, T. Feng, C. Jia, P. M. Ajayan, C. M. Portela, M. Wegener, J. Howe, C. V. Singh, Y. Zou, S. Ryu, T. Filleter, "Ultrahigh Specific Strength by Bayesian Optimization of Carbon Nanolattices," *Adv. Mater.* (2025) 2410651. [Link]

J. Kulikowski, D. Delghandi, C. Wu, S. D. Figueroa, W. S. Cunningham, D. S. Gianola, C. M. Portela, X. W. Gu, "Mechanical Behavior of Nanocluster-Based Nanocomposites Made Using Two-Photon Lithography," *ACS Appl. Mater. Interfaces* 17 (2025) 34582–34591. [Link]

R. Sun, J. Lem, Y. Kai, W. DeLima, C. M. Portela, "Tailored Ultrasound Propagation in Microscale Metamaterials via Inertia Design," *Sci. Adv. 10* (2024) eadq6425. [Link]

P. Thakolkaran, M. Espinal, S. Dhulipala, S. Kumar, C. M. Portela, "Experiment-informed Finite-strain Inverse Design of Spinodal Metamaterials," *Extreme Mech. Lett.* 74 (2025) 102274. [Link]

W. Chen, R. Sun, D. Lee, C. M. Portela, W. Chen, "Generative Inverse Design of Metamaterials with Functional Responses by Interpretable Learning," *Adv. Intell. Syst.* (2024) 2400611. [Link]

Negar Reiskarimian

Associate Professor

Department of Electrical Engineering & Computer Science

Integrated circuits and systems and applied electromagnetics with a focus on analog, RF, millimeter-Wave (mm-Wave) and optical integrated circuits, metamaterials and systems for a variety of applications.

Rm. 39-427a | 617-253-0726 | negarr @ mit . edu

POSTDOCTORAL ASSOCIATE

Mohammad Barzgari, EECS

GRADUATE STUDENTS

Soroush Araei, EECS Haibo Yang, EECS Sarina Sabouri, EECS (co-supervised with A. Chandrakasan) Melania St. Cyr, EECS, Draper Scholars Fellowship

SUPPORT STAFF

Maria Markulis. Administrative Assistant

SELECTED PUBLICATIONS

- S. Araei, M. Barzgari, H. Yang, and N. Reiskarimian, "A Harmonic-Suppressing Gain-Boosted N-Path Receiver with Clock Bootstrapping for IoT Applications," *IEEE Radio Frequency Integrated Circuits Symposium (RFIC)*, Jun. 2025.
- S. Araei and N. Reiskarimian, "Implementation and Application of Harmonic Reset Switching in Passive Mixers," *IEEE J. of Solid-State Circuits (JSSC)*, vol. 59, no. 12, pp. 4009-4021, Dec. 2024 (invited).
- A. Nagulu, N. Reiskarimian, T. Chen, S. Garikapati, I. Kadota, T. Dinc, S.L. Garimella, M. Kohli, A.S. Levin, G. Zussman, and H. Krishnaswamy, "Doubling Down on Wireless Capacity: A Review of Integrated Circuits, Systems, and Networks for Full-Duplex," *Proceedings of the IEEE*, vol. 112, no. 5, pp. 405-432, May 2024 (invited).
- S. Mohin, S. Araei, M. Barzgari, and N. Reiskarimian, "A Blocker-Tolerant mm-Wave MIMO Receiver with Spatial Notch Filtering Using Non-Reciprocal Phase-Shifters for 5G Applications," in *IEEE Radio Frequency Integrated Circuits Symposium (RFIC)*, pp. 15-18, Jun. 2024. (Best Student Paper Award 1st place).
- S. Araei, S. Mohin, and N. Reiskarimian, "0.25-4GHz Harmonic-Resilient Receiver with Built-in HR at Antenna and BB Achieving +14/+16.5dBm 3rd/5th IB Harmonic 1dB," in IEEE International Solid-State Circuits Conference (ISSCC), pp 90-91, Feb. 2024 (ISSCC 2024 Jack Kilby Outstanding Student Paper Award).
- S. Araei, S. Mohin, and N. Reiskarimian "Harmonic-Resilient Fully Passive Mixer-First Receiver for Software-Defined Radios," *IEEE J. of Solid-State Circuits (invited)*, vol. 58, no. 12, pp. 3396-3407, Dec. 2023.

- S. Araei, S. Mohin, and N. Reiskarimian "Realization of Low-Loss Fully Passive Harmonic Rejection N-Path Filters," *IEEE Microwave and Wireless Technology Letts.* (invited), vol. 33, no. 6, pp. 823-826, Jun. 2023.
- S. Araei, S. Mohin, and N. Reiskarimian, "Realization of Low-Loss Fully-Passive Harmonic Rejection N-Path Filters," in *IEEE International Microwave Symposium (IMS)*, Jun. 2023 (Selected as one of the top-50 IMS submissions).
- S. Araei, S. Mohin, and N. Reiskarimian, "An Interferer-Tolerant Harmonic-Resilient Receiver with >+10dBm 3rd Harmonic Blocker P1dB for 5G NR Applications," in *IEEE International Solid-State Circuits Conference (ISSCC)*, pp. 294-295, Feb. 2023.
- N. Reiskarimian, "A Review of Nonmagnetic Nonreciprocal Electronic Devices: Recent Advances in Nonmagnetic Nonreciprocal Components," *IEEE Solid-State Circuits Magazine* vol. 13, no. 4, pp. 112-121, Fall 2021.
- N. Reiskarimian, M. Khorshidian, and H. Krishnaswamy, "Inductorless, Widely Tunable N-Path Shekel Circulators Based on Harmonic Engineering," *IEEE J. of Solid-State Circuits (JSSC)* (invited), vol. 56, no. 4, Apr. 2021.
- A. Nagulu, N. Reiskarimian, and H. Krishnaswamy, "Non-reciprocal Electronics Based on Temporal Modulation," *Nature Electronics*, May 2020.

Charles G. Sodini

LeBel Professor

Department of Electrical Engineering & Computer Science

Electronics and integrated circuit design and technology. Specifically, his research involves technology intensive integrated circuit and systems design, with application toward medical electronic devices for personal monitoring of clinically relevant physiological signals.

Rm. 39-527b | 617-253-4938 | sodini @ mtl . mit . edu

COLLABORATORS

Sam Fuller, Analog Devices, Inc Joohyun Seo, Analog Devices, Inc. Thomas Heldt, MIT Vivienne Sze. MIT

CO-ADVISED STUDENTS

Isabella Romero Estevez Jamie Koerner Ana Pascual Lopez

SUPPORT STAFF

Ava Bowen, Administrative Assistant

SELECTED PUBLICATIONS

H.-Y. Lai, C. G. Sodini, T. Heldt, and V. Sze, "Individualized Tracking of Neurocognitive-state-dependent Eye-movement Features Using Mobile Devices," *Proceedings of the ACM on Interactive, Mobile, Wearable and Ubiquitous Technologies* 7(1): 1–23, 2023.

M. I. Syed, C. G. Sodini, and T. Heldt, "Deconvolution-based partial volume correction for volumetric blood flow measurement," *IEEE Transactions on Ultrasonics, Ferroelectrics, and Frequency Control* 69(8): 2484–2498, Apr. 2022.

J. Seo, H.-S. Lee, and C. G. Sodini, "Non-Invasive Evaluation of a Carotid Arterial Pressure Waveform Using Motion-Tolerant Ultrasound Measurements During the Valsalva Maneuver," *IEEE J. of Biomedical and Health Informatics* 25(1), Jan. 2021.

H.-Y. Lai, G. Saavedra-Peña, C. G. Sodini, V. Sze, and T. Heldt, "App-based saccade latency and error determination across the adult age spectrum," *IEEE Transactions on Biomedical Engineering* 69(2): 1029–1039, 2021.

H.-Y. Lai, G. Saavedra-Peña, C. G. Sodini, V. Sze, and T. Heldt, "Measuring Saccade Latency Using Smartphone Cameras," *IEEE J. of Biomedical and Health Informatics* 24(3): 885–897, Mar. 2020.

Frances M. Ross

TDK Professor

Department of Materials Science and Engineering

Electron microscopy as a tool to measure dynamic processes such as crystal growth and materials transformations.

Rm. 13-5046 | 617-452-2535 | fmross @ mit . edu

POSTDOCTORAL ASSOCIATES

Zhenjing Liu, DMSE Hanglong Wu, DMSE

GRADUATE STUDENTS

Chen Chang, DMSE, Think Global Education Trust Fellow Kaiyuan Chen, DMSE Rishabh Kothari, DMSE, NSF Fellow Pip Knight, DMSE Paul Miller, DMSE, Mathworks Fellow Jane Park, DMSE

SUPPORT STAFF

Kathy Simons, Administrative Assistant

SELECTED PUBLICATIONS

F. M. Ross, "Liquid Cell Transmission Electron Microscopy for Real-World Problems," *Microscopy Today*, 32: 17-22, 2024.

- J. Klein and F. M. Ross, "Materials Beyond Monolayers: The Magnetic Quasi-1D Semiconductor CrSBr," *J. Materials Research*, 39: 3045–3056, 2024.
- E. Park, J. P. Philbin, H. Chi, J. J. Sanchez, C. Occhialini, G. Varnavides, J. B. Curtis, Z. Song, J. Klein, J. D. Thomsen, M.-G. Han, A. C. Foucher, K. Mosina, D. Kumawat, N. Gonzalez-Yepez, Y. Zhu, Z. Sofer, R. Comin, J. S. Moodera, P. Narang, and F. M. Ross, "Anisotropic 2D Van Der Waals Magnets Hosting 1D Spin Chains," *Advanced Materials*, 36: 2401534, 2024.
- J. D. Thomsen, Y. Wang, H. Flyvbjerg, E. Park, K. Watanabe, T. Taniguchi, P. Narang, and F. M. Ross, "Direct Visualization of Defect-Controlled Diffusion in Van Der Waals Gaps," *Advanced Materials*, 36: 2403989, 2024.
- T. Pham, K. Reidy, J. D. Thomsen, B. Wang, N. Deshmukh, M. A. Filler, and F. M. Ross, "Salt-Assisted Vapor–Liquid–Solid Growth of 1D Van Der Waals Materials," *Advanced Materials*, 36: 2309360, 2024.
- S. F. Tan, H. Wu, J. S. Manser, D. Zhang, M. Ronchi, S. Smullin, Y.-M. Chiang, and F. M. Ross, "Electrochemical Reactivity and Stability of the Fe Electrode in Alkaline Electrolyte," *Advanced Functional Materials*, 2407561, 2024.
- S. Lee, K. Gadelrab, L. Cheng, J. P. Braaten, H. Wu, and F. M. Ross, "Simultaneous 2D Projection and 3D Topographic Imaging of Gas-Dependent Dynamics of Catalytic Nanoparticles," *ACS Nano*, 18: 21258–21267, 2024.

- A. C. Foucher, W. Mortelmans, W. Bing, Z. Sofer, R. Jaramillo, and F. M. Ross, "Structural Changes in HfSe₂ and ZrSe₂ Thin Films With Various Oxidation Methods," *J. Materials Chemistry C*, 12: 9677–9684, 2024.
- S. Han, J. S. Kim, E. Park, Y. Meng, Z. Xu, A. C. Foucher, G. Y. Jung, I. Roh, S. Lee, S. O. Kim, J.-Y. Moon, S.-I. Kim, S. Bae, X. Zhang, B.-I. Park, S. Seo, Y. Li, H. Shin, K. Reidy, A. T. Hoang, S. Sundaram, P. Vuong, C. Kim, J. Zhao, J. Hwang, C. Wang, H. Choi, D.-H. Kim, J. Kwon, J.-H. Park, A. Ougazzaden, J.-H. Lee, J.-H. Ahn, J. Kim, R. Mishra, H.-S. Kim, F. M. Ross, and S.-H. Bae, "High Energy Density in Artificial Heterostructures Through Relaxation Time Modulation," *Science*, 384: 312-317, 2024.
- T. Defferriere, B. Wang, J. Klein, F. M. Ross, and H. L. Tuller, "Field-Driven Solid-State Defect Control of Bilayer Switching Devices," *ACS Applied Materials & Interfaces*, 16: 46461-46472, 2024.
- S. Lee, T. Watanabe, F. M. Ross, and J. H. Park, "Temperature Dependent Growth Kinetics of Pd Nanocrystals: Insights From Liquid Cell Transmission Electron Microscopy," *Small*, 2403969, 2024.
- K. Mosina, B. Wu, N. Antonatos, J. Luxa, V. Mazánek, A. Söll, D. Sedmidubsky, J. Klein, F. M. Ross, and Z. Sofer, "Electrochemical Intercalation and Exfoliation of CrSBr Into Ferromagnetic Fibers and Nanoribbons," *Small Methods*, 8: 2300609, 2024.
- Y. Zhang, B. Wang, C. Miao, H. Chai, W. Hong, F. M. Ross, and R.-T. Wen, "Controlled Formation of Three-Dimensional Cavities During Lateral Epitaxial Growth," *Nature Communications*, 15: 2247, 2024.
- J. D. Thomsen, M.-G. Han, A. N. Penn, A. C. Foucher, M. Geiwitz, K. S. Burch, L. Dekanovsky, Z. Sofer, Y. Liu, C. Petrovic, F. M. Ross, Y. Zhu, and P. Narang, "Effect of Surface Oxidation and Crystal Thickness on the Magnetic Properties and Magnetic Domain Structures of Cr₂Ge₂Te₈," *ACS Nano*, 18: 13458–13467, 2024.
- Z. Wang, H. Wang, R. Caudillo, J. Wang, Z. Liu, A. Foucher, J.-H. Park, M.-C. Chen, A. Lu, P. Wu, J. Zhu, X. Zheng, T. S. Pieshkov, S. A. Vitale, Y. Han, F. M. Ross, I. I. Abate, and J. Kong, "Interfacial Oxidation of Metals on Graphene," ACS Applied Nano Materials, 7: 24537–24546, 2024.

Vivienne Sze

Professor of Electrical Engineering & Computer Science Department of Electrical Engineering & Computer Science Joint design of signal processing algorithms, architectures, VLSI and systems for energy-efficient implementations. Applications include computer vision, machine learning, autonomous navigation, image processing and video coding.

Rm. 38-260 | 617-324-7352 | sze @ mit . edu

GRADUATE STUDENTS

Tanner Andrulis, EECS (co-advised with Joel Emer)
Zih-Sing Fu, EECS (co-advised with Sertac Karaman)
Dasong Gao, EECS (co-advised with Sertac Karaman)
Michael Gilbert, EECS (co-advised with Joel Emer)
Keshav Gupta, EECS (co-advised with Sertac Karaman)
Jamie Koerner, EECS (co-advised with Thomas Heldt)
Peter Li, EECS (co-advised with Sertac Karaman)
Soumya Sudhakar, AeroAstro (co-advised with Sertac Karaman)

Zi Yu Fisher Xue, EECS (co-advised with Joel Emer)

UNDERGRADUATE STUDENTS

Eyan Forsythe, EECS Yicheng Huang, EECS Kailas Kahler, EECS Ezra Kang, EECS Pau Ilerbaig-Bajona, EECS Noah Wiley, EECS Reng Zheng, EECS

SUPPORT STAFF

Janice L. Balzer. Administrative Assistant

SELECTED PUBLICATIONS

Z.-S. Fu*, S. Sudhakar*, S Karaman, V. Sze, "DecTrain: Deciding When to Train a Monocular Depth DNN Online," *IEEE Robotics and Automation Letts.*, Vol. 10, No. 3, pp. 2822 - 2829. Mar. 2025.

D. Gao*, P. Z. X. Li*, V. Sze, S. Karaman, "GEVO: Memory-Efficient Monocular Visual Odometry Using Gaussians," *IEEE Robotics and Automation Letts.*, Vol. 10, No. 3, pp. 2774 - 2781, Mar. 2025.

J. Koerner, V. Sze, "ClearDepth: Addressing Depth Distortions Caused by Eyelashes for Accurate Geometric Gaze Estimation on Mobile Devices," *IEEE International Conference on Image Processing (ICIP)*, Oct. 2024.

M. Gilbert, Y. N. Wu, J. S. Emer, V. Sze, "LoopTree: Exploring the Fused-layer Dataflow Accelerator Design Space," *IEEE Transactions on Circuits and Systems for Artificial Intelligence (TCASAI)*, Vol. 1, No. 1, pp. 97-111, Sep. 2024.

T. Andrulis, J. S. Emer, V. Sze, "CiMLoop: A Flexible, Accurate, and Fast Compute-In-Memory Modeling Tool," *IEEE International Symposium on Performance Analysis of Systems and Software (ISPASS)*, May 2024.

Luis Fernando Velásquez-García

Principal Research Scientist Microsystems Technology Laboratories Micro- and nano-enabled, multiplexed, scaled-down systems that exploit high electric field phenomena; microelectromechanical systems (MEMS) and nanoelectromechanical systems (NEMS); powerMEMS; additively manufactured MEMS and NEMS. Actuators, cold cathodes, ionizers, microfluidics, microplasmas, CubeSat hardware, portable mass spectrometry, pumps, sensors, X-ray sources.

Rm. 39-415B | 617-253-0730 | Ifvelasq @ mit . edu

GRADUATE STUDENTS

Zoey Bigelow, EECS Jorge Canada Perez-Sala, EECS Colin Eckhoff, EECS Alex Kashkin, MechE Hyeonseok Kim, MechE B. Quintanar and L. F. Velásquez-García, "Fully 3D-printed, triaxial electrospray microfluidics for uniform coreshell-shell microparticle generation," to be presented at the 23rd International Conference in Solid-State Sensors, Actuators, and Microsystems (Transducers 2025), Orlando FL, USA, Jun. 29 to Jul. 3, 2025.

VISITORS

Bryan Quintanar Abarca, Instituto Tecnológico y de Estudios Superiores de Monterrey Jose-María López-Villegas, Universität de Barcelona Neus Vidal, Universität de Barcelona

SUPPORT STAFF

Jami L. Mitchell, Project Coordinator

SELECTED PUBLICATIONS

C. Eckhoff, H. Kim, L. Metzler, R. E. Pedder, and L. F. Velásquez-García, "3D-printed quadrupole mass filter with high filter resolution for detecting carbon-13 isotopes," *Technical Digest 37th International Vacuum Nanoelectronics Conference (IVNC 2024)*, Brno, Czech Republic, July 15 – 19 2024, doi: 10.1109/IVNC63480.2024.10652515

J. Cañada and L. F. Velásquez-García, "Semiconductor-free, Monolithically 3D-printed Logic Gates and Resettable Fuses," *Virtual and Physical Prototyping*, vol. 19. no. 1, e2404157, Sep. 2024, doi: 10.1080/17452759.2024.2404157

J. Cañada, S. F. Nagle, N. Vidal, J. M. López-Villegas, and L. F. Velásquez-García, "3D-printed soft magnetic cores for compact electromechanical devices via material extrusion," *Technical Digest 23rd International Conference on Micro and Nanotechnology for Power Generation and Energy Conversion Applications* (PowerMEMS+ 2024), Tonsberg, Norway, pp. 255 – 258, Nov. 18-21, 2024 doi: 10.1109/PowerMEMS63147.2024.10814238

A. L. Beckwith, J. Borenstein, N. Moore, D. Doty, and L. F. Velásquez-García, "Systems and Methods for Fabricating Microfluidic Devices," *US Patent* 12,208,385 B2 (Publication Date Jan. 28, 2025).

H. Kim and L. F. Velásquez-García, "High-impulse, modular, 3D-printed CubeSat electrospray thrusters throttleable via pressure and voltage control," *Advanced Science*, vol. 12, no. 13, 2413706, Apr. 2025, doi: 10.1002/advs.202413706

Theses Awarded

S.B.

• Gaurab Das (A. CHANDRAKASAN)
Minor in Mathematics

S.M.

- Andres Garcia Coleto (J. NOTAROS)
 Integrated Visible-Light Liquid-Crystal-Based Modulators and Grating-Based Antennas
- Patrick Darmawi-Iskander (T. PALACIOS)
 Highly Scaled p-GaN-gate HEMTs for Low Voltage
 Power Electronics
- Daniel DeSantis (J. NOTAROS)
 Spatially-Adaptive LiDAR and Underwater
 Communications Using Integrated Optical Phased Arrays
- Hannah Gold (s. v. BORISKINA)
 Genetic Algorithm Gradient Ascent (GAGA)
 Optimization of Compact Symmetry-breaking Photonic Crystals
- Ayush Gupta (T. PALACIOS)
 Dipole Contact Engineering for Field-Effect Transistors
 Based on Two-Dimensional Materials
- Zhiping He (L. LIU)
 Magnetic Weyl Semimetals for Spintronic Applications
- Amy Huynh (s. v. BORISKINA)
 Sustainable Engineering of Polyethylene Fiber
 Materials: Advancing Functional Properties of Diverse
 Textile-Based Structures
- Yixuan Jiao (T. PALACIOS)
 CMOS-Compatible Wafer-Scale Synthesis and Rapid
 Characterization of Two-Dimensional Transition Metal
 Dichalcogenides
- Junghyun Kim (W. OLIVER)
 Design and Engineering of Protected Superconducting Qubits
- Jungsoo Lee (J. DEL ALAMO)
 Analog On-chip Training and Inference with Non-volatile Memory Devices
- Christian Lopez Angeles (T. PALACIOS)
 Highly Integrated Graphene-Based Sensing Platform for Structural Monitoring Applications
- Abhishek Mukherjee (S. V. BORISKINA)
 Optical Characterization of Strain and Defects in 2D
 Photonic Materials

- Hridibrata Pal (T. PALACIOS)
 High Al-content AlGaN Transistors for RF applications
- Aijia Yao (T. PALACIOS)
 Design-technology Co-optimization for Sub-2 nm
 Technology Node Based on 2D Materials

M. ENG

- Eyan Forsythe (v. SZE)
 Architectural Effects on the Accuracy of Analog
 Neural Network Accelerators
- Kailas Kahler (v. SZE)
 Hardware Acceleration for Gaussian Compression
- Ezra Kang (v. SZE) Energy Efficient Real-time Operating Systems on Chip
- Monica Liu (H.-S. LEE)
 Fully Differential Programmable Gain Chiplet for Integrated Data Acquisition Systems
- Aklilu Aron (s. CODAY)
 Condensed Buck-Boost Switched Capacitor Converter for Efficient Voltage Distribution in Electrified
 Aircraft
- Gaurab Das (A. CHANDRAKASAN)
 Vigilis: Leveraging Language Models for Fraud
 Detection in Mobile Communications and Financial
 Transactions
- Raiphy Jerez (S. CODAY)
 Novel Topology for Capacitively Isolated Switched Capacitor Converter
- Lejla Skelic (A. CHANDRAKASAN)
 CIRCUIT: A Benchmark for Circuit Interpretation and Reasoning Capabilities of LLMs
- Jade Sund (S. CODAY)
 A Hybrid Switched-Capacitor Converter for Capacitive
 Wireless Power Transfer in Biomedical Applications

PH.D.

- Soroush Araei (N. REISKARIMIAN)
 Reconfigurable and Interference-Tolerant Receivers for
 Next-Generation Wireless Systems
- Maitreyi Ashok (A. CHANDRAKASAN)
 Integrated Hardware Security for Practical and Low Overhead Protections
- Colin C. Eckhoff (L. F. VELASQUEZ)
 Development of Additively Manufactured Quadrupole
 Mass Filters for Low-Cost and High-Performance
 Applications

PH.D. (CONTINUED)

• Gerardo Perez Goncalves (C. L. DRENNAN)

Structural and Biochemical Investigation of a Multiprotein Complex between Human Ribonucleotide Reductase and a Protein-based Activity Regulator

• Tushar Karnik (J. HU)

Integration of Quantum Cascade Lasers with Photonic Circuits

• Serin Lee (F. ROSS)

In situ electron microscopy of nanomaterials dynamics in heterogenous phase environments

• Yujun Lin (S. HAN)

Advancing Deep Learning Efficiency: from Specialized Co-Design to Automated Generation

• Owen Medieros (K. BERGGREN)

Superconducting Nanowire Integrated Circuits for Scalable Cryogenic Memorys

• John Niroula (T. PALACIOS)

Thermally Hardened RF GaN HEMTs in Extreme Environments

• Joshua Perozek (T. PALACIOS)

Novel Structures for Scalable Vertical Gallium Nitride Power Devices

• Jorge Cañada Pérez-Sala (L. F. VELASQUEZ)

Additive Manufacturing of Electrical Machines and Electronic Devices

• Cosmin Popescu (J. HU)

Improving the Reliability of Optical Phase Change Materials-Based Devices

• Luigi Ranno (J. HU)

Scalable Packaging and Integration Solutions for Next-Generation Photonic Systems

• Kate Reidy (F. ROSS)

Atomic-scale Design at the 2D/3D Interface Using Electron Microscopy

• David Rower (W. OLIVER)

Exploring Anisotropic Noise and Fast Gates with Superconducting Qubits

• Margaret Schroeder (E. S. BOYDEN)

Postnatal Specialization of Astrocyte Regional Heterogeneity in the Mammalian Brain and Improved Tools for Studying Glia

• John Simonaitis (K. BERGGREN)

Low-energy Electron-Photon Interactions in a Scanning Electron Microscope

• Corban Swain (E. S. BOYDEN)

Technological Innovation and Integration of Whole Brain Imaging, Olfactory Stimulation, and Correlative Microscopy in Larval Zebrafish

Haotian Tang (S. HAN)

Co-Designing Efficient Systems and Algorithms for Sparse and Quantized Deep Learning Computing

• Deniz Umut Yildirim (A. CHANDRAKASAN)

Wireless, Battery-Free, High-Sensitivity 5G RF Energy Harvesters for Next Generation IoT Sensor Tags

• Kevin Ye (R. JARAMILLO)

Chalcogenide Perovskite Thin Films for Photovoltaics

• Arina Yu (J. A. DEL ALAMO)

Characterization of pGaN-gate power HEMTs

Ruihan Zhang (E. S. BOYDEN)

Mapping the Spatial Transcriptome Across Whole Organisms

• Jiadi Zhu (T. PALACIOS)

System-Technology Co-Optimization of Scaled Electronics Based on Two-Dimensional Materials

• Weikun (Spencer) Zhu (F. NIROUI)

Additive Integration from Nanomaterials to Devices

Startups Affiliated with MTL and MIT.nano Faculty

Polina Anikeeva

• Neurobionics | https://neurobionics.io/

Vladimir Bulović

- QD Vision
- Kateeva | https://kateeva.com/
- Ubiquitous Energy | https://ubiquitous.energy
- Swift Solar | https://www.swiftsolar.com
- Optigon | https://www.optigon.us
- Active Surfaces | https://www.linkedin.com/company/activesurfaces

Tonio Buonassisi

• Xinterra Pte.Ltd. | https://xinterra.tech

Jesús A. del Alamo

• Eva Corp. | https://evacorp.ai/

Dirk R. Englund

- QuEra Computing, Inc | https://www.quera.com
- Lightmatter Inc | https://www.lightmatter.ai
- Quantum Network Technologies, Inc | https://www.qunett.com
- Dust Identity Inc | https://dustidentity.com/
- Axiomatic_Al | https://www.axiomatic-ai.com/

Eugene Fitzgerald

• nsc pte ltd | https://www.nscinnovation.com/

Ruonan Han

• Cambridge Terahertz | https://www.thzcorp.com

Juejun (JJ) Hu

- 2Pi Inc. | https://www.2pioptics.com/
- $\bullet \ \mathsf{InSpek} \ \mathsf{SAS} \ | \ \mathsf{https://www.inspek-solutions.com/}$
- LyteChip Inc. | https://lytechip.com/

Hae-Sueng (Harry) Lee

• Omni Technologies | https://www.omnidesigntech.com

Scott Manalis

- Travera | https://www.travera.com
- Affinity Biosensors | https://affinitybio.com

William D. Oliver

• Atlantic Quantum | https://www.atlantic-quantum.com

Tomás Palacios

- Finwave Semiconductor | https://www.finwavesemi.com
- FabuBlox | https://www.fabublox.com
- Vertical Horizons | https://www.vertical-horizons.com
- CDimension Inc. | https://www.cdimension.com

David Perreault

- Artic Sand
- Onchip power/Finsix
- Eta Devices | https://www.linkedin.com/company/eta-devices-inc-/about/
- Eta Wireless | https://www.etawireless.com

Charlie Sodini

• Prescient Devices | https://www.prescientdevices.com

Kripa Varanasi

- LiquiGlide Inc. | https://liquiglide.com
- Dropwise Corp. | https://www.drop-wise.com
- Infinite Cooling | https://www.infinite-cooling.com
- AgZen Inc. | https://www.agzen.com
- Alsym Energy | https://www.alsym.com
- CoFLo Medical | https://www.coflo-medical.com

Luis Fernando Velásquez-García

• FORAY Bioscience | https://www.foraybio.com



TECHNICAL ACRONYMS

ADC Analog-to-Digital Converters

CMOS Complementary Metal-Oxide-Semiconductor

CNT Carbon Nanotubes

FET Electro-Chemical Plating
FET Field-Effect Transistor
HSQ Hydrogen Silsesquioxane

InFO Integrated Fan Out

MOSFET Metal-Oxide-Semiconductor Field-Effect Transistor

nTRON Nanocryotron

RDL Re-distribution Layers
RIE Reactive Ion Etching

SNSPDs Superconducting Nanowire Single Photon Detectors

SS Subthreshold Swing

TMAH Tetramethylammonium Hydroxide

TREC Thermally Regenerative Electrochemical Cycle

MIT ACRONYMS & SHORTHAND

BE Department of Biological Engineering

Biology Department of Biology

ChemE Department of Chemical Engineering
CICS Center for Integrated Circuits and Systems
CMSE Center for Materials Science and Engineering

LIRG Interdisciplinary Research Group

DMSE Department of Materials Science & Engineering

EECS Department of Electrical Engineering & Computer Science

ISN Institute for Soldier Nanotechnologies

KI David H. Koch Institute for Integrative Cancer Research

LL Lincoln Laboratory

MAS Program in Media Arts & Sciences

MechE Department of Mechanical Engineering

MEDRC Medical Electronic Device Realization Center

MIT-CG MIT/MTL Center for Graphene Devices and 2D Systems

MITEI MIT Energy Initiative

MIT-GaN MIT/MTL Gallium Nitride (GaN) Energy Initiative

MIT International Science and Technology Initiatives

MIT-Surgapore University of Technology and Design Collaboration Office

MIT Skoltech Initiative

MTL Microsystems Technology Laboratories

NSE Department of Nuclear Science & Engineering

Physics Department of Physics

Sloan School of Management

SMA Singapore-MIT Alliance

LSMART Singapore-MIT Alliance for Research and Technology Center

SMART-LEES SMART Low Energy Electronic Systems Center

SUTD-MIT MIT-Singapore University of Technology and Design Collaboration Office

UROP Undergraduate Research Opportunities Program

U.S. GOVERNMENT ACRONYMS

AFOSR U.S. Air Force Office of Scientific Research

FATE-MURI Foldable and Adaptive Two-dimensional Electronics

Multidisciplinary Research Program of the University Research Initiative

AFRL U.S. Air Force Research Laboratory

ARL U.S. Army Research Laboratory

LARL-CDQI U.S. Army Research Laboratory Center for Distributed Quantum Information

ARO Army Research Office

ARPA-E Advanced Research Projects Agency - Energy (DOE)

DARPA Defense Advanced Research Projects Agency

DREaM Dynamic Range-enhanced Electronics and. Materials

DoD Department of Defense **DoE** Department of Energy

LEFRC U.S. Department of Energy: Energy Frontier Research Center (Center for Excitonics)

DTRA U.S. DoD Defense Threat Reduction Agency

IARPA Intelligence Advanced Research Projects Activity

RAVEN Rapid Analysis of Various Emerging Nanoelectronics

NASA National Aeronautics and Space Administration

LGSRP NASA Graduate Student Researchers Project

NDSEG National Defense Science and Engineering Graduate Fellowship

NIH National Institutes of Health

LNCI National Cancer Institute

NNSA National Nuclear Security Administration

NRO National Reconnaissance Office

NSF National Science Foundation

LCIQM NSF Center for Brains, Minds, and Machines **LCIQM** Center for Integrated Quantum Materials

LESS NSF Center for Sensorimotor Neural Engineering

NSF Center for Energy Efficient Electronics Science

CARFP Graduate Research Fellowship Program

LIGERT NSF The Integrative Graduate Education and Research Traineeship

NEEDSNSF Nano-engineered Electronic Device Simulation Node

Presidential Early Career Awards for Scientists and Engineers

NSF Science, Engineering, and Education for Sustainability

LSTC NSF Science-Technology Center

ONR Office of Naval Research

OTHER ACRONYMS

CONACyT Centre National de la Recherche Scientifique
CONACyT Consejo Nacional de Ciencia y Tecnología (Mexico)

IEEE Institute of Electrical and Electronics Engineers

IHP Germany Innovations for High Performance Microelectronics Germany

KIST Korea Institute of Science and Technology

KFAS Kuwait Foundation for the Advancement of Sciences

MASDAR Masdar Institute of Science and Technology

NTU Nanyang Technological University
 NUS National University of Singapore
 NYSCF The New York Stem Cell Foundation
 SRC Semiconductor Research Corporation

NSF/SRC Nano-Engineered Electronic Device Simulation Node

SUTD Singapore University of Technology and Design

TEPCO Tokyo Electric Power Company

TSMC Taiwan Semiconductor Manufacturing Company

Principal Investigator Index

| A | K |
|--|--|
| A | K |
| Agarwal, Anuradha Miv, 202 | Karaman, Sertac63, 65 |
| Akinwande, Akintunde I 67 | Keathley, Phillip D |
| Anikeeva, Polina243 | Kim, Jeehwan |
| Anthony, Brianiv | Kong, Jingv, 32, 40, 73, 79, 81, 88, 100, 139, 171, 172, 186 |
| Antoniadis, Dimitri A. 29, 91, 99 | |
| В | L |
| D | Lang, Jeffrey H, ii, 66, 144, 226 |
| Bahai, Ahmad23, 200 | LeBeau, James M |
| Baldo, Marc A | Lee, Hae-Seung22, 227, 243, 244 |
| Barbastathis, George98, 204 | Li, Mingda |
| Bawendi, Moungi G132, 140 | Liu, Luqiao27, 229 |
| Berggren, Karl K. v, 17, 77, 106, 130, 135, 136, 158, 163, 175, 205 | L. Ju |
| Boning, Duane S | Lozano, Paulov, 60 |
| Boriskina, Svetlana V | ** |
| Boyden, Edward S | M |
| Bulović, Vladimir i, iii, iv, v, 42, 66, 86, 88, 140, 209, 207, 243 | Manalis. Scott R |
| Buonassisi, Tonio | 250, 244 |
| C | N |
| Casamento, Joseph43, 210 | Niroui, Farnaz |
| Chandrakasan, Anantha P 23, 113, 211 | Notaros, Jelena |
| Chen, Kevin | |
| Coday, Samantha142, 149, 213 | 0 |
| Comin, Riccardo | Oliver, William Dv, 160, 233, 244 |
| 5 | Onver, william D |
| D | P |
| del Alamo, Jesús Av, 29, 36, 90, 91, 93, 99, 101, 103, 108, | |
| | Palacios, Tomás i, ii, iii, v, 11, 19, 31, 32, 34, 35, 39, 40, 52, 62, |
| Drennan, Catherine L. | |
| _ | Portela, Carlos Mv, 60, 61, 74, 75, 235 |
| E | 101tela, Galios II |
| Emer, Joel S | R |
| Englund, Dirk R | •• |
| | Ram, Rajeev |
| F | Reiskarimian, Negar |
| | Ross, Caroline Av |
| Fitzgerald, Eugene A243 | Ross, Frances M. v, 27, 71, 165, 166, 167, 169, 188, 189, 190, 191, 239 |
| H | S |
| Han, Jongyoon54, 55, 217 | Sarkar, Deblinav |
| Han, Ruonanii, 12, 14, 24, 31, 62, 195, 218, 243 | Sodini, Charles G. 197, 198, 237, 198 |
| Han, Song | Soljačić, Marin 121, 138 |
| Hart, A. Johnv | Strano, Michael S 82 |
| Heldt, Thomas47, 197 | S. V. Boriskina 173 |
| Hu, Juejun v, 124, 126, 220, 243 | Sze, Vivienne ii, 18, 63, 65, 105, 106, 109, 114, 238 |
| Hu, Qing | - |
| | Т |
| J | Thompson, Carl Vv |
| Jaramillo, Rafael | Tisdale, William A |
| Jarillo-Herrero. Pablo | Traverso, Giovanni |
| Jossou, Ericmoore | Tuller, Harry L180 |
| Ju, Longv, 33, 159, 162, 178, 223 | - |
| , 55, 55, 55, 57, 57, 57 | |

| V | |
|---|------------------------------------|
| Varanasi, Kripa K Velásquez-García, Luis F | v, 244 ii, 2, 4, 6, 9, 240, 244 |
| W | |
| Wardle, Brian L. | 8, 185 |
| Υ | |
| Yildiz, Bilgeii, v You, Sixian | |

IN APPRECIATION OF OUR MICROSYSTEMS INDUSTRIAL GROUP MEMBER COMPANIES:

Analog Devices
Applied Materials
Edwards
Ericsson
GlobalFoundries
Hitachi High-Tech Corporation
IBM
Intel
Lam Research Corp.
Lockheed Martin
muRata
NEC
Soitec
Taiwan Semiconductor Manufacturing Company
Texas Instruments

AND MIT.NANO CONSORTIUM MEMBER COMPANIES:

Analog Devices, Inc.
Applied Materials
Edwards
Fujikura
IBM Research
Lam Research
Lockheed Martin
NC
NEC Corporation
Shell
SLB



